Developing blood-based biomarkers of disease progression in Amyotrophic Lateral Sclerosis

Ching-Hua Lu

UCL Institute of Neurology

PhD Supervisors:

Professor Linda Greensmith & Dr Andrea Malaspina

A Thesis submitted for the degree of

Doctor of Philosophy

(Clinical Neuroscience)

University College London

2013

Declaration

I, Ching-Hua Lu, confirm that the work presented in this Thesis is my own. Where information has been derived from other sources, I confirm that this has been indicated in the Thesis.

Abstract

Amyotrophic Lateral Sclerosis (ALS) is a fatal neurodegenerative disorder, for which there is no effective treatment. Clinical trials in ALS are hindered by the lack of reliable biomarkers to enable an early diagnosis and monitoring of disease progression. There is therefore an urgent need to develop biomarkers for ALS. In this Thesis, I examined the possibility that plasma Neurofilament levels may be a biomarker of disease progression in mouse models and ALS patients.

I first developed an enzyme-linked immunosorbent assay (ELISA) method that overcomes a well-known technical obstacle, the NfH 'Hook Effect', to enable accurate quantification of plasma Neurofilament Heavy Chain (NfH). Using this ELISA, I next examined the longitudinal changes in plasma NfH levels in $SOD1^{G93A}$ mice that model ALS. I observed a significant increase in plasma NfH levels as disease progressed, which correlated with the decrease in functional and morphological read-outs of neuromuscular function and motor neuron survival. Moreover, treatment of $SOD1^{G93A}$ mice with different disease-modifying agents, Arimoclomol, Cogane and Riluzole, was found to not only ameliorate disease but also reduce plasma NfH levels compared to untreated controls. Plasma NfH levels may therefore be of use in monitoring drug efficacy and disease progression in clinical trials. Examination of plasma NfH levels in an alternative ALS model with a slower disease progression, the $SOD1^{G93Adl}$ mouse, confirmed that plasma NfH levels increase during disease progression in models other than the rapidly progressing $SOD1^{G93A}$ model. The relevance of these findings of increased plasma NfHs in SOD1 mice as a biomarker of disease progression in the human disease were examined in the final Results Chapter using serial samples longitudinally collected from a cohort of 136 ALS patients with follow-up up to three years.

To sum up, the results presented in this Thesis detail the investigation of plasma NfH levels as a disease progression marker in SOD1 mice and in ALS patients.

Acknowledgements

The idea of coming to UK for a PhD was formed in 2005 after the Tsunami hit the island where I was originally supposed to stay on that chaotic day. I started ALS research at a time, which I consider with hindsight, that there was also a Tsunami taking place in the ALS field where we were entering a whole new world of RNA research in ALS, although RNA is nothing to do with this Thesis. Nonetheless, I feel very happy to have taken part in ALS research and hope that the work presented in this Thesis has contributed to a better understanding of ALS. Thanks must go to the ALS patients and their families who generously gave their blood as well as the SOD1 mice I've come across during these years.

I would not be able to complete this PhD project and this Thesis without my supervisors Professor Linda Greensmith and Dr Andrea Malaspina, who gave me the opportunity to do this fantastic project, and full support and guidance throughout these years. Their passion and dedication to ALS research is a constant inspiration for me. Special thanks must go to Dr Axel Petzold, my unofficial supervisor, who guided me to the world of neurofilament and ELISA, which are the backbones of this Thesis. In addition, I would not be able to simply focus on the project itself without the perfect admin support and friendship from Kully. Special thanks must also go to Jim, our superb lab manager, whose support has been crucial to the research and for my getting-to-know British culture!

I have enjoyed working in Watts Laboratory in UCL Institute of Neurology and the Blizard Institute, Queen Marry University of London in the past years and considered myself quite fortunate to be able to work alongside my brilliant labmates and to have their friendships: Adrian, Alec, Alex, Amy, Anna, Barney, Bernadett, Bilal, Emem, Karli, Leonie, Mhoriam, Jing, Phil, and Virginie. You have enriched my life in London, both scientifically and socially!

Lastly, but by no means least, I would like to dedicate this Thesis to my family: Father, Yeo-Lee Lu, Mother, Hsiu-Er Chang, and my sisters, Shu-Fang Lu and Tzu-Wan Lu. I can't thank them enough for their love and support, which is so vital and so dear to me, as always!

TABLE OF CONTENTS

Title …… 1
Developing blood-based biomarkers of disease progression in 1
Amyotrophic Lateral Sclerosis 1
Declaration 2
Abstract 3
Acknowledgements 4
List of Figures 12
List of Tables 15
List of Abbreviations 17
Chapter 1 21
General Introduction 21
1.1 Amyotrophic Lateral Sclerosis 21
1.1.1 Clinical phenotypes of ALS 22
1.1.2 Cognitive involvement in ALS 25
1.1.2.1 Frontotemporal lobar degeneration (FTLD) 25
1.1.2.2 The clinical spectrum of ALS and FTLD 25
1.1.3 Cognitive and clinical characteristics in ALS patients with the chromosome 9 open reading frame 72 gene *(C9orf72)* expansion 26
1.2 Genetics of Amyotrophic Lateral Sclerosis 26
1.2.1 Causative genes for ALS 29
1.2.2 Susceptibility and modifier genes 32
1.3 Disease pathomechanisms in ALS 33
1.3.1 New insights into the pathogenesis of ALS 33
1.3.1.1 A failure of proteostasis: new findings about this long-known mechanism 33
1.3.1.1.1 Both mutant SOD1 and oxidised wild-type SOD1 misfold and result in increased cellular stress 33
1.3.1.1.2 Impaired protein degradation 38
1.3.1.2 Dysregulated transcription and RNA processing 39
1.3.1.2.1 Loss-of-function mechanism of TDP-43 and FUS 39
1.3.1.2.2 Gain-of-function toxicity of TDP-43 and FUS 39
1.3.1.3 A failure of axons 40
1.3.1.4 Neuroinflammation 43
1.4 ALS Therapeutics 44
1.5 Clinimetrics in ALS 50
1.6 Biomarkers for ALS 54

1.6.1 Biomarkers for the development of disease-modifying treatments in ALS 54
1.6.2 Current strategies for the development of Biomarkers in ALS 56
1.6.2.1 Physiological biomarkers 56
1.6.2.1.1 Motor unit number estimation 57
1.6.2.1.2 Electrical impedance myography 58
1.6.2.1.3 Neurophysiological index 58
1.6.2.1.4 Transcranial magnetic stimulation 59
1.6.2.2 Neuroimaging 60
1.6.2.2.1 Magnetic Resonance Imaging 60
1.6.2.2.1.1 Standard sequence 60
1.6.2.2.1.2 Diffusion tensor imaging 61
1.6.2.2.1.3 Functional MRI 61
1.6.2.2.1.4 Magnetic resonance spectroscopy imaging 62
1.6.2.2.2 Positron emission tomography scan 62
1.6.2.2.3 Muscle ultrasonography 62
1.6.2.3 Neurochemical biomarkers 63
1.6.2.3.1 Choice of samples for biomarker analysis 64
1.6.2.3.2 Biomarker discovery platforms 64
1.6.2.3.2.1 Proteomics 64
1.6.2.3.2.2 Metabolomics 66
1.6.2.3.2.3 Lipidomics 67
1.6.2.3.2.4 Gene expression profiling and transcriptomics 67
1.6.2.3.2.5 High throughput techniques 69
1.7 Aims of this thesis 75
Chapter 2 76
Development of a sensitive, quantitative immunoassay for the measurement of plasma neurofilaments for ALS 76
2.1 Introduction 76
2.1.1 Neurofilament heavy chain (NfH) as a biomarker of ALS 76
2.1.2 Established approaches for the detection of NfH in the peripheral blood of ALS 77
2.1.3 Limitations of existing methods to quantify NfH levels from blood: lack of parallelism 78
2.1.4 Hypothesis and Aims 79
Hypothesis 79
Aims 79
2.2 Methods and Materials 81
2.2.1 Experimental animals 81

2.2.1.1 Genotyping of SOD1^{G93A} mice 81
2.2.1.2 Plasma collection 82
2.2.2 ELISA 82
2.2.2.1 Antibodies 82
2.2.2.2 Chemicals and Reagents 82
2.2.2.3 NfH Standards 84
2.2.2.4 Plasma samples 84
2.2.2.5 Existing method for detection of NfH 84
2.2.3 Western blot analysis 85
2.2.3.1 Samples 85
2.2.3.2 Sample preparation 85
2.2.3.3 Blot management 85
2.2.3.4 Band specificity validation 86
2.2.3.5 Densitometry 86
2.2.4 Statistical analysis 86
2.3 Results 86
2.3.1 Plasma NfH aggregates cause a NfH 'Hook shaped curve' 86
2.3.2 Disruption of NfH aggregates in plasma 90
2.3.3 A comparison of plasma NfH levels in end-stage SOD1^{G93A} mice with age-matched WT littermates, using the modified in-house ELISA 96
2.4 Discussion 96
2.4.1 From CNS to Peripheral circulation 96
2.4.2 A breakthrough for NfH immunoassay 98
2.4.2.1 The 'Hook Effect' in Oncology and Endocrinology 99
2.4.2.2 Overcoming the NfH 'Hook Effect' 99
2.4.3 Plasma NfH levels significantly increase in end-stage SOD1^{G93A} mice that model ALS 100
2.4.4 Conclusions 102
Chapter 3 103
Plasma neurofilament heavy chain levels correlate with disease progression and are biomarkers of treatment response in SOD1^{G93A} mouse model of ALS 103
3.1 Introduction 103
3.1.1 The need for biomarkers in ALS 103
3.1.2 Neurofilament Heavy Chain (NfH) as a candidate biomarker for ALS 103
3.1.3 Current and potential therapeutics tested in SOD1^{G93A} mice 105
3.1.3.1 Riluzole 105

3.1.3.2 Arimoclomol 105
3.1.3.3 Cogane 107
3.1.4 Hypotheses and Aims 107
3.2 Methods and Materials 108
3.2.1 Experimental animals 108
3.2.1.1 Breeding of SOD1^{G93A} mice 108
3.2.1.2 SOD1^{G93Adl} mice 108
3.2.2 Drug treatment 109
3.2.3 Arimoclomol trial 109
3.2.3.1 Experimental groups in Arimoclomol trial 109
3.2.3.2 Longitudinal plasma sampling in Arimoclomol treated SOD1^{G93A} mice 110
3.2.4 Cogane Trial 110
3.2.4.1 Experimental groups in Cogane trial 110
3.2.4.2 Longitudinal plasma sampling in Cogane trial 110
3.2.5 Plasma Collection 111
3.2.5.1 Plasma collection in Arimoclomol Trial 111
3.2.5.2 Plasma collection in Cogane Trial 111
3.2.5.3 Plasma collection in SOD1^{G93Adl} 111
3.2.6 Functional assessments of neuromuscular functions 112
3.2.6.1 Longitudinal assessment of Grip Strength 112
3.2.6.2 Acute *in vivo* physiological assessment of muscle force 112
3.2.6.3 Acute *in vivo* physiological assessment of motor unit survival 113
3.2.7 Morphological assessment of motor neuron survival 113
3.2.8 NfH ELISA 113
3.2.9 ELISA Data analysis 113
3.2.10 Statistical analysis 114
3.2.10.1 Longitudinal Biomarker and Arimoclomol treatment study 114
3.2.10.2 SOD1^{G93Adl} study and SOD1^{G93A} Cogane drug trial 114
3.3 Results 114
3.3.1 Plasma NfH levels in SOD1^{G93A} mice increase significantly from a late symptomatic stage 115
3.3.2 Correlations between plasma NfH levels and functional measures of disease progression in SOD1^{G93A} mice 118
3.3.2.1 Increased plasma NfH levels inversely correlate with grip strength in SOD1^{G93A} mice 119
3.3.2.2 Increased plasma NfH levels correlate with the decline in isometric muscle force in hindlimb muscles of SOD1^{G93A} mice 119

3.3.2.3 Increased plasma NfH levels correlate with motor unit loss in SOD1^{G93A} mice 126
3.3.2.4 Increased plasma NfH levels directly correlate with the extent of motor neuron death in the spinal cord of SOD1^{G93A} mice 126
3.3.3 Plasma NfH levels reflect the disease-modifying effects of arimoclomol in SOD1 mice 129
3.3.3.1 Longitudinal assessment of disease progression in Arimoclomol-treated SOD1^{G93A} mice 132
3.3.3.2 The effect of Arimoclomol on muscle force, motor unit and motor neuron survival in SOD1^{G93A} mice 132
3.3.3.3 Plasma NfH levels reflect the beneficial effects of Arimoclomol in SOD1^{G93A} mice132
3.3.4 Using plasma NfH levels as a biomarker in a novel preclinical trial in SOD1^{G93A} mice 140
3.3.5 Plasma NfH levels reflect disease progression in a slowly progressing mouse model of ALS 143
3.4 Discussion 148
3.4.1 Plasma NfH levels are a biomarker of disease progression in the SOD1^{G93A} mouse model of ALS and reflect the beneficial effects of a disease-modifying therapy 148
3.4.2 The use of NfHs as a biomarker of disease 149
3.4.3 Plasma NfH levels correlate with functional and morphological read-outs of neuromuscular decline in SOD1^{G93A} mice 151
3.4.4 Plasma NfH levels reflect the effects of disease-modifying therapies in SOD1^{G93A} mice 152
3.5 Conclusions 155
Chapter 4 156
Plasma neurofilaments as a biomarker of disease progression in ALS: 156
Insights from a longitudinal study 156
4.1 Introduction 156
4.1.1 Current limitations and merits in biomarkers of disease progression in ALS 156
4.1.2 Recent progress in developing neurofilaments as a biomarker of disease progression in ALS 158
4.1.3 Hypotheses and Aims of this Chapter 159
4.2 Method and Materials 159
4.2.1 Experimental participants 159
4.2.1.1 ALS patients 160
4.2.1.2 Control subjects 160
4.2.2 Characterisation of disease progression ALS 160
4.2.2.1 Change in function 160
4.2.2.1 Disease duration to baseline 162

4.2.3 Plasma collection 162
4.2.3.1 Cross-sectional study sampling 166
4.2.3.2 Longitudinal study sampling 166
4.2.4 NfH ELISA 166
4.2.2.1 Analytical procedure using ELISA method originally designed for CSF samples 166
4.2.2.2 Analytical procedure using ELISA method designed for plasma samples (developed in Chapter 2) 166
4.2.2.3 ELISA data analysis 166
4.2.4 Western Blots 167
4.2.4.1 Sample preparation 167
4.2.4.2 Blotting procedures 167
4.2.5 Statistical analysis 168
4.3 Results 168
4.3.1 A NfH 'hook effect' is present in human plasma 168
4.3.2 The NfH 'Hook Effect' in human plasma is overcome by urea 169
4.3.3 Plasma levels of NfH in ALS patients and controls 169
4.3.3.1 Changes in plasma NfH levels in ALS patients 176
4.3.3.1.1 Cross-sectional study of plasma NfH levels in ALS patients and control subjects 176
4.3.3.1.1.2 Plasma NfH levels may change during disease progression 178
4.3.3.1.2 Longitudinal changes in plasma NfH levels in ALS patients 178
4.3.3.1.2.1 Total plasma NfH levels in ALS patients are affected by the progression rate during disease 179
4.3.3.1.3 Longitudinal changes in levels of hyperphosphorylated NfH in ALS patients: the change in expression from symptom onset 179
4.3.3.1.3.1 Hyperphosphorylated NfH^{SMI34} plasma levels in ALS patients and the effects of disease duration and progression rate 179
4.3.3.2 Do changes in plasma NfH levels have any prognostic value? 183
4.3.3.2.1 Plasma NfH levels correlate with progression of disease between visits 183
4.3.3.2.2 Changes in plasma NfH levels do not predict patterns of disease progression 186
4.3.3.3 Sampling bias leads to misinterpretation of relevance of NfH levels in cross-sectional studies in ALS 188
4.3.4 The immune response to neurofilaments; NfH fragments co-localise with anti-human IgG immunoglobulin 192
4.4 Discussion 197
4.4.1 Plasma NfH levels are related to disease duration and disease progression in ALS and may also be affected by the immune response: NfH is not a ready-to-use biomarker of disease progression for ALS 198
4.4.2 Plasma NfH levels do not always increase as disease progresses in ALS 199

4.4.3 Immune response against neuroglia-specific proteins in the peripheral blood 200

4.4.4 Possible explanations for the discrepancy in plasma NfH levels between animal models and men 201

4.4.5 The impact of this study for biomarker studies in ALS 202

4.5 Conclusions 203

Chapter 5 205

Discussion 205

5.1 The development of a sensitive, reliable immunoassay for the quantification of NfH in plasma of SOD1 mice and ALS patients. 205

5.2 Plasma NfH levels in clinically homogeneous SOD1 mouse models of ALS 205

5.2.1 Plasma NfH levels increase during disease progression is detected in both rapidly-progressing $SOD1^{G93A}$ and slowly-progressing $SOD1^{G93Adl}$ mouse models of ALS 206

5.2.2 Plasma NfH levels correlate with readouts of disease progression in $SOD1^{G93A}$ mice 206

5.2.3 Plasma NfH levels reflect the therapeutic effects of established and new agents in $SOD1^{G93A}$ mice 207

5.3 Plasma NfH levels in a cohort of clinically heterogeneous ALS patients 207

5.3.1 Plasma NfH levels are influenced by disease duration, rate of disease progression, composition of study cohorts, and likely auto-antibody to NfH as well 208

5.3.2 Sampling bias is likely in small homogeneous cross-sectional studies of ALS patients: The need to re-think the use of baseline sampling 209

5.4 Conclusion 209

List of References 213

List of Figures

1.1	Clinical disease continuum and molecular relationships between FTLD and ALS	28
1.2	Molecular pathogenesis of amyotrophic lateral sclerosis	35
1.3	The protein quality control machinery	37
1.4	Changes to RNA metabolism upon cellular stress	41
1.5	Novel therapeutic targets currently/to be under clinical trials in ALS	45
1.6	Timeline of key clinical events and related types of biomarkers in ALS	55
2.1	Antibody concentration calculations by using a standard curve prepared from a serial dilution of *H. influenzae type b* standard reference serum (FDA 1983) (oval) and two serially diluted serum samples (square) plotted on a fully specified logit-log scale	80
2.2	Lack of parallelism from plasma samples impresses with a typical 'hook shaped curve' for NfH	87
2.3	Disruption of NfH aggregates	89
2.4	The effect of pre-thawing and calcium chelators on disruption of NfH aggregates	91
2.5	The effects of urea at different concentration on NfH levels in plasma of $SOD1^{G93A}$ mice	92
2.6	The effects of incubation period in $Barb_2EDTA$ buffer with urea at various concentration on NfH levels in plasma of $SOD1^{G93A}$ mice	93
2.7	The effects of 1 hour incubation of 0.5 M Urea-Barb2EDTA buffer at room temperature on plasma NfH levels in $SOD1^{G93A}$ mice	94
2.8	NfH levels in plasma of 120 days old $SOD1^{G93A}$ mice compared to WT littermates	97
3.1	Longitudinal assessment of plasma NfH^{SMI34} levels in WT and SOD1 mice	116
3.2	Longitudinal assessment of plasma NfH^{SMI35} levels in WT and SOD1 mice	117
3.3	Longitudinal assessment of grip strength and body weight in WT and SOD1 mice during disease progression	120
3.4	The correlation between grip strength and plasma NfH levels in	122

	SOD1 mice during disease progression	
3.5	The correlation between plasma NfH phosphoform levels and hindlimb muscle force in SOD1 mice during disease progression	124
3.6	The correlation between plasma NfH phosphoform levels and motor unit survival in EDL muscles in SOD1 mice during disease progression	127
3.7	The correlation between plasma NfH phosphoform levels and motor neuron survival in SOD1 mice during disease progression	130
3.8	Longitudinal assessment of grip strength and body weight in SOD1 and SOD1+A mice during disease progression	133
3.9	Longitudinal assessment of plasma NfH^{SMI34} levels in Arimoclomol-treated SOD1 mice	136
3.10	Longitudinal assessment of plasma NfH^{SMI35} levels in Arimoclomol-treated SOD1 mice	138
3.11	Functional and morphological assessment of $SOD1^{G93A}$ mice treated with Cogane and Riluzole from onset of disease (70 days of age)	141
3.12	Summary of plasma NfH levels in $SOD1^{G93A}$ mice treated with Cogane and Riluzole from onset of disease (70 days of age)	144
3.13	The decline in neuromuscular function and motor neuron survival and change in plasma NfH levels during disease progression in $SOD1^{G93Adl}$ mouse model of ALS	146
4.1	The 'Hook Effect' and lack of parallelism for NfH in human plasma	170
4.2	The effects of 1 hour incubation of 0.5 M Urea-$Barb_2$EDTA buffer at room temperature on plasma NfH levels in human plasma	172
4.3	A shorter diagnostic latency is associated with a poorer prognosis in ALS	175
4.4	Cross-sectional analysis of plasma NfH levels in ALS patients and controls at baseline	177
4.5	The profile of total plasma NfH levels in a 15-month follow-up from baseline in ALS patients with different rates of disease progression	181
4.6	The longitudinal profile of plasma NfH^{SMI34} levels in a 2 year follow-up varies according to the rate of disease progression and duration	184

4.7	NfH plasma levels correlate with the decline in the monthly ALSFRS_R slope.	187
4.8	Analysis of the change in plasma NfH levels and ALSFRS_R score during a follow-up period of up to 32 months identifies four main groups of ALS patients	189
4.9	A comparative cross-sectional analysis of plasma NfH levels in ALS patients and healthy controls: NfH levels vary according to the chosen sampling time	193
4.10	Immune response to NfH and NfH aggregates.	195
5.1	Timeline of key clinical events and the use of biomarkers in SOD1 mice and in ALS patients.	210

List of Tables

1.1	Summary of epidemiological and clinical characteristics of ALS phenotypes	24
1.2	Diagnostic categories of FTLD-ALS disease spectrum	27
1.3	Genes associated with familial ALS	30
1.4	Summary of susceptibility and modifier genes in ALS	34
1.5	Summary of ALS novel therapeutic targets recently being/to be tested in clinical trials	47
1.6	Summary of current clinimetrics in use in ALS	52
1.7	Advantages and disadvantages of different sample sources used in neurochemical biomarker studies	65
1.8	Selected studies of putative CSF and blood-based biomarkers in ALS	70
1.9	Current leading candidates of neurochemical biomarkers in ALS	72
2.1	Summary of the cycles involved in PCR analysis of $SOD1^{G93A}$ samples	83
2.2	A summary of initial plasma NfH^{SMI34} levels obtained from 120-day-old WT and $SOD1^{G93A}$ mice, using the ELISA method originally designed for CSF samples in Human	88
2.3	The optimised protocol for an ELISA detecting NfH in the plasma	95
3.1	Arimoclomol delays disease progression in $SOD1^{G93A}$ mice.	135
3.2	A summary of the statistical analysis (Mann-Whitney test) of the difference in the plasma levels of the two NfH phosphoforms in vehicle-treated SOD1 and Arimoclomol-treated SOD1+A mice at 65, 90, 105 and 120 days of age	139
4.1	Diagnostic guidelines for ALS	161
4.2	ALS Functional Rating Scale _ Revised (ALSFRS_R)	163
4.3	Characteristics of ALS patients and controls in the cross-sectional study for plasma NfH levels	174
4.4	Patient characteristics of the ALS patients studied longitudinally and sub-grouped according to their overall progression rates. Serial plasma NfH levels for all ALS patients were recorded from the baseline visit	180
4.5	Characteristics of ALS patients followed longitudinally: ALS patients are sub-grouped according to the time interval between ALS onset and their first study visit	182
4.6	Change in plasma NfH levels and its prognostic value for	191

disease progression: summary of the statistical analysis

List of Abbreviations

2D-DIGE: Two-dimensional fluorescence difference gel electrophoresis

Ab: antibody

AD: Alzheimer's Disease

ADC: Apparent Diffusion Coefficient

ADM: abductor digiti minimi

ALS: amyotrophic lateral sclerosis

ALSbi: ALS with minor behavioural impairment

ALSci: ALS with minor cognitive impairment

ALS-F: ALS individuals with a fast disease development

ALSFRS_R: ALS functional rating scale_Revised

ALS-S: ALS individuals with a slow disease development

Barb2EDTA buffer: a buffer containing 13.1g Sodium Barbitone, 2.1g Barbital, 0.25mg EDTA per litter of distilled water

BBB: blood-brain barrier

BDNF: brain-derived neurotrophic factor

bNfH: bovine neurofilament heavy chain subunit

BSA: bovine serum albumin

BSCB: blood-spinal cord barrier

bvFTD: behavioural variant frontotemporal lobar degeneration

BW: body weight

C9orf72: chromosome 9 open reading frame 72

CAFS: Combined Assessment of Function and Survival

CC: corpus callosum

cDNA: complementary deoxyribonucleic acid

CMAP: compound muscle action potential

CNS: central nervous system

CSF: cerebral spinal fluid

CST: corticospinal tract

CV: coefficient of variation

DNA: deoxyribonucleic acid

dNTP: deoxyribonucleotide triphosphate

DTI: diffusion tensor imaging

ECF: extracellular fluid

EDL: Extensor Digitorum Longus muscle

EDTA: ethylene diamine tetraacetic acid

EGTA: ethylene glycol tetraacetic acid

EI: echo intensity
EIM: Electrical impedance myography
ELISA: Enzyme-linked immunosorbent assay
EMG: electromyography
ER: endoplasmic reticulum
FA: fractional anisotropic
fALS: familial ALS
FDA: U.S. Food and Drug Administration
fMRI: Functional magnetic resonance imaging
FTD: frontotemporal dementia
FTLD: frontotemporal lobar degeneration
FUS: fused in sarcoma
FVC: forced vital capacity
GDNF: glial cell-derived neurotrophic factor
GEP: gene expression profiling
GLT1: Glial glutamate transporter 1
GS: Grip strength
GS/BW: the ratio of grip strength and body weight
GTPase: a hydrolase enzyme of guanosine triphosphate
GWAS: genome-wide association studies
HC: healthy controls
HHD: handheld dynamometry
Hib: *Haemophilus influenza type b*
HRP: horseradish peroxidase
HSE: heat shock element
HSF1: heat shock transcription factor 1
Hsp: heat shock protein
HSR: heat shock response
IgG: immunoglobulin G
i.p.: intra-peritoneal
IQR: interquartile range
LMN: lower motor neuron
microRNA: small non-coding RNA molecule
MN: motor neuron
MND: motor neuron disease
MRC: UK Medical Research Council
MRI: magnetic resonance imaging

mRNA: messenger RNA
MRSI: magnetic resonance spectroscopy imaging
MS: multiple sclerosis
mSOD1: mutant SOD1
MU: motor unit
MUNE: motor unit number estimation
MUS: muscle ultrasonography
MW: molecular weight
NC: neurological disease controls
NCS: nerve conduction studies
Nfs: neurofilament proteins
NfL: neurofilament light chain subunit
NfM: neurofilament median chain subunit
NfH: neurofilament heavy chain subunit
NfH^{SMI34}: hyperphosphorylated NfH detected by using SMI-34R (Covance, USA) as primary antibody
NfH^{SMI35}: variably-phosphorylated NfH detected by using SMI-35R (Covance, USA) as primary antibody
NI: neurophysiological index
NMJ: neuromuscular junction
NOD: normalised optical density
OD: optical density
P-body: processing body
PBP: progressive bulbar palsy
PCR: polymerase chain reaction
PD: Parkinson's disease
PET: positron emission tomography
PFA: paraformaldehyde
PLS: primary lateral sclerosis
PLMN: pure lower motor neuron
PMA: progressive muscular atrophy
PNFA: progressive non-fluent aphasia
pNfH: phosphorylated Neurofilament heavy chain subunit
PRL: prolactin
PUMN: pure upper motor neuron
RNA: ribonucleic acid
RNP: RNA-binding protein

ROS: reactive oxygen species
RT: room temperature
sALS: sporadic ALS
SDS gel: sodium dodecyl sulphate polyacrylamide gel
SELDI: surface-enhanced laser desorption/ionization
S.E.M.: standard error of mean
SD: semantic dementia
SG: stress granules
S-MUP: single motor unit potential
SNP: single nucleotide polymorphism
SOD1: superoxide dismutase 1
TA: Tibialis Anterior muscle
TDP-43: Tar DNA-binding protein 43
TIF: translation initiation factor
TMB: 3, 3', 5, 5'-tetramethylbenzidine
TMS: transcranial magnetic stimulation
UMN: upper motor neuron
UPR: unfolded protein response
VEGF: vascular endothelial growth factor
WB: western blot
WT: wild-type
wtSOD1: wild-type SOD1

Chapter 1

General Introduction

In this Thesis, I undertook a series of experiments aimed at developing a plasma-based biomarker of disease progression in the neurodegenerative disease Amyotrophic Lateral Sclerosis (ALS).

In this Introduction, I will first review the recent advances in our understanding of the genetics and molecular pathomechanisms involved in ALS. In addition, I will review the recent progress in clinical trials and discuss possible solutions to improve the design of clinical trials in ALS. An overview of the current status of biomarker development in ALS is also presented.

1.1 Amyotrophic Lateral Sclerosis

Amyotrophic Lateral Sclerosis (ALS) is an adult-onset, fatal neurodegenerative disorder, characterised by the selective degeneration of motor neurons in the spinal cord, brainstem and motor cortex, resulting in muscle paralysis and death, usually within 3-5 years of symptom onset. At present, there is no specific diagnostic test or biomarker for ALS, and the diagnosis relies on the fulfilment of clinical criteria defined by the main clinical manifestations of each disease stage (Brooks et al., 2000). This lack of diagnostic aids results in a typical gap of 9-15 months between symptom onset and diagnosis, a delay that not only reduces the patient's chance of maximising benefit from Riluzole, the only therapeutic agent currently available for ALS, but also hinders the early recruitment of ALS patients into clinical trials, thereby reducing the likelihood of success (Cellura et al., 2012; Chio et al., 2009; Iwasaki et al., 2002). Despite extensive efforts to develop effective treatments, Riluzole remains to date the only FDA-approved drug for ALS. This drug prolongs survival in ALS patients by 3 months after 18-month treatment (Miller et al., 2007). Other supportive treatments deal with the consequences of disease progression, such as immobility, malnutrition and respiratory failure (Kiernan et al., 2011; Miller et al., 2007).

The mean incidence of ALS is approximately 1.7-3.0 cases per 100,000 per year, and men have a slightly higher incidence than women (1.2-1.5:1). The age of clinical onset of ALS is highly variable: peak age at onset is 58-63 years for sporadic ALS (sALS) and 47-52 for familial ALS (fALS). The incidence of ALS decreases after 80 years of age. The prevalence of ALS is around 6 per 100,000 per year, and the life time risk for ALS is 1:400 in women

and 1:350 in men in the European population (Beghi et al., 2006; Hardiman et al., 2011; Johnston et al., 2006; Logroscino et al., 2010).

1.1.1 Clinical phenotypes of ALS

The clinical presentation of ALS is the presence of upper motor neuron (UMN) and lower motor neuron (LMN) signs, resulting from motor neuron (MN) degeneration in the motor cortex, brainstem and spinal cord. Patients can present with bulbar onset (25%), limb onset (70%) or trunk/respiratory onset (5%), followed by subsequent spreading to the adjacent regions (Vucic et al., 2007). UMN involvement in the limbs leads to spasticity, muscle weakness, brisk deep tendon reflexes, while UMN involvement in the bulbar region causes spastic dysarthria, brisk gag and jaw jerk. LMN involvement in the limbs features muscle weakness, wasting and fasciculation, whilst bulbar LMN dysfunction results in flaccid dysarthria, dysphagia, as well as weakness, wasting, and fasciculations in the tongue (Kiernan et al., 2011).

Thus, the phenotype of ALS is highly heterogeneous due to the varying involvement of spinal and bulbar UMNs and LMNs, site of onset, and rate of progression (Ravits and La Spada, 2009). In general, the main presentations of ALS can be sub-classified as i) limb-onset ALS with a combination of UMN and LMN signs in the limb, ii) bulbar-onset ALS, with speech and swallowing difficulties first and followed by later limb involvement; iii) the less common pure UMN involvement of primary lateral sclerosis (PLS), and iv) the pure LMN involvement of progressive muscular atrophy (PMA) (Kiernan et al., 2011).

According to a recent study, the ALS phenotypes reported in the literature can be further sub-classified into 8 sub-groups, with distinct epidemiological and clinical characteristics (Chio et al., 2011a). These phenotypes were determined from 1132 ALS patients, and are defined as follows:

i) Classic (Charcot's) phenotype: onset of symptoms in the upper or lower limbs, with clear but not predominant pyramidal signs;

ii) Bulbar phenotype: a bulbar onset with dysarthria and/or dysphagia, tongue wasting and fasciculation for the first 6 months, followed by limb involvement later on;

iii) Flail arm phenotype: progressive, predominantly proximal, weakness and wasting in the upper limbs, may or may not present with pathological deep tendon reflexes or Hoffman sign

in the upper limbs. Functional involvement had to be confined to the flail limbs for at least 12 months after symptom onset;

iv) Flail leg phenotype: progressive distal onset of weakness and wasting in the lower limbs, with or without pathological deep tendon reflexes or Babinski sign. However, symptoms/signs beginning proximally in the legs without distal involvement at presentation were classified as classic ALS;

v) Pyramidal phenotype (UMN predominant ALS): dominant pyramidal signs of severe spastic para/tetraparesis, associated with Babinski or Hoffmann sign, hyperactive reflexes, clonic jaw jerk, dysarthric speech and pseudobulbar signs, are accompanied by clear cut features of LMN impairment from onset of the disease and by the presence of EMG findings of acute and chronic denervation in at least two different sites;

vi) Respiratory phenotype: predominant respiratory involvement at onset with orthopnoea or dyspnoea at rest or during exertion, accompanied by only mild spinal or bulbar signs in the first 6 months. UMN involvement is evident;

vii) Pure LMN (PLMN): clinical and electrophysiological evidence of progressive LMN signs. Clinical UMN signs are excluded;

viii) Pure UMN (PUMN): pure UMN involvement. Patients with clinical and electrophysiological involvement of LMN signs are excluded.

The epidemiological and clinical characteristics of these sub-groups are summarised in Table 1.1. Classic and bulbar phenotypes are the most common sub-groups and have similar annual incident rates. Men are predominant in classic, flail arm, respiratory, PLMN phenotypes. Age at onset is significantly lower in pyramidal, PLMN and PUMN phenotypes, while bulbar phenotype has the highest age at onset. In addition, the better outcome in tracheostomy-free survival are found in PLMN, pyramidal, PUMN, and flail arm phenotypes, whist the bulbar phenotype has the worst outcome. Factors influencing outcomes include age at onset, certain phenotypes and co-morbidity of frontotemporal dementia (FTD) (Chio et al., 2011a).This sub-classification might render in full the clinical heterogeneity of ALS, which may be relevant to the underlying pathogenesis of ALS and of use in the design of clinical trials.

Table 1.1. Summary of epidemiological and clinical characteristics of ALS phenotypes.

Phenotype	No of cases (%)	Annual incidence rate Mean	Men to women incidence rate ratio	Age at onset (years) Mean (SD)* Median (IQR)‡	Diagnostic latency (months) Mean (SD)* Median (IQR)‡	Cases with FTD (%)†
Classic	404 (30.3)	0.94	1.65:1	62.8 (11.3) 64.6 (56.1, 70.6)	10.9 (9.6) 8 (5,13)	16 (4.0)
Bulbar	456 (34.2)	1.05	0.98:1	68.8 (9.7) 69.9 (62.9, 75.0)	9.8 (7.0) 8 (5,12)	41 (9.0)
Flail arm	74 (5.5)	0.17	4:1	62.6 (11.8) 63.3 (54.8, 72.2)	12.8 (11.0) 9 (5, 15)	1 (1.4)
Flail leg	173 (13.0)	0.40	1.03:1	65.0 (9.6) 65.6 (58.5, 71.2)	13.1 (10.1) 11 (7, 17)	7 (4.1)
Pyramidal	120 (9.1)	0.28	1.04:1	58.3 (13.5) 60.1 (49.2, 68.3)	15.9 (13.4) 12 (6, 22)	3 (2.5)
Respiratory	14 (1.1)	0.03	6:1	62.2 (8.6) 62.0 (58.3, 65.3)	6.4 (4.3) 5 (3, 9)	-
PUMN	38 (2.9)	0.08	2.04:1	56.2 (11.3) 55.2 (45.7, 61.3)	15.5 (12.4) 14 (10, 19)	-
PLMN	53 (4.0)	0.12	0.98:1	58.9 (10.9) 56.5 (48.3, 62.6)	15.9 (14.3) 15 (10, 19)	2 (3.8)
Overall ALS	1322	3.07	1.29:1	64.3 (11.3) 65.3 (59.7, 71.8)	10.8 (10.4) 9 (5,14)	70 (5.4)

Adapted from Chio et al., 2011

* sd: Standard deviation, ANOVA test, p=0.0001

‡ IQR: Interquartile range

† chi-Squared test, p=0.0001

1.1.2 Cognitive involvement in ALS

Cognitive changes in ALS were not described in Charcot's original description of ALS and cognition was regarded to be largely spared in ALS until recent years following the development of consensus on clinical diagnostic criteria of frontotemporal lobar degeneration (FTLD) (Neary et al., 1998) and the findings of the connection between ALS and FTLD (Achi and Rudnicki, 2012; Neary et al., 2000).

1.1.2.1 Frontotemporal lobar degeneration (FTLD)

FTLD is defined by focal neurodegeneration in the frontal and anterior temporal lobes of the brain and is one of the leading causes of dementia, particularly in patients before 65 years of age. The incidence rate of FTLD is 3.5-4.1 per 100,000 population and its prevalence rate is 10-20 per 100,000 population among the population aged between 45-65 years of age (Van Langenhove et al., 2012). The median disease duration of FTLD is 6-8 years (Hodges et al., 2003). According to its clinical manifestations, FTLD can be divided into three sub-types, which can gradually overlap as disease progresses (Kertesz et al., 2005; Van Langenhove et al., 2012). The three sub-types of FTLD are:

i) Behavioural variant FTLD (bvFTD): the most frequently diagnosed variant, with predominant prefrontal neurodegeneration. Patients present with marked changes in behaviour and personality;

ii) Progressive non-fluent aphasia (PNFA): predominant left perisylvian atrophy. Patients present with loss of motor speech fluency and agrammatism, but language comprehension is relatively preserved;

iii) Semantic dementia (SD): pathology is mainly in the anterior temporal lobes. Patients develop progressive comprehension deficits and naming errors in speech.

1.1.2.2 The clinical spectrum of ALS and FTLD

The association between dementia or psychiatric disturbances and ALS has become increasingly important during the last decade (Bak and Hodges, 2001). It is now known that of the total population of ALS patients, 15-18% also have FTLD with TAR deoxyribonucleic acid (DNA)-binding protein 43 (TDP-43)-positive inclusions in cortical neurons (Lomen-Hoerth et al., 2003; Mackenzie et al., 2007; Ringholz et al., 2005), and at least 50% have evidence for more subtle cognitive and/or behavioural dysfunction (Ringholz et al., 2005). FTD symptoms in ALS patients are usually those of bvFTD (Lillo et al., 2010), and typically

precede the onset of ALS (Hu et al., 2009). On the other hand, of patients with FTLD, 15% have ALS and many more have only some lower motor neuron involvement (Burrell et al., 2011; Lomen-Hoerth et al., 2002). Patients with ALS-FTD typically have onset of symptoms in their 50's, which, in most cases, present first with cognitive changes. The interval between cognitive symptoms and weakness varies, with a mean of 2 years (Lillo et al., 2010), and bulbar onset is found more often than in pure ALS patients in some studies (Bak and Hodges, 2004; Lillo et al., 2010). Survival in patients with ALS-FTLD is worse than those with ALS alone or FTLD alone, particularly in those with dysexecutive function (Elamin et al., 2011; Lillo et al., 2010). These findings suggest that ALS and FTLD are at two ends of a clinical continuum. Table 1.2 summarises the diagnostic categories of the FTLD-ALS disease spectrum. It is now known that genetics and underlying molecular mechanism may explain the relationship between ALS and FTLD (Van Langenhove et al., 2012). Figure 1.1 shows the molecular relationships between ALS and FTLD.

1.1.3 Cognitive and clinical characteristics in ALS patients with the chromosome 9 open reading frame 72 gene *(C9orf72)* expansion

The hexanucleotide repeat expansion in the *C9orf72* gene accounts for a significant proportion of fALS (34.2%), sALS (5.9%), familial FTLD (25.9%) and sporadic FTLD (5.1%) and is currently the major genetic cause of ALS and/or FTLD (Cooper-Knock et al., 2012a; DeJesus-Hernandez et al., 2011; Majounie et al., 2012; Renton et al., 2011; van Blitterswijk et al., 2012). Although the function of *C9orf72* remains to be established, it appears that ALS patients carrying this repeat expansion present a recognisable phenotype among the ALS population (Byrne et al., 2012). ALS patients with the *C9orf72* repeat expansion have an earlier onset, more co-morbid FTLD and a shorter survival, compared to those without the expansion (Byrne et al., 2012; Cooper-Knock et al., 2012a).

1.2 Genetics of Amyotrophic Lateral Sclerosis

Although the majority of ALS cases are sporadic ALS (sALS), approximately 10% of cases are familial (fALS) with a Mendelian pattern of inheritance. fALS cases are clinically indistinguishable from and share similar pathological features with sALS cases. Identifying causative fALS genes offers a direct approach to investigate the underlying pathomechanisms of ALS and thus may help identifying therapeutic targets. However, there is also growing evidence that sALS may also have a genetic basis. Although the genetic effect in sALS might be smaller than those in fALS, such so called 'susceptibility' genes, together with possible environmental factors may predispose the development of sALS (Sreedharan and Shaw, 2009).

Table 1.2. Diagnostic categories of FTLD-ALS disease spectrum.

Disease	Subtypes	Main clinical characteristics
FTLD	bvFTD	Disinhibition, apathy, lack of emotional concern, hyperorality, stereotypic behaviour and executive dysfunction
	PNFA	Laboured speech, agrammatism with relatively spared comprehension
	SD	Comprehension deficits, naming errors with fluent speech
FTLD-MND		FTLD with minor motor system dysfunction
ALS-FTLD		FTLD and ALS
ALSci		ALS with minor cognitive impairment
ALSbi		ALS with minor behavioural impairment
ALS		Pure ALS motor symptoms

Adapted from van Langenhove et al., 2012.

Abbreviations: ALSbi: ALS with a mild behavioural impairment; ALSci: ALS with a mild cognitive impairment; bvFTD: behavioural variant FTLD; PNFA: progressive non-fluent aphasia; SD: semantic dementia; MND: Motor neuron disease.

Figure 1.1

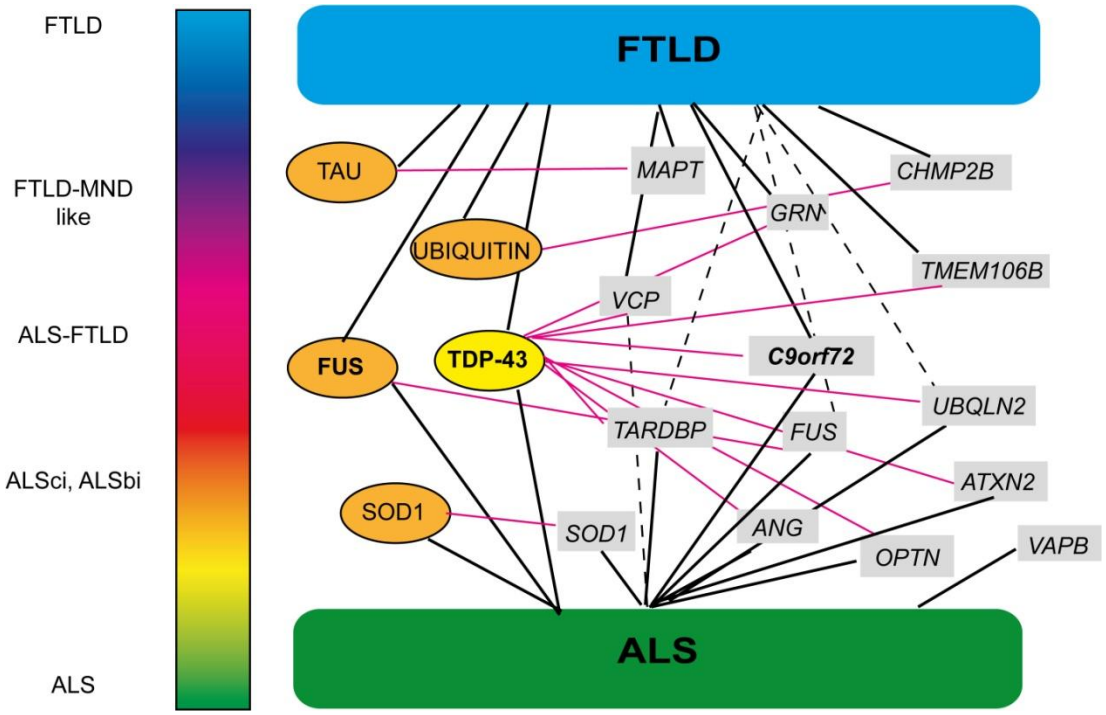

Figure 1.1. Clinical disease continuum and molecular relationships between FTLD and ALS. Pure FTLD and pure ALS are the two ends of a clinical disease continuum. Patients who present clinical features of both disorders are classified as ALS-FTLD. ALS patients showing some cognitive or behavioural changes but not meeting the criteria for FTLD are classified as ALSci (ALS with cognitive impairment) or ALSbi (ALS with behaviour impairment). FTLD patients who show minor motor neuron involvement without developing ALS are classified as FTLD-MND like. Pathological proteins involved in ALS and FTLD are shown in ovals, while causal genes are shown in rectangles. Black solid and dashed between diseases and pathological proteins/genes indicate strong and putative correlations, respectively. Pink solid lines show the correlations between genes and pathological proteins. **Adapted from van Langenhove et al., 2012.**

1.2.1 Causative genes for ALS

To date, at least 20 genes and chromosomal loci have been associated with fALS (Al-Chalabi et al., 2012; Andersen and Al-Chalabi, 2011; Beleza-Meireles and Al-Chalabi, 2009; Ferraiuolo et al., 2011), and these genes are summarised in Table 1.3.

Mutations in the superoxide dismutase 1 *(SOD1)* gene account for 20% of fALS cases (Rosen et al., 1993), and can be found in approximate 2-7 % sALS cases (Ticozzi et al., 2011). To date, over 165 different genetic mutations spanning the entire *SOD1* gene have been discovered (http://alsod.iop.kcl.ac.uk/Als/index.aspx). Transgenic mice carrying a mutant human *SOD1* gene develop motor dysfunction, muscle wasting and death, reflecting the symptoms of human ALS, and have contributed enormously to our understanding of the underlying pathophysiology of ALS and as the test bed of preclinical drug trials (Gurney et al., 1994).

Furthermore, recent genetic discoveries have identified a number of new important ALS-causing genes, including genes involved in **protein quality control** *(UBQLN2, VCP)*, **endosomal trafficking** and **cell signalling** *(ALS2, VAPB, FIG4, OPTN)*, **cytoskeletal function** *(MAPT, PFN1)* and **glutamate excitotoxicity** *(DAO).* However, the most significant mutations have been identified in genes that code for proteins involved in **RNA** (ribonucleic acid) **processing,** specifically *TARDBP, FUS, SETX, ANG, HNRNPA1 and C9orf72*, as shown in Table 1.3. The identification of these new ALS-causing genes has widened our understanding of the underlying molecular pathophysiology in ALS.

Mutations in the Tar DNA-binding protein 43 (*TARDBP*) and in the Fused in Sarcoma (*FUS*) genes (Neumann et al., 2009; Neumann et al., 2006), which have been identified in both sALS and fALS patients, account for 5% and 4% of the fALS cases respectively. Moreover, a hexanucleotide repeat expansion in the *C9orf72* gene has recently been identified in more than half of fALS cases in a Finnish cohort and may indeed account for more than 30-40% of all fALS cases in the USA and North England and for about 10% of the overall sporadic ALS population (Cooper-Knock et al., 2012a; DeJesus-Hernandez et al., 2011; Renton et al., 2011). These most recent genetic discoveries have also revealed important links between ALS and other neurodegenerative diseases, in particular FTLD, as well as important clues regarding the pathomechanisms of disease, which can be used in developing novel therapeutic targets (Andersen and Al-Chalabi, 2011).

Table 1.3. Genes associated with familial ALS.

Genetic subtype (Estimated % of fALS)	Gene locus	Gene	Inheritance/ Onset	Phenotypic MND variants	Other features	Reference
Oxidative Stress						
ALS1 (20%)	21q22	Superoxide dismutase 1 (*SOD1*)	AD/Adult	ALS, PMA, PBP (rare) BFA (rare)	Cognitive impairment, Autonomic dysfunction, FTD (rare); Cerebellar ataxia	(Rosen et al., 1993)
Endosomal trafficking and cell signalling						
ALS2 (<1%)	2q33.2	Alsin (*ALS2*)	AR/Juvenile	Juvenile PLS, juvenile ALS or infantile HSP	Unknown	(Hadano et al., 2001; Yang et al., 2001)
ALS8 (<1%)	20q13.3	Vesicle-associated membrane protein-associated protein B (*VAPB*)	AD/Adult	ALS, PBP, or PMA	Motor neuropathy	(Chen et al., 2010; Nishimura et al., 2004)
ALS11	6q21	Polyphosphoinositide phosphatase (*FIG4*)	AD/Adult	ALS, PLS, HSP	CMT4J‡, Cognitive impairment	(Chow et al., 2009)
ALS12 (<1%)	10p13	Optineurin *(OPTN)*	AD and AR /Adult	ALS-FTD	POAG‡, FTD	(Maruyama et al., 2010)
RNA binding and/or processing dysfunctions						
ALS4	9q34	Senataxin (*SETX*)	AD/Juvenile	ALS	AOA2, cerebellar ataxia, motor neuropathy	(Chen et al., 2004)
ALS6 (1-5%)	16p11.2	Fused in sarcoma (*FUS*)	AD/Adult	ALS, ALS-FTD	Parkinsonism, FTD	(Kwiatkowski et al., 2009; Vance et al., 2009)
ALS9 (<1%)	14q11.2	Angiogenin (*ANG*)	AD/Adult	ALS, PBP or ALS-FTD	Parkinsonism	(Greenway et al., 2006; van Es et al., 2009)
ALS10 (1-5%)	1p36.2	Tar DNA-binding protein (*TARDBP*)	AD/Adult	ALS, ALS-FTD	PSP, PD, FTD, Chorea	(Kabashi et al., 2008; Sreedharan et al., 2008)
ALS-FTD (40-50%)	9p21.2	Chromosome 9 open reading frame 72 *(C9orf72)*	AD/Adult	ALS, ALS-FTD, ALS-Parkinsonism	FTD, Psychosis, Parkinsonism	(DeJesus-Hernandez et al., 2011; Morita et al., 2006; Renton et al., 2011; Vance et al., 2006; Williams et al., 2013)
ND	12q13.13	Heterogeneous nuclear ribonucleoprotein A1 (*HNRNP A1*)	AD/NA	ALS	IBM‡	(Kim et al., 2013)
Ubiquitin/protein degradation						
ND (<1%)	9p13-p12	Valosin-containing protein (*VCP*)	AD/Adult	ALS, ALS-FTD	IBMPFD‡, Dementia, FTD	(Johnson et al., 2010)
ALSX (<1%)	Xp11	Ubiquilin 2 (*UBQLN2*)	X-linked/ Adult and Juvenile	ALS, ALS/dementia	Dementia, FTD	(Deng et al., 2011)
Cytoskeleton						

ALS-dementia-PD	17q21	Microtubule-associated protein tau *(MAPT)*	AD/Adult	ALS-FTD	FTD; PSP, PD, CBD	(Hutton et al., 1998)
ND	17p13.2	Profilin 1 (*PFN1*)	AD/Adult	ALS	NA	(Wu et al., 2012)
Glutamate excitotoxicity						
ND (<1%)	12q24	D-amino acid oxidase (*DAO*)	AD/Adult	ALS	NA	(Mitchell et al., 2010)
Other genes						
ALS5	15q15-q21	Spatacsin (*SPG11*)	AR/Juvenile	Juvenile ALS	NA	(Orlacchio et al., 2010)
ALS-FTD	9p13.3	Ơ Non-opioid receptor 1 (*SIGMAR 1*)	AD/Adult AR/Juvenile	ALS, ALS-FTD	FTD	(Al-Saif et al., 2011; Luty et al., 2010)
Unknown genes						
ALS3	18q21	Unknown	AD/Adult	ALS	NA	(Hand et al., 2002)
ALS7	20ptel-p13	Unknown	AD/Adult	ALS	NA	(Sapp et al., 2003)

Adapted from Andersen and Al-Chalabi, 2011 and Ferraiuolo et al., 2011.

‡Clinical features reported in non-ALS patients with mutations not associated with ALS.

Abbreviations: AD: autosomal dominant; ALS, amyotrophic lateral sclerosis; AOA2, ataxia with oculomotor apraxia type 2; AR: autosomal recessive; BFA, benign focal amyotrophy; CMT4J: Charcot-Marie-Tooth disease type 4J; FTD, frontotemporal dementia; HSP, hereditary spastic paraparesis; IBM, inclusion body myopathy; IBMPFD, Inclusion body myopathy with Paget disease and frontotemporal dementia; MND, motor neuron disease; NA, information not available; ND: not defined; PBP, progressive bulbar palsy; PD, Parkinson's disease; PLS, primary lateral sclerosis; PMA, progressive muscular atrophy; POAG, Primary open-angle Glaucoma; PSP, progressive supranuclear palsy.

1.2.2 Susceptibility and modifier genes

The search for susceptibility and modifier genes in sALS can be approached by a number of experimental approaches:

i) Candidate gene-based approaches: Targets are chosen according to the molecular mechanisms identified through known causative genes in fALS such as cytoskeletal structure [neurofilament heavy chain subunit *(NEFH)*, dynactin *(DCTN1)*], hypoxia and oxidative stress [vascular endothelial growth factor *(VEGF)*, paraoxonase *(PON)*], motor neuron survival [survival motor neuron *(SMN)*, ciliary neurotrophic factor *(CNTF)*, leukaemia inhibitory factor *(LIF)*] and neurodegenerative disorders [hemochromatosis *(HFE)*, apolipoprotein E4 allele *(APOE4)*] (Valdmanis and Rouleau, 2008);

ii) Genome-wide association studies (GWAS): GWAS enables the identification of novel genes and pathways without any assumptions about the genomic nature or location of the casual variants (Sreedharan and Shaw, 2009). With large-scale GWAS, it has been possible to identify reliable single nucleotide polymorphism (SNPs) and copy number variants for sALS, which are then verified by replication in another cohort. This approach has identified five significant associations in sALS:

a) *FLJ10986*: an uncharacterised gene (Dunckley et al., 2007);
b) *ITPR2*: the inositol 1,4,5-triphosphate receptor 2 gene (van Es et al., 2007);
c) *DPP6*: dipeptidyl peptidase 6 gene (van Es et al., 2008);
d) *ELP3*: elongator protein 3 gene (Simpson et al., 2009);
e) *KIFAP3*: kinesin-associated protein 3 (Landers et al., 2009).

The effect of these identified variants still requires further investigation (Dupre and Valdmanis, 2009). However, some subsequent GWAS in smaller German *(FLJ10986 & ITPR2)*, Italian *(DPP6)*, French-Canadian *(DPP6 & FGGY)* and Chinese *(FLJ10986, ITPR2, DPP6 & KIFAP3)* cohorts failed to replicate the association found in large-scale surveys (Chen et al., 2012; Daoud et al., 2010; Fernandez-Santiago et al., 2011; Fogh et al., 2011), whilst others confirmed the initial findings in *KIFAP3* (Orsetti et al., 2011). These results suggest that a geography/population-specific effect may be present in these variants.

Table 1.4 summarises the susceptibility and modifier genes for ALS identified through candidate gene-based approaches and large-scale GWAS approach.

1.3 Disease pathomechanisms in ALS

ALS is a complex disease involving dysfunction of several cellular pathways in both motor neurons as well as neighbouring glial cells (Ferraiuolo et al., 2011). Several of the main molecular pathways that have been proposed to be affected in ALS include: i) Oxidative stress; ii) Mitochondrial dysfunction; iii) Excitotoxicity; iv) Endoplasmic reticulum (ER) stress; v) Protein aggregation; vi) Dysregulation of endosomal trafficking; vii) Aberrant axonal transport; viii) Dysregulated transcription and RNA processing; ix) Neuroinflammation and non-cell-autonomous processes. These pathways are summarised in Fig. 1.2.

1.3.1 New insights into the pathogenesis of ALS

Several recent breakthroughs in our understanding of the genetic and molecular pathology of ALS have led to important changes in our understanding of ALS pathomechanisms.

1.3.1.1 A failure of proteostasis: new findings about this long-known mechanism

Intracellular aggregates of mutant protein are established pathological hallmarks of a number of neurodegenerative disorders including ALS. Increased oxidative stress, excitotoxicity, mitochondrial dysfunction, neuroinflammation, and aberrant RNA metabolism all contribute to aberrant protein folding, facilitating the formation of aggregates, which can further cause downstream subcellular dysfunctions (Ferraiuolo et al., 2011). Hence, an effective protein quality control is an important cellular defence system to prevent toxic protein aggregation due to cellular stress. Figure 1.3 shows four main protein quality control machineries present in cells, which are protein refolding, proteasomal degradation, autophagy and ER unfolded protein response.

1.3.1.1.1 Both mutant SOD1 and oxidised wild-type SOD1 misfold and result in increased cellular stress

SOD1, a ubiquitous cytoplasmic and mitochondrial antioxidant enzyme, catalyses the harmful reactive oxygen species (ROS) products, hence prevents oxidative

Table 1.4 Summary of susceptibility and modifier genes in ALS.

Genes	Identified in patients group	Nature of variation	Function	Effect of variation	References
GWAS					
FLJ10986	sporadic	SNP*	unknown	unknown	(Dunckley et al., 2007)
ITPR2	sporadic	SNP	Glutamate-mediated neurotransmission, Intracellular Ca^{2+} homeostasis, Apoptosis.	unknown	(van Es et al., 2007)
DPP6	sporadic	SNP	Neuropeptide homeostasis, Modulation of voltage-gated K^{+} channels	unknown	(van Es et al., 2008)
ELP3	sporadic	SNP	RNA processing, Gene expression, Neuroprotection.	unknown	(Simpson et al., 2009)
KIFAP3	sporadic	SNP	Kinesin motor subunit	Reduced expression; longer survival	(Landers et al., 2009)
Candidate gene-based studies					
NEFH	Sporadic /familial	KSP in/del**	Cytoplasmic type II intermediate filament	Accumulation	(Al-Chalabi et al., 1999; Figlewicz et al., 1994)
PRPH	Familial /sporadic	SNP, In/del	Type III intermediate filament	Accumulation, Disruption of Neurofilament assembly	(Corrado et al., 2011; Gros-Louis et al., 2004; Leung et al., 2004)
VEGF	sporadic	SNP in promotor	Mitogen involved in angiogenic activity	Reduced expression	(Lambrechts et al., 2003)
PON1	sporadic	SNP	Anti-oxidant and detoxifying properties	Reduced activity	(Slowik et al., 2006)
SMN	sporadic	Copy number	mRNA metabolism, neuronal development and synapse formation	unknown	(Corcia et al., 2002)
CNTF	familial	Null mutation	Neurotrophic factor	inactive	(Giess et al., 2002)
LIF	sporadic	SNP	Neurotrophic factor	unknown	(Giess et al., 2000)
HFE	sporadic	SNP	Cellular iron regulation	Decreased expression of Cu/Zn-SOD1, α-tubulin and β-actin; Disruption of axonal transport	(Wang et al., 2004)
APOE	sporadic	Haplotype	Lipid metabolism	unknown	(Li et al., 2004; Zetterberg et al., 2008)

Adapted from Valdmanis and Rouleau 2008, Sreedharan and Shaw, 2004, Anderson and Al-Chalabi, 2011.

Abbreviations: * SNP, single nucleotide polymorphism; **KSP in/del, lysine-serine-proline insertion/deletion

Figure 1.2

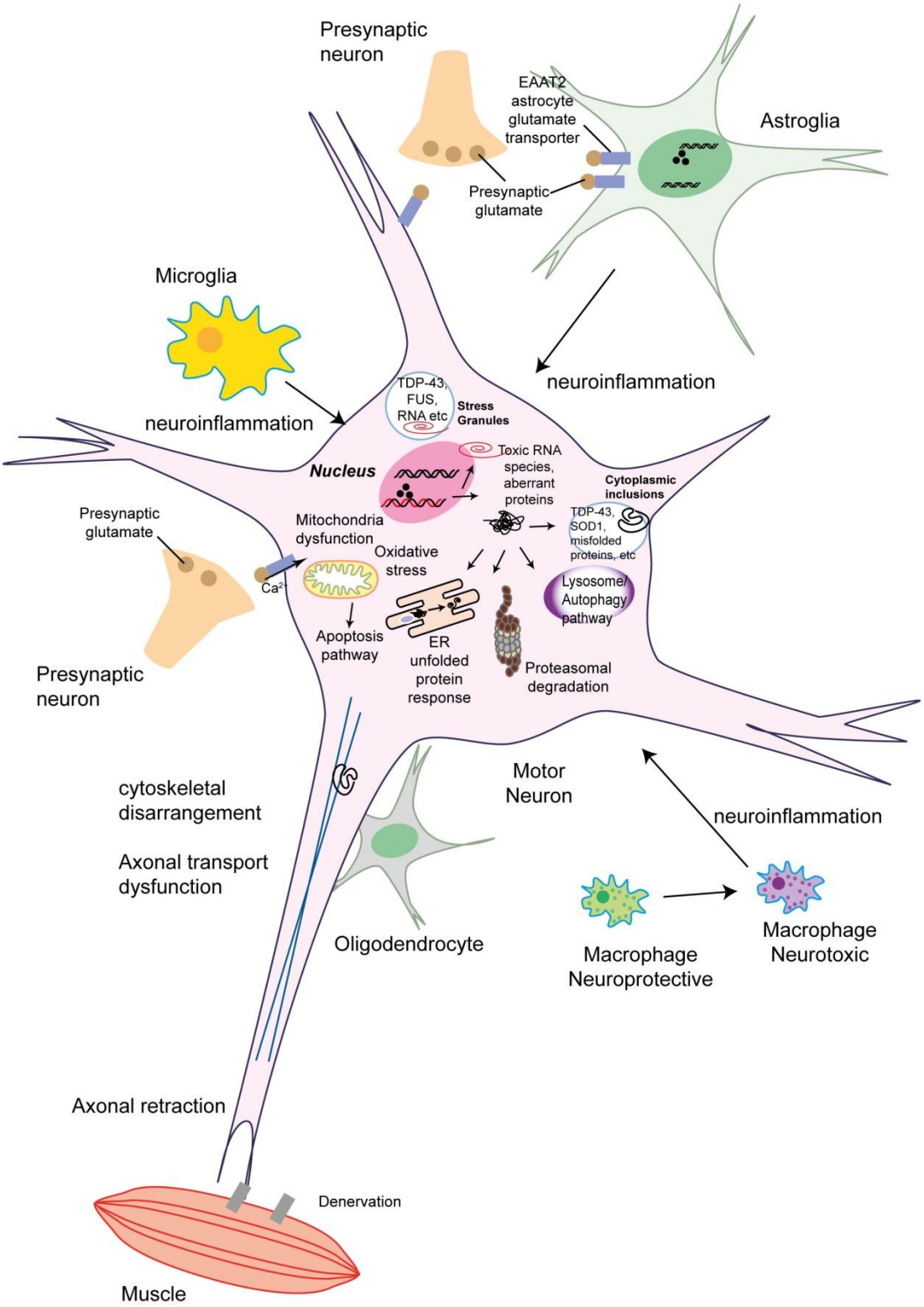
Presynaptic neuron
EAAT2 astrocyte glutamate transporter
Astroglia
Presynaptic glutamate
Microglia
neuroinflammation
neuroinflammation
TDP-43, FUS, RNA etc
Stress Granules
Nucleus
Toxic RNA species, aberrant proteins
Cytoplasmic inclusions
TDP-43, SOD1, misfolded proteins, etc
Presynaptic glutamate
Mitochondria dysfunction
Oxidative stress
Ca2+
Lysosome/ Autophagy pathway
Apoptosis pathway
ER unfolded protein response
Proteasomal degradation
Presynaptic neuron
Motor Neuron
cytoskeletal disarrangement
Axonal transport dysfunction
neuroinflammation
Oligodendrocyte
Macrophage Neuroprotective
Macrophage Neurotoxic
Axonal retraction
Denervation
Muscle

Figure 1.2. Molecular pathogenesis of amyotrophic lateral sclerosis. ALS is a complex disease involving activation of several cellular pathways in motor neurons and surrounding neighbours. Up-regulated oxidative stress, aberrant RNA processing contribute to aberrant protein folding, resulting in aggregates which can lead to proteasome impairment, ER stress, activation of autophagy and apoptotic pathways. Mitochondrial dysfunction and dysregulation of calcium influx can also lead to apoptosis. The failure of axons, in cytoskeletal and in cargo transport, contributes to dying-back axonopathy, denervation and muscle atrophy. Astrocytes are involved in the expression of the glutamate reuptake transporter EAAT2 as well as the secretion of inflammatory mediators, while oligodendrocytes take part in the supply of lactate. Microglia activate a serious of inflammatory mediators and is a key player of neuroinflammation, which is associated with the function of T-cells. **Adapted from Robberecht and Philips, 2013 and Kalmar et al., 2013.**

Figure 1.3

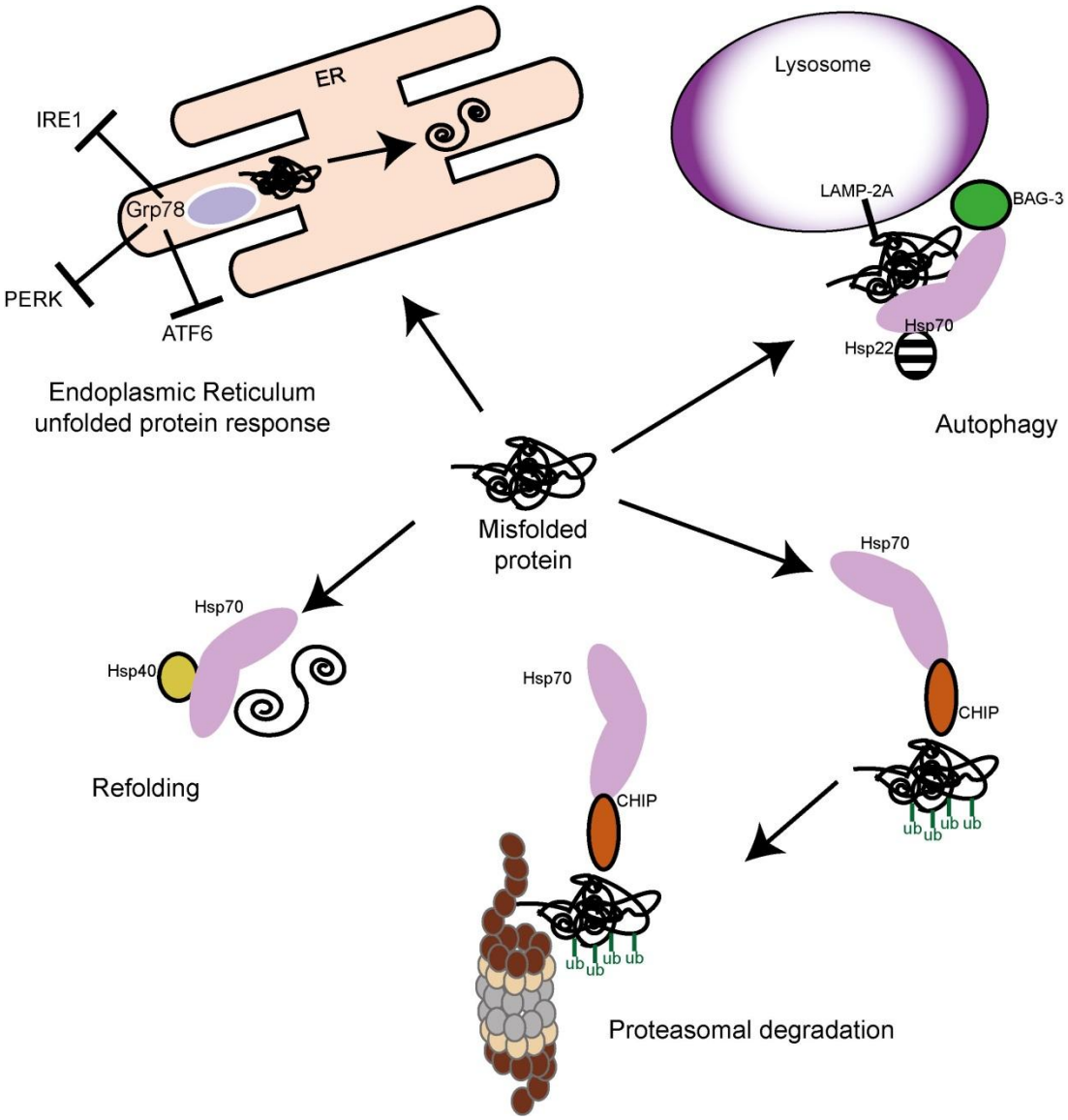

Figure 1.3. The protein quality control machinery. This Figure summarises schematically the protein quality control machineries and the chaperone-co-chaperone network. Hsp70 is a crucial component of all pathways, including refolding, proteasomal degradation, autophagy and ER unfolded protein response. **Abbreviations:** ATF6, Activating transcription factor 6; BAG-3, Bcl-2-associated athanogene 3; Grp78, 78 kDa glucose-regulated protein; IRE1, inositol-requiring enzyme 1; LAMP2A, Lysosome-associated membrane protein 2A; PERK, protein kinase RNA-like endoplasmic reticulum kinase. **Adapted from Kalmar et al., 2013.**

stress. Mutant SOD1 (mSOD1) not only reduces the cellular antioxidant capacity but is also detrimental to the proteasomal and autophagy protein degradation pathways. Escaping from protein degradation, mSOD1 accumulates and forms oligomers and, eventually, aggregates, which then increase cellular stress and activate the unfolded protein response (UPR) in the ER (Saxena et al., 2009). This can result in activation of ER-stress induced apoptosis. It is now known that these reactions occur not only in mSOD1-related fALS but also in non-mSOD1-related fALS and sALS, as oxidised wild-type SOD1 (wtSOD1) can acquire similar toxic properties to mSOD1 (Bosco et al., 2010b; Ezzi et al., 2007).

1.3.1.1.2 Impaired protein degradation

A failure of the protein degradation machinery in ALS has become more evident following the discovery of mutations in genes involved in proteostasis (Table 1.3 and 1.4), including:

i) Ubiquilin 2 *(UBQLN2):* delivers ubiquitylated proteins to the proteasomal pathway, and is found in skein-like inclusions in fALS, sALS, non-*UBQLN2*-related fALS, and FTLD (Deng et al., 2011);

ii) Valosin-containing protein *(VCP):* encodes a multifunctional ubiquitine-sensitive chaperone, which plays key roles in ER-, proteasomal- and autophagy-associated protein degradation (Johnson et al., 2010);

iii) Charged multivesicular body protein 2b *(CHMP2B)*: involved in the sorting of integral membrane proteins in multivesicular bodies and subsequent clearance in autophagy (Parkinson et al., 2006);

iv) Phosphatidylinositol 3,5-bisphosphate 5-phosphatase *(FIG4)*: located in vacuolar membrane and is essential for normal lysosome function (Chow et al., 2009).

Motor neurons have high metabolic activity and intrinsically high energy demands in order to maintain a baseline physiological function, which makes them more vulnerable to cellular stress (Bento-Abreu et al., 2010). However, motor neurons have an extremely high threshold for the activation of the heat shock response (HSR) (Batulan et al., 2003), the first line of defence to cellular stress, which renders motor

neurons less able to cope with cellular stress and to handle misfolded proteins, hence increases their vulnerability to cell death (Kalmar and Greensmith, 2008).

1.3.1.2 Dysregulated transcription and RNA processing

The identification of mutations in genes encoding proteins involved in RNA metabolism and regulation, including *TARDBP, FUS, TAF15, EWSR1, SMN, ANG, SETX,* and *C9orf72,* has provided new hypotheses to be tested to unravel ALS pathogenesis. There is now emerging evidence for dysregulated RNA processing in ALS, including, i) Transcriptional regulation (Ayala et al., 2008; Greenway et al., 2006; Kieran et al., 2008; Law et al., 2006; Polymenidou et al., 2011); ii) Alternative slicing (Bose et al., 2008; Polymenidou et al., 2011); iii) mRNA transport (Volkening et al., 2009); iv) microRNA processing (Campos-Melo et al., 2013); v) Nucleus-cytoplasm shuttling (Dormann et al., 2010; Lagier-Tourenne et al., 2010); vi) Stress granules (Dewey et al., 2012; Gal et al., 2011; McDonald et al., 2011).

1.3.1.2.1 Loss-of-function mechanism of TDP-43 and FUS

TDP-43 targets more than 6000 mRNAs, including a good number of long pre-mRNAs that are enriched in motor neurons. Upon the loss of TDP-43, the abundance of more than 600 mRNAs and the splicing of more than 900 mRNAs are changed (Polymenidou et al., 2011). Similarly, FUS binds more than 5500 genes, most of which are different from the targets of TDP-43, and the loss of FUS also affects the abundance of other mRNAs (Lagier-Tourenne et al., 2012). These findings suggest a loss-of-function mechanism of TDP-43 and FUS.

1.3.1.2.2 Gain-of-function toxicity of TDP-43 and FUS

TDP-43 is mainly a nuclear protein, but translocates from the nucleus to the cytoplasm in response to stress, where it is incorporated into stress granules (SGs). This process allows the cell to prioritise protein synthesis in response to the stressor, such as heat shock proteins (Lindquist, 1986), whilst, simultaneously, the on-going translated mRNAs are held-up and directed into SGs and processing bodies (P-bodies) (Li et al., 2013). P-bodies are also RNA-binding protein granules that serve key roles in mRNA homeostasis (Jain and Roy, 2013). P-bodies represent sites of mRNA degradation, translation repression, non-translating mRNAs, and RNA-binding proteins. P-bodies mediate mRNA decay, including nonsense-mediated decay and RNA interference by serving as sites of co-localization for RNA processing components such as the RNA decapping machinery (Parker and Sheth,

2007). However, the relationship between TDP-43 and P-bodies remains to be established.

Once the cellular stress is resolved, SGs disaggregate and allow TDP-43 to relocate back to nucleus and the RNA translation to be presumed or discarded (McDonald et al., 2011; Shorter, 2011). Figure 1.4 illustrates this proposed mechanism. Despite being a nuclear protein, FUS is also present in the cytoplasm and post-synaptic density via transportin-mediated nuclear import, which is perturbed in most of mutations in FUS (Dormann et al., 2010). Both TDP-43 and FUS contain a prion-like domain. This domain contains sequences which enable proteins to adopt a range of alternative structures, each capable of conformational self-replication. This is achieved through templating the conversion of other copies of the same protein in order to radically alter protein function (King et al., 2012). This prion-like domain is essential to form SGs and P-bodies and is prone to form aggregates, particularly in ALS-associated mutant forms (Johnson et al., 2009; Li et al., 2013). These insoluble mutant TDP-43 and FUS aggregates alter the SG dynamics even after the resolution of stress and result in persistent presence of SG that subsequently increase cellular stress due to aggregates at protein levels as well as prevention of the translation of mRNAs critical to cell survival and recovery, which consequently contribute to motor neuron vulnerability and death in a toxic 'gain-of-function' mechanism (Bosco et al., 2010a; Dormann et al., 2010; Johnson et al., 2009; Li et al., 2013; Liu-Yesucevitz et al., 2010)

1.3.1.3 A failure of axons

As observed in animal models and in ALS patients, muscle denervation and subsequent axonal retraction is one of the first pathological changes in ALS, which occurs prior to the death of motor neurons and the onset of symptoms (Fischer et al., 2004; Frey et al., 2000). The failure involves structural and functional disruption in axons. This deficit has been reaffirmed by recent genetic (Table 1.3 & 1.4) and molecular findings, including:

i) Structure proteins: NfH, Peripherin, Dynactin, Profilin1, Elongator complex protein 3 and Kinesin-associated protein 3. Mutations in genes encoding these proteins have been shown to be causative or susceptibility genes in ALS (Al-Chalabi et al., 1999; Figlewicz et al., 1994; Gros-Louis et al., 2004; Landers et al., 2009; Leung et al., 2004; Munch et al., 2004; Simpson et al., 2009; Wu et al., 2012);

Figure 1.4

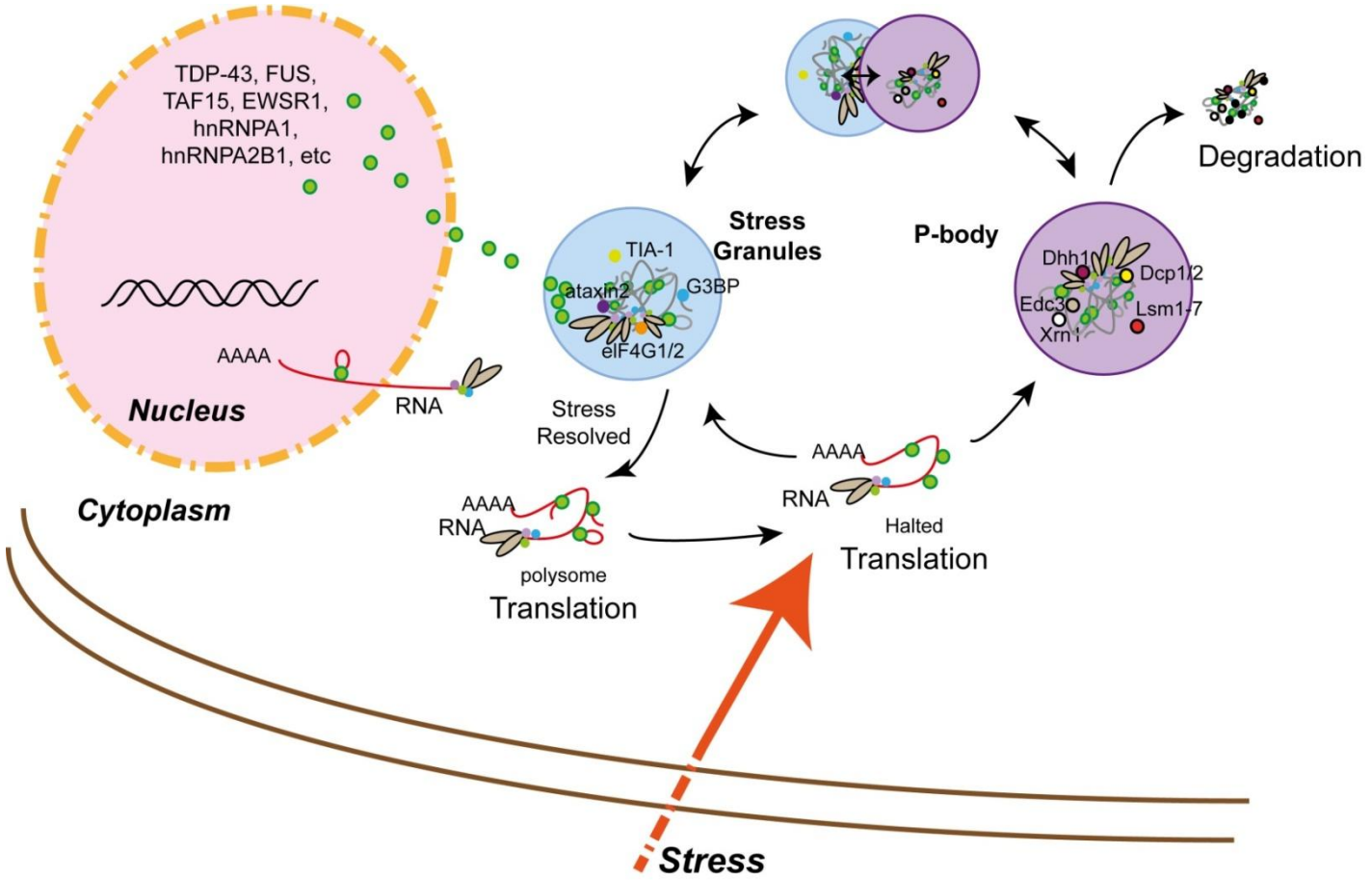
TDP-43, FUS,
TAF15, EWSR1,
hnRNPA1,
hnRNPA2B1, etc
AAAA
RNA
Nucleus
Cytoplasm
TIA-1
ataxin2
G3BP
eIF4G1/2
Stress
Granules
Stress
Resolved
AAAA
RNA
polysome
Translation
AAAA
RNA
Halted
Translation
P-body
Dhh1
Dcp1/2
Edc3
Lsm1-7
Xrn1
Degradation
Stress

Figure 1.4. Stress granules and P-bodies are sites of RNA triage. Upon cellular stress, one of the cellular stress responses is to halt the translation initiation, leading to the formation of stress granules (SG). SGs are cytoplasmic RNA-protein complexes that contain RNA-binding proteins (RNPs), mRNAs, and translation initiation factors (TIF). Once the stress exposure is resolved, the SGs disassemble and RNA translation resumes. Nontranslating mRNAs can be directed to Processing bodies (P-bodies), which are sites of halted translation and mRNA degradation. SGs and P-bodies are independently regulated, but can interact with each other. RNPs such as TDP-43, FUS, TAF15, EWSR1, hnRNPA1, hnRNPA2B1, are predominantly nuclear proteins that can be recruited to SGs upon cellular stress. **Adapted from Li et al., 2013.**
Abbreviations: Dcp1/2: mRNA-decapping enzyme 1/2, a decapping enzyme; Dhh1: DEAD box Helicase Homolog 1, a decapping activator; Edc3: Enhancer of mRNA decapping 3, a decapping activator; eIF4G1/2 Eukaryotic initiation factors 4G1/2, translation initiation factors and a scaffolding protein that interacts with eIF3; G3BP: GAP SH3 domain-binding protein, an hnRNA-binding protein and endoribonuclease. LSm1-7: like Sm (small) proteins 1-7, decapping activators; TIA1: T-Cell-Restricted Intracellular Antigen-1 Cytotoxic Granule-Associated RNA-Binding Protein, a 3'UTR mRNA binding protein; Xrn1: 5'-3' exoribonuclease 1.

ii) Axonal signalling: Vesicle-associated membrane protein-associated protein B/C (VAPB) and Alsin. VAPB normally interacts with ephrin A4, a receptor of the ephrin axonal repellent system via RHOA GTPase. Alsin also belongs to RHO-family GTPases (Linseman and Loucks, 2008; Nishimura et al., 2004; Tsuda et al., 2008; Yang et al., 2001);

iii) Neurite outgrowth inhibitor: Nogo-A is up-regulated in muscles of ALS patients and SOD1 mouse models. It is currently a therapeutic target in a clinical trial in ALS (Dupuis et al., 2002; Jokic et al., 2006; NCT01753076);

iv) Trophic factors: VEGF, a trophic factor for MNs and an axon guidance molecule. *VEGF* is a modifier gene in ALS, and either overexpressed or intracerebroventricularly administered of VEGF attenuates the phenotype in SOD1 rat model (Lambrechts et al., 2003; Storkebaum et al., 2005).

1.3.1.4 Neuroinflammation

A common characteristic of ALS and other neurodegenerative disorders is the neuroinflammatory reaction involving activated glial cells (astrocytes, microglia, and oligodentrocyte) and T cells (Philips and Robberecht, 2011).

Astrocytes provide trophic support for surrounding neurons, regulate extracellular neurotransmitter concentrations, such as glutamate, metabolic and ionic homoeostatic functions, repair and regulate immune response of CNS (Sofroniew and Vinters, 2010). Although astrocytes are not immune cells, upon activation they are able to recognise non-self and endogenous danger signals (via PRRs, the pattern-recognition receptors) and also secret soluble mediators, such as CXCL10, CCL2, Interleukin-6, and BAFF (B cell survival factor), which have an impact on both the innate and adaptive immune response (Farina et al., 2007). Selective knock-out of mSOD1 in astrocytes of SOD1 mice significantly slows disease progression (Yamanaka et al., 2008). Improved survival was observed in SOD1 rat model that have wild-type glial restricted precursor cells transplanted into cervical spinal cord, which later differentiated into wild-type astrocytes (Lepore et al., 2008). These findings suggest that regulating astrocyte function may be a therapeutic target for ALS.

Microglia, the resident macrophages in the nervous system, are the first line of defence against infection or injury to the nervous system. Upon activation, microglia

secrete, firstly, proinflammatory molecules to protect against the injuries, and, subsequently, anti-inflammatory molecules to repair (Hanisch and Kettenmann, 2007), events which are influenced by the subsets of surrounding astrocytes and inflammatory T-cell (Henkel et al., 2009). Microglia can therefore be induced to be detrimental M1 microglia or beneficial M2 microglia. Their contribution to motor neuron degeneration is T-cell dependent (Appel et al., 2010). In $SOD1^{G93A}$ mice, $CD4^{+}$ T helper cells can modulate the inflammatory response through down-regulation of the neurotoxic reaction of microglia and astrocytes (Beers et al., 2008; Chiu et al., 2008). Regulatory T-cells (Tregs) infiltrating the spinal cord are beneficial during early disease stages in $SOD1^{G93A}$ mice (Beers et al., 2011). Tregs are correlated with disease progression in ALS patients: i) reduction in numbers of Tregs in the blood are found in rapidly progressing ALS patients (Beers et al., 2011), and ii) early reduction in the expression of FOXP3 (forkhead box P3), the transcription factor for the development and function of Tregs, is predictive of rapid disease progression (Henkel et al., 2013).

Recent evidence has also revealed that oligodendrocytes and their progenitor cells NG2 cells, play a crucial part in axonal maintenance by providing neurons with lactate through the monocarboxylate lactate transporter MCT1; loss of MCT1 is toxic to MNs both *in vitro* and *in vivo* (Lee et al., 2012). However, the roles of oligodendrocytes in neuroinflammation are not yet well understood.

1.4 ALS Therapeutics

One of the most important steps forward in our understanding of the pathogenesis of ALS in the last two decades was the identification of the first mutations in the *SOD1* gene, which was rapidly followed by the discovery of other causal genetic mutations (Table 1.3). This important development led to the generation of transgenic mouse models engineered with human mutated genes, which have functioned as test beds for preclinical testing of potential therapeutic agents targeting underlying pathomechanisms in ALS. Figure 1.5 summarises the main molecular pathways which have been targeted by different compounds tested in recent clinical trials in ALS. Table 1.5 summarises novel therapeutic targets recently or currently under studies in clinical trials in ALS patients (Zinman and Cudkowicz, 2011). It is clear that quite a large number of Phase III clinical trials have failed despite the promising pre-clinical and Phase I/II results, including studies involving Gabapentin,

Figure 1.5

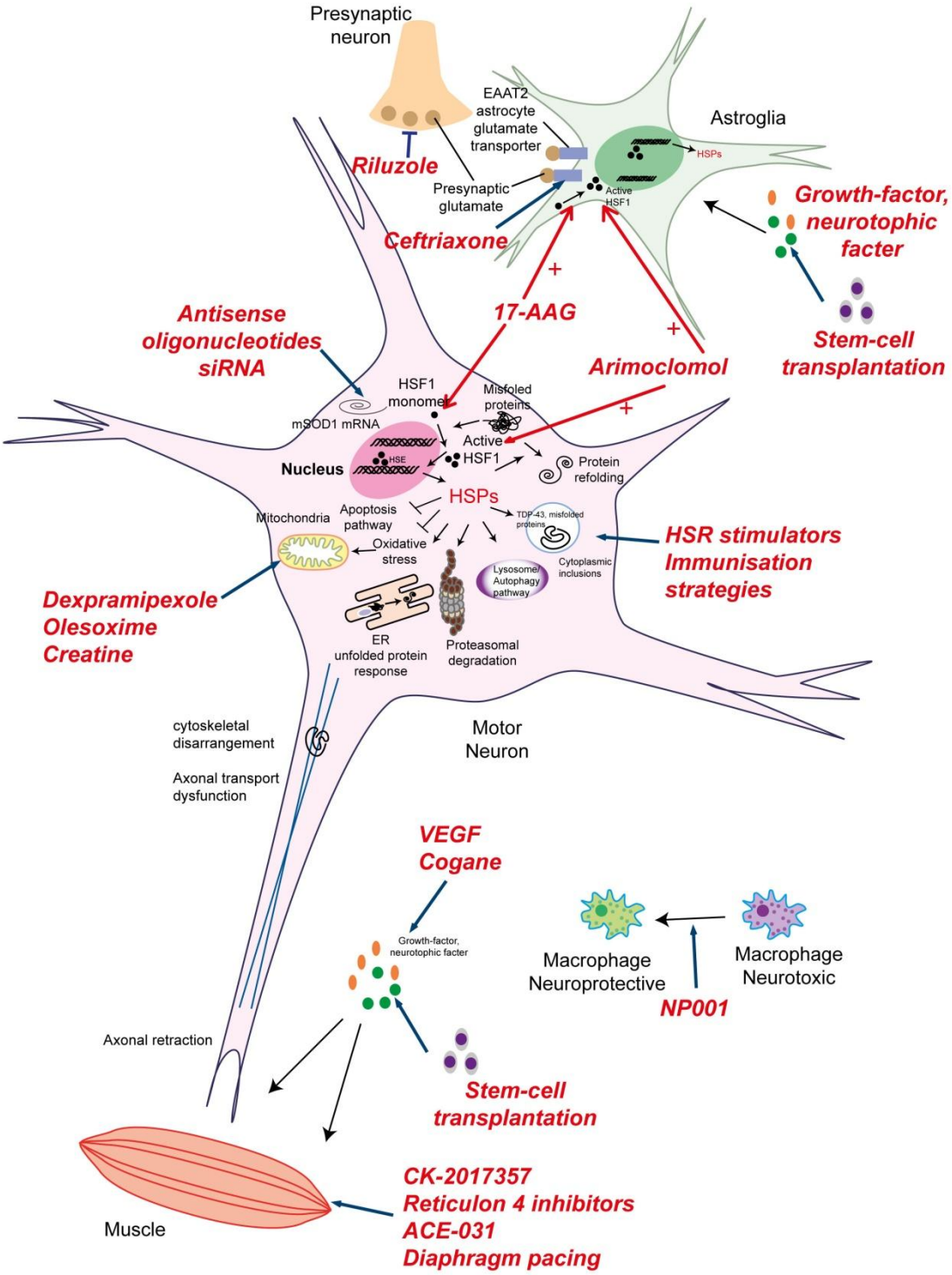
Presynaptic neuron
EAAT2 astrocyte glutamate transporter
Astroglia
HSPs
Riluzole
Presynaptic glutamate
Active HSF1
Ceftriaxone
Growth-factor, neurotophic facter
17-AAG
Antisense oligonucleotides siRNA
Arimoclomol
Stem-cell transplantation
HSF1 monomer
Misfoled proteins
mSOD1 mRNA
Active HSF1
Nucleus
HSE
Protein refolding
HSPs
Mitochondria
Apoptosis pathway
TDP-43, misfolded proteins
Oxidative stress
Cytoplasmic inclusions
Lysosome/ Autophagy pathway
HSR stimulators
Immunisation strategies
Dexpramipexole
Olesoxime
Creatine
ER unfolded protein response
Proteasomal degradation
cytoskeletal disarrangement
Axonal transport dysfunction
Motor Neuron
VEGF
Cogane
Growth-factor, neurotophic facter
Macrophage Neuroprotective
Macrophage Neurotoxic
NP001
Axonal retraction
Stem-cell transplantation
CK-2017357
Reticulon 4 inhibitors
ACE-031
Diaphragm pacing
Muscle

Figure 1.5. Novel therapeutic targets in recent or current clinical trials in ALS. A number of molecular pathomechanisms of ALS have been identified and therapeutically targeted in ALS. Glutamate-mediated excitotoxicity can be targeted by reducing presynaptic glutamate, for example by treatment with the only FDA-approved drug Riluzole. Glutamate can also be reduced by increasing EAAT2 expression to inactivate synaptic glutamate, as targeted by Ceftriaxone. For fALS patients with a known mutation, reducing the effects of the mutant protein by targeting the mRNA may be a novel approach and a slowing of disease progression has been achieved in animal models of ALS. A number of drugs targeting mitochondria have been tested, although all of these drugs failed in Phase III trials. Targeting skeletal muscle function may also improve quality of life. Stem cell transplantation may provide trophic support for motor neurons to reduce degeneration. Enhancement of the HSR may reduce the proteotoxic stress and prevent motor neuron degeneration. **Adapted from Zinman and Cudkowicz, 2011.**
Abbreviation: siRNA, small interfering RNA

Table 1.5 Summary of ALS novel therapeutic targets recently or currently under test in clinical trials.

Target (drugs)	Mechanisms	Stage of development	Preliminary results	References
1. Glutamate				
1.1 Ceftriaxone	Reduce synaptic glutamate by increase expression of EAAT2	Phase III study	Criteria for tolerability met, but insufficient efficacy at the Phase III stage. The results raise key questions of trial design, the enrolment number!	(NCT00349622; Pflumm, 2012)
2. RNA/post-transcriptional modification				
2.1 Antisense SOD1 oligonucleotides (ISIS 333611)	Reduce expression levels of mutant SOD1 mRNA	Phase I study completed. Phase 2B study underway.	Criteria for safety and tolerability met in the Phase 1 study.	(Miller et al., 2013; NCT01041222)
2.2 Pyrimethamine	Reduce SOD1 levels, possibly through posttranscriptional modification	Phase I/II study recruiting.	Decreases levels of SOD1 in leukocytes and cerebrospinal fluid (CSF) of ALS patients in a Phase I pilot study; further investigation required.	(Lange et al., 2013; NCT01083667)
3. Protein misfolding				
3.1 Arimoclomol	Augmentation of Heat Shock Response (HSR)	Phase II/III study ongoing.	Safe, well-tolerated and CSF penetration in placebo-controlled study.	(Cudkowicz et al., 2008; NCT00706147)
3.2 Immunisation	Removal of misfolded SOD1	Preclinical studies	Promising preclinical data in both active and passive immunisation in SOD1 mouse model of ALS.	(Gros-Louis et al., 2010; Takeuchi et al., 2010; Urushitani et al., 2007)
4. Mitochondria				
4.1 Dexpramipexol	Improve mitochondrial function	Phase III	Phase II stage 1 study showed safety, tolerability, motor decline attenuation and dose-responsive improvement in survival.	(Bozik et al., 2009; NCT00647296; NCT00931944; NCT01281189)
4.2 Olesoxime (TRO19622)	Mitochondria pore modulation	Phase III terminated	Preclinical animal data showed efficacy, but Olesoxime failed to meet endpoints in Phase III clinical trial. However, questions about trial designs might need to re-address in the future.	(ALSTDI; NCT00868166; Sunyach et al., 2012)
5. Growth factors				
5.1 VEGF (sNN0029)	Angiogenesis and neuroprotection	Phase II open-labelled study	Intracerebroventricular injection. Initial safety and tolerability met; final report pending.	(NCT00800501; NCT01384162)
5.2 VEGF (SB-509)	A Zinc Finger Protein Transcription Factor (ZFP-TF) of the VEGF	Phase II completed	Initial results showed criteria for safety and tolerability met, and slow in deterioration of muscle force in ALS.	(BioSciences; NCT00748501)
5.3 Cogane	Neurotrophic factor inducer; neuroprotection	Preclinical study	Improved neuromuscular physiological function and motor neuron survival in $SOD1^{G93A}$ mouse model of ALS	(Kalmar et al., 2012a)

6. Immune				
6.1 NP001	transform macrophages from a neurotoxic state to a neuroprotective state	Phase I and II studies completed. Phase III under way.	Initial results show safe and tolerable. Beneficial effect observed in patients with high dose, enhanced by a post-hoc analysis.	(NCT01091142; NCT01281631; Pflumm, 2012)
7. Stem-cell (SC)				
7.1 Embryonic SC into CNS (Neuralstem)	Neuroprotection	Phase I study completed.	The initial results of the Phase I study appear to be safe for the procedure itself, but note some serious adverse events to immunosuppressant drugs. Stem cells could last and be detected in the spinal cord of autopsied tissue of some trial participants.	(Glass et al., 2012; NCT01348451)
7.2 Induced pluripotent Stem Cells (iPS cells)	Neuroprotection	Phase I study pending.	A trial using existing collections of cells to develop human iPS cells is due to complete soon. A new trial to set up a fibroblast bank for studying molecular, cellular and genetic pathology in fibroblast, iPS, and differentiated cells is recruiting.	(NCT00801333; NCT01639391)
8. Muscle				
8.1 Diaphragm pacing	Promote diaphragm contraction	Phase I study completed. Post-Approval study recruiting.	The initial results show safety in DPS implantation and improved survival. FDA approval for humanitarian designation exemption pending.	(NCT00420719; NCT01605006; Onders et al., 2010)
8.2 GDF-8 (myostatin) inhibitor (ACE-031)	Increase muscle growth	Phase I study in healthy postmenopausal women completed, but phase II study for Duchenne Muscular Dystrophy terminated.	Initial criteria for safety and tolerability in Phase I study met, but participants with muscular dystrophy experienced adverse effects such as increasing nosebleeds, gum bleeding, and small dilated blood vessels within the skin, which raised safety concern and led to its termination.	(MuscularDystrophyCampaign; NCT00952887; NCT01099761)
8.3 Skeletal muscle troponin activator (CK-2017357; Tirasemtiv)	Improve fast muscle contraction	Phase IIb trial recruiting.	Initial criteria and tolerability met; need to reduce the dose of Riluzole when use in combination.	(NCT01709149; Pflumm, 2012; Russell et al., 2012)
8.4 Reticulon 4 (Nogo-A) inhibitor (GSK1223249; Ozanezumab)	Promote neurite outgrowth	Phase II study recruiting.	Initial criteria and tolerability met.	(NCT01753076)

Ceftriaxone, Talampanel, Topiramate, and Lamotrigine (Cudkowicz et al., 2003; Miller et al., 2001; NCT00349622; Ryberg et al., 2003; Shefner et al., 2010). In light of these failed clinical trials, and considering the increasing demand of clinical trials in response to the significant advances which have uncovered the underlying molecular mechanisms of ALS, there is a clear need for clinical trials in ALS to be improved. The challenges faced to achieve this goal are multiple; the disease is clinically extremely heterogeneous with an unpredictable rate of progression, whilst the pharmacokinetics and bioavailability of most of the drugs examined to date is far from clear (Zinman and Cudkowicz, 2011). ALS is clearly not a prevalent disorder and patients often manifest concerns over being treated with placebo. All of these factors contribute to poor recruitment for clinical trials in ALS. The delay in providing a firm diagnosis of ALS reduces the already short treatment window and it is likely to have a major effect in reducing the efficacy of most test drugs since the spared and 'rescuable' motor neuron population is likely to be significantly reduced the more advanced the disease is. In addition, the high costs, large sample size requirement, difficulty in retaining participants and the unavoidable missing data in the development of trials may all play a crucial role in the failure of most clinical trials in ALS. Possible solutions to improve trial design have been recently proposed (Zinman and Cudkowicz, 2011) and are summarised below:

i) Time-to-event study design: enable participants cross-over to active treatment;

ii) 2:1 randomisation: increase the proportion of participants being treated with active compound;

iii) Replacement of the currently most used primary outcome, survival, by either one of the **co-primary outcome measures**, used for example in the Phase III Ceftriaxone study (EMPOWER) (Berry et al., 2013), or an **alternative outcome** measure such as the change in ALS functional rating scale_Revised (ALSFRS_R), used as a primary outcome measure in a recent study on Lithium and Riluzole (Aggarwal et al., 2010);

iv) Randomised sequential trials with multiple interim analyses: traditionally, the sample size of clinical trials should be determined in advance, and data analysis should only proceed after the data collection is completed. The technique of sequential trials has enabled the examination of data at a series of interim analyses, so that a decision of whether to continue, stop or adjust therapy in the trials can be

formed (Todd et al., 2001; Whitehead, 1999). In this case, when a novel therapy is significantly effective, patients can receive the drug as soon as possible. In contrast, if a novel therapy is evidently not beneficial or even detrimental, patients should not be at any further risk testing with this drug and all other resources should be put into better use for other treatment strategies. A sequential trial design has become increasingly popular in ALS, and has been used to reduce the number of ALS patients required, for example to show that Creatine (Groeneveld et al., 2003), Valproic acid (Piepers et al., 2009) and Lithium (Verstraete et al., 2012b) are ineffective.

It should be noted that the associated parameter measuring treatment difference and the stopping rule should be chosen appropriately. More flexible and sophisticated statistical tests for interim analysis to compare the effects between experimental and placebo groups should be employed. Lastly, the conclusion drawn from the interim analysis is only appropriate for deciding whether or not the trial should continue and a final analysis should still be carried out (Todd et al., 2001);

v) Multidrug phase II selection studies considered as an effective way to speed up trials;

vi) Multistage adaptive design by reducing the time and the costs for a drug with positive phase II to move on to a phase III of the study.

1.5 Clinimetrics in ALS

Clinimetrics are characterised as '…arbitrary ratings, scales, indexes, instruments or other expressions that have been created as ''measurements'' for those clinical phenomena that cannot be measured in the customary dimensions of ''laboratory data''.' These rating scales have been developed in order to be used to describe the clinical condition of patients with a disease process (Feinstein, 1987). The clinical changes due to the disease progression can be covered by recording elements of impairment, disability and/or handicaps (Brooks, 1997). Clinimetric scales, as a measure of a complex clinical phenomenon, usually contain multiple items representing different aspects of a disease such as pathology, impairment, disability and handicap, the combination of which varies in the different ALS clinical functional rating scales developed over the last two decades (Brooks, 2002). Most of these scales require either the patient's self-reporting or the clinician's reporting of the

current functional state, referable to the four major anatomical domains involved in ALS (bulbar, breathing, arms and legs) in an ordinal-scaled questionnaire. In addition, attributes being measured in clinimetric scales need to vary over the entire range of clinical presentation among patients in order to provide adequate coverage of clinimetric scale score variability. Hence, limited variability of attributes may not be representative of the whole population (Brooks, 2002), although it might be more sensitive to reflect the change of function.

Reliable clinimetric scales need to fulfil i) consistent intra-rater reliability (or so-called test-retest reliability) in assessments of a patients with stable condition by the same assessor at different occasions, either being tested in the clinic or via telephone, ii) consistent inter-rater reliability across examiners, iii) the ability to detect change over time within a patients, i.e. the clinimetric scale score responsiveness, and iv) good clinimetric scale score sensitivity to detect clinically differences between groups. Table 1.6 summarises markers related to function which are used in ALS trials (Cudkowicz et al., 2004).

One of the most widely used clinimetric scale in ALS is the ALS Function Rating Scale_Revised (ALSFRS_R), a revised version of ALSFRS, which strengthens the ALSFRS with regard to the assessment of respiratory function (Cedarbaum et al., 1999). In a study of 267 ALS patients in the clinic, 4.4-fold increased risk to death or tracheotomy was found in patients with baseline ALSFRS_R score below the median (38), suggesting ALSFRS_R score is a good predictor of survival (Kaufmann et al., 2005) and its progression rate at diagnosis was found to subordinate to the score itself in another study (Kimura et al., 2006).

Progression rate measured by ALSFRS_R between i) First symptom to First examination, ii) the whole follow-up period, and iii) within 100 days during follow-up were all found correlate with survival time (Kollewe et al., 2008). Hence, the ALSFRS_R is currently widely used as a screening measure for entry into clinical trials and as a sensitive outcome measure with sufficient validation to be recommended as a primary endpoint (Leigh et al., 2004). Indeed, a new endpoint for ALS was recently introduced, which combines survival time and change in the ALSFRS_R score as co-primary endpoints, the Combined Assessment of Function and Survival (CAFS) (Berry et al., 2013). CAFS provides a balanced analysis of a drug which might have preferential benefit on function and survival, a powerful

Table 1.6 Summary of current clinimetrics in use in ALS.

Measures	Method		*Pros and cons*	Reference
Muscle Strength				
Maximum Voluntary Isometric Contraction (MVIC)	Quantify the strength of individual muscle groups and normalise the score to obtain megascores. Numerically continuous data.	Fixed device with strain gauges	Good intra- and inter-rater reliability; has been used as primary outcome measure in clinical trials. Inconsistent association with survival found in different trials. Long testing time (approximately 45 minutes), expensive equipment, vigorous training for evaluators required, nor applicable for home visit, not usable for very weak muscles, high dropout rate in the trials using MVIC as an outcome measure	(Andres et al., 1986; Cudkowicz et al., 2004; Hoagland et al., 1997)
		Hand-held dynamometre	Been validated against MVIC with good correlation; good intra-rater reliability; portable; inexpensive; shorter testing time.	(Beck et al., 1999; Cudkowicz et al., 2004)
Manual Muscle Testing (MMT)	Using the Medical Research Council (MRC) grading scale. Ordinal qualitative data.		Trained evaluators and standardised patient positioning required; speed, low cost, but low sensitive to change in muscle strength.	(Cudkowicz et al., 2004; Lakes and Group, 2003)
Pulmonary function				
Forced vital capacity (FVC)	Volume of air forcefully expired in one breath, reported as a percentage of a predicted vital capacity based on the height, gender and age.		Widely available, non-invasive, and portable. Baseline FVC and the rate of decline in FVC are predictive of survival. The decline of FVC overtime is a sensitive measure of disease progression. However, this test is difficult to perform in patients with significant bulbar symptoms.	(Cudkowicz et al., 2003; Kaufmann et al., 2005; Magnus et al., 2002; Varrato et al., 2001)
Maximal Inspiratory Pressure (MIP)	The maximal negative pressure at the mouth after complete exhalation by single sustained maximal inspiratory effort against an occluded airway.		Widely available, non-invasive, and portable, but increased variability in patients with bulbar involvements.	(Black and Hyatt, 1969; Cudkowicz et al., 2004)
Maximal Expiratory Pressure (MEP)	The maximal positive pressure measured in the mouth after inhalation to total lung capacity followed by a maximal expiratory effort against an occluded airway		Widely available, non-invasive, and portable, but increased variability in patients with bulbar involvements.	(Black and Hyatt, 1969; Cudkowicz et al., 2004)
Functional rating scales: access the activities of daily living (ADL)				
Appel ALS rating scale	Evaluate 5 categories: Bulbar, Respiratory, Muscle Strength, Lower limbs and Upper limbs function, ranging from 30 (normal) to 164 (maximum impairment).		Simple, validated, sensitive. Rate of change in the score is a predictor of survival. Several team members required to finish the test; time-consuming. Difficult to use in severely affected patients. Unclear relation to function.	(Appel et al., 1987; Haverkamp et al., 1995)
ALS Functional Rating Scale (ALSFRS)	Evaluate 4 motor areas (fine motor, gross motor, bulbar, and respiratory) in 10 questions, score ranging from 40 (normal)		The first functional scale independent to strength testing. Good correlation with survival and other measures. Disproportionate weighing of limb and bulbar measurements to respiratory dysfunction.	(Guiloff, 2002; Mora, 2002)

	to 0 (worst function)		
ALS Functional Rating Scale_Revised (ALSFRS_R)	Evaluate 4 motor areas (fine motor, gross motor, bulbar, and respiratory) in 12 questions, score ranging from 48 (normal) to 0 (worst function)	The revised test of ALSFRS. Currently the most widely used functional test in ALS clinical trials. The rate of progression of ALSFRS_R from onset of disease is a predictor of survival time.	(Cedarbaum et al., 1999; Gordon et al., 2010; Kaufmann et al., 2007)
Combined Assessment of Function and Survival (CAFS)	A recently developed endpoint which combines two primary outcomes: the ALSFRS_R and survival.	Has been applied in a phase II and phase III study, and show CAFS may provide a balanced analysis for a testing drug with disproportionate effect on function and survival, which weights mortality as the most clinically important outcome. However, CAFS scores between treatment groups cannot be compared across trials directly and it requires sophisticated analysis of the data for function arm and survival arm.	(Archibald et al., 2011; Berry et al., 2013; Cudkowicz et al., 2011; Ferreira-Gonzalez et al., 2007; Rudnicki et al., 2013; Wittkop et al., 2010)

statistical analysis, and yet prevent false-positive results from drugs beneficial in function but detrimental in survival (Berry et al., 2013). If CAFS can be further validated in more trials, then it may help to improve design and outcome of clinical trials in ALS.

1.6 Biomarkers for ALS

If improving the trial design is one approach to improve clinical trials in ALS, the other rests on the development of disease biomarkers. A biomarker is defined as 'an objective measurement that acts as an indicator of normal biological processes, pathogenic processes or pharmacologic response to therapeutic intervention' by the UK Medical Research Council (MRC).

1.6.1 Biomarkers for the development of disease-modifying treatments in ALS

A biomarker should be able to reflect an important feature of the disease, so that it could be used for disease diagnosis, predict disease susceptibility, monitor disease progression, and evaluate treatment efficacy/toxicity (Ryberg and Bowser, 2008). Figure 1.6 shows the timeline of key clinical events and their relation to different types of biomarkers.

Ideal biomarkers for ALS should have the following characteristics and positive effects in the conduct of trials (Turner et al., 2009; Zinman and Cudkowicz, 2011):

i) speed up the diagnostic process of ALS, which would enable early participation in clinical trials;

ii) help differentiation between clinical phenotypes, reducing the confounding effect that clinical heterogeneity has in clinical trials;

iii) help to define the true efficacy of drugs designed to target specific pathogenic mechanism which are related to the biomarker itself;

iv) change with the natural progression of the disease and hence help to monitor more efficiently drug efficacy, which would in turn reduce the size and time the trials need;

v) expedite the drug screening process;

Figure 1.6

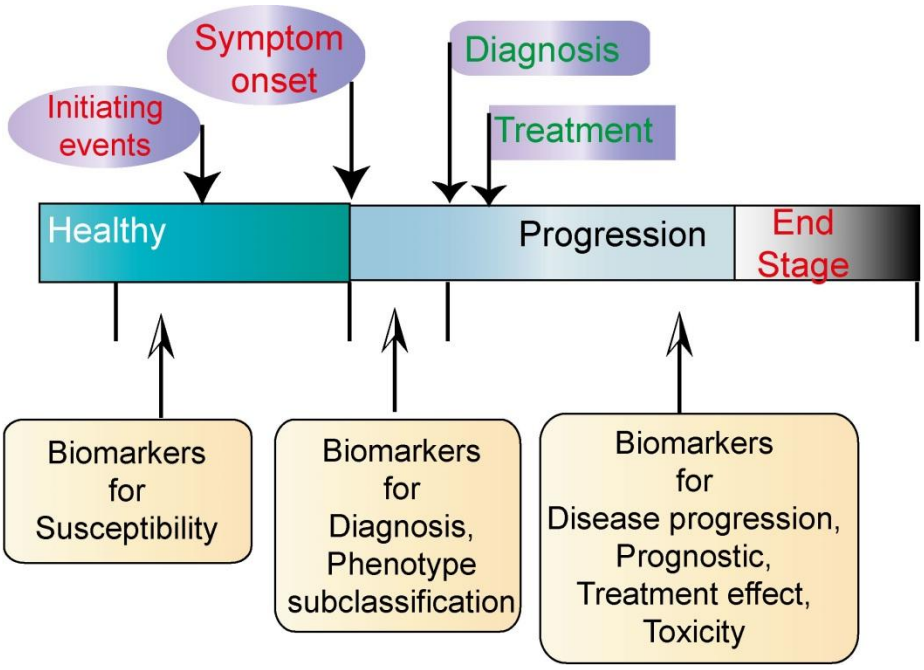

Figure 1.6. Timeline of key clinical events and related types of biomarkers in ALS. As disease initiating events are usually genetically determined or occur long before the onset of symptoms, it is important to be able to identify these subjects as soon as possible. Therefore onset should be detected earlier and the diagnosis made quicker, so that treatment can be initiated as soon as possible. Biomarkers can be used to aid diagnosis and to help clarify disease phenotypes, thereby shortening the current lengthy diagnostic process and reducing heterogeneity in clinical trials. Biomarkers for disease progression can speed-up drug screening, monitor the drug efficacy/toxicity and predict poor prognosis, to allow appropriate treatment to be provided. **Adapted from Ryberg and Bowser, 2008**

vi) predict poor prognosis and the rate of disease progression so that early intervention as well as adequate care can be planned;

vii) provide new insights on pathogenesis;

viii) be quantifiable with easy accessibility and affordable technology.

And yet there are currently no validated biomarkers for diagnosis, phenotype determination, disease progression, or therapeutic monitoring in ALS, the current approaches to the development of biomarker identification in ALS are discussed below.

1.6.2 Current strategies for the development of Biomarkers in ALS

Biomarker discovery in ALS has been prioritised by the drive to develop new treatment strategies and strengthened by recent advances in technology. A number of leading candidates have been identified to date; however, there are currently no validated biomarkers for ALS.

1.6.2.1 Physiological biomarkers

Assessments of the physiological features of the neuromuscular structures involved in the disease process in ALS can provide direct information of disease progression in ALS patients. A number of tests have been developed to examine the motor deficits in both LMNs and UMNs.

LMN function is routinely assessed using nerve conduction studies (NCS) and electromyography (EMG). UMN function can be assessed through transcranial magnetic stimulation (TMS). Loss of muscle strength is one of the most direct measures of disease progression in ALS, but the maximal compound muscle action potential (CMAP) amplitude, which reflects the function of the motor unit, will fall only when the extent of denervation exceeds the compensation of re-innervation, when approximately 50-80% of axons have been lost (Bromberg, 2004). Although routine EMG is essential in the diagnosis of ALS, it is not regarded as a good tool for monitoring disease progression due to its invasive nature and its poor correlation with pathological changes during disease progression. The development of non-

invasive, disease progression-related physiological measures would be highly desirable.

1.6.2.1.1 Motor unit number estimation

Motor unit number estimation (MUNE) is a non-invasive clinical neurophysiological measure that provides quantitative information on the number of intact motor units innervating a single muscle and on the size of individual motor units. MUNE is calculated by dividing the size of an average surface recorded single motor unit potential (S-MUP) into the maximal CMAP, and is not affected by collateral innervation (Bromberg, 2004; Bromberg et al., 1993; McComas, 1995).

A number of analytical techniques have been employed to monitor motor unit loss during disease progression in ALS (Armon and Brandstater, 1999; Felice, 1997), amongst which statistical MUNE has been used more often in ALS clinical trials due to the feasibility of standardising results from site to site. A study assessing statistical MUNE in *SOD1*-related ALS patients showed that carriers are not different from controls at a pre-symptomatic stage (Aggarwal and Nicholson, 2001). However, in another longitudinal study where MUNE was assessed at 6-month intervals, two carriers were observed to have 12-23% reduction in MUNE in thenar or extensor digitorum brevis, while the muscle strength was still preserved (Aggarwal and Nicholson, 2002). MUNE has been used as a secondary endpoint measure in ALS clinical trials; a change of MUNE after 1 year was found to have a superior correlation with disease progression than other measures, such as CMAP, hand grip and vital capacity (Felice, 1997).

However, the results from two more recent multicentre clinical trials raise concerns about using statistical MUNE as an outcome measure. In the multicentre drug trials for creatine, there was a 23% decline of MUNE over a 6-month study period, although S-MUP amplitude was found stable over the same period, in contrast to previous MUNE studies (Shefner et al., 2004). Several modifications of the statistical methods were implemented to address this problem before statistical MUNE was employed as a secondary outcome measure in a drug trial for Celecoxib over a 12-month study period (Shefner et al., 2007). However, S-MUP amplitude still remained stable during the follow-up of Celecoxib/ALS trial. Meanwhile, it was also discovered that S-MUPs from ALS patients displayed increased amplitude variability when stimulated repeatedly (Jillapalli and Shefner, 2004). Therefore, the assessment of

the motor unit in ALS patients presents not only quantitative problems. It was previously assumed that the variability of response to a repeated stimulus detected by MUNE in ALS patients is due to the number of motor unit responding in an intermittent manner; the newly identified qualitative problem of motor unit suggests that this may be due to dysfunction of motor unit itself (Shefner et al., 2007). Although this problem could be addressed, it has reduced the potential for statistical MUNE to become a secondary outcome measure in a multicentre clinical trial (Shefner et al., 2007).

1.6.2.1.2 Electrical impedance myography

Electrical impedance myography (EIM) is a non-invasive electrophysiological technique in which low-intensity, high-frequency alternating current is applied through surface electrodes measuring the underlying muscle impedance (Rutkove et al., 2002). Two of the components of muscle impedance, the resistance (R) and the reactance (X) change in ALS. As R is reversely proportional to the cross-sectional area of the muscle, ALS patients will have increased R due to muscle atrophy. In contrast, X is decreased in ALS as a result of an increased total capacitance due to muscle atrophy (Tarulli et al., 2009). A third parameter, phase (θ), is then calculated from the formula: $\theta = \arctan(X/R)$, which is used as the main outcome parameter for EIM studies as it is less sensitive on muscle shape and size (Rutkove et al., 2002), but sensitive enough to detect muscle abnormalities in ALS (Tarulli et al., 2009).

A recent multicentre study has compared EIM with existing clinimetrics, the handheld dynamometry (HHD) and ALSFRS_R, to examine the potential of EIM to monitor disease progression in ALS (Rutkove et al., 2012). The three measures were compared by assessing the coefficient of variation (CV) in the rate of decline and each technique's correlation with survival. All three measures correlated with survival, and EIM was found to be able to reduce the sample size needed for detection of a 20% treatment effect, plus 80% power for 95 subjects per arm, compared to 220 subjects per arm for ALSFRS_R (Rutkove et al., 2012). It appears EIM may therefore be a promising biomarker to accelerate Phase II clinical trials.

1.6.2.1.3 Neurophysiological index

The neurophysiological index (NI) was developed to quantify peripheral neuromuscular deficits in ALS, by mathematical derivation *(NI=CMAP (mV) X F wave frequency/distal motor latency (ms))* from three combined standardised

neurophysiological measurements: compound motor action potential amplitude, distal motor latency and F-wave frequency, representing aspects of denervation and re-innervation (de Carvalho and Swash, 2000). This approach is non-invasive, and simple to measure from abductor digiti minimi (ADM). In subsets of ALS patients grouped according to the progression rate, NI was found to be the most sensitive measure of change among other existing clinimetrics such as MRC muscle strength scale, forced vital capacity (FVC) and ALSFRS scores (de Carvalho et al., 2003a). It has been shown that in patients progressing rapidly, NI can decline by as much as 50% over 1 year (de Carvalho et al., 2003a, 2005). ALS patients with bulbar-onset disease were found to have a greater NI value (0.88) than patients with upper limb-onset disease over a 12-week follow-up period, but the rate of decline was not found to be different among different phenotypes (averaged 0.04 per week). In addition, the change in NI was found to weakly correlate with the change of functional impairment (Cheah et al., 2011). Validation in multicentre studies is needed to further evaluate the utility of NI in ALS clinical trials.

1.6.2.1.4 Transcranial magnetic stimulation

Transcranial magnetic stimulation (TMS) provides the only neurophysiological assessment of UMN function and cortical abnormalities. This technique exploits electromagnetic induction, which in turn induces weak electric currents to measure activity and function of specific brain circuits. An UMN lesion is considered either if the response to cortical stimulation is absent or the central conduction time is delayed, while the peripheral conduction time and amplitude of the M-wave (evoked by supramaximal peripheral nerve stimulation) remains within the normal range (Urban et al., 1998). A number of TMS measurements have been performed in patients with ALS, including:

i) Cortical motor threshold: The current needed to stimulate the motor cortex increases during disease progression in ALS (de Carvalho et al., 2002);

ii) Cortical silent period: The pause in EMG activity after motor-cortex stimulation is reduced in ALS (Eisen and Swash, 2001; Siciliano et al., 1999);

iii) Peri-stimulus time histograms: desynchronized, complex, primary peak that has an increased duration were observed, suggesting a supraspinal defect, as this

abnormality was not detected in Kennedy's disease, a LMN disorder (Eisen and Swash, 2001; Eisen and Weber, 2000; Siciliano et al., 1999);

iv) Central conduction time: The latency from cortex to a selected limb muscle is normal or modestly prolonged in ALS (Eisen and Swash, 2001);

v) Motor evoked potentials: small or absent motor-evoked response is observed in ALS patients (de Carvalho et al., 2003b).

Most of the findings in ALS patients using TMS suggested cortico-motor neuron pathways dysfunction and reduced inhibition (Winhammar et al., 2005). Indeed cortical hyperexcitability was found to precede the onset of *SOD1*-related fALS, when the short-interval intracortical inhibition was massively reduced in pre-symptomatic carriers, but not in asymptomatic carriers (Vucic et al., 2008). Although validation through multicentre studies is still required, TMS may be a potential tool to allow early identification of symptom onset in carriers of fALS and hence allow early intervention in these patients.

1.6.2.2 Neuroimaging

Neuroimaging provides a non-invasive approach to monitor disease progression and to identify biomarkers for ALS. With the advance in magnetic resonance imaging (MRI), neuroimaging has contributed to ALS not only as a diagnostic tool to exclude ALS mimics (Brooks et al., 2000), but also as a mean of biomarker discovery (Turner and Modo, 2010).

1.6.2.2.1 Magnetic Resonance Imaging

ALS is a disease of upper motor neurons (UMN) and lower motor neurons (LMN). Recent progresses in ALS also demonstrate a clinicopathological overlap with FTLD. MRI neuroimaging therefore provides excellent non-invasive tools to investigate the UMN component of ALS, the involvement of the primary motor cortex and corticospinal tract (CST).

1.6.2.2.1.1 Standard sequence

Standard T1-weighted MRI imaging in general is not sensitive enough to detect subtle changes of brain atrophy in ALS patients apart from those patients with an extensive FTD phenotype (Turner and Modo, 2010). With the development of voxel-

based morphometry, subtle volumetric changes in both grey-matter and white-matter tissue compartments can be identified when compared to healthy controls (Abrahams et al., 2005; Chang et al., 2005), and atrophy in the right precentral gyrus is the most consistent finding in ALS patients (Chen and Ma, 2010). This technique has largely improved the detection power of the standard T1-weighted clinical MRI in detecting brain atrophy.

1.6.2.2.1.2 Diffusion tensor imaging

Diffusion tensor imaging (DTI) is sensitive to the movement of water, which moves as a highly directional element (fractional anisotropic; FA) and behave as freely diffusible (isotropic; diffusivity, ADC: Apparent Diffusion Coefficient) in intact and damaged white matter tract, respectively. DTI image acquisition can then reconstruct the connectivity of white matter tracks, as diffusion tensor tractography (Ciccarelli et al., 2008). This technique has demonstrated the involvement of the CST and corpus callosum (CC) in ALS and other forms of UMN degeneration, such as primary lateral sclerosis and hereditary spastic paraparesis (Ellis et al., 1999; Filippini et al., 2010; Iwata et al., 2011; Muller et al., 2012; van der Graaff et al., 2011). Therefore DTI might be a potential biomarker to help the early identification of UMN failure, which would ultimately speed up the diagnosis of ALS. In addition, longitudinal DTI studies have showed significant UMN progression (decreased FA) over a period of 6-8 months, and also correlated with the clinimetric ALS Functional Rating Scale_Revised (ALSFRS_R) score and decline of ALSFRS_R score (Keil et al., 2012; Zhang et al., 2011b). These results indicate that DTI might be a promising diagnostic and disease progression marker for ALS.

1.6.2.2.1.3 Functional MRI

Functional MRI (fMRI) examines the differential magnetic properties of oxygenated and deoxygenated haemoglobin which is a by-product of neuronal activation in response to specific tasks. Expanded areas of cortical activation have been shown in ALS patients in a number of studies (Lule et al., 2009). Moreover, interhemispheric disconnection has been demonstrated in resting-state fMRI (Jelsone-Swain et al., 2010; Mohammadi et al., 2009), which echoes the findings in DTI tractography.

1.6.2.2.1.4 Magnetic resonance spectroscopy imaging

The magnetic resonance spectroscopy imaging (MRSI) allows the quantification of proton-containing cerebral metabolites within areas of interests. Metabolites most studied to date are the ratio of N-Acetylaspartate to choline or creatine (NAA/Cho or NAA/Cr ratios). A longitudinal study focused on the motor cortex showed a significant change in absolute concentration and ratio of metabolites in ALS patients. These changes also correlated to the lateralisation of clinical symptoms, to disease duration, and to disease progression (Pohl et al., 2001). A recent advance is the availability of whole-brain MRSI which enables metabolic profile from the whole brain to be studied during a single scan and also provides a stronger correlation with the ALSFRS_R score than the correlation found in DTI studies with the same rating scale (Stagg et al., 2013). Hence MRSI might also be considered a potential source of biomarker for ALS, particularly if a multimodal analysis is chosen combining different techniques of imaging.

1.6.2.2.2 Positron emission tomography scan

The use of positron emission tomography (PET) scans in ALS studies relies on the development of ligands for more accessible neuronal receptors, so that monitoring ALS progression can be carried out, similar to the used of PET amyloid images in Alzheimer's disease (AD) (Quigley et al., 2011). The requirement for intravenous injection and radiation exposure are inherent disadvantages in the development of a PET-based biomarker. However, using PK11195, a ligand for a microglia specific peripheral benzodiazepine receptor, PET scanning has been used to demonstrate the widespread cerebral neuroinflammatory activity in ALS patients (Turner et al., 2004), an increasingly important pathomechanism in ALS.

1.6.2.2.3 Muscle ultrasonography

Muscle ultrasonography (MUS), a safe and non-invasive diagnostic tool performed in a more relaxing environment compared to MRI and PET imaging, can visualise muscle pathology, record muscle contraction and detect fasciculations caused by neuromuscular disorders (Pillen et al., 2008). Affected muscles present with diminished muscle thickness and increased echo intensity (EI), which are also associated with aging and gender. With a quantification based on age and gender, MUS can differentiate neuromuscular disorders with a high specificity and sensitivity (Arts et al., 2010; Pillen et al., 2008). Studies have shown MUS can differentiate ALS and controls with a sensitivity of 96.3% and a specificity of 84.4% and is

superior in detection of regional LMN degeneration (fasciculations) than EMG (Arts et al., 2012; Misawa et al., 2011), which can be used to improve diagnostic certainty.

MUS has been used to predict survival in ALS in a cross-sectional study (n=31) which showed the combination of EI and the ALSFRS_R pre-slope (Change in ALSFRS_R score from onset to diagnosis), is a good predictor of survival (Arts et al., 2011b). However, results from two longitudinal studies carried out by different research groups using the same MUS protocol, show different results (Arts et al., 2011a; Lee et al., 2010). In a small cohort of patients (n=10), where few muscles examined (3 groups) in few follow-up tests (total 3) were undertaken in a 6-month study period, the rate of change of muscle thickness was found to correlate well with the ALSFRS_R score, though variation between muscle groups was noted (Lee et al., 2010). However, in a larger cohort (n=31), where more muscles were examined (6 groups) at more follow-up points (total 5) over a 5-month study period, the pattern of MUS muscle changes was found to be highly variable, with no correlation in functional measures observed (Arts et al., 2011a). These studies demonstrated the discrepancy in results in single and serial follow-up, small and large cohort biomarker studies and reveals potential problems caused by sampling bias, cohort heterogeneity, and intra- and inter-individual variation in ALS biomarker studies.

1.6.2.3 Neurochemical biomarkers

Disease-related proteins may be produced by tissues primarily affected by ALS or by other tissues that may become involved during the disease process. These disease-related proteins may be released into body fluids or remain confined within these tissues; the test biomarker can be sampled to obtain quantitative and qualitative analyses which establish the feasibility of using these factors as disease biomarkers. For rare and complex diseases like ALS, national and international collaborations are essential to undertake effective biomarker studies, enabling sharing of sources and throughput of analyses. Developing a consensus over the most appropriate annotated clinical information to be collected, as well as standardised protocols and standard operating procedures for sample collection and processing, are crucial steps for any shared effort in biomarker validation and to minimise pre-analytical and analytical variables. This groundwork in biomarker research enables collaboration and comparisons across studies (Otto et al., 2012; Schrohl et al., 2008).

1.6.2.3.1 Choice of samples for biomarker analysis

Relevant neurochemicals for biomarker analysis can be studied in different bio-fluids and tissues from patients as well as in post-mortem tissue samples. Cerebrospinal fluid (CSF) and blood are the current leading bio-fluids in ALS biomarker research. With the identification of new therapeutic targets and the improvement in stem cell technology, fibroblasts from skin biopsies have also become increasingly important. Table 1.7 summarises the strengths and the weaknesses of the most common biomarker sources (Otto et al., 2012).

1.6.2.3.2 Biomarker discovery platforms

Biomarker development is usually a two-step process, i) Screening for non-hypothesis driven studies, such as Gene Expression Profiling (GEP) and 'omic' studies, in order to identify targets, ii) Validation of previously identified putative disease biomarkers through large-scale analyses from step i). The recent development of new analytical techniques, which has improved biomarkers discovery in ALS, are discussed in the below sections.

1.6.2.3.2.1 Proteomics

Proteomics is the large-scale analysis of the protein content of a selected biological sample. The information obtained concerns protein profiles and the analysis is not hypothesis-driven, in-so-far that there is no pre-defined molecular target. The main methods employed in proteomics include:

i) Two-dimensional fluorescence difference gel electrophoresis (2D-DIGE): readily interfaced with mass spectrometry for protein identification, but under-representation of all potentially relevant proteins, low sensitivity and restricted multiplexing capabilities are its main limitations;

ii) Surface-enhanced laser desorption/ionization (SELDI) allows the analysis of a large number of samples compared to 2D-DIGE, but does not directly reveal the identity of the protein peaks detected. Further analytical work is required to characterise the initial targets, which could be a considerable challenge for this technology.

Generally, proteomics relies on a preliminary identification of protein spots by gel electrophoresis. The subsequent quantification and definition of the protein content

Table 1.7 Advantages and disadvantages of different sample sources used in neurochemical biomarker studies.

Characteristics	CSF	Blood	Muscle	Skin	Urine	Saliva
Proximity to CNS pathology	+++	++	+	+	+	+
Resistance to exogenous drug contamination	+++	+	++	++	+	++
Practicality of sampling	++	+++	+	+	+++	++
Less invasive	+	++	+	+	+++	+++
Ease of handling for storage	+	++	+	+	++	+
Potential for DNA/RNA analysis	+	+++	+++	+++	+	++
Less molecular complexity	+	+	++	++	++	+++
Candidate molecules to date	+++	++	+	+	+	+

Adapted from Otto et al., 2012.

+++: highly significant; ++: significant; + low significance.

can be achieved using a mass spectrometry-based technology, in combination with isotope labelling or label-free assay (Otto et al., 2012).

A proteomic study of CSF from newly diagnosed ALS patients and from mixed controls (a combination of healthy controls and neurological disease controls) has identified 3 protein candidates that have distinct expression in ALS (Ranganathan et al., 2005). These proteins are i) the 3.42 kDa 7B2CT, a carboxy-terminal fragment of the neuroendocrine protein 7B2, ii) the 13.38 kDa Cystatin C, and iii) the 6.88 kDa of Transthyretin (TTR), a carrier protein for thyroxine and Vitamin A, which is predominantly synthesised by the choroid plexus and glial cells (Ranganathan et al., 2005).

Cystatin C, a cysteine protease inhibitor and a constituent of the Bunina body inclusions found in motor neurons of ALS patients (Okamoto et al., 1993; Okamoto et al., 2008), has also been identified in another proteomic study carried out in ALS patients and control subjects (Pasinetti et al., 2006). Cystatin C was then further examined in CSF and in plasma from ALS patients using a quantitative ELISA method (Wilson et al., 2010). The levels of Cystatin C in CSF appeared to be reduced, whilst it was elevated in plasma samples from the same patients, compared to healthy controls; however, these changes could not differentiate ALS from other neurological disease controls. Moreover, Cystatin C levels in CSF and its change in longitudinal samples were found to correlate with disease progression and survival in ALS (Wilson et al., 2010). In addition, TTR CSF levels were found in a recent proteomic study to have distinct levels in ALS patients with rapid disease progression and in ALS patients with slow disease progression (Brettschneider et al., 2010).

Proteomic profiling is a promising tool to identify potential biomarker candidates for ALS, although this technique requires further work towards the clarification of the pathogenetic relevance of the newly identified targets, as well as the screening of the same proteins in large populations of patients and controls.

1.6.2.3.2.2 Metabolomics

Metabolomics is a technique that aims at identifying and quantifying small molecules (60-1000 kDa) retained in biological tissues which are thought to reflect biochemical changes linked to the pathological process. This approach can be applied to large

platforms of drug screening and biomarker discovery (Quinones and Kaddurah-Daouk, 2009). Rozen and colleagues used a screening platform of 300 plasma metabolites in the attempt to define the metabolic profile of ALS pathology. They found that the differential expression of subsets of metabolites could separate ALS patients from healthy controls and included i) significantly decreased or elevated molecules in ALS patients, ii) metabolites significantly elevated by treatment with Riluzole, and iii) a set of metabolites highly represented in patients with a predominantly lower motor neuron disease (Rozen et al., 2005). A recent metabolomics study using CSF samples also discovered a perturbation of glucose metabolism in ALS patients at diagnosis, and observed a distinct metabolomic profile in ALS patients with mutations in the *SOD1* gene (Blasco et al., 2010; Wuolikainen et al., 2012). With a consensus among researchers supporting strict pre-analytical handling and the sharing of the same technology for the analysis, the use of metabolomics might therefore become a useful approach for ALS biomarker discovery (Otto et al., 2012; Wuolikainen et al., 2009)

1.6.2.3.2.3 Lipidomics

Lipidomics targets the lipid component of biological tissues. With the development of tandem mass spectrometry and of liquid chromatography for the resolution of lipid chemistry, lipidomics has acquired the potential for large-scale lipid profiling and facilitated the development of methods for large datasets analysis (Otto et al., 2012; Wolf and Quinn, 2008). The rationale for using lipidomic analysis as means of biomarker discovery in ALS is based on observation that energy metabolism disturbances and dyslipidemia have been reported in ALS, with some reports suggesting that the latter may have some prognostic value (Dupuis et al., 2011). Whilst lipidomics may be a promising tool for biomarker discovery in ALS, it is important to remember that diet may be a major confounding factor interfering with the analysis of the lipid profile observed in ALS pathology.

1.6.2.3.2.4 Gene expression profiling and transcriptomics

The complementary DNA microarray has been an important tool in the identification of dysregulated biological pathways in ALS. By using an oligonucleotide/cDNA microarray, RNA samples from a particular cell type or tissue are extracted, fluorescently labelled and then hybridized to the microarray to be quantified. Gene expression profiling (GEP) of post-mortem tissue has shown an ALS-specific expression profile and has led to the identification of important aspects of ALS

pathogenesis (Dangond et al., 2004; Malaspina and de Belleroche, 2004; Malaspina et al., 2001). Recent advances in the development of laser capture microdissection techniques have allowed the investigation by GEP of single cell types (Cooper-Knock et al., 2012b). The gene expression profile of peripheral cells, from blood or muscles, has opened new experimental opportunities, for example, the possibility of monitoring patients during disease progression and the use of the differential regulation of defined RNA species as prognostic factors in the disease (Mougeot et al., 2011; Pradat et al., 2012; Saris et al., 2009; Shtilbans et al., 2011; Zhang et al., 2011a).

In ALS, GEP studies have consistently identified gene expression changes reflecting the involvement of defined biological pathways, such as the cytoskeleton, inflammation, protein turnover and RNA splicing, irrespectively of tissue type (CNS or peripheral) or sample types (mixed-cell or single cell) under investigation (Cooper-Knock et al., 2012b). The next-generation sequencing of RNA is a new technology that allows sequencing of long stretches of DNA or RNA, i.e. every base of the whole transcriptome. This technique has improved the detection rate, allowing a better definition of novel transcripts compared to hybridization-based microarray assays, although relatively larger amount of starting material is required (Cooper-Knock et al., 2012b). With the capacity to simultaneously screen a vast number of biological pathways, GEP might be in a privileged position to become the platform of choice for biomarker discovery in ALS.

Recent advances in ALS GEP studies also include the newly developed approach to integrate multiple species and tissue-type microarray-based GEP to identify biomarkers (Kudo et al., 2010). Using microarray coupled with the laser capture microdissection, the transcriptomic changes were identified in pre-symptomatic spinal motor neurons and surrounding glial cells in transgenic mouse models of fALS and tauopathy, the $SOD1^{G93A}$ and TAU^{P301L} mice, respectively. The pathways regulated in these mouse models were then verified with pre-symptomatic peripheral blood transcriptome in $SOD1^{G93A}$ mice, using custom-designed microarray. The relevance of these genes was next confirmed by high-throughput immunoassays using tissue microarrays from post-mortem spinal cord tissues. Despite the difference that may exist between the pre-symptomatic transcriptome in animal models and the post-mortem human transcriptome, a number of relevant proteins and putative blood biomarkers were identified (Kudo et al., 2010). The underlying molecular mechanisms of these identified proteins in ALS pathology now require

further investigation. Nonetheless, this approach demonstrates how GEP can be utilised and further exploited in the search of biomarkers for ALS.

1.6.2.3.2.5 High throughput techniques

Apart from the biomarker discovery platforms discussed above, quantification of protein candidates in biological samples can also be achieved by using antibody-based techniques, such as enzyme-linked immunosorbent assay (ELISA), which target single or multiple proteins in each assay. Currently, in ALS the preferred target tissues are CSF and blood. Table 1.8 summarises a broad range of targets that have been investigated in ALS in CSF and peripheral blood using this method (Ryberg and Bowser, 2008; Tarasiuk et al., 2012; Turner et al., 2009). Divergent results have been found by different groups for some of the target proteins, and a common major shortfall in the quality of these studies is the generally small cohort size of these studies and single sampling. Table 1.9 summarises the current leading candidates of protein-based biomarker in ALS (Bowser et al., 2011).

1.6.3.2.5.1 Neurofilament: one of the best validated candidates

Neurofilaments (Nfs) are neurofibrils of 10 nm in diameter, classified as type IV intermediate filaments, interacting with microtubule (24 nm) and actin microfilament (7 nm) to form the cytoskeleton scaffolding in the neurons (Petzold, 2005). Nfs are composed by neurofilament light chain (NfL; coded on chromosome 8p21, 61.5 kDa), neurofilament medium chain (NfM; coded on chromosome 8p21, 102.5 kDa), neurofilament heavy chain (NfH; coded on chromosome 22q12.2112.5 kDa), and α-internexin (coded on chromosome 10q24, 66 kDa) (Yuan et al., 2006; Perrot et al., 2008). Post-translational modifications such as phosphorylation and glycosylation of NfL, NfM, and NfH are responsible for the higher molecular weights from sodium dodecyl sulfate polyacrylamide gel electrophoresis in the earlier literature with 68, 150, 190-210 kDa, respectively (Petzold, 2005). NfH is a particularly challenging protein as non-phosphorylated it is a near neutral polyampholyte (-2e), while fully phosphorylated the charge is -82e (Kim et al., 2011). This has implications for the qualitative analysis of NfH phosphoforms by electrophoresis from body fluids, resulting in a blurred smear which can be abolished by enzymatically phosphorylation/dephosphorylation (Petzold et al., 2011b). Each Nf subunit is composed of a non-helical amino region (head domain) and a carboxy-terminal regions (tail domain), which are linked by a central α-helical rod domain that is highly conserved of approximately 310 amino acids (Perrot et al., 2008). The tail

Table 1.8 Selected studies of putative CSF and blood-based biomarkers in ALS.

Evaluated biomarkers	Findings in ALS		Findings (Dx, Phe, Pro)‡	References
	CSF	Blood (S/P)*		
Neuroaxonal degeneration markers				
NfH	↑	↑(S)	Dx: Increased CSF and serum levels in ALS vs. controls Phe: High CSF levels of NfH in UMN predominant Prg: High CSF NfH levels with faster rate of disease progression and survival	(Boylan et al., 2009; Brettschneider et al., 2006c; Ganesalingam et al., 2011)
NfL	↑		Dx: Increased CSF levels Phe: High CSF levels of NfL in ALS vs. PMA Pro: High CSF levels associated with shorter survival; shorter disease duration	(Rosengren et al., 1996; Tortelli et al., 2012; Zetterberg et al., 2007)
Markers of inflammation and immune activation				
MMP-2	↑/-	↑(S)	Dx: Increased serum levels in ALS vs. controls	(Lorenzl et al., 2003; Niebroj-Dobosz et al., 2010)
MMP-9	-/↓	↑(S)	Dx: Increased serum levels in ALS vs. controls	(Beuche et al., 2000; Niebroj-Dobosz et al., 2010)
MCP-1	↑	↑/- (S)	Dx: Increased levels Pro: correlated with ALSFRS_R and disease progression	(Baron et al., 2005; Kuhle et al., 2009; Tanaka et al., 2006; Wilms et al., 2003)
Interleukin-6	↑/-	↑/- (S)	Dx: CSF levels higher in ALS vs. NDC; serum levels higher in ALS vs. NDC; both CSF/serum levels found no difference with HC in another study	(Moreau et al., 2005; Ono et al., 2001; Sekizawa et al., 1998)
TNF-α		↑/- (S)	Dx: Conflict results from different studies	(Moreau et al., 2005; Poloni et al., 2000)
Complement C3, C4	↑		Dx: CSF C3, C4 levels in ALS higher than HC; pNfH/C3 ratio predict the diagnosis of ALS	(Ganesalingam et al., 2011; Goldknopf et al., 2006)
Markers of neuroprotective				
VEGF	↓/-/↑	↑/- (S) -(P)	Dx: Decreased CSF levels in hypoxaemic ALS vs. ND; increased serum levels in end-stage ALS. Phe: Increased CSF levels in limb-onset	(Devos et al., 2004; Ilzecka, 2004; Moreau et

			Prg: Increased CSF levels with long duration; Serum levels inversely correlate with disease duration	al., 2006; Nygren et al., 2002)
sVEGFR1		↓	Phe: Decreased levels in Definite ALS vs. Probable ALS	(Anand et al., 2012)
Cystatin C†	↑/↓		Dx: Increased levels in ALS vs. HC; one proteomic study show decreased levels in ALS Pro: correlate with disease progression and survival	(Pasinetti et al., 2006; Ranganathan et al., 2005; Wilson et al., 2010)
TDP-43	↑	↑ (P)	Dx: Higher CSF levels in ALS vs. NDC; Higher plasma levels in ALS vs. HC Pro: CSF levels correlate with shorter survival time; plasma levels correlate with age	(Kasai et al., 2009; Noto et al., 2011; Verstraete et al., 2012a)

Adapted from Tarasiuk et al., 2012; Turner, et al., 2009; Ryberg and Bowser, 2008.

*Blood (S/P): (Serum/Plasma)

‡(Dx, Phe, Pro): (Diagnosis. Phenotype, Progression)

†: contain findings from proteomic studies

Abbreviation: HC: healthy controls; MCP-1: Monocyte chemoattractant protein-1; MMPs: Matrix metalloproteinases; NDC: neurological disease controls; NfH: Neurofilament heavy chain; NfL: Neurofilament light chain; pNfH: phosphorylated NfH; sVEGFR1: soluble vascular endothelial growth factor receptor 1; TNF-α: Tumour necrosis factor-α; VEGF: Vascular endothelial growth factor.

Table 1.9. Current leading candidates of neurochemical biomarkers in ALS.

Method used to identify these candidates	Reference
Methods measuring single-protein antibody concentrations	
pNfH in CSF or blood	(Boylan et al., 2009; Boylan et al., 2012; Brettschneider et al., 2006c; Lu et al., 2012)
Ratio of CD14 to S100β in CSF	(Sussmuth et al., 2010)
Ratio of pNfH to complement C3 in CSF	(Ganesalingam et al., 2011)
Cystatin C levels as prognostic indicator of disease progression	(Wilson et al., 2010)
Methods measuring concentrations of multiple antibodies	
Levels of IL-2, IL-6. IL-10, IL-15, and GM-CSF in CSF	(Mitchell et al., 2009)
Levels of MCP-1 and IL-8 in CSF plus IL-8, CCL11, CCL24, and CCL26 in blood	(Kuhle et al., 2009)
MS-based methods	
Cystatin C, TTR, neuroendocrine protein 7B2 in CSF	(Ranganathan et al., 2005; Ryberg et al., 2010)
A2-glycoprotein in CSF	(Brettschneider et al., 2008)
C3 and other complement in blood	(Goldknopf et al., 2006)
Cystatin C and neurosecretory protein VGF in CSF	(Pasinetti et al., 2006)
Fetuin-A and TTR in CSF as disease progression	(Brettschneider et al., 2010)

Adapted from Bowser et al., 2011

Abbreviations: CCL, CC-chemokine ligand; C3, complement 3; GM-CSF, granulocyte macrophage-colony stimulating factor; MCP-1, monocyte chemoattractant protein-1; pNfH, phosphorylated neurofilament heavy chain.

domain is the distinctive feature for NfL, NfM and NfL: short in NfL, longer and rich in repeats of phosphorylation site Lys-Ser-Pro (KSP) for NfM and NfH (Julien and Mushynski, 1982; Julien and Mushynski, 1983). Nfs are heteropolymers, with a subunit stoichiometry of 4:2:2:1 (NfL-α-internexin-NfM-NfH) (Yuan et al., 2006). As mentioned, Nfs undergo post-translation modifications, such as phosphorylation, glycosylation, nitration, oxidation and ubiquitination, in response to physiological (such as development, neurite outgrowth, interactions with other proteins) and pathological situations including anterograde (Wallerian degeneration) and retrograde axonal degenerations as seen in a number of neurodegenerative conditions (Perrot et al., 2008).

When growing axons reach their targets, NfL is the first subunit to be expressed, together with α-internexin and peripherin, and followed by NfM (Carden et al., 1987; Willard and Simon, 1983). At this stage, the expression levels of NfL and NfM is low (Carden et al., 1987). The appearance of NfH occurs after the synaptogenesis and accompanied by robust up-regulation of NfL and NfM expression (Carden et al., 1987). These subunits are then assembled in the perikaryon, followed by slow axonal transport toward the nerve terminal (Hoffman and Lasek, 1975). It is known that about 80% of axonal Nfs are highly phosphorylated and integrated in the structure of axons, while the remaining 20% of non- or hypophosphorylated Nfs is involved in ante- and retrograde axonal transport (Nixon, 1993; Roy et al., 2000). At nerve terminal, Nfs are degraded by calcium-activated proteases, such as calpain, and non-specific proteases like lysosomal cathepsin D, trypsin and α-chymotrypsin (Chin et al., 1983; Malik et al., 1983; Roots, 1983). Susceptibility of Nfs to proteases decreases with increase of phosphorylation (Goldstein et al., 1987; Sternberger and Sternberger, 1983; Pant, 1988).

Nfs are not essential for axonogenesis, but have critical roles on axonal diameter. Neurofilament numbers and density are correlated with axonal calibre in myelinated axons (Griffin and Watson, 1988), which is directly related to nerve conduction velocity. Nfs interact with a number of partners that can modulate functions (through enzymes, such as kinases and phosphatases) and structure (through molecular motors, such as Dynein, Kinesin) of Nf, as well as the dynamic interactions (through MAP2, STOP, Hamartin, Fodrin, Synapsin I, etc) with other cytoskeletal proteins such as microtubules, tubulin, actin, and orgenelles (Perrot et al., 2008). Genetically reduction of Nfs expression in experimental animals causes reduced neurofilament

content, axonal caliber, and conduction velocities (Griffin and Watson, 1988; Julien, 1999).

Due to dysfunction of Nf synthesis, phosphorylation, distribution by axonal transport and their degradation, abnormal aggregations of Nfs are a hallmark of a number of human neurological disorders, including Alzheimer's Disease, Parkinson's Disease, Charcot-Marie-Tooth, neuronal intermediate filament inclusion disease, diabetic neuropathy, giant axonal neuropathy, multiple sclerosis, glaucoma, as well as amyotrophic lateral sclerosis (Hermann and Griffin, 2002; Perrot et al., 2008).

One of the pathological characteristics in ALS is the intraneuronal aggregates of Nfs (named spheroids) in affected neurons (Carpenter, 1968; Delisle and Carpenter, 1984; Hirano et al., 1984; Munoz et al, 1988). Codon deletions or insertions in the KSP repeat of NfH have been identified in sporadic ALS (Al-Chalabi et al., 1999; Figlewicz, et al., 1994; Tomkins et al., 1998). Expression of a mutant NfL subunit (Lee et al., 1994) and the overexpression of NfL (Xu et al., 1993), NfM (Wong et al., 1995), or human NfH (Cote et al, 1993) induces Nf pathology in experimental animals similar to those in observed in ALS patients. The pathology caused by excess human NfH can be rescued by co-overexpression of human NfL in a dosage-dependent pattern, suggesting the importance of subunit stoichiometry in ALS pathogenesis (Meier et al., 1995). Mice expressing mutant SOD1 display Nf pathology and a phenotype similar to mice overexpression NfL or human NfH (Borchelt et al., 1998; Tu et al., 1996). Depletion of axonal NfH, by preventing NfH entering the axons, and hence perikaryal accumulation of NfH is not beneficial for $SOD1^{G37R}$ mice; in fact, neither initiation nor progression of pathology is not affected in this $SOD1^{G37R}$ mouse model (Eyer et al., 1998). However, depletion of axonal NfL, the main subunit for Nf assembly, with subsequently reduced axonal NfM and NfH and increased perikaryal NfM and NfH levels, delays onset and slows disease progression in $SOD1^{G85R}$ mice (Williamson et al., 1998). Furthermore, overexpression of NfL or NfH delays onset and extend lifespan in $SOD1^{G93A}$ mice (Kong and Xu, 2000). Similarly, overexpression of human NfH in $SOD1^{G37R}$ mice also extends lifespan in these mice (Couillard-Despres et al., 1998). These findings suggest that a protective effect of perikaryal accumulation of Nfs is responsible for slowing disease in these models. Possible mechanisms of this protective effect include Nfs may act i) as calcium chelators (Roy et al., 1998), ii) to interfere with glutamate receptor function and prevent glutamate excitotoxicity (Ehlers et al., 1998),

and iii) as a phosphorylation sink for cyclin-dependent kinase 5 dysregulation induced by mutant SOD1, and hence reducing the detrimental hyperphosphorylation in neurons (Nguyen et al., 2001).

Nfs therefore play a crucial role in ALS, although the pathology-causing and pathology-relieving mechanisms of Nfs in ALS and SOD1 mouse models remain to be further clarified. Together with the physiological role in maintaining normal neuronal structure and physiological functions as well as their pathological involvements in other neurodegenerative disorders, Nfs have become surrogate markers for axonal injury, degeneration and loss, which led to quite a number of quantification studies, essentially in CSF samples (Petzold, 2005).

1.7 Aims of this thesis

The Hypothesis tested in the experiments described in this Thesis is that plasma NfH levels may extend on earlier CSF work and be a biomarker of disease progression in ALS patients. The specific Aims of this research project are:

i) To develop and validate a reliable ELISA method for the sensitive and accurate detection of NfH in plasma;

ii) To evaluate whether plasma NfH levels could be used to monitor disease progression in a mouse model of ALS with a homogeneous and well characterised pattern of disease progression;

iii) To examine whether plasma NfH levels can reflect therapeutic effects of known and novel disease-modifying agents for ALS;

iv) To examine whether plasma NfH levels can be used to monitor disease progression in a large, heterogeneous cohort of ALS patients.

Chapter 2

Development of a sensitive, quantitative immunoassay for the measurement of plasma neurofilaments for ALS

2.1 Introduction

There is an urgent need to develop reliable biomarkers for ALS not only for monitoring disease progression, accelerating diagnosis and predicting prognosis, but also for improving the efficacy of clinical trials for the development of new therapeutic strategies. Neurofilaments (Nfs) are one of the leading candidate biomarkers in ALS. However, most of studies undertaken to date were conducted using cerebrospinal fluid (CSF) as sample source, which is not an appropriate tissue for long-term repetitive sampling in debilitating diseases such as ALS. In the experiment discussed in this Chapter, I examined the possibility that plasma Nfs may be a useful biomarker of disease progression in ALS.

2.1.1 Neurofilament heavy chain (NfH) as a biomarker of ALS

Protein aggregation is a characteristic feature of neurodegenerative disorders including ALS. Nfs are components of the protein aggregates found in affected tissues from ALS individuals and animal models of ALS (Strong et al., 2005). Nfs are a major component of the neuroaxonal cytoskeleton and are important for maintaining axonal calibre, and thereby modulation of conduction velocity. Nfs also interact with other cytoskeletal proteins to ensure axonal transport of key organelles, growth factors, and signalling factors (Perrot et al., 2008). Nfs are assembled into a unique heteropolymer structure with a specific stoichiometric composition of at least four subunits: neurofilament light chain (NfL, 68 kDa), neurofilament medium chain (NfM, 150 kDa), and neurofilament heavy chain (NfH, 190-210 kDa) and alpha-internexin (Petzold, 2005). The three neurofilament subunits differ mainly in the length of the carboxy-terminal tail domain, which results in different states of phosphorylation and of susceptibility to proteases (Goldstein et al., 1987). Mutations in Nfs have been reported in several neurodegenerative diseases, such as Alzheimer's disease (AD), Parkinson's disease (PD), Charcot-Marie-Tooth disease, giant axonal neuropathy, diabetic neuropathy, progressive supranuclear palsy, spinal muscular atrophy, as well as ALS (Perrot et al., 2008). Although only a small number of variants in the NfH gene have been identified in approximately 1% of sporadic ALS (sALS) patients (Al-Chalabi et al., 1999; Figlewicz et al., 1994), one

common pathological finding of both sALS and familial ALS (fALS) is the accumulation of phosphorylated Nfs in the perikaryon and in axonal spheroids, which are normally only present in distal axons and nerve terminals (Manetto et al., 1988). Manipulations of the stoichiometry of the three Nfs subunits have been shown to facilitate the development of early-onset motor neuron death in transgenic mouse models of ALS (Cote et al., 1993; Lee et al., 1994; Xu et al., 1993), thus supporting the critical involvement of Nfs in ALS pathology.

Monitoring of tissue-specific components released into biological fluids during disease progression can be used to aid diagnosis and as readouts of pathological severity (Ganesalingam and Bowser, 2010; Sussmuth et al., 2008). Nfs levels in the CSF, the closest body fluid compartment to the central nervous system (CNS), have been investigated as potential disease biomarkers in several neurological disorders. Recent studies have shown that CSF Nf levels might serve as a prognostic marker in multiple sclerosis (Salzer et al., 2010), may assist in the differential diagnosis between frontotemporal dementia (FTD) and early onset AD, particularly in combination with Aβ42 and phosphorylated-tau proteins (de Jong et al., 2007), and may help distinguish Parkinsonian syndromes in combination with CSF tau levels (Brettschneider et al., 2006b; Constantinescu et al., 2009). Furthermore, CSF Nf levels are much higher in ALS than in other neurodegenerative disorders such as AD (Brettschneider et al., 2006c; Ganesalingam et al., 2011; Norgren et al., 2003; Rosengren et al., 1996) and correlate inversely with disease duration (Zetterberg et al., 2007). Studies have also suggested that the phosphorylation state of Nfs can be indicative of neuronal pathology, with high phosphorylated levels present in neurodegenerative disorders (Perrot et al., 2008). However, because of its invasive nature, serial CSF sampling is not tolerated by all patients and is clearly not an ideal source of bio-fluids for repeated bioassays for the purpose of monitoring progression in ALS. Thus, a functionally validated Nf-based blood biomarker for the longitudinal monitoring of disease development and informative of treatment response would be highly desirable.

2.1.2 Established approaches for the detection of NfH in the peripheral blood of ALS

Boylan and colleagues have previously shown that phosphorylated NfH (pNfH) is detectable in the blood from both SOD1 murine models and ALS patients, using an in-house ELISA method (Boylan et al., 2009). However, pNfH was only detectable

after 74 days of age and reached a peak concentration of only 35 ng/mL at 133 days of age (end-stage) in $SOD1^{G93A}$ mice, and was undetectable in wild-type (WT) mice. In ALS (n=19) and control subjects (n=19), median pNfH in the plasma was 0.53 and 0.17 ng/mL, respectively ($p<0.001$) (Boylan et al., 2009). These levels observed in human samples were surprisingly low, considering that the average concentration of overall proteins in the blood is 60 ng/mL in humans (Boylan et al., 2009). In addition, pNfH in $SOD1^{G93A}$ mice was only detected relatively late in the disease, which is surprising as motor neuron degeneration occurs earlier in the disease. Furthermore, pNfH was undetectable in WT animals, in contrast to the findings in human control subjects. These findings suggested that this existing ELISA method may not be ideal in quantifying pNfH in the blood of either mice or humans.

2.1.3 Limitations of existing methods to quantify NfH levels from blood: lack of parallelism

Several studies have examined Nf levels as a potential biomarker in ALS, significant limitations have been subsequently identified which limit the extrapolation of data derived from CSF samples to blood samples: Notably, a lack of parallelism.

Precise quantification of NfH levels from biological samples using immunoassays can be compromised by at least four factors: (1) the change in solubility and polymerisation characteristics of Nfs subunits, leading to the formation of Nfs aggregates; (2) differential resistance to proteases, resulting in variable stability; and (3) differential interactions with other proteins, such as ubiquitin and (4) presence of auto-antibodies. These factors can result in the masking of those NfH epitopes relevant to immunoassays, resulting in a different bio-dilution curve compared to that observed with the soluble, stable NfH protein standard curve for such immunoassays from different bio-fluids.

Typically, in immunoassays using biological samples such as blood, CSF or other body fluids, it had been possible to obtain a dilution-optical density curve in a linear range, which is parallel to the curve obtained with the purified protein standard. If the bio-dilution curve from biological samples diverges from, and is not parallel to that obtained with the standard curve, this is referred to as 'lack of parallelism.' ‘Lack of parallelism’ suggests that the protein in the biological sample and that in the protein standard presents different bio-properties, and as a consequence the standard curve may not be suitable for use in accurate quantification of protein levels from the

respective biological fluid (Plikaytis et al., 1994). Consequently the results may be inconclusive or mis-leading, since after correcting for the dilution factor, the protein concentrations calculated from a 1:1 dilution will be very different to the protein concentrations calculated from other sample dilutions.

To illustrate this further, an example of such a lack of parallelism is shown for human serum samples assayed for *Haemophilus influenza type b* (Hib) antibody (Ab) in the data presented in Fig. 2.1, taken from Plikaytis et al (1994). The Figure shows the results of two typical ELISA for *Hib* Ab in which the OD readings for serum samples are shown alongside the results obtained with the standards. In the results shown in Fig. 2.1A, the samples show clear parallelism with the standard curve, indicating that the *Hib* Ab at the concentration presented in the samples has the same bio-properties as the Hib Ab in the standard curve. However, in the data presented in Fig. 2.1B, the serum samples show a clear lack of parallelism with the standard OD readings, so that the calculated *Hib* Ab concentration will be very different in the samples at different dilutions. For example, compare the data identified by the large and small arrows in Fig. 2.1B, which represent *Hib* Ab concentrations of 2 and 9.25 µg/mL, respectively, for the same serum sample at two different dilutions (Plikaytis et al., 1994). This finding clearly illustrates the confounding effects of the lack of parallelism of the bio-sample with the standard curve in an immunoassay.

2.1.4 Hypothesis and Aims

Hypothesis

In this Chapter, I examined the probability that accurate measurement of plasma NfH levels could be obtained by the development of a highly sensitive, reproducible ELISA, that specifically overcome the lack of parallelism from plasma samples, which causes a 'Hook' shape on the bioassay dilution curve.

Aims

The aims of the work described in this Chapter are to develop a new ELISA method for the detection of plasma NfH, both hyperphosphorylated and variably phosphorylated NfH, from an existing method developed for use in CSF (Petzold et al., 2003). Since the $SOD1^{G93A}$ mouse is a well characterised, widely used model of ALS, with a reproducible progressive phenotype, plasma from $SOD1^{G93A}$ mice at end stage of disease was therefore used as a platform for development of the NfH

Figure 2.1

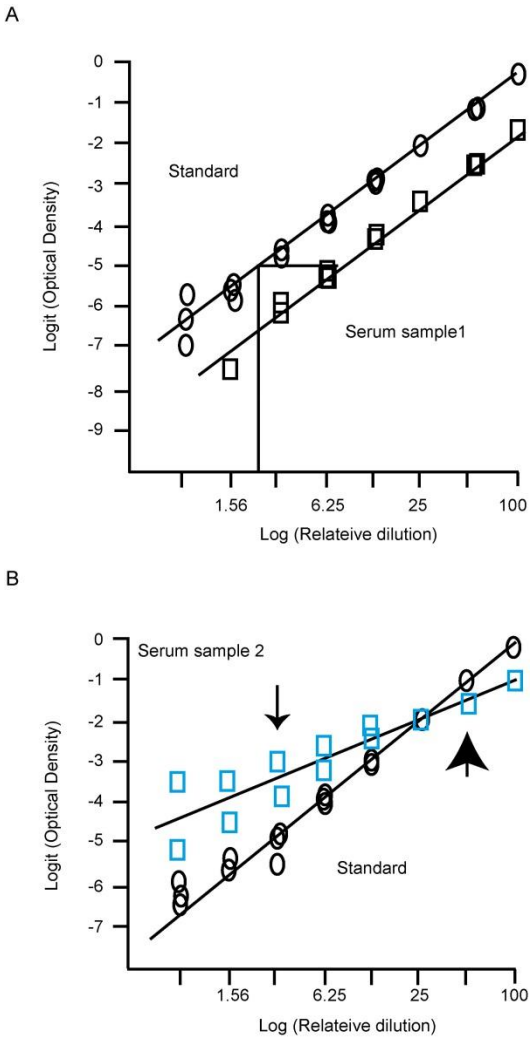

Figure 2.1. Antibody concentration calculations by using a standard curve prepared from a serial dilution of *H. influenzae type b* standard reference serum (FDA 1983) (oval) and two serially diluted serum samples (square) plotted on a fully specified logit-log scale. (A) The parallel case; the slopes for the standard reference and serum sample 1 (black square) curves are 1.370 and 1.366, respectively. **(B)** The nonparallel case; the slopes for the standard reference and serum sample 2 (blue square) curves are 1.361 and 0.677, respectively. Serum antibody concentrations for points with big arrow head and small arrow head are 2.00 and 9.25 µg/ml, respectively. **Adapted from Pikaytis et al., 1994.**

assay. In view of the very small volumes of plasma that can be obtained from mice, the method developed also has to be suitable for use in very small volumes of plasma.

2.2 Methods and Materials

2.2.1 Experimental animals

2.2.1.1 Genotyping of SOD1^{G93A} mice

Mice expressing the human SOD1^{G93A} mutant protein (TgN[SOD1-G93A]1Gur) were maintained by breeding male heterozygous carriers with female (F57BL/6 x SJL) F1 hybrids within the biological services facility of UCL Institute of Neurology under licence from the UK Home Office and following ethical approval from UCL Institute of Neurology. The presence of the SOD1^{G93A} mutation was confirmed by PCR reaction from ear biopsies of 3-week-old mice. Male SOD1^{G93A} mice were examined at 120 days of age, near to end stage in our colony of SOD1^{G93A} mice in which male mice live for a mean 123±2 days (Kalmar et al., 2008). WT, age- and sex-matched mice were used as controls. Each experimental group consisted of 10 mice from 6 different litters.

Genotyping of SOD1^{G93A} mice by polymerase chain reaction

The mice carrying a mutant human *SOD1* transgene were identified by polymerase chain reaction (PCR) amplification of the transgene from genomic DNA. Ear notches were collected soon after the mice were weaned. The tissue sample was then digested using rapid digestion buffer.

For PCR, 2.5 µl of each DNA sample was added to a reaction tube, which contained 17.65 µl sterile water, 2.5 µl PCR buffer, 0.75 µl MgCl2 (50 mM), 0.5 µl dNTP solution, 0.25 µl of both forward and reverse primers for the endogenous SOD1 enzyme and human mutant SOD1 enzyme, and 0.1 µl Taq polymerase, to make the final volume of 0.25 µl. In order to differentiate the human transgene from murine *SOD1*, primers with the following sequences were used:

5’ CAT CAG CCC TAA ATC TGA 3’
5’ CGC GAC TAA CAA TCA AAG 3’

The samples were then temperature cycled, as summarised in Table 2.1. The PCR products were subsequently visualised by gel electrophoresis by running 15 µl of each PCR product on a 2% gel agarose gel at 85 V for 20 minutes.

2.2.1.2 Plasma collection

Blood from 120-day-old SOD1 mice and their age-matched WT littermates was collected via cardiac puncture under terminal anaesthesia into an EDTA-coated tube (Greiner bio-one; K3EDTA). Each tube was then centrifuged at 14,000 rpm for 8 minutes. The plasma was collected, protease inhibitor added (Sigma; v/v: 1/100), the sample was then aliquoted and stored at -80°C freezer until assayed.

2.2.2 ELISA

The in-house sandwich ELISA developed in this Chapter was modified from a method originally designed for assessment of NfH levels in CSF samples. Here we adhere to a previously proposed nomenclature and indicate that the capture antibodies used for NfH phosphoform quantification in superscript NfH^{SMI35} for variably-phosphorylated NfH and NfH^{SMI34} for hyperphosphorylated NfH (Petzold et al., 2003).

2.2.2.1 Antibodies

The capture antibodies used in this study were mouse monoclonal anti-NfH antibodies, SMI-34R and SMI-35R (Covance, USA) and the detector antibody was rabbit polyclonal anti-Neurofilament 200 (N4142; Sigma, UK). The reporter antibody was horseradish peroxidase (HRP)-labelled swine polyclonal anti-rabbit antibody (P0217; DAKO, Denmark).

2.2.2.2 Chemicals and Reagents

The following reagents were used in this study: Sodium barbitone (No. 27283; BDH, USA); Barbitone (B-0375), ethylenediaminetetraacetic disodium salt (EDTA; E4884), protease inhibitor cocktail (PI, P8340), NaHCO3, Na2CO3, Tween20 (P1379), urea and bovine serum albumin (BSA) (all purchased from Sigma, UK); One step HRP substrate, TMB (3, 3', 5, 5'-tetramethylbenzidine; DAKO, Denmark); Hydrochloric acid (HCl; Merck, Germany); Bovine Neurofilament H, 200kD (N2160-15B; USBiological, USA).

Table 2.1. Summary of the cycles involved in PCR analysis of $SOD1^{G93A}$ samples.

No. of cycles	Temperature	Duration of cycle
1	95°C	3 minutes
36	95°C	30 seconds
36	60°C	30 seconds
36	72°C	45 seconds
1	72°C	2 minutes

2.2.2.3 NfH Standards

Gel determined bovine NfH (bNfH; USBiology) was reconstituted and aliquots stored at -20°C. The standard curve used for the NfH assay was calculated from dilution of 200 µg bovine NfH in Barb2EDTA buffer (Sodium Barbitone, Barbitone, 6 mM EDTA at pH 8.6) containing 0.1% BSA and ranged from 0 to 100 ng/mL.

2.2.2.4 Plasma samples

In these experiments, plasma obtained from $SOD1^{G93A}$ mice at end stage of disease was used as a biological sample in which NfH levels would be expected to be high compared to WT controls. For measurement of NfH levels, plasma was thawed and each sample analysed in duplicate on a single plate.

2.2.2.5 Existing method for detection of NfH

As a platform to develop a reliable immunoassay for the quantification of plasma NfH, using very small amount of samples obtained from mice, I first examined the feasibility of using an already established method developed for the detection of NfH in CSF in human (Petzold et al., 2003). This existing method was therefore used as a starting point from which further steps for optimisation were taken as needed to extend this method for the use of plasma samples.

The microtitre plates were coated with 100 µl of capture antibodies, either SMI-34R or SMI-35R, in 0.05 M carbonate buffer, pH 9.5 (w/v, 2/10000), at 4ºC overnight. The plates were rinsed in Barb2EDTA buffer containing 0.05% Tween 20 and 0.1% BSA (wash solution) once and then blocked with 150 µl of Barb2EDTA buffer containing 1% BSA at room temperature (RT) for 1 hour. After 2 rinses with wash solution, 95 µl of Barb2EDTA buffer containing 0.1% BSA (sample diluent) was added into each well. Five microliters of standard, quality control or plasma sample were then loaded in duplicate into the plate. The plate was then incubated on a shaker for 1 hour (RT). After washing (3x5 minutes), 100 µl of detector antibody (w/v. 10/10000 in sample diluent) was added into each well and incubated for 1 hour on a shaker (RT). The plate was then washed (3x5 minutes) before 100 µl of reporter antibody (w/v, 10/10000 in sample diluent) was loaded into each well and incubated for 1 hour on a shaker (RT). After washing (6x5 minutes), 100 µl of TMB substrate was added into each well and incubated for approximately 20 minutes in the dark on a shaker (RT). The reaction was then stopped by adding 50 µl of 1M HCl into each well. The absorbance was read immediately at 450 nm, with 750 nm as the

reference wavelength, on an Omega plate reader (Software version: 1.02; BMG LABTECH).

2.2.3 Western blot analysis

2.2.3.1 Samples

Western blot (WB) analysis of NfH^{SMI34} was carried out in plasma from 120-day-old $SOD1^{G93A}$ and WT mice and purified bovine NfH protein (USBiological; N2160-15B). Each set of samples contained plasma from 3 mice from different litters. All sets of samples were firstly filtered twice through the Amicon® Ultra Centrifugal filter (Millipore; UFC510024) to remove low molecular weight proteins in the plasma.

2.2.3.2 Sample preparation

Plasma samples were incubated at three conditions, all at 1:1 dilution factor: i) 4 M urea-Barb2EDTA buffer incubation at 4ºC for 48 hours, ii) 4 M urea-Barb2EDTA buffer incubation for 1 hour (RT), and iii) Barb2EDTA buffer incubation for 1 hour (RT). Samples were then mixed with lithium dodecyl sulfate sample buffer and 0.5 M dithiothreitol before being denatured at 70ºC in a water bath for 10 minutes. Purified bovine NfH protein was incubated using the above conditions ii) and iii).

2.2.3.3 Blot management

HiMark™ Pre-stained HMW protein standard (ranged between 460-30 kDa; Invitrogen, LC5699), purified bNfH protein and plasma samples were loaded into 3-8% NuPAGE® Noves® Tris-Acetate gels (Invitrogen, EA0375BOX). The gel electrophoresis was set at 150 volt for 100 minutes, and the proteins were then wet blotted to a nitrocellulose membrane as previously described (Petzold et al., 2011b). The membrane was then blocked with Barb2EDTA buffer containing 5% skimmed milk at room temperature for 1 hour. After washing (4x10 minutes), the membrane was incubated in Barb2EDTA buffer containing 0.1% skimmed milk with SMI-34R (1:1000) at 4ºC overnight. The membrane was then washed (6x15 minutes), followed by 2-hour incubation with HRP-labelled rabbit anti-mouse IgG (Dako, P0260, 1:1000, RT) and washed (6x15 minutes). The membrane was then treated with the chemiluminescence substrate (SuperSignal West Pico, Thermo Scientific, #34078) for 5 minutes. The dried membrane was visualised on an AlphaEase SP CCD camera (2 minutes exposure).

2.2.3.4 Band specificity validation

Pre-absorption of the primary antibodies, using high concentration of NfH standard proteins, abolished all the bands at high molecular weight.

2.2.3.5 Densitometry

The immunoblot bands were quantified using AlphaEase®FC software version 5.0.2. Densitometric values of bands from urea-treated conditions were normalised to non-urea treated conditions.

2.2.4 Statistical analysis

Statistical analyses were undertaken using SAS software (V9.1). Non-parametric analysis Mann-Whitney U test was used.

2.3 Results

2.3.1 Plasma NfH aggregates cause a NfH 'Hook shaped curve'

In the first set of experiments, I examined whether an existing published method used for the detection of NfH in CSF samples was suitable for reliable measurement of NfH in plasma samples. In order to optimise the chance of detecting NfH, plasma from end-stage $SOD1^{G93A}$ mice was examined as it was expected that NfH levels would be significant at this stage in this model of ALS. As can be seen in the bio-dilution curve presented in Fig. 2.2, a hook shape curve was observed in the serial dilution of plasma samples from 120-day-old $SOD1^{G93A}$ mice. (This phenomenon was termed NfH 'Hook Effect' in my publication about the work presented in this Chapter (Lu et al., 2011)). In addition, it can be seen that the plasma levels of NfH from age-matched WT littermates were undetectable (Table 2.2). Figure 2.2 shows a clear lack of parallelism between the clinical course of $SOD1^{G93A}$ plasma samples and that of the NfH standards. This lack of parallelism introduced an analytical error, averaging at 300% for a 1:16 dilution (comparison of the 4^{th} dilution and the 1^{st} dilution) (Fig. 2.2B).

Subsequent immunoblotting showed that this lack of parallelism was likely to be due to a combination of NfH aggregate formation (see 238-460 kDa bands in Fig. 2.3A, lanes 4&7) and endogenous binding of NfH cleavage products (Fig. 2.3A, 5 bands below the expected ~205 kDa on a SDS gel, lanes 4-9). Addition of 4 M Urea partly dissolved the aggregates after one hour (Fig. 2.3A, lanes 5&8, solid arrows). The NfH aggregates were completely broken up by a longer incubation for 48 hours (Fig.

Figure 2.2

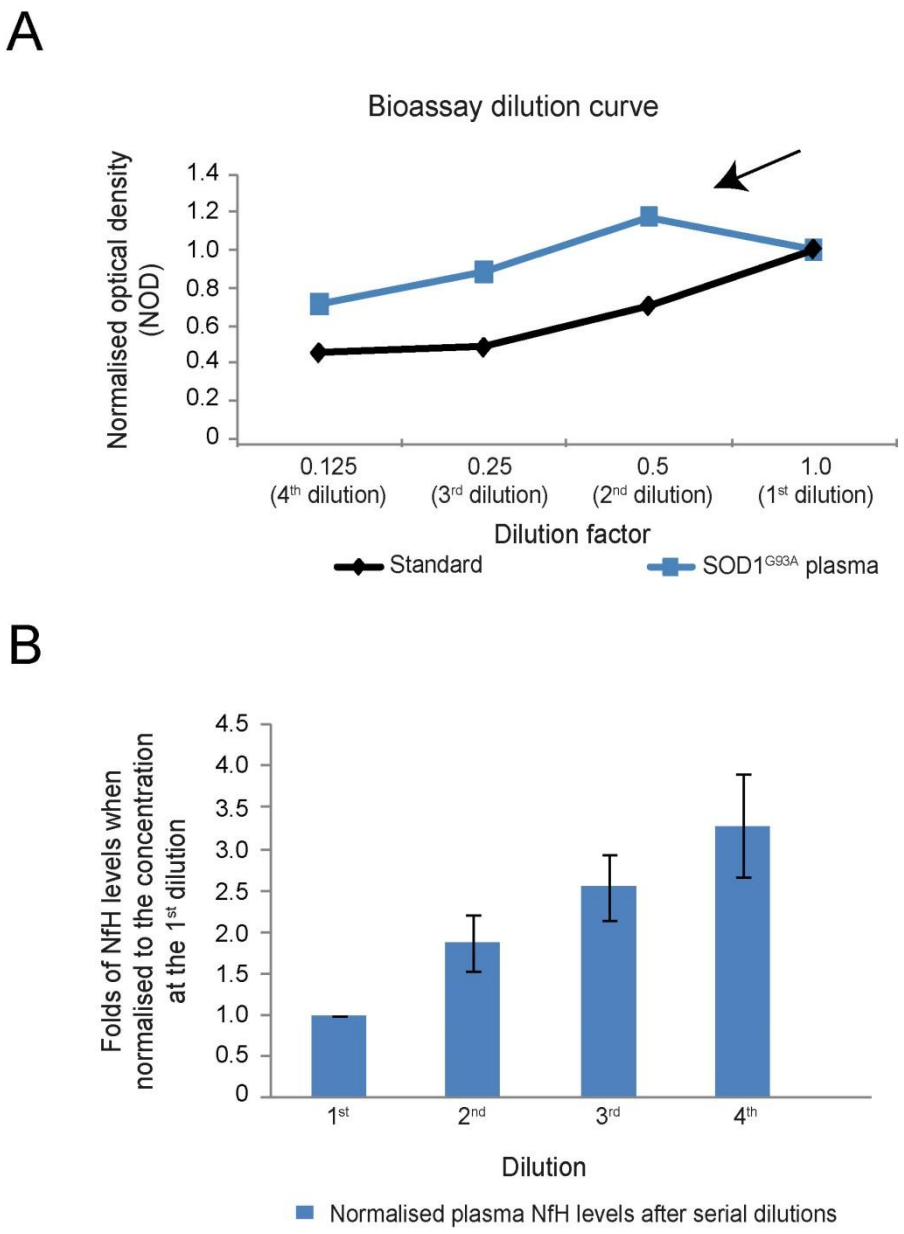

Figure 2.2. Lack of parallelism from plasma samples impresses with a typical 'hook shaped curve' for NfH. (A) Normalised optical density (NOD) in doubling dilution of plasma samples from 120-day SOD1^{G93A} mice showed a hook shape at the start of the dilution curve (arrow), i.e. an increase in NOD, while the NOD of the NfH standard attenuated. **(B)** Averaged concentration of an undiluted sample was approximately a third of the levels at a dilution 1:16. Error bars: ±SEM.

Table 2.2. A summary of initial plasma NfH^{SMI34} levels obtained from 120-day-old WT and $SOD1^{G93A}$ mice, using the ELISA method originally designed for CSF samples in Human.

Group		Sample Dilution	NfH^{SMI34} levels (ng/mL)
WT	Mouse 1	1:2	All undetectable
		1:4	
		1:8	
		1:16	
	Mouse 2	1:2	All undetectable
		1:4	
		1:8	
		1:16	
	Mouse 3	1:2	All undetectable
		1:4	
		1:8	
		1:16	
SOD1	Mouse 1	1:2	154.42
		1:4	396.71
		1:8	500.82
		1:16	655.68
	Mouse 2	1:2	169.83
		1:4	230.17
		1:8	314.04
		1:16	375.96
	Mouse 3	1:2	313.37
		1:4	518.17
		1:8	715.21
		1:16	790.01

Figure 2.3

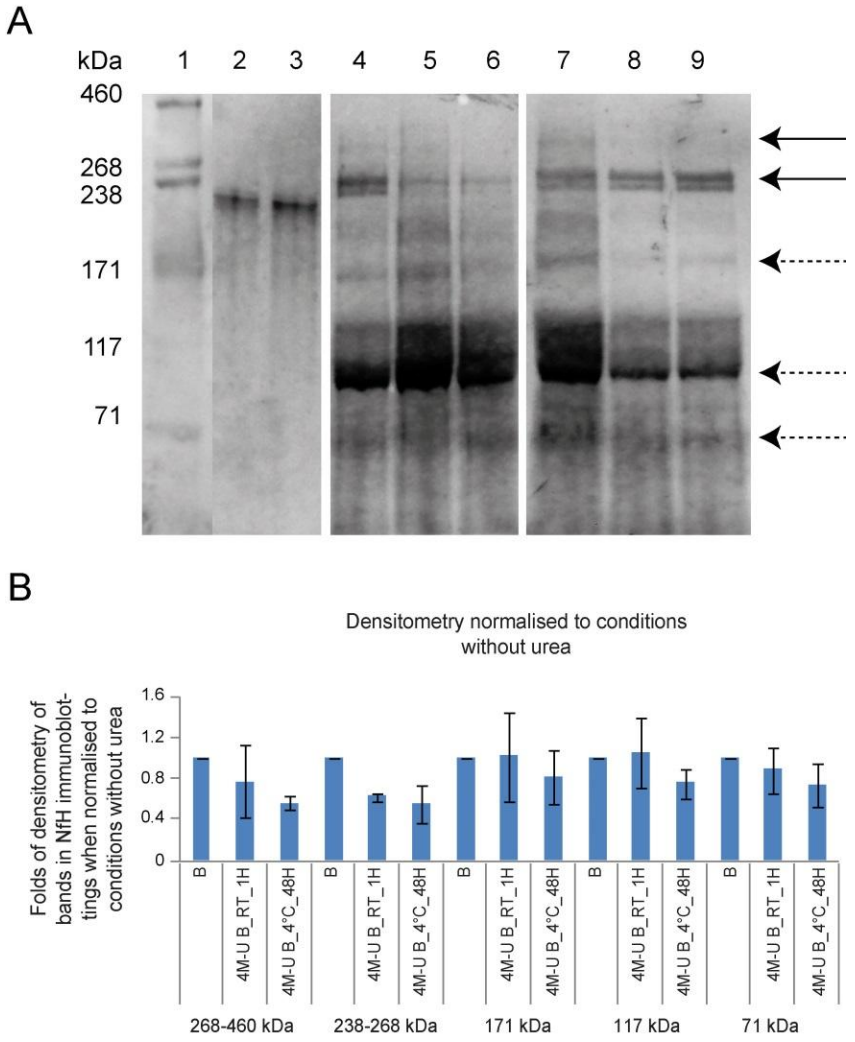

Figure 2.3: Disruption of NfH aggregates. (A) The western blot shows the effect of urea in disrupting NfH aggregates in plasma of SOD1^{G93A} mice. Lane 1: the molecular weight (MW) standards; Lanes 2 and 3: Purified bovine NfH; Lanes 4-6: SOD1^{G93A} plasma sample Set A; Lanes 7-9: SOD1^{G93A} plasma sample Set B; Lanes 2, 4, and 7: 1 hour incubation in Barb$_2$EDTA buffer at RT; Lanes 3, 5, and 8: 1 hour incubation in Barb$_2$EDTA buffer with 4 M urea at RT; Lanes 6 and 9: 48 hours incubation in Barb$_2$EDTA buffer with 4 M urea at 4°C. **(B)** Densitometry of bands i) between 268-460 kDa, ii) around 238 and 268 kDa, iii) around 171 kDa, iv) around 117 kDa, and v) around 71 kDa. All densitometric values for bands with urea incubation were normalised to corresponding non-urea incubation condition. Error bars represent the SEM of Densitometric values normalized to non-urea condition of corresponding bands in three repeats of samples. Error bars: ±SEM.

2.3A, lanes 6&9, solid arrows; Fig. 2.3B). As aggregates were broken up the lower molecular weight bands became stronger (Fig. 2.3A, lanes 5&6). However, in contrast to the consistent break up of aggregates, the appearance of cleavage products (dashed arrows) was less consistent (Fig. 2.3A, lanes 5, 6, 8, 9; Fig. 2.3B).

2.3.2 Disruption of NfH aggregates in plasma

In view of the finding that NfH aggregates in plasma might contribute to the 'hook shaped curve' shown in Fig. 2.2, I next developed a method to overcome this effect. Using plasma samples from 120-day-old $SOD1^{G93A}$ mice and age-matched WT controls, a number of established methods for the gentle disruption of NfH aggregates were therefore tested, including addition of a calcium chelator, such as EGTA or EDTA (Yabe et al., 2001a; Yabe et al., 2001b) or the pre-thawing of samples at 4°C (Petzold et al., 2003). As the results presented in Fig. 2.4 show, both of these methods improved the quantification of NfH levels during serial dilution. However, the error remained high, averaging 36% for pre-thawing (Fig. 2.4A), 63% for EDTA and 33% for EGTA (Fig. 2.4B). The effects of calcium chelators and/or prethawing were therefore not consistent enough to achieve parallelism.

As shown in Fig. 2.5, the most effective method for the disruption of NfH aggregates was found to be incubation in urea (Fig. 2.5). Urea incubation had a dose-dependent effect (0.5 M - 4 M) with the highest NfH^{SMI34} and NfH^{SMI35} levels detected following incubation of the sample diluent in 0.5 M urea at RT, 1 hour prior to incubation in the ELISA. Longer incubation periods (up to 24 hours at 4ºC) reduced the levels of NfH phosphoforms detected, with a decrease of up to 75% for NfH^{SMI34} and a 60% decrease for NfH^{SMI35} (Fig. 2.6).

Incubation of the plasma samples in 0.5 M urea-Barb2EDTA buffer at a 1:8 dilution for 1 hour at RT before adding to the ELISA abolished the hook shaped dilution curve and substantially improved parallelism (Fig. 2.7A & 2.7B).

A summary of the final optimised method for the detection of NfH phosphoforms in plasma is shown in Table 2.3. The Table details the protocol which overcomes the lack of parallelism and is therefore suitable for detection of NfH phosphoforms in i) plasma, and ii) small sample volumes.

Figure 2.4

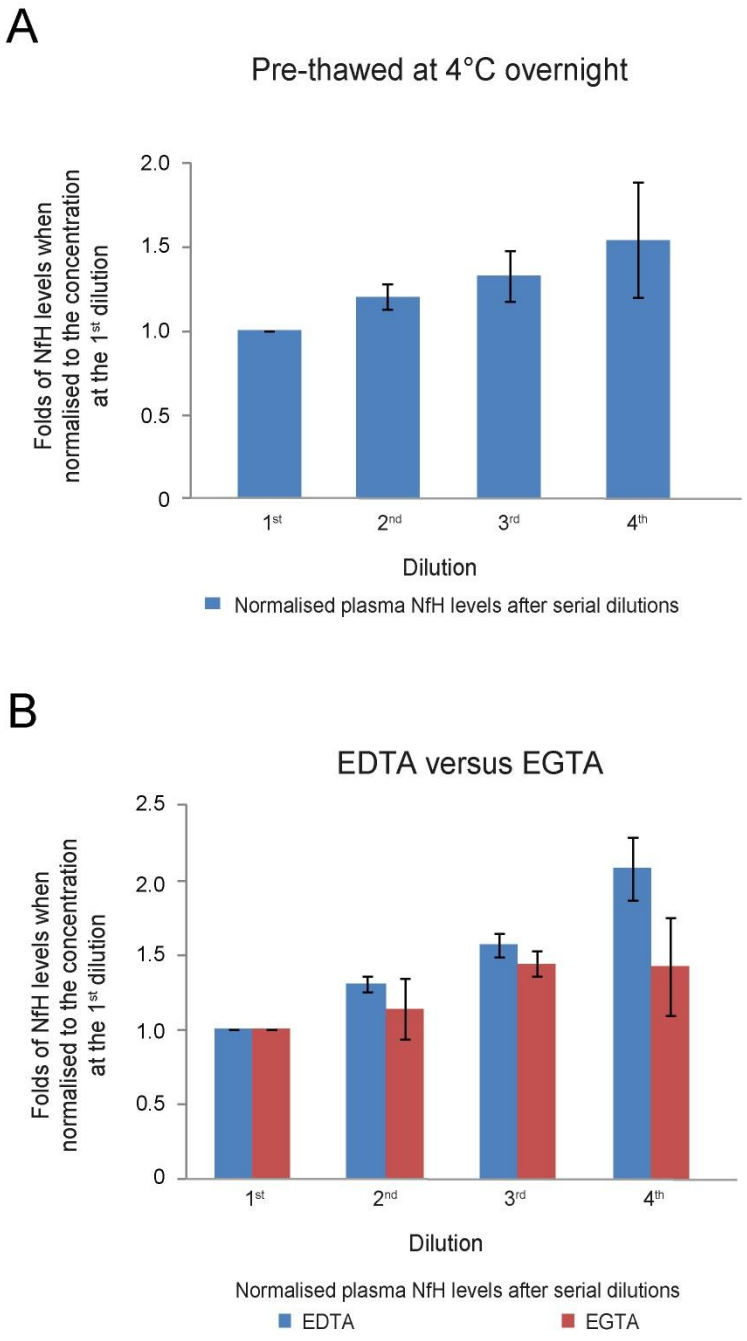

Figure 2.4. The effect of pre-thawing and calcium chelators on disruption of NfH aggregates. Both pre-thawing plasma samples **(A)** and addition of calcium chelators **(B)** reduced the NfH "Hook Effect" observed during doubling dilutions, resulting in an averaged elevation of NfH levels during serial dilution of 36%, 63% and 33% for pre-thawing, EDTA and EGTA, respectively. Error bars: ±SEM.

Figure 2.5

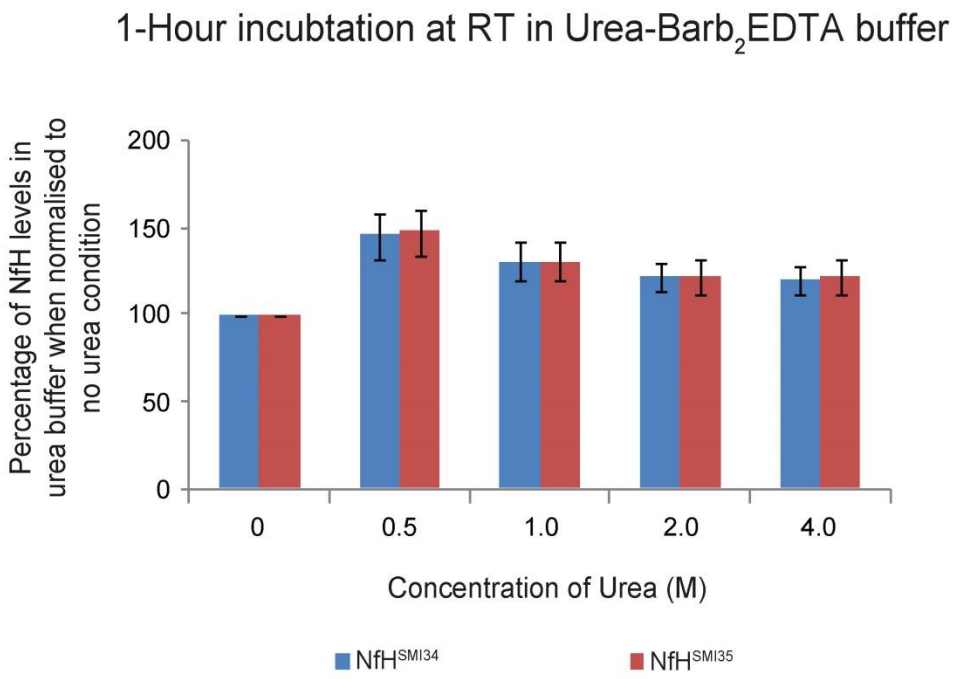

Figure 2.5. The effects of urea at different concentration on NfH levels in plasma of SOD1^{G93A} mice. Plasma levels of both NfH^{SMI34} and NfH^{SMI35} largely increased after 1 hour urea-Barb$_2$EDTA buffer incubation at room temperature, up to 47% at 0.5 M urea. Error bars: ±SEM.

Figure 2.6

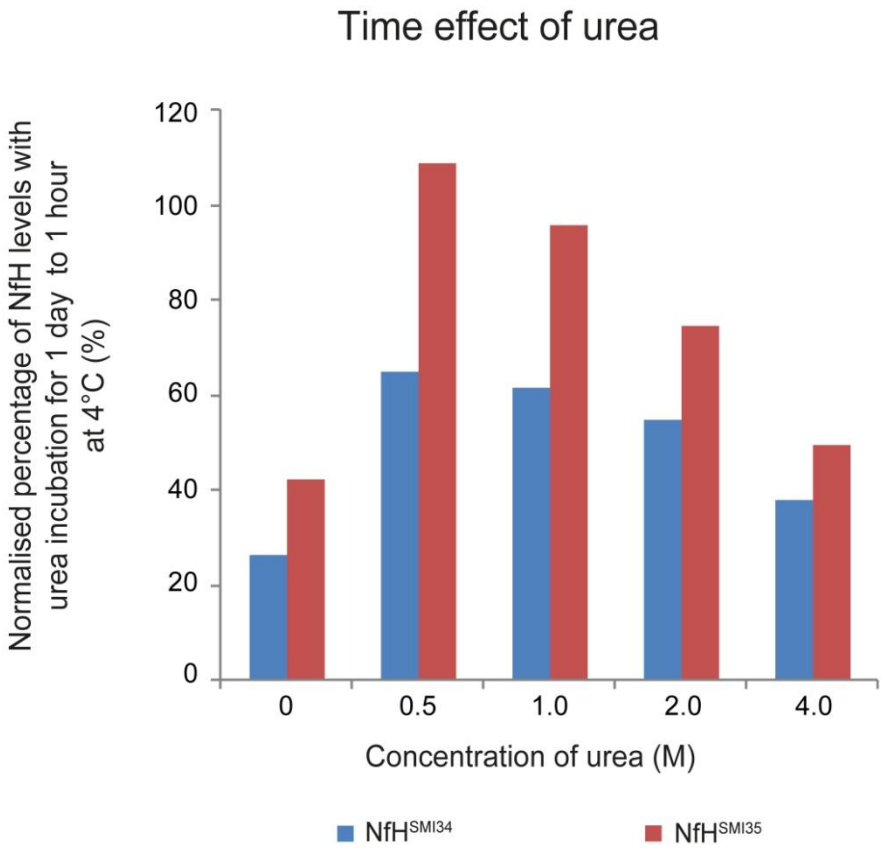

Figure 2.6. The effects of incubation period in $Barb_2EDTA$ buffer with urea at various concentration on NfH levels in plasma of $SOD1^{G93A}$ mice. Levels of NfH^{SMI34} and NfH^{SMI35} largely attenuated after 24-hour incubation at 4°C up to 75% and 60%, respectively.

Figure 2.7

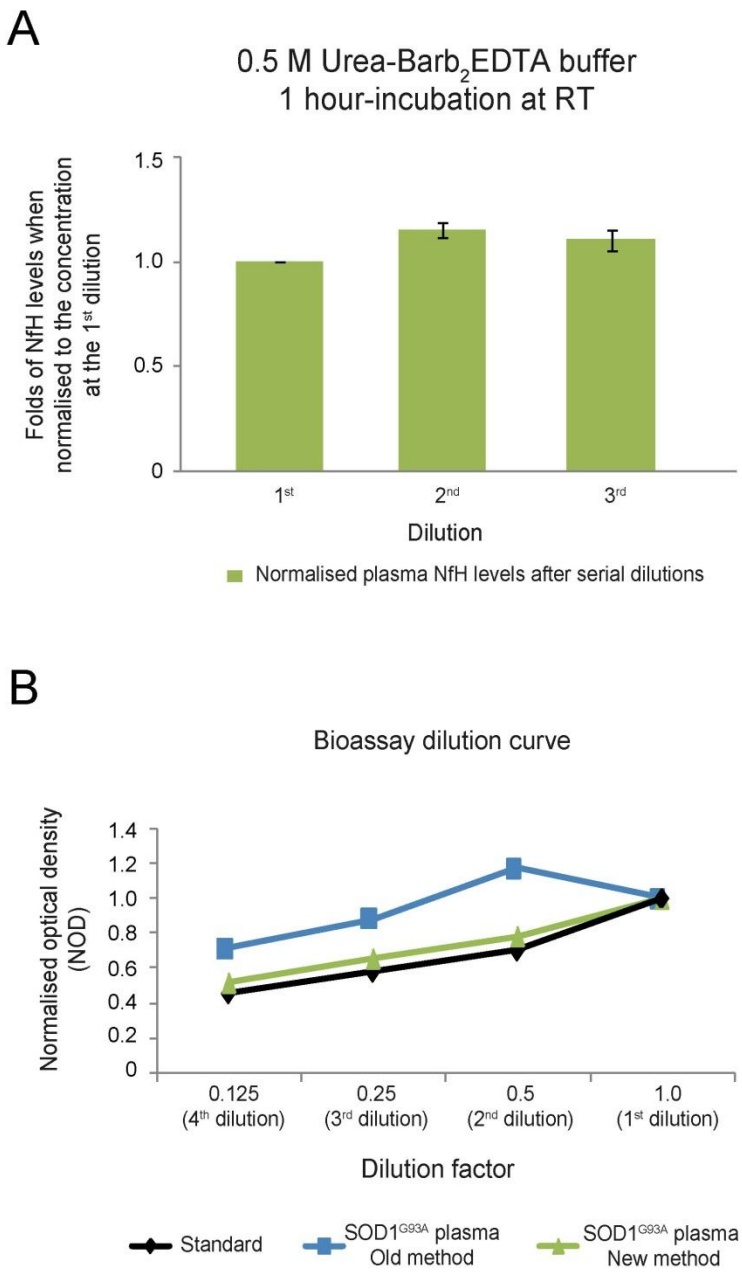

Figure 2.7. The effects of 1 hour incubation of 0.5 M Urea-Barb$_2$EDTA buffer at room temperature on plasma NfH levels in SOD1^{G93A} mice. (A) Using serial dilution of samples, more consistent NfH levels were detected at the 2nd (16%) and 3rd (11%) dilution. **(B)** In addition, the NfH 'Hook Effect' disappeared and parallelism was improved using the new urea-timed method (Incubation in 0.5 M Urea-Barb$_2$EDTA buffer at room temperature for 1 hour). Error bars: ±S.E.M.

Table 2.3 The optimised protocol for an ELISA detecting NfH in the plasma.

Capture antibody	Load 100 µl of Capture antibody (Covance SMI-34R or SMI-35R in carbonate buffer[1]; v/w, 2/10000) into a 96-well microtitre plate*. Incubate the plate at 4°C overnight.
Block the plate	Decant the Capture antibody. Rinse the plate twice with 150 µl wash solution[3]. Block the plate with 100 µl blocking solution4 at RT for 1 hour on the shaker.
Sample preparation	Add 5 µl of original plasma into 35 µl of Barb2EDTA buffer[2] containing 0.5 M urea. Well-mixed and incubate at RT for 1 hour----diluted plasma.
Load the samples	Decant the blocking solution. Rinse the plate twice with 150ul wash solution. Load 95 µl of sample diluent5 into each well of the plate. Apply 5 µl of NfH standard (ranging from 0-100 ng/mL), the diluted and pre-incubated plasma, and the quality control sample in duplicates. Incubate at RT for 1 hour on the shaker.
Detector antibody	Decant the samples. Wash the plate 3 times with 150 µl wash solution for 5 minutes on the shaker. Load 100 µl of detector antibody (Sigma Rabbit anti-neurofilament 200 in sample diluent; v/w, 10/10000) into the plate. Incubate at RT for 1 hour on the shaker.
Reporter antibody	Decant the detector antibody. Wash the plate 3 times with 150 µl wash solution for 5 minutes on the shaker. Load 100 µl of reporter antibody (DAKO Swine anti-rabbit HRP-linked antibody in sample diluent; v/w, 10/10000) into the plate. Incubate at RT for 1 hour on the shaker.
Chemiluminescence readout	Decant the reporter antibody. Wash the plate 6 times with wash solution for 5 minutes on the shaker. Load 100 µl of TMB into the plate. Incubate at RT for 20 minutes on the shaker in the dark. Stop the reaction with 50 µl of 1M HCL. Read the plate at 450 nm, with 750 nm as the reference wavelength.

*All loading volume refers to volume adding into each well of the microtire plate.

[1]Carbonate Buffer (pH 9.6): 13.85g anhydrose sodium carbonate and 26.10g sodium hydrogen carbonate in per litre distilled water

[2]$Barb_2$EDTA buffer (pH 8.6): 13.1g sodium barbitone, 2.1g barbitone, and 0.25g EDTA in per litre distilled water

[3]Wash solution: 0.1% bovine serum albumin (BSA) and 0.05% Tween 20 in $Barb_2$EDTA buffer

[4]Blocking solution: 1% BSA in $Barb_2$EDTA buffer

[5]Sample diluent: 0.1% BSA in $Barb_2$EDTA buffer

2.3.3 A comparison of plasma NfH levels in end-stage SOD1^{G93A} mice with age-matched WT littermates, using the modified in-house ELISA

Using the modified, optimal ELISA described above and detailed in Table 2.3, plasma NfH levels in WT and 120-day-old SOD1^{G93A} mice were next compared. Plasma NfH^{SMI34} levels from SOD1^{G93A} mice (n=10) were significantly higher (median: 304.19.1 ng/mL) than in plasma from age-matched WT littermates (median: 28.33 ng/mL, n=11, p=0.001, Mann-Whitney U test; Fig. 2.8A). A similar pattern was observed for NfH^{SMI35} and in plasma of SOD1^{G93A} mice (n=10) NfH^{SMI35} levels were significantly higher (median: 77.61 ng/mL) than WT levels (median: 13.53 ng/mL, n=10, p=0.019, Mann-Whitney U test; Fig. 2.8B). Examination of WT mouse plasma therefore revealed that this optimised ELISA developed in the experiments developed in this Chapter was also sensitive enough to detect normal levels of plasma NfH in WT mice.

2.4 Discussion

In this Chapter, I examined whether an existing ELISA method, developed for measurement of NfH phosphoforms in CSF was suitable for use in plasma samples. Having confirmed that a clear 'hook shaped curve' prevented accurate measurement of plasma NfH, using end-stage SOD1^{G93A} mouse plasma, I next developed a sensitive in-house ELISA that overcame the NfH 'Hook Effect.' Using this assay, I then established that levels of plasma NfH^{SMI34} and NfH^{SMI35} were elevated in plasma of 120-day-old SOD1^{G93A} mice that model ALS compared to age-matched WT mice and revealed that even WT plasma contains NfH, albeit at low levels.

2.4.1 From CNS to Peripheral circulation

Although the blood-brain barrier and the blood-spinal cord barrier both have a robust effect in limiting CNS-to-blood transfer, molecules expressed in the CNS still may enter the blood under both physiological conditions and also during pathological disruptions of the CNS. One of the commonest pathological hallmarks in ALS is the accumulation of phosphorylated Nf in perikaryon and axonal spheroids (Manetto et al., 1988), as the consequence of a failed protein quality control machinery. Detection of neuron-specific and glia-specific proteins in CSF has been observed in a number of neurodegenerative disorders such as AD, MS and ALS (Brettschneider et al., 2006c; de Jong et al., 2007; Salzer et al., 2010). Therefore it is not surprising that Nfs can enter the circulation system in a mouse model of ALS.

Figure 2.8

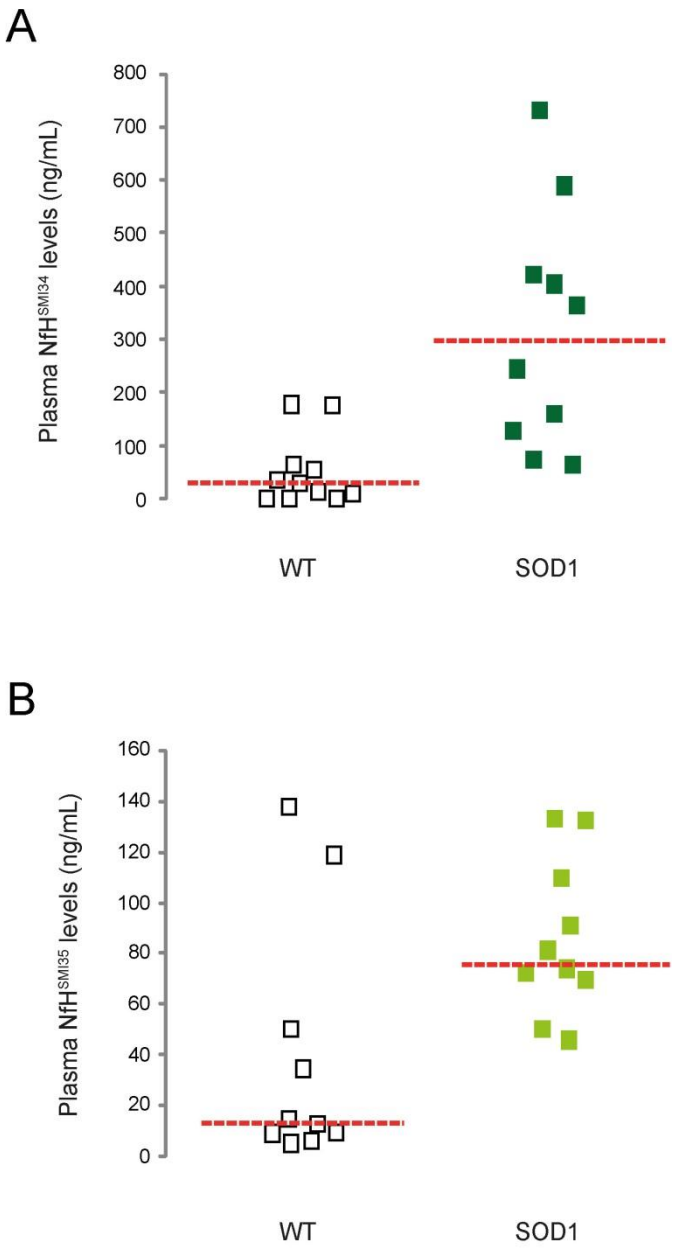

Figure 2.8. NfH levels in plasma of 120 days old SOD1^{G93A} mice compared to WT littermates. (A) NfH^{SMI34} and **(B)** NfH^{SMI35} levels were both significantly elevated in the plasma of SOD1^{G93A} (filled circles) mice at 120 days, compared to levels in WT (open squares) littermates. *: p<0.05, **: p<0.01, ***: p<0.0001, N.S.: p>0.05. Mann-Whitney U test. Red dash lines: median values of each group.

Previous studies have reported significantly higher CSF levels of phosphorylated Nfs in ALS patients compared to both healthy controls and to other neurodegenerative disorders such as Alzheimer's disease (Brettschneider et al., 2006c; Norgren et al., 2003; Rosengren et al., 1996). It is therefore reasonable to hypothesise that similar patterns of Nf levels may be found in the plasma of such patients. In view of the far greater accessibility to plasma and the problems associated with repeated CSF sampling, particularly in patients with severe diseases like ALS, it seems appropriate to develop a sensitive and reliable immunoassay for the quantification of plasma Nf levels. Plasma is clearly a readily accessible body fluid compartment, from where sampling can easily continue during longitudinal follow-up of the disease, causing minimal impact on the quality of like of patients.

2.4.2 A breakthrough for NfH immunoassay

Here I describe a new method for the accurate quantification of NfH levels which overcomes a crucial analytical problem. Researchers have previously experienced significant analytical difficulties with reliable and reproducible quantification of NfH levels in blood samples of mutant SOD1 mice and patients suffering from ALS. A typical example of this problem is illustrated in the results of measurement of NfH levels in serial dilutions of blood shown in Figure 2.2. These data are resembled to the so called 'Hook Effect' when high concentrations of protein (e.g. undiluted samples) produce a decline in the dose response curve, resembling the shape of a hook, and leads to a lack of parallelism between plasma samples and standards (Fig. 2.1 and Fig. 2.2A). This NfH 'hook shaped curve' was not previously observed when measuring NfH levels in CSF samples (Petzold et al., 2003), but has been reported with serial dilutions of homogenate from brain/spinal cord tissue (Petzold, unpublished observations). Because of the 'hook shaped curve' observed in Fig. 2.2, we previously termed the lack of parallelism for NfH from blood samples the NfH 'Hook effect' (Lu et al., 2011). Subsequently, the work presented in this Chapter has since been reproduced independently by pioneering and leading experts in the field on neurofilament proteins and experimental models for ALS (Swarup et al., 2011). Following our protocol, these researchers found a concentration of 0.3 M urea to be optimal for their own in-house ELISA for the use of spinal cord homogenate samples, which is very close the 0.5 M concentration originally described by us.

2.4.2.1 The 'Hook Effect' in Oncology and Endocrinology

The 'Hook Effect', otherwise known as the 'high dose Hook Effect', was first described in the 1970s in a two-site immunoradiometric assay for ferritin (Miles et al., 1974). This effect resulted in low values from undiluted samples with extremely high concentrations of the analytes that saturated both the capture and detector antibodies concurrently, which consequently failed to form the so-called sandwich complex for the final readout. The phenomenon was later widely observed in clinical immunoassays examining hormones and tumour markers, such as prolactin in macroprolactinoma (Frieze et al., 2002; St-Jean et al., 1996), prostate specific antigen (Charrie et al., 1995; Furuya et al., 2001), alpha-fetoprotein in hepatoblastoma (Jassam et al., 2006), and calcitonin in metastatic medullary thyroid carcinoma (Leboeuf et al., 2006). This effect can be overcome by serial sample dilutions to keep the analytes in each well within the detection threshold of immunoassays.

2.4.2.2 Overcoming the NfH 'Hook Effect'

In the first set of experiments in this Chapter, I examined the suitability of the existing method for detection of plasma NfH in $SOD1^{G93A}$ mice that has been used for measuring CSF NfH (Petzold et al., 2003). As can be seen in Table 2.2 for NfH, the assayed values for serial sample dilution increased as the dilution factor increased. However, we found that serial sample dilution itself within detectable limits still failed to give constant analytical results for each sample from $SOD1^{G93A}$ mice as shown in Fig. 2.2B. Furthermore, for NfH there was no antigen excess as in the case of most of the hormone/tumour marker immunoassay. The NfH 'Hook Effect' was therefore considered to be due to endogenous binding. Further immunoblotting confirmed that plasma samples of $SOD1^{G93A}$ mice contain NfH aggregates in the higher molecular range (238-460 kDa) (Fig. 2.3A).

The use of urea to manipulate protein folding and unfolding properties (Saha and Das, 2007; Zangi et al., 2009), as well as protein dynamics and conformational changes such as Nf assembly (Cohlberg et al., 1995; Hisanaga and Hirokawa, 1990; Shea, 1994; Tokutake, 1990) is well established. Not surprisingly, in the experiment described in this Chapter, pre-incubation with urea solubilised the NfH aggregates at a concentration of 4 M (Fig. 2.3A). Since pre-absorption of the primary antibody abolished all the bands in the immunoblot, it is likely that bands below 205 kDa on the blot (Fig. 2.3) represent fragments of NfH rather than unspecific binding. In

addition, previous studies of immunoblotting using SMI-34R and SMI-35R (NfH specific antibodies), have shown no cross-reaction with NfM and NfL (Petzold et al., 2011a), since SMI-34R and SMI-35R are specific for the epitopes in the tail region of neurofilament heavy chain. The densities of these lower molecular bands changed after timed-urea incubation, also suggesting that smaller fragments of NfH were produced during the incubation with urea. Bands at 117 kDa were found coincidently at a similar range to bands detected in brain tissue in patients of traumatic brain injury; these 117 kDa bands were considered as a cleavage product by enterokinase in CNS (Petzold et al., 2011a). Therefore, it is very likely that pre-cleavage of NfH in the CNS occurred prior to the release of NfH into the peripheral blood and was dissembled from the high MW aggregates of NfH after urea incubation.

Nonetheless, 4 M urea was not compatible with the NfH ELISA. By titrating the molar concentration of urea, we found that aggregates could be sufficiently broken up to achieve analytical parallelism at 0.5 M urea. Consistent with the data from previous studies (Kushkuley et al., 2010; Yabe et al., 2001a; Yabe et al., 2001b), the addition of EDTA and EGTA partly disrupted NfH aggregates following 24-hour incubation. Although I did not test longer incubation periods as these make the protocol less practical, but I note that Kushkuley et al., 2009 observed a peak effect of EGTA incubation after 7 days of incubation (Kushkuley et al., 2009). For routine laboratory purposes, shorter (1 hour) incubation periods with 0.5 M urea are preferable to longer (7 days) incubation periods with EGTA.

A similar approach to that used in these experiments, using low dose urea pre-incubation, to overcome NfH 'Hook Effect' in ELISA testing the spinal cord homogenates has also been tested and developed by another group (Swarup et al., 2011).

2.4.3 Plasma NfH levels significantly increase in end-stage SOD1^{G93A} mice that model ALS

Exploiting the ability of urea to release NfH from aggregates, I proceeded to investigate the levels of NfH^{SMI34} and NfH^{SMI35} in an established mouse model of a neurodegenerative disease, the SOD1^{G93A} mouse model of ALS. Plasma was collected near to disease end-stage, at 120 days of age, and NfH levels were compared to levels in control, age- and sex-matched WT mice. The first conclusion

that can be drawn from these experiments is that the assay was sensitive enough even to detect very low levels of NfH in WT mice, both hyperphosphorylated and variably-phosphorylated NfH (Fig. 2.8). This is an important methodological improvement compared to previous studies (Boylan et al., 2009; Petzold et al., 2003) where plasma NfH levels in WT mice were undetectable using conventional NfH ELISA. The method developed in this Chapter also disrupts NfH aggregates and overcomes the problem of endogenous binding, thereby abolishing the 'Hook Effect' and improving analytical sensitivity, reliability and reproducibility. This finding suggests firstly that plasma is a compartmentalised bio-fluid where neurofilaments ultimately appear following intracellular clearance from the CNS, not only under pathological conditions but also under normal physiological conditions. Secondly, the existence of hyperphosphorylated NfH in plasma itself is not a pathological indicator since it is present even in WT undiseased mice, although it has long been thought to be abundant in pathological conditions (Perrot et al., 2008). In view of this finding, it is clear that the detection of NfH in plasma is not disease specific and therefore not of diagnostic value for ALS or any other neurodegenerative disease.

In 120-day-old $SOD1^{G93A}$ mice, the median plasma NfH^{SMI34} (hyperphosphorylated) and NfH^{SMI35} (variably-phosphorylated) forms of NfH levels were 10.7-fold and 5.7-fold higher in $SOD1^{G93A}$ mice compared to WT controls, respectively. This elevation in NfH levels is consistent with the known motor neuron and motor axon degeneration which is a feature of the $SOD1^{G93A}$ mouse model of ALS, resulting in the release of Nf into the blood. Previous studies have shown that by 120 days of age in male $SOD1^{G93A}$ mice, approximately 70% of motor neurons have died (Kalmar et al., 2008). In addition, the differential alteration of the two forms of NfH observed in this study is consistent with immunohistochemical evidence showing a pathological increase in perikaryal accumulation of phosphorylated Nf in ALS (Manetto et al., 1988; Wong et al., 2000). The chemical properties of Nf aggregate formation and dissociation have been intensively investigated and phosphorylation of NfH has been found to be a key feature facilitating Nf formation (Kushkuley et al., 2009; Kushkuley et al., 2010). This finding is in line with my data showing that the increase in hyperphosphorylated NfH (NfH^{SMI34}) from NfH aggregates was much more than that of the less phosphorylated NfH (NfH^{SMI35}).

2.4.4 Conclusions

The results presented in this Chapter describe the development of an in-house ELISA for the detection of two phosphoforms of NfH in plasma. This method is a substantial improvement on existing immunoassays for the detection of NfH phosphoforms since it: i) overcomes the 'Hook Effect'; ii) is highly sensitive; iii) is reproducible, and iv) is suitable for detection of NfH in plasma.

- Some of the results described in this Chapter have been published.
  Ching-Hua Lu, Bernadett Kalmar, Andrea Malaspina, Linda Greensmith, Axel Petzold. (2011). A method to solubilise protein aggregates for immunoassay quantification which overcomes the neurofilament "hook" effect. Journal of Neuroscience Methods, 195, 143-150.

Chapter 3

Plasma neurofilament heavy chain levels correlate with disease progression and are biomarkers of treatment response in SOD1^{G93A} mouse model of ALS

3.1 Introduction

In Chapter 2, I described the development of a quantitative, sensitive immuoassay that can reliably detect NfH phosphoforms in plasma from SOD1^{G93A} mice. In this Chapter, using this mouse model of ALS as a test-bed, I examined whether plasma NfH levels could be used to monitor disease progression and the effects of disease modifying treatments in SOD1^{G93A} mice.

3.1.1 The need for biomarkers in ALS

Riluzole remains the only FDA-approved treatment for ALS, which prolongs median survival by only 2-3 months in patients treated for at least 18 months (Miller et al., 2007). Importantly, the greatest benefit of Riluzole is observed when treatment is initiated early in the course of disease (Zoing et al., 2006). In the absence of reliable diagnostic biomarkers, the recognition of ALS relies largely on clinical assessment and electrophysiological findings, which provide evidence of upper and lower motor neuron involvement (Carvalho and Swash, 2009). The lack of more specific investigative tools and of easily measurable biomarkers typically results in a 9-14-month delay between symptom onset to diagnosis, for both sporadic (sALS) and familial ALS (fALS) (Cellura et al., 2012; Iwasaki et al., 2002). This delay not only prevents patients from receiving early administration of Riluzole, reducing the benefit of the only available therapy, but also impedes their early recruitment to clinical trials, thereby reducing the likelihood of success of potential disease-modifying agents. Therefore, there is a critical need to develop biomarkers for ALS, to both speed up diagnosis and to monitor disease progression. This is particularly true for clinical trials, where such a biomarker would be invaluable for statistical power and as an indicator of both positive and negative responses to treatment.

3.1.2 Neurofilament Heavy Chain (NfH) as a candidate biomarker for ALS

Although the precise underlying pathology of ALS is not yet fully understood, a number of molecular mechanisms have been identified that play a part in ALS both in humans and in mouse models of the disease (see Chapter 1 Section 3). Transgenic mice carrying the mutant human superoxide dismutase 1 *(SOD1)* gene

which is responsible for approximately 10-20% of familial ALS cases (Rosen et al., 1993), have a disease phenotype that resembles that of ALS patients, including progressive motor neuron degeneration accompanied by gradual muscle paralysis and premature death (Gurney et al., 1994). These mice have been invaluable in research efforts to evaluate several pathological changes that contribute to ALS. ALS is now known to be a multifactorial disorder, and protein aggregation plays an important role in its pathophysiology (Bento-Abreu et al., 2010). Several proteins have been shown to aggregate in tissues of ALS patients and animal models of ALS, including structural proteins of the axonal cytoskeleton such as neurofilaments (Strong et al., 2005). A common pathological finding in both sALS and fALS is the accumulation of phosphorylated Nfs in the perikaryon and in axonal spheroids, which are normally only present in distal axons and nerve terminals (Manetto et al., 1988). NfH has been implicated in the pathogenesis of ALS also based on genetic investigations. A small number of allelic variants of the *NEFH* gene have been identified in approximately 1% sALS patients (Al-Chalabi et al., 1999; Figlewicz et al., 1994), Manipulations of the stoichiometry of the three Nf subunits has been shown to facilitate the development of early-onset motor neuron death in transgenic mouse models of ALS (Cote et al., 1993; Lee et al., 1994; Xu et al., 1993), thus supporting the critical involvement of Nfs in ALS pathology.

The measurement of specific components of the affected tissue which are released into biological fluids during disease progression can be used to aid diagnosis and evaluate/predict disease severity in ALS (Ganesalingam and Bowser, 2010; Otto et al., 2012; Sussmuth et al., 2008). It has also been suggested that the phosphorylation state of Nfs can be indicative of neuronal pathology and high levels of phosphorylated NfH have been detected in neurodegenerative disorders (Perrot et al., 2008). Nfs levels in the CSF have been investigated as potential disease biomarkers in several neurological disorders (Brettschneider et al., 2006a; Brettschneider et al., 2006b; Constantinescu et al., 2009; de Jong et al., 2007; Ganesalingam et al., 2011; Norgren et al., 2003; Rosengren et al., 1996; Salzer et al., 2010; Zetterberg et al., 2007). However, because of its invasive nature, serial CSF sampling is not tolerated by all patients and CSF is clearly not the ideal bio-fluid for repeated sampling in order to monitor progression and evaluate treatment response in frail and advanced ALS patients. Thus, a functionally validated Nf-based blood biomarker for the longitudinal monitoring of disease development and informative of treatment response would be highly desirable.

3.1.3 Current and potential therapeutics tested in SOD1^{G93A} mice

It would be highly valuable if a biomarker can reflect the beneficial or detrimental effect of a testing drug so that it can be used as a surrogate outcome measure in the clinical trial. In this Chapter, whether the expression levels of plasma NfH reflect the effects of known and novel therapeutics was examined in SOD1^{G93A} mice.

3.1.3.1 Riluzole

Riluzole is the only FDA approved drug for ALS and has a modest effect on the progression of ALS. However, there is limited information about the effect of this drug in animal models of ALS. Its mechanism of action is not fully understood, although it is generally believed to inhibit glutamate release and reduce excitotoxicity (Nirmalananthan and Greensmith, 2005). A number of studies have suggested that Riluzole may also has an effect in up-regulating the HSR in the cells, and has been shown to increase the active form of HSF1 under physiological conditions in Hela cells (Yang et al., 2008). A more recent study has suggested that Riluzole can increase amount of HSF1 by slowing down the turnover rate of HSF1 and concurrently, via HSF1, may also increase the activity of the Glial Glutamate Transporter 1 (GLT1) promoter, which contains multiple Heat Shock Elements (HSE), leading to increased expression of GLT1 protein, Hsp70 and Hsp90 (Liu et al., 2011). Overall, these experiments have demonstrated a potentially synergistic effect of the various routes through which Riluzole can promote neuronal survival under stress (Liu et al., 2011).

3.1.3.2 Arimoclomol

Arimoclomol is a hydroximic acid derivative which acts as an amplifier of Hsp expression by stabilisation of the active phosphorylated trimer of HSF1 and prolongation of the binding of HSF1 to HSE, which encodes a number of major Hsps in response to cell stresses (Crul et al., 2013). Importantly, compounds in the Arimoclomol family act as a ‘smart drugs’ to co-induce the HSR, but only in cells already under stress (Hargitai et al., 2003; Kalmar and Greensmith, 2009), which is an important characteristic when considering their use as therapeutic agents in humans.

In the SOD1^{G93A} mouse model of ALS, daily intraperitoneal administration of Arimoclomol prolonged survival by 22% and 18%, when the treatment started from pre-symptomatic stage and at disease onset, respectively (Kieran et al., 2004).

Arimoclomol-treated SOD1^{G93A} mice treated pre-symptomatically also presented with a displayed a delay of disease onset, showed improved hindlimb neuromuscular functions and spinal motor neuron survival at end-stage. Whether given at symptom onset (75 days of age), when the loss of body weight is the only disease manifestations (Kieran et al., 2004) or later, at 90 days of age when SOD1 mice have lost 40% of their sciatic motor neurons (Hegedus et al., 2007; Sharp et al., 2005), Arimoclomol-treated SOD1^{G93A} mice had significantly improved hindlimb muscle strength and an increased number of motor units and spinal motor neurons compared to untreated animals (Kalmar et al., 2008).

It has become clear that non-neuronal cells that interact with motor neurons, particularly glial cells within the CNS, play a critical role in disease progression in ALS (Appel et al., 2011; Clement et al., 2003; Phatnani et al., 2013). Astrocytes are known to have a robust HSR and up-regulate Hsps in response to stress (Batulan et al., 2003; Choi et al., 2011; Imuta et al., 1998). This effect can be further augmented by Arimoclomol following peripheral nerve injury (Kalmar et al., 2002). It is therefore possible that the increased expression of Hsps within astrocytes observed following treatment with Arimoclomol, results in an improved function of the astrocytes themselves, which in turn acts to support and protect vulnerable motor neurons.

In addition to their interaction with non-neuronal cells within the CNS, motor neurons also interact with their target muscle fibres in the periphery. The very first physical manifestation of disease in ALS occurs at the neuromuscular junction (NMJ), much earlier than the degeneration of motor neuron in both ALS mouse models and in ALS patients (Fischer et al., 2004; Frey et al., 2000; Kalmar et al., 2012b). It has been shown that the first signs of the disease-modifying effects of Arimoclomol in SOD1^{G93A} mice manifest in the muscle, at an early pre-symptomatic stage, rather than the spinal cord, where Arimoclomol-induced up-regulation of Hsps only occurs later in the disease (Kalmar et al., 2012b). Treatment with Arimoclomol improves muscle innervation as well as markers of neuromuscular transmission in SOD1^{G93A} mice, prior to any central effect on the HSR within the spinal cord, indicating an early peripheral effect of this Hsp-based therapy in ALS (Kalmar et al., 2012b). Similar beneficial effects of systemic treatment with a single Hsp have also been reported in SOD1^{G93A} mice, following intraperitoneal injection with recombinant Hsp70 protein (Gifondorwa et al., 2012).

The broad-based effect of Arimoclomol may be an effective approach in the development of a disease-modifying therapy for ALS. Arimoclomol has also been tested in humans. Seven Phase I studies in healthy volunteers have established that Arimoclomol has no significant effect of food or fasting on the pharmacokinetics or tolerability (Lanka et al., 2009). The Phase IIa clinical trial showed oral administration of Arimoclomol is safe and well-tolerated up to 300mg/day, with a good level of CSF penetration (Cudkowicz et al., 2008). A Phase II/III trial is currently undergoing in patients with *SOD1*-related fALS (NCT00706147).

3.1.3.3 Cogane

Cogane (Phytopharm plc) is an orally bioavailable neurotrophic factor inducer that readily crosses the blood brain barrier. Cogane has been shown to be neuroprotective in a model of Parkinson's disease, where it induces the expression of brain-derived neurotrophic factor (BDNF) and glial cell line-derived neurotrophic factor (GDNF) (Visanji et al., 2008). In ALS, treatment with Cogane from the onset of symptoms around 70 days of age has shown beneficial effects in improving hindlimb muscle functions and motor neuron survival in $SOD1^{G93A}$ mice (Kalmar et al., 2012a).

3.1.4 Hypotheses and Aims

In this Chapter, I tested the hypothesis that plasma NfH levels may be a biomarker of disease progression in ALS and may be used to monitor the effects of disease modifying agents in $SOD1^{G93A}$ mice. For this purpose, I undertook a series of experiments with the following Aims:

i) To establish whether plasma NfH levels increase with disease progression in the $SOD1^{G93A}$ mouse model of ALS;

ii) To investigate whether increased plasma NfH levels correlate with physiological and morphological changes linked to disease progression in $SOD1^{G93A}$ mice;

iii) To test whether the NfH ELISA developed in the experiment phase of this project and presented in Chapter 2, was sensitive enough to detect the effects of an established and potential disease-modifying therapies in $SOD1^{G93A}$ mice;

iv) To assess whether the method was suitable for use in monitoring disease progression in less aggressive form of ALS, using an alternative mouse model of ALS.

3.2 Methods and Materials

3.2.1 Experimental animals

All animals were bred and maintained by Biological Services in the UCL Institute of Neurology. The experiments described in this study were carried out under licence from the UK Home Office and following approval from the UCL Institute of Neurology's Ethical Review Panel. In these experiments, I examined plasma NfH levels in the most widely used SOD1 mouse model of ALS, the high copy SOD1^{G93A} strain. In addition, in some experiments, plasma NfH levels were also examined in a more slowly progressing SOD1 model, the SOD1^{G93Adl} strain.

3.2.1.1 Breeding of SOD1^{G93A} mice

Transgenic mice expressing human SOD1^{G93A} mutant protein (TgN[SOD1-G93A]1Gur; Jackson Laboratories, Bar Harbour) were maintained by breeding male heterozygous carriers with female (C57BL/6 x SJL) F1 hybrids. The presence of the SOD1^{G93A} mutation was confirmed by PCR reaction from ear biopsies in all mice, at the age of 3 weeks (see Chapter 2, Section 2.1.1).

The high copy strain SOD1^{G93A} mice have approximately 25 copies of the mutant transgene. Most of the experiments discussed in this Chapter were undertaken using this strain of SOD1 mice. However, this strain has a very aggressive disease and progresses very rapidly after symptom onset. Therefore, in addition to measuring plasma NfH levels in the high copy strain of SOD1 mice, in one set of experiments I also examined plasma NfH in SOD1^{G93Adl} B6 (SOD1^{G93Adl}) mice

3.2.1.2 SOD1^{G93Adl} mice

The SOD1^{G93Adl} mice have a number of transgene copies of 8-10 and display a slower course of disease than the high copy strain, so that end-stage is reached by 37.8 weeks. These mice have been comprehensively characterised (Acevedo-Arozena et al., 2011). In this study, plasma NfH levels in SOD1^{G93Adl} mice were examined before they met their study end-point, at 38 weeks of age.

3.2.2 Drug treatment

In this Chapter, I examined the possibility that changes in plasma NfH levels are significant enough to reflect the effects of agents that modify disease progression in SOD1^{G93A} mice. In the first test, I examined NfH levels in SOD1^{G93A} mice that were treated with Arimoclomol, a pharmaceutical compound with proven efficacy in SOD1^{G93A} mice (Kalmar et al., 2008; Kieran et al., 2004). In a separate preclinical trial of a novel compound with unknown efficacy in SOD1 mice, I examined the utility of plasma NfH levels as a biomarker of drug efficacy to establish whether changes in plasma NfH levels could reflect the positive or negative effects of a new test compound. In this trial a novel compound called Cogane was under treatment and as part of this preclinical trial some mice were also treated with Riluzole, the standard ALS treatment, either alone or in combination with Cogane. Therefore, in different experiments in this Chapter, mice were treated with the following compounds:

i) Arimoclomol (a kind gift of Biorex R&D Co., Hungary) was dissolved in sterile saline (2mg/mL) and the solution stored at 4°C for a maximum of 1 week; mice were treated with a dose of 10mg/Kg/day via intra-peritoneal (i.p.) injection;
ii) Cogane (Provided from Phytopharm plc) was dissolved into food pellets for mice, achieving an oral dose of 30mg/Kg/day;
iii) Riluzole hydrochloride (from TOCRIS) was dissolved into drinking water, achieving an oral dose of 30mg/Kg/day;
iv) Vehicle: a) sterile saline, i.p. for Arimoclomol trial;
b) normal chow or drinking water for Cogane trial.

3.2.3 Arimoclomol trial

In the first treatment trial the effect of Arimoclomol on NfH levels in SOD1^{G93A} mice was examined. In order to obtain the maximum blood sample volume from mice aged between 65-120 days whilst still complying with the UK Home Office Regulations (less than 15% of the blood volume should be removed in any 30-day period, i.e. 10.5 ml/kg) (Wolfensohn, 2003), only **male** mice were examined in this part of study.

3.2.3.1 Experimental groups in Arimoclomol trial

Depending on genotype, the mice were randomly assigned to one of 3 treatment groups:

i) Transgenic mice carrying human SOD1^{G93A} mutant gene treated daily with Arimoclomol (10mg/Kg; i.p.) from 35 days of age (SOD1+A mice);
ii) Transgenic mice carrying human SOD1^{G93A} mutant gene treated daily with vehicle (i.p.) from 35 days of age (SOD1 mice);
iii) Untreated, age-matched WT littermates (WT mice).

3.2.3.2 Longitudinal plasma sampling in Arimoclomol treated SOD1^{G93A} mice

The effect of Arimoclomol on plasma NfH levels was longitudinally examined in,
i) Arimoclomol treated SOD1^{G93A} mice (SOD1+A; n=19);
ii) Vehicle treated SOD1^{G93A} mice (SOD1; n=19);
iii) Untreated wild-type (WT; n=13).

The mice were repeatedly examined at various stages of disease progression ranging from pre-symptomatic to end-stage disease, i.e. 65 days; 90 days; 105 days; 120 days.

3.2.4 Cogane Trial

Cogane (5β,20α,25R-spirostan-3β-ol) is a novel small molecule, orally bioavailable neurotrophic factor inducer, which has shown beneficial effects in a mouse model of Parkinson's disease (Visanji et al., 2008) and ALS (Kalmar et al., 2012a). In this study, the effect of a novel agent, Cogane, on plasma NfH levels was examined in test experiments, using Riluzole as the standard treatment arm.

3.2.4.1 Experimental groups in Cogane trial

All treatment was given to **female** SOD1^{G93A} mice from 70 days of age, at the time of symptom onset.

i) Group COG: Mice treated with Cogane, 30mg/kg/day (in food);
ii) Group COG+RIL: Mice treated with Cogane, 30mg/kg/day (in food) in addition to Riluzole, 30mg/kg/day (in drinking water);
iii) Group RIL: Mice treated with Riluzole, 30 mg/kg/day (in drinking water);
iv) Group VEH: Vehicle treatment of normal chow for Cogane or normal drinking water for Riluzole.

3.2.4.2 Longitudinal plasma sampling in Cogane trial

The effect of Cogane on plasma NfH levels was longitudinally examined in,

i) Cogane treated SOD1^{G93A} mice (COG; n=16);
ii) Cogane plus Riluzole treated SOD1^{G93A} mice (COG+RIL; n=17);
iii) Riluzole treated SOD1^{G93A} mice (RIL; n=15);
iv) Vehicle treated SOD1^{G93A} mice (VEH; n=12).

The mice were repeatedly examined at two stages of disease progression after symptom onset, i.e. 105 days; 120 days.

3.2.5 Plasma Collection

Blood sampling was carried out in mice from each experimental group at various stages of disease, ranging from pre-symptomatic, early-symptomatic, late-symptomatic and end stage disease. At each sampling time point before mice reached their end stage, the mice were placed in a recovery chamber (Peco Service; V1200), set at 38.5°C, for 15 minutes and then transferred into a plastic tube with the tail exposed. Blood was collected from the tail veins into an EDTA-coated tube (BD Microtainer®, K2E). In mice at end stage (87.5% at 120 days [range between 111-121 days] for SOD1^{G93A} mice and 36±2 weeks for SOD1^{G93Adl} mice), blood was collected by a cardiac puncture, under terminal anaesthesia using pentobarbital. Each tube was then centrifuged at 14,000 rpm for 8 min. The plasma was collected and protease inhibitor added (Sigma; v/v: 1/100). Each sample was then aliquoted and stored at -80°C until further analysis.

3.2.5.1 Plasma collection in Arimoclomol Trial

All experimental animals received blood sampling at age 65, 90, 105 and 120 days.

3.2.5.2 Plasma collection in Cogane Trial

All experimental animals received blood sampling at age 105 and 120 days.

3.2.5.3 Plasma collection in SOD1^{G93Adl}

Blood samples were taken every month between 22 weeks of age and their end-stage (36±2 weeks) where possible. Although samples were collected from 15 mice, not all of them were available for serial samplings of plasma at all stages of disease progression. Although it would have been very desirable to also have samples from the WT littermates of these SOD1^{G93Adl} mice, they were not available at the time of

collection as that original study was not set-up for biomarker study and I only started to collect samples from quite late stage of that original study.

3.2.6 Functional assessments of neuromuscular functions

In this Chapter, levels of plasma NfH levels were correlated with established markers of disease progression in SOD1^{G93A} mice, using behavioural, physiological and morphological readouts of disease progression.

3.2.6.1 Longitudinal assessment of Grip Strength

In the same mice selected for plasma collection, grip strength was determined longitudinally at the same ages, immediately prior to blood collection, according to the manufacturer's instruction (Bioseb, BIO-GS3). Mice were placed on a horizontal grid and pulled by the tail against the direction of the force gauge until the animal released the grid. An average of four readings for each mouse was obtained at each occasion.

3.2.6.2 Acute *in vivo* physiological assessment of muscle force

In a separate set of mice, physiological analysis of hindlimb muscle function was undertaken at 105 days of age, corresponding to a late symptomatic stage of disease. WT (muscle n=10), SOD1 (muscle n=12) and SOD1+A (muscle n=16) mice were deeply anesthetised (4.5% chloral hydrate; 1 ml/100g of body weight, i.p.) and prepared for in vivo analysis of isometric muscle force (as described in Kalmar et al., 2008). The distal tendons of the Tibialis Anterior (TA) and Extensor Digitorum Longus (EDL) muscles in both hindlimbs were dissected free and attached by silk thread to isometric force transducers (Dynamometer UFI Devices, Welwyn Garden City, UK). The sciatic nerve was exposed and sectioned. The length of the muscles was adjusted for maximum twitch tension. The muscles and nerve were kept moist with saline throughout the recordings and all experiments were carried out at room temperature. Isometric contractions were elicited by stimulating the nerve to TA and EDL using square-wave pulses of 0.02 ms duration at supra-maximal intensity, via silver wire electrodes. Contractions were elicited by trains of stimuli at frequencies of 40, 80 and 100 Hz. The maximum twitch and tetanic tension was measured using a computer and appropriate software (PicoScope).

3.2.6.3 Acute *in vivo* physiological assessment of motor unit survival

The number of motor units innervating the EDL muscles was also determined by stimulating the motor nerve with stimuli of increasing intensity, resulting in stepwise increments in twitch tension due to successive recruitment of motor axons with increasing stimulus thresholds. The number of stepwise increments was counted to give an estimate of the number of functional motor units (MUNE) present in each muscle.

3.2.7 Morphological assessment of motor neuron survival

Following physiological assessment of muscle function, the mice (n=5 per group) were terminally anaesthetised and perfused transcardially with saline followed by fixative containing 4% paraformaldehyde (PFA). The spinal cords were then removed and post-fixed in 4% PFA and cryopreserved in 30% sucrose overnight at 4°C. Transverse sections (20 µm) of the fixed lumbar spinal cords (L3-L6) were cut on a freezing cryostat and collected serially onto glass slides and subsequently stained for Nissl (gallocyanin). Large polygonal neurons, with a minimum diameter of 20 µm, within the sciatic motor pool, which had a clear nucleolus and a distinct Nissl-dense cytoplasm were counted in every 3rd section, in order to prevent counting the same neuron twice in consecutive sections (McHanwell and Biscoe, 1981).

3.2.8 NfH ELISA

For a full description of the 4-layer sandwich ELISA and the reagents used in these experiments see the detailed method outlined in Table 2.3, Chapter2.

3.2.9 ELISA Data analysis

Hyperphosphorylated NfH was detected with the SMI-34R capture antibody labelled as NfH^{SMI34} (averaged intra-assay coefficient of variation (CV): 3.53%, averaged inter-assay CV: 3.01% at 12.5 ng/mL), while variably phosphorylated NfH was detected with the SMI-35R capture antibody, labelled as NfH^{SMI35} (averaged intra-assay CV: 3.03%, averaged inter-assay CV: 5.87% at 12.5 ng/mL). The sensitivity (blank + 3SD) of the assay calculates to 0.74 ng/mL, with a detection limit of 1.56 ng/mL. Measurements with a CV value higher than 10% (Petzold et al., 2003) were repeated. Quality control samples were used throughout and absorbance readouts from different microtitre plates were adjusted to the quality control readout to allow comparison of results across different plates.

3.2.10 Statistical analysis

3.2.10.1 Longitudinal Biomarker and Arimoclomol treatment study

The results from the study in which NfH phosphoforms levels were determined at different ages in $SOD1^{G93A}$ mice in vehicle-treated and arimoclomol-treated mice were statistically analysed using SPSS software (V17). The normality of data was checked, using a Kolmogorov-Smirnov test, to determine the approach of parametric or nonparametric analysis. The repeated Friedman test was used for analysis of NfH levels within groups in the longitudinal biomarker study. The Mann-Whitney test or t-test, according to the normality of data, was used for analysis of NfH levels between groups at each time point (WT vs. SOD1; SOD1 vs. SOD1+A), and for analysis of the levels of the two NfH phosphoforms in each group, at different time points (NfH^{SMI34} vs. NfH^{SMI35}). Bivariate correlation analysis, using Spearman's correlation coefficient, was examined for plasma NfH levels and grip strength. A minor, moderate and strong correlation is considered if Spearman's rho (R) is <0.3, 0.3-0.5, >0.5, respectively. Statistical significance was set at $p<0.05$. Exponential analysis was used to determine the correlation of plasma NfH levels and functional readouts in SOD1 mice at various disease stages. A strong correlation was considered when the coefficient of determination (R^2) obtained from the exponential analysis was greater than 0.8.

3.2.10.2 $SOD1^{G93Adl}$ study and $SOD1^{G93A}$ Cogane drug trial

For a comparison of the data obtained in the Cogane drug trial and that obtained in the study examining NfH phosphoforms levels in an alternative mouse model of ALS, the $SOD1^{G93Adl}$ mice, the data were statistically analysed using the Mann-Whitney U test for group comparison using SPSS (v20). A p value <0.05 is considered as significant.

3.3 Results

In this Chapter, the Results of 4 studies are presented:

i) A longitudinal assessment of plasma NfH levels during disease progression in $SOD1^{G93A}$ mice to establish whether plasma NfH levels correlate with markers of decline in neuromuscular function;

ii) An examination of whether the beneficial effect of an established disease-modifying therapy, Arimoclomol, is reflected in changes in plasma NfH levels in $SOD1^{G93A}$ mice;

iii) An investigation of plasma NfH levels in a trial of a new therapeutic agent in $SOD1^{G93A}$ mice to establish whether plasma NfH levels predict efficacy of new agents;

iv) Examination of plasma NfH levels in an alternative mouse model of ALS to determine whether the ELISA assay developed in Chapter 2 was of use in models other than $SOD1^{G93A}$ in which it was developed.

3.3.1 Plasma NfH levels in $SOD1^{G93A}$ mice increase significantly from a late symptomatic stage

In the first set of experiments, I examined longitudinal changes in plasma NfH levels at various stages of disease progression in $SOD1^{G93A}$ mice, using the ELISA developed in Chapter 2.

Hyperphosphorylated (NfH^{SMI34}) and variably-phosphorylated (NfH^{SMI35}) NfH levels in plasma from mice in each experimental group were determined at various stages of disease. Figure 3.1A shows the level of plasma NfH^{SMI34} in individual WT (black squares) and SOD1 (green circles) mice at 65, 90, 105, and 120 days of age, and Fig. 3.1B shows the mean plasma NfH^{SMI34} levels in WT and SOD1 mice at each age. As can be seen in Fig. 3.1, hyperphosphorylated NfH^{SMI34} was detected in plasma of WT mice, but the levels remained unchanged during the duration of the study, up to 120 days of age (Friedman test, $p=0.518$). In contrast, in SOD1 mice, there was a significant increase in NfH^{SMI34} levels during disease progression (Friedman test, $p<0.0001$). Plasma NfH^{SMI34} levels were higher in SOD1 mice than in WT littermates at all ages examined, although this difference only reached statistical significance from 105 days of age onwards (65 days: SOD1 46.2±13.1 ng/mL, WT 40.6±8.9 ng/mL; 90 days: SOD1 81.8±15.8 ng/mL, WT 52.7±12.2 ng/mL; 105 days: SOD1 155.4±19.3 ng/mL, WT 26.7±6.8 ng/mL, $p<0.0001$; 120 days: SOD1 328.4±40.3 ng/mL, WT 43.5±17.3 ng/mL, $p<0.0001$; mean±S.E.M ng/mL; Mann-Whitney test; Fig. 3.1).

Levels of the variably-phosphorylated NfH^{SMI35} were also examined. Figure 3.2A

Figure 3.1

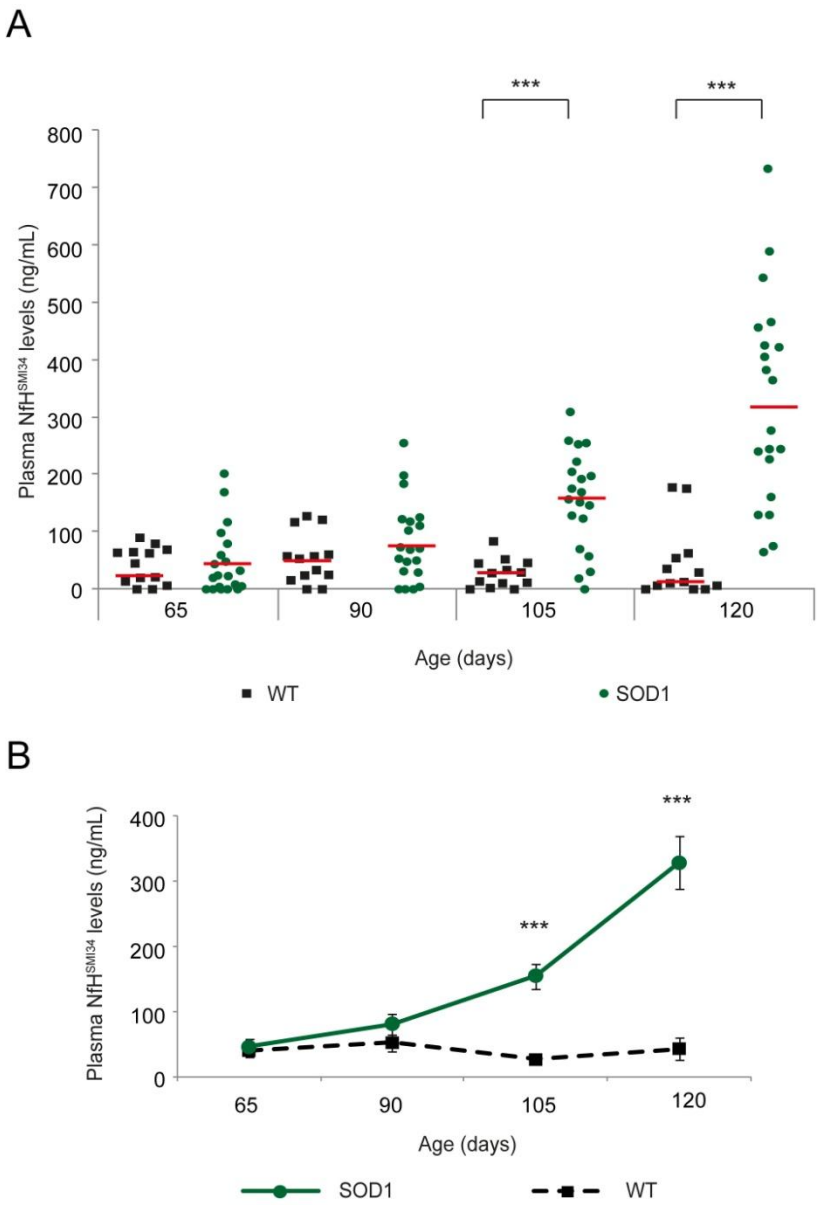

Figure 3.1. Longitudinal assessment of plasma NfH^{SMI34} levels in WT and SOD1 mice. The graphs show the plasma level (ng/mL) of NfH^{SMI34} in **(A)** individual mice and in **(B)** the mean values in SOD1 (green circles; n=19) and WT (black squares; n=13) mice at 65 (pre-symptomatic), 90 (early symptomatic), 105 (late symptomatic), and 120 (end stage) days of age. Red lines depict the median values of plasma NfH^{SMI34} levels in each group. Error bars: ±S.E.M. Friedman test was used for analysis of the pattern of plasma NfH levels during disease progression, and Mann-Whitney U test was then used for group comparison at each time point. *** $p < 0.0001$.

Figure 3.2

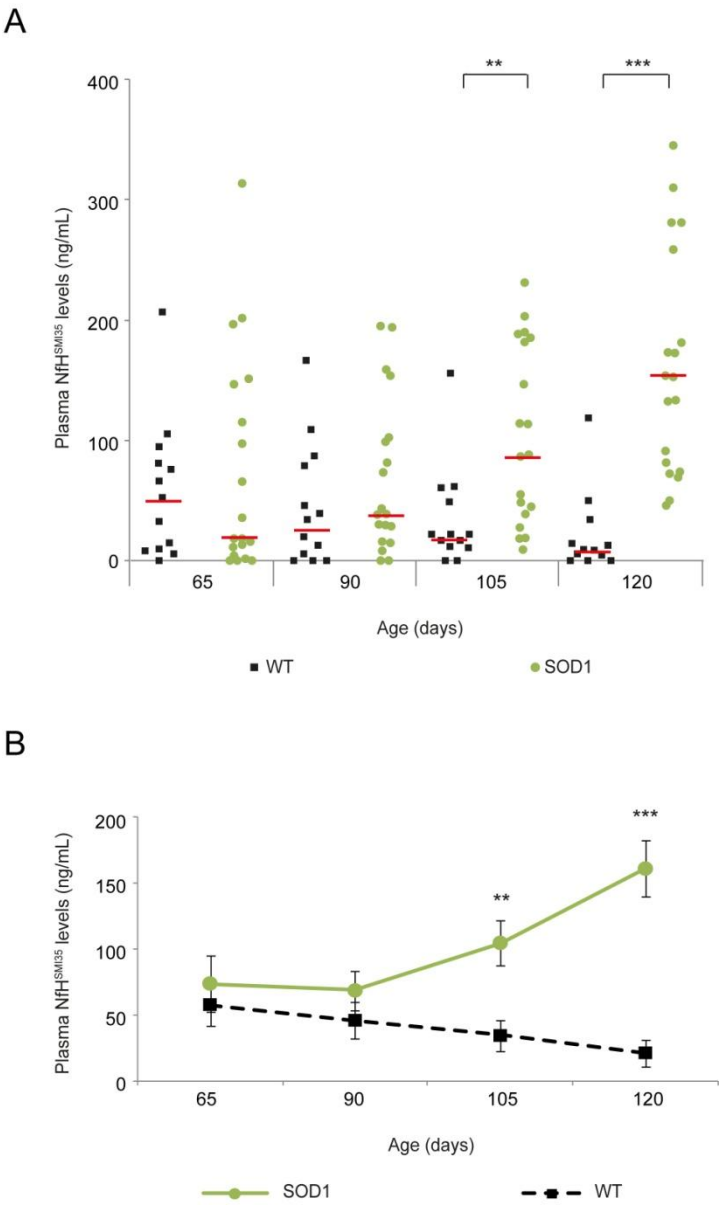

Figure 3.2. Longitudinal assessment of plasma NfH^{SMI35} levels in WT and SOD1 mice. The graphs show plasma levels (ng/mL) of NfH^{SMI35} in **(A)** individual mice and **(B)** the mean values in SOD1 (green circles; n=19) and WT (black squares; n=13) mice at 65 (pre-symptomatic), 90 (early symptomatic), 105 (late symptomatic), and 120 (end stage) days of age. Red lines depict the median values of plasma NfH^{SMI35} levels in each group. Error bars: ±S.E.M. Friedman test was used for analysis of the pattern of plasma NfH levels during disease progression, and Mann-Whitney U test was then used for group comparison at each time point. ** p =0.002, *** p < 0.0001.

shows the plasma NfH^{SMI35} levels in individual WT (black square) and SOD1 (green circles) mice at 65, 90, 105, and 120 days of age, and Fig. 3.2B shows the mean plasma NfH^{SMI35} levels in WT and SOD1 mice at each age. Plasma NfH^{SMI35} (Fig. 3.2), considered to be the less pathological form of NfH, was detected in plasma of WT mice, but levels remained stable throughout the study period (Friedman test, p=0.405). In contrast, in SOD1 mice, plasma NfH^{SMI35} levels increased significantly throughout disease progression (Friedman test, p<0.0001), although not as dramatically as NfH^{SMI34}, the more pathological phosphoform. Levels of NfH^{SMI35} in SOD1 mice became significantly higher than WT from 105 days of age onwards (65 days: SOD1 74.0±20.8 ng/mL, WT 58.0±16.0 ng/mL; 90 days: SOD1 68.8±14.8 ng/mL, WT 46.2±14.2 ng/mL; 105 days, SOD1 104.8±17.0 ng/mL, WT 34.7±11.6 ng/mL, p=0.002; 120 days, SOD1 161.0±21.5 ng/mL, WT 21.6±9.9 ng/mL, p<0.0001; mean±S.E.M; Mann-Whitney U test; Fig 3.2).

In addition, in WT mice, a comparison of NfH^{SMI35} and NfH^{SMI34} levels showed that plasma levels of NfH were not only low, but that there was also no difference in the relative levels of the two NfH phosphoforms at any age examined (Mann-Whitney test, p=0.479, 0.353, 0.817, 0.565 at 65, 90, 105, and 120 days, respectively; data not shown). In contrast, in SOD1 mice, a comparison of the relative levels of the two NfH phosphoforms revealed that levels of NfH^{SMI34} compared to NfH^{SMI35} increased as disease advanced (comparison NfH^{SMI34}: NfH^{SMI35} at 65days: p=0.507; 90days: p=0.546; 105 days: p=0.068; 120days: p=0.004; Mann-Whitney U Test). Thus, in SOD1 mice plasma levels of the more pathological NfH^{SMI34} phosphoform increased to a greater extent than the less pathological NfH^{SMI35} phosphoform.

3.3.2 Correlations between plasma NfH levels and functional measures of disease progression in SOD1^{G93A} mice

In the next set of experiments, I examined whether the increase in plasma NfH phosphoforms correlated with disease progression. A number of markers of disease progression were examined: both functional and morphological parameters as well as longitudinal and acute parameters. Thus longitudinal assessment of body weight and grip strength was under taken, as well as functional analysis of *in vivo* muscle force and motor unit survival, and morphological assessment of motor neuron survival. For each of these outcome measures, a correlation analysis with NfH levels at each age was carried out.

3.3.2.1 Increased plasma NfH levels inversely correlate with grip strength in SOD1^{G93A} mice

Body weight (BW) and grip strength (GS) were measured twice a week in both WT and SOD1 mice from 65 days of age until 120 days of age. These mice were the same experimental animals in which blood was samples for assessment of plasma NfH levels. The longitudinal change in mean GS of WT (black squares) and SOD1 (green circles) mice during disease progression is shown in Fig. 3.3A. It can be seen that SOD1 mice have lower GS than WT mice even at the start of the study, at 65 days. The Figure also illustrates the gradual decline in GS in SOD1 mice, which becomes apparent from approximate 93 days and becomes significant from the baseline strength from 105 days onwards. The longitudinal pattern of BW in WT and SOD1 mice is summarised in Fig. 3.3B, which shows the graduate decrease in BW in SOD1 mice. It can be seen that a reduction in BW in SOD1 mice only manifests relatively late in the disease, after their BW reaches maximum at around 90 days. In Fig 3.3C, the ratio of GS/BW is shown in order to account for the effect of changes in BW on GS. It can be seen that even when the decrease in BW is accounted for, there is a clear decrease in grip strength in SOD1 mice from approximately 93 days onward, in contrast to WT mice, where the ratio of GS/BW remains constant throughout the study.

In order to establish the relationship between the changes in plasma NfH levels detected in SOD1 mice and the decline in neuromuscular function that occurs as disease progresses in these mice a correlation analysis between plasma NfH levels and the corresponding mean grip strength was undertaken and the results are summarised in Fig. 3.4. No such correlation in plasma NfH levels and grip strength was observed in WT mice at any age examined (Fig. 3.4A & 3.4B, left panel). The results show that in SOD1 mice, there was a moderate- to-strong inverse correlation between plasma NfH levels and grip strength at all the time points examined, 65, 90, 105 and 120 days (Spearman's rho (R) : NfH^{SMI34} vs. GS: -0.583, $p<0.0001$; NfH^{SMI35} vs. GS: -0.335, $p<0.0001$; Fig. 3.4A & 3.4B, right panel).

3.3.2.2 Increased plasma NfH levels correlate with the decline in isometric muscle force in hindlimb muscles of SOD1^{G93A} mice

In order to obtain a more detailed assessment of the relationship between plasma NfH levels and quantitative functional markers of disease progression, an *in vivo* physiological assessment of isometric muscle force in the hindlimb muscles of

Figure 3.3

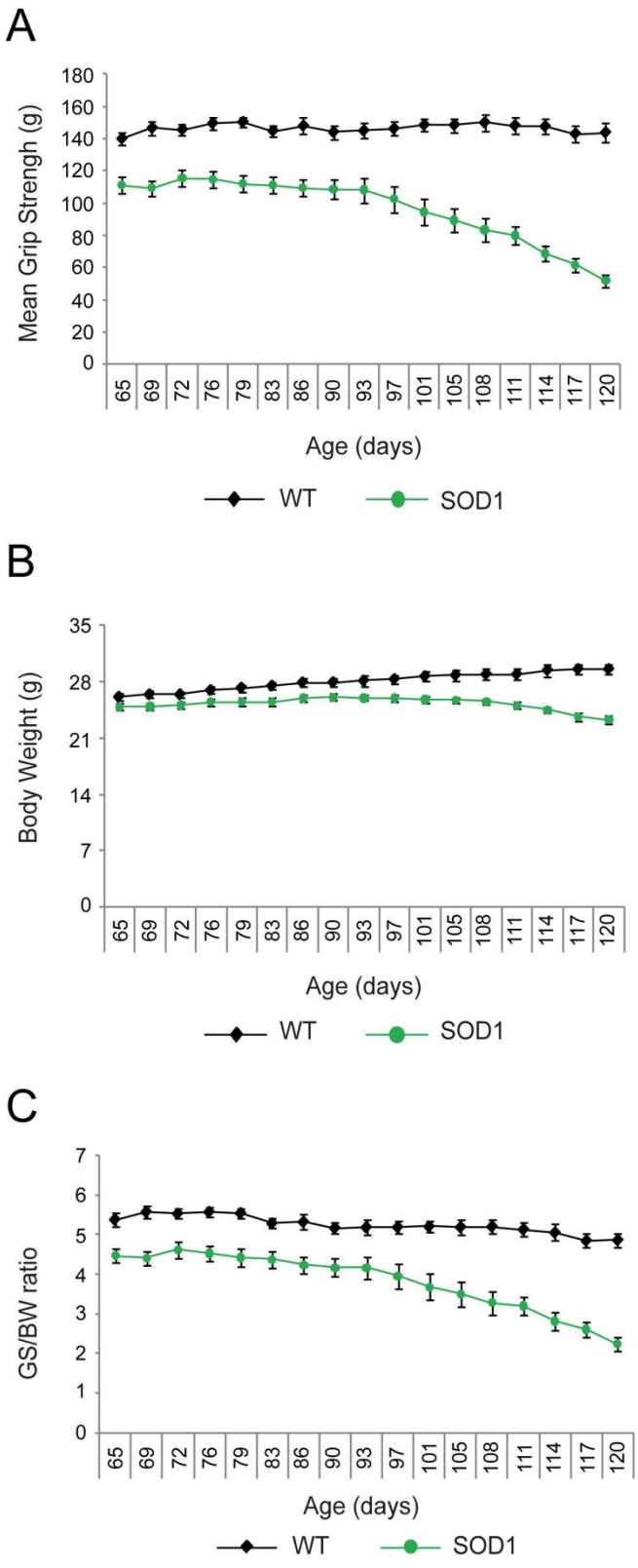
A
Mean Grip Strengh (g)
180
160
140
120
100
80
60
40
20
0
65 69 72 76 79 83 86 90 93 97 101 105 108 111 114 117 120
Age (days)
WT
SOD1
B
Body Weight (g)
35
28
21
14
7
0
65 69 72 76 79 83 86 90 93 97 101 105 108 111 114 117 120
Age (days)
WT
SOD1
C
GS/BW ratio
7
6
5
4
3
2
1
0
65 69 72 76 79 83 86 90 93 97 101 105 108 111 114 117 120
Age (days)
WT
SOD1

Figure 3.3. Longitudinal assessment of grip strength and body weight in WT and SOD1 mice during disease progression. (A) Mean grip strength (GS) was determined weekly in mice of each group from 65-120 days of age. SOD1 mice appeared to be significantly weaker than their WT littermates from the beginning of the assessment period, at 65 days of age ($p<0.05$, one-way within subject ANOVA, with Bonferroni correction). In SOD1 mice, GS began to decrease significantly from 105 days ($p<0.05$, t-test with the baseline). **(B)** Body weight (BW) was determined weekly from 65-120 days in mice of each group. WT mice weighed more than SOD1 mice at the start of the study and continued to increase weight throughout the study ($p<0.05$, one-way within subject ANOVA, with Bonferroni correction). In SOD1 mice, BW began to decline steadily from a maximum at 90 days. **(C)** Mean grip strength was expressed relative to body weight (GS/BW) for WT and SOD1 mice during disease progression. In WT mice, GS/BW remained constant throughout the study. In contrast, in SOD1 mice, there was a steady decrease in the GS/BW ratio as disease progressed. Error bars: ±S.E.M. Black diamonds, WT mice; green circles, SOD1 mice.

Figure 3.4

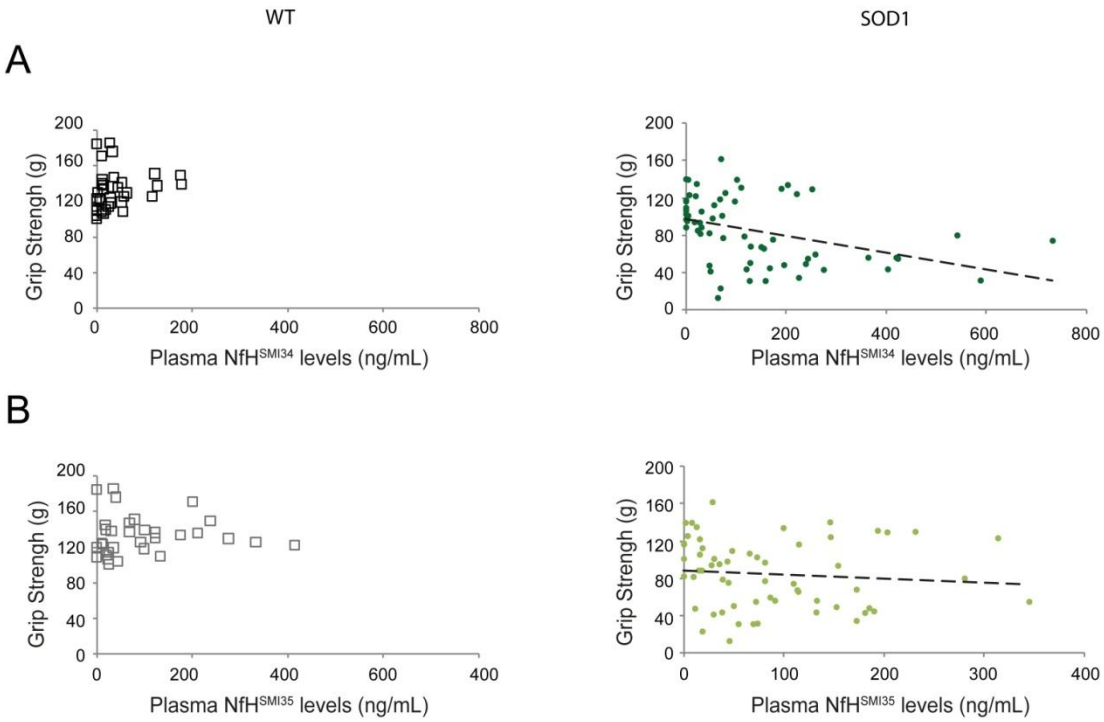

Figure 3.4. The correlation between grip strength and plasma NfH levels in WT and SOD1 mice between 65 and 120 days of age. The graphs show the relationship between mean grip strength (g) and plasma NfH phosphoform levels (ng/mL) in individual WT and SOD1 mice (n=16) at 65, 90, 105, and 120 days of age. **(A)** There is no correlation in WT mice (black squares), while a strong inverse correlation between plasma NfH^{SMI34} levels and grip strength is observed in SOD1 mice (dark green circles; Spearman's rho=-0.583, $p<0.0001$). The best-fit line (dashed line) is shown. **(B)** There is no correlation in WT mice (grey squares), whilst a moderate inverse correlation between plasma NfH^{SMI35} and grip strength is observed in SOD1 mice (light green circles; Spearman's rho=-0.335, $p<0.0001$). The best-fit line (dashed line) is shown.

SOD1^{G93A} mice were undertaken. This physiological assessment of isometric muscle force of specific muscles provides a more sensitive and quantitative assessment of functional decline than grip strength analysis, which can only detect general motor deficits in SOD1^{G93A} mice relatively late in the disease process, when many motor neurons have already died. We have previously generated similar physiological data in our lab in SOD1^{G93A} mice at various stages of disease ranging from early symptomatic (90 days) to end-stage disease (130 days) (Kalmar et al., 2008; Kieran et al., 2004; Sharp et al., 2005). Using these measures of the decrease in muscle force I examined whether plasma NfH levels correlated with this profile of functional decline in SOD1^{G93A} mice.

Typical examples of tetanic and twitch force traces from the TA muscles of 105-day-old WT and SOD1 mice are shown in Fig. 3.5A. The mean maximum twitch and tetanic force of the Tibialis Anterior (TA) and Extensor Digitorum Longus (EDL) muscles of WT and SOD1 at various stages of disease is summarised in Fig. 3.5B (Twitch) and Fig. 3.5C (Tetanus). These results show the well-established, progressive decrease in muscle force in both TA and EDL muscles that occurs in SOD1 mice as they age (Sharp et al., 2005). The results also show that in SOD1 mice, TA muscles were affected earlier in disease and to a greater extent than EDL muscles. Thus, the maximum tetanic force (Fig. 3.5C; mean±S.E.M.) in SOD1 TA (dark green bars) was 56.7±5 g (n=13) at 90 days, 21.1±3 g (n=16) at 105 days and 19.5± 3.5 g (n=12) at 120 days. When expressed as a percentage of WT TA (black bars) muscle force in age-matched WT mice, the force produced by SOD1 TA was 41.7% at 90 days, 15.3% at 105 days and 12% at 120 days ($p<0.0001$ at each time point; Mann-Whitney U test). The decline in force in SOD1 EDL (light green bars) muscles occurred at a steadier, slower pace. Thus, in SOD1 EDL muscles the force produced was 24.7±1.5 g (n=15) at 90 days, 15.7±1.6 g (n=19) at 105 days and 13.7±1.0 g (n=11) at 120 days, which was 68.6%, 43.9% and 33.3% of the force produced in WT EDL (grey bars) muscles at the respective ages ($p< 0.01$; <0.0001; <0.0001, respectively; Mann-Whitney U test). A similar pattern of decline was also found in the twitch tension of TA and EDL muscles of SOD1 mice (Fig. 3.5B).

As shown in Fig. 3.5D, an exponential regression analysis of the decline in maximum TA muscle force at 90, 105 and 120 days of age (indicated by the respective arrows) and their corresponding plasma NfH^{SMI34} (dark green squares) or NfH^{SMI35} (light green triangles) levels in SOD1 mice was undertaken. It can be seen

Figure 3.5

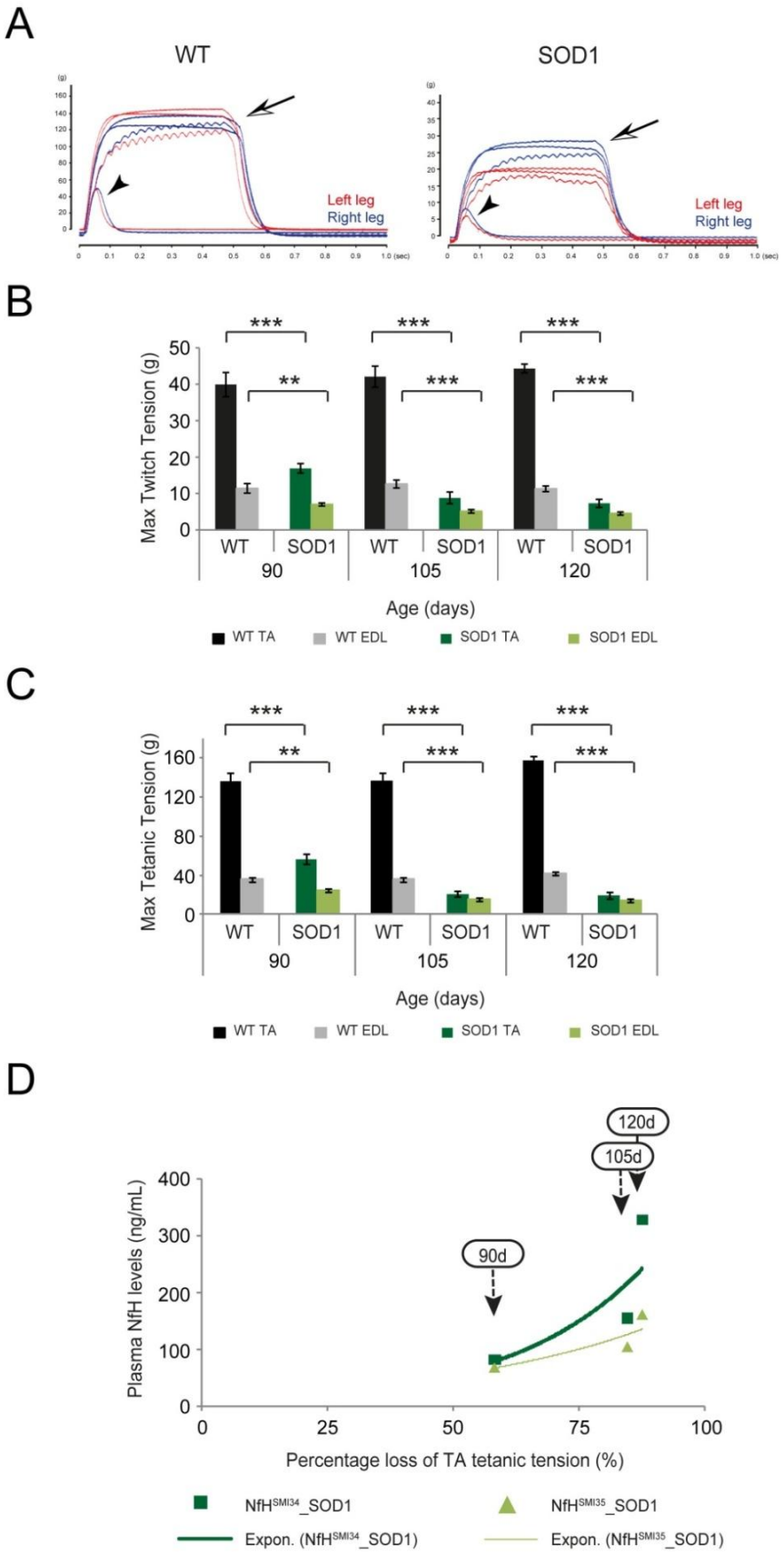
A
WT
SOD1
Left leg
Right leg
B
Max Twitch Tension (g)
WT
SOD1
90
105
120
Age (days)
WT TA
WT EDL
SOD1 TA
SOD1 EDL
C
Max Tetanic Tension (g)
D
Plasma NfH levels (ng/mL)
120d
105d
90d
Percentage loss of TA tetanic tension (%)
NfHSMI34_SOD1
NfHSMI35_SOD1
Expon. (NfHSMI34_SOD1)
Expon. (NfHSMI35_SOD1)

Figure 3.5. The correlation between plasma NfH phosphoform levels and hindlimb muscle force in SOD1 mice during disease progression. (A) Examples of recordings of maximum tetanic (arrow) and twitch (arrow head) tension in TA muscles of WT and vehicle treated SOD1 mice at 105 days of age. **(B)** The bar chart shows the mean maximum twitch tension (g) of TA (WT: black bars; SOD1: dark green bars) and EDL (WT: grey bars; SOD1: light green bars) muscles. **(C)** The bar chart shows the mean maximum tetanic tension (g) of TA (WT: black bars; SOD1: dark green bars) and EDL (WT: grey bars; SOD1: light green bars) muscles. **(D)**The graph shows the percentage loss of TA maximum tetanic tension, relative to WT, and the corresponding plasma NfH^{SMI34} (dark green squares) and NfH^{SMI35} (light green triangles) levels in vehicle treated SOD1 mice at each stage of disease (indicated by arrows). Exponential regression lines are shown for NfH^{SMI34} (dark green line) and NfH^{SMI35} (light green line). Error bars: ±S.E.M. Mann-Whitney U test: ** $p < 0.01$; *** $p < 0.0001$.

that there is a moderate-strong correlation between muscle force and plasma NfH levels in SOD1 mice (R^2=0.79 and 0.82 for NfH^{SMI34} and NfH^{SMI35} respectively).

3.3.2.3 Increased plasma NfH levels correlate with motor unit loss in $SOD1^{G93A}$ mice

Next, the number of functional motor units innervating the EDL muscle of WT and SOD1 mice was determined. Examples of typical motor unit traces from the EDL muscle of 105-day-old SOD1 and WT mice are shown in Fig. 3.6A. The number of functional motor units that survived in EDL muscles was also determined in SOD1 mice at 90, 105 and 120 days of age and the results are summarised in Fig. 3.6B. In WT mice, the number of motor units innervating EDL muscles remained constant over the course of the study, and the number of motor units innervating EDL (mean±S.E.M.) was found to be 26.6±0.4 (n=14) at 90 days, 30.8±0.4 (n=10) at 105 days and 25.7±0.5 (n=6) at 120 days. In contrast, in SOD1 mice, a significant number of motor units had already died by 90 days, with 22.7±1.2 (n=17) motor units innervating EDL, a 15% decline compared to WT ($p<0.05$). Between 90-105 days, there was a 60% decrease in the number of motor units innervating EDL units innervating EDL, a 15% decline compared to WT ($p<0.05$). Between 90-105 days, there was a 60% decrease in the number of motor units innervating EDL muscles of SOD1 mice and by 105 days only 12.6±0.5 (n=15) motor units innervated EDL ($p<0.01$). This decline in motor unit survival in SOD1 mice plateaued at this level, so that by 120 days, 10.7±1.0 (n=11; $p<0.01$) motor units innervated EDL.

Fig. 3.6C shows the results of an exponential regression analysis of the decline in motor unit survival in EDL muscles at 90, 105 and 120 days (indicated by the respective arrows) and the corresponding plasma NfH^{SMI34} (dark green squares) or NfH^{SMI35} (light green triangles) levels in SOD1 mice. Motor unit loss, expressed as a percentage of motor unit survival in age-matched WT mice, can be fitted into an exponential regression with R^2=0.70 for NfH^{SMI34} and R^2=0.73 for NfH^{SMI35}, indicating a modest correlation between the extent of EDL motor unit loss and plasma NfH levels in SOD1 mice.

3.3.2.4 Increased plasma NfH levels directly correlate with the extent of motor neuron death in the spinal cord of $SOD1^{G93A}$ mice

The defining disease characteristic in both ALS patients and in the $SOD1^{G93A}$ mouse model of ALS is motor neuron degeneration. Therefore, in order to determine if

Figure 3.6

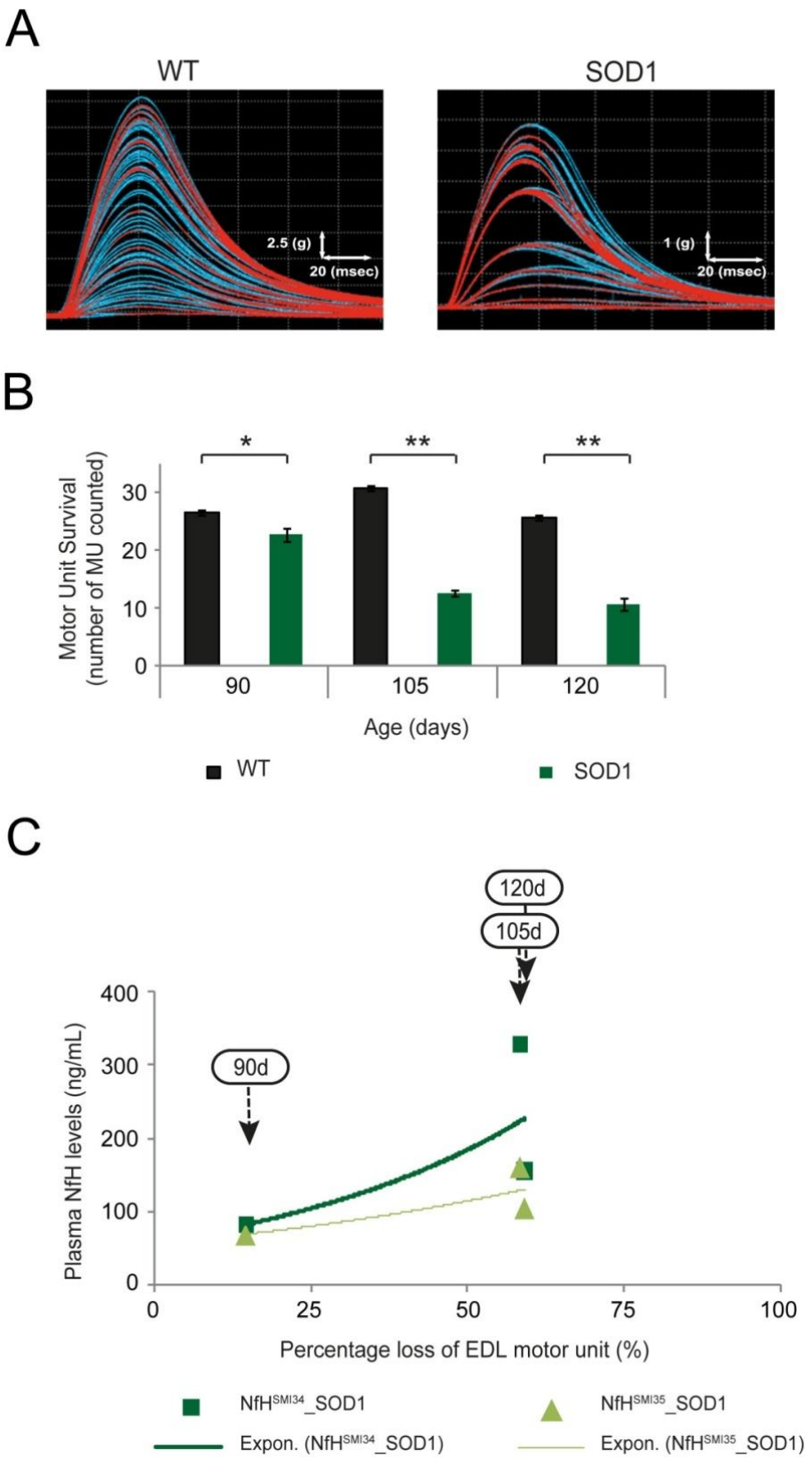
A
WT
SOD1
2.5 (g)
20 (msec)
1 (g)
20 (msec)
B
Motor Unit Survival (number of MU counted)
*
**
**
30
20
10
0
90
105
120
Age (days)
WT
SOD1
C
120d
105d
90d
400
300
200
100
0
Plasma NfH levels (ng/mL)
0
25
50
75
100
Percentage loss of EDL motor unit (%)
NfHSMI34_SOD1
NfHSMI35_SOD1
Expon. (NfHSMI34_SOD1)
Expon. (NfHSMI35_SOD1)

Figure 3.6. The correlation between plasma NfH phosphoform levels and motor unit survival in EDL muscles in SOD1 mice during disease progression. **(A)** Typical examples of motor unit traces in the EDL muscle of a WT and a vehicle treated SOD1 mouse at 105 days of age. Blue lines indicate traces that have not been replicated, and red lines indicate traces that have been replicated. **(B)** The bar chart shows the mean motor unit survival (numbers) in EDL muscles of WT (open bars) and vehicle treated SOD1 (green bars) mice. **(C)** The percentage loss of EDL motor units, relative to WT, and plasma NfH^{SMI34} (dark green squares) and NfH^{SMI35} (light green triangles) levels in SOD1 mice at each stage of disease (indicated by arrows). Exponential regression lines are shown for NfH^{SMI34} (thick dark green line) and NfH^{SMI35} (thin light green line). Error bars: ±S.E.M. Mann-Whitney Test: * $p < 0.05$; ** $p < 0.01$.

changes in plasma NfH levels in SOD1^{G93A} mice were a good reflection of the extent of motor neuron degeneration, we next established the extent of motor neuron survival in the lumbar spinal cord of WT and SOD1 mice at various stages of disease. Examples of Nissl-stained spinal cord sections, showing the lumbar ventral horn of 105-day-old WT and SOD1 mice are shown in Fig. 3.7A. The results are summarised in Fig. 3.7B, which shows the mean motor neuron survival in 90, 105 and 120 day old SOD1 mice expressed as a percentage of WT. It can be seen that by 90 days, a significant number of motor neurons have already died in SOD1 mice and only 60.8±1.4% of motor neurons survive compared with WT littermates ($p<0.01$). Motor neurons continue to die in SOD1 mice as disease progresses, so that by 105 days, 44.8±1.2% of motor neurons survive ($p<0.01$) and by 120 days this is further reduced and only 29.0±1.3% of motor neurons survive ($p<0.01$; Mann-Whitney U test).

In order to establish whether the changes detected in plasma NfH levels correlate with the extent of motor neuron degeneration in SOD1 mice, an exponential regression analysis of motor neuron survival and plasma NfH levels was undertaken. Figure 3.7C summarises the results and shows the decline in motor neuron survival in SOD1 mice at 90, 105 and 120 days of age (indicated by the respective arrows) and corresponding plasma NfH^{SMI34} (dark green squares) or NfH^{SMI35} (light green triangles) levels. It can be seen that the decline in motor neuron survival observed in SOD1 mice during disease progression fits into an exponential regression with $R^2=0.99$ for both NfH^{SMI34} and NfH^{SMI35} (p-value of coefficient: 0.03 and 0.006, respectively). This analysis shows that there is a very strong correlation between the extent of motor neuron death and plasma levels of both NfH^{SMI34} and NfH^{SMI35} in SOD1 mice.

3.3.3 Plasma NfH levels reflect the disease-modifying effects of arimoclomol in SOD1 mice

Since plasma NfH levels correlate with the decline in neuromuscular function in SOD1^{G93A} mice, I next examined whether changes in plasma NfH levels could detect the effects of agents that modify disease progression, i.e. whether they could be a biomarker in the setting of a clinical trial. Therefore in the next set of experiments, I investigated whether the beneficial effects of Arimoclomol, an established disease-modifying therapy in SOD1^{G93A} mice (Kalmar et al., 2008; Kieran et al., 2004), were reflected in changes in plasma NfH levels. Therefore, in this study a separate group

Figure 3.7

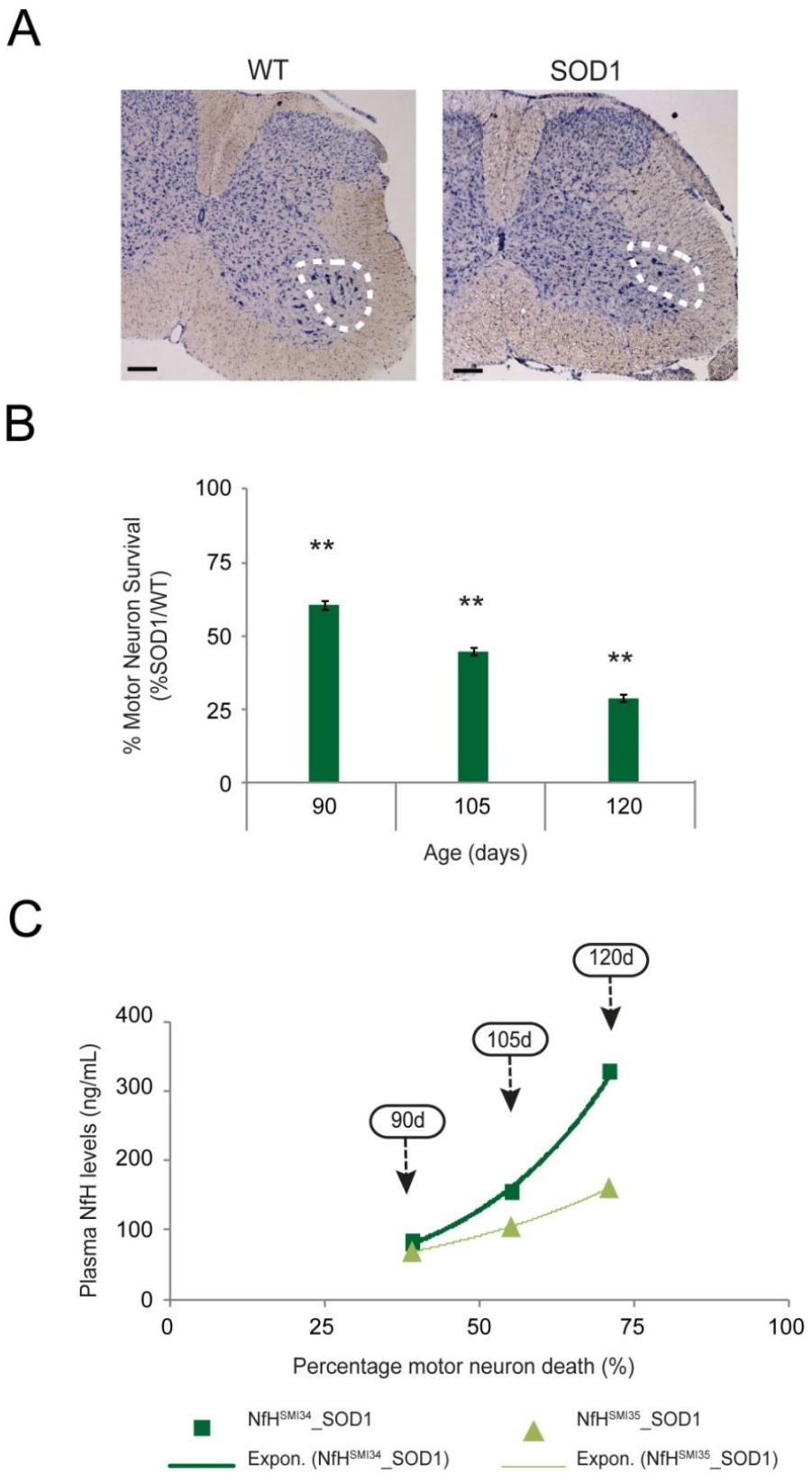
A
WT
SOD1
B
% Motor Neuron Survival (%SOD1/WT)
100
75
50
25
0
**
**
**
90
105
120
Age (days)
C
Plasma NfH levels (ng/mL)
400
300
200
100
0
120d
105d
90d
0
25
50
75
100
Percentage motor neuron death (%)
NfHSMI34_SOD1
Expon. (NfHSMI34_SOD1)
NfHSMI35_SOD1
Expon. (NfHSMI35_SOD1)

Figure 3.7. The correlation between plasma NfH phosphoform levels and motor neuron survival in SOD1 mice during disease progression. (A) The photomicrographs show cross-sections of the lumbar region at L5 level of spinal cords from a WT and a vehicle treated SOD1 mouse at 105 days of age stained for Nissl. The location of the sciatic motor pool is indicated within the broken circle. Magnificent: 5X. Scale bar = 250µm. **(B)** The bar chart shows the mean motor neuron survival in SOD1 mice expressed as a percentage of that in age-matched WT littermates at various stages of disease. The motor neuron count (mean±SEM) in WT/SOD1 mice at 90, 105, and 120 days were 433±7.8/264±10.5, 422±8.9/189.2±5.0 and 439±2.3/125.5±5.6, respectively. **(C)** The percentage motor neuron death in SOD1 mice and levels of plasma NfH^{SMI34} (dark green squares) and NfH^{SMI35} (light green triangles) at each disease stage (indicated by arrows). Exponential regression lines are shown for NfH^{SMI34} (thick dark green line) and NfH^{SMI35} (thin light green line). Error bars: ±S.E.M. Mann-Whitney U Test: ** $p < 0.01$.

of SOD1^{G93A} mice were treated with Arimoclomol (10 mg/Kg; i.p.; SOD1+A) from 35 days and their plasma was collected at 65, 90, 105 and 120 days of age for analysis of NfH levels.

3.3.3.1 Longitudinal assessment of disease progression in Arimoclomol-treated SOD1^{G93A} mice

The effect of Arimoclomol on disease progression was determined by longitudinal assessments of body weight (BW) and grip strength (GS). The results are summarised in Fig. 3.8, which shows that Arimoclomol had no detectable effect on either BW or GS compared to vehicle-treated SOD1 littermates.

3.3.3.2 The effect of Arimoclomol on muscle force, motor unit and motor neuron survival in SOD1^{G93A} mice

In order to determine if arimoclomol did improve disease progression in SOD1^{G93A} mice as previously reported (Kalmar et al., 2008; Kieran et al., 2004), I next examined the muscle force, motor unit survival and motor neuron survival in Arimoclomol-treated SOD1 mice and vehicle-treated SOD1 littermates, at 105 and 120 days of age. The results are summarised in Table 3.1 and confirm that there is a significant improvement in muscle force, functional motor unit survival and motor neuron survival in Arimoclomol-treated SOD1 mice compared to their vehicle-treated SOD1 littermates, both at a symptomatic (105 day) stage and more clearly at a late stage (120 day) of disease. These results confirm that Arimoclomol delays the decline in muscle function and motor neuron survival that occurs in vehicle-treated SOD1 mice between 105 and 120 days of age.

3.3.3.3 Plasma NfH levels reflect the beneficial effects of Arimoclomol in SOD1^{G93A} mice

I next examined whether the improvements in disease observed in Arimoclomol-treated SOD1 (SOD1+A) mice was reflected in a reduction in plasma NfH levels compared to their vehicle-treated SOD1 littermates (SOD1).

Levels of plasma NfH in SOD1+A mice and SOD1 mice were determined between 65 and 120 days of age. The results are summarised in Fig. 3.9, which shows that even at 65 days, a pre-symptomatic age, the effects of arimoclomol were reflected in a reduction in the plasma mean levels of NfH^{SMI34} in treated SOD1+A mice (red) compared to vehicle-treated SOD1 littermates (green). Thus, at 65 days, the

Figure 3.8

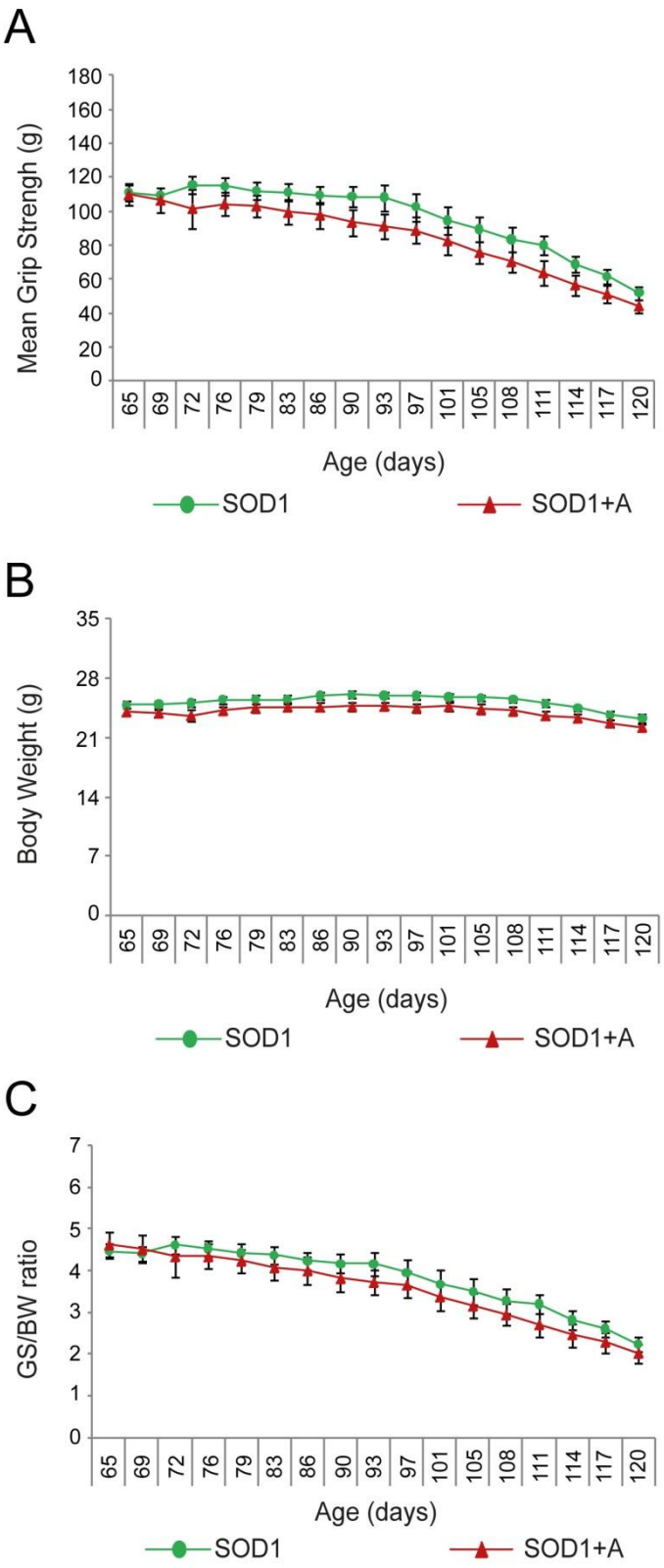
A
Mean Grip Strengh (g)
180
160
140
120
100
80
60
40
20
0
65
69
72
76
79
83
86
90
93
97
101
105
108
111
114
117
120
Age (days)
SOD1
SOD1+A
B
Body Weight (g)
35
28
21
14
7
0
Age (days)
SOD1
SOD1+A
C
GS/BW ratio
7
6
5
4
3
2
1
0
Age (days)
SOD1
SOD1+A

Figure 3.8. Longitudinal assessment of grip strength and body weight in SOD1 and SOD1+A mice during disease progression. (A) Mean grip strength (GS) was determined weekly in mice of each group from 65-120 days of age. No significant difference was observed in GS in SOD1 and SOD1+A mice at any age (two-sample *t*-test, $p>0.05$ at all the time points). **(B)** Body weight (BW) was determined weekly from 65-120 days in mice of each group. In both SOD1 and SOD1+A mice, BW began to decline steadily from a maximum at 90 days, although there was no significant difference between SOD1 and SOD1+A mice at any age studied. **(C)** Mean grip strength was expressed relative to body weight (GS/BW) for SOD1 and SOD1+A mice during disease progression. In SOD1 and SOD1+A mice, there was a steady and similar decrease in the GS/BW ratio as disease progressed. Error bars: ±S.E.M. Green circles, SOD1 mice; red triangles, SOD1+A mice.

Table 3.1. Arimoclomol delays disease progression in $SOD1^{G93A}$ mice.

Age (days)	Group	Maximum TA Tetanic Force (g±sem) (n=muscle examined)	EDL MU survival (n±sem) (n=muscle examined)	MN survival (%WT) (n= sciatic motor pool examined)
105	SOD1	21.1±3.0 (16)	12.6±0.5 (15)	44.8 (10)
	SOD1+A	49.2±9.9 (11) **	14.8±0.5 (12) **	58.0 (10) **
120	SOD1	19.5±3.5 (12)	10.7±0.7 (11)	29 (10)
	SOD1+A	36.9±9.0 (10) **	14.0±0.6 (10) **	65 (10) **

The Table shows the maximum TA tetanic force, EDL Motor Unit survival and Motor Neuron Survival in vehicle-treated SOD1 and Arimoclomol-treated SOD1+A mice at 105 and 120 days of age. The results are the mean ± S.E.M. **p <0.01

Figure 3.9

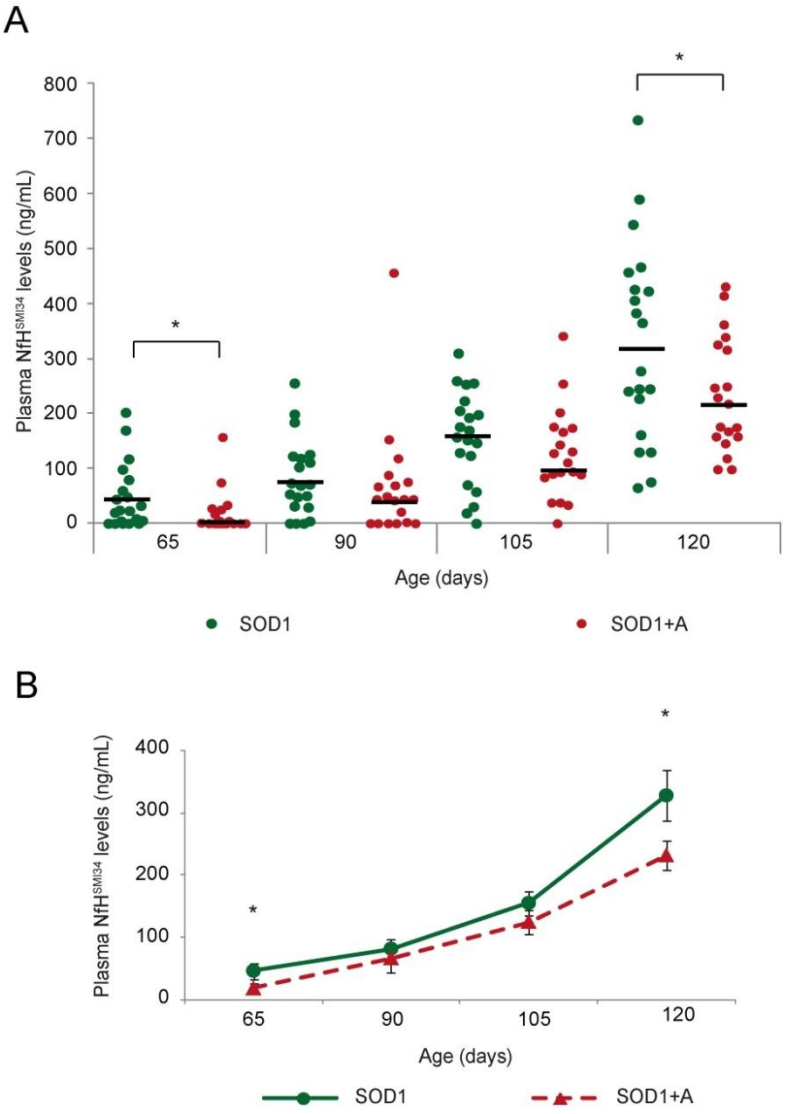

Figure 3.9. Longitudinal assessment of plasma NfH^{SMI34} levels in Arimoclomol-treated SOD1 mice. The graphs show the mean plasma level (ng/mL) of NfH^{SMI34} in (**A**) individual values and in (**B)** group mean values in vehicle treated SOD1 mice (dark green; n=19) and Arimoclomol-treated SOD1+A mice (dark red; n=19), at 65 (pre-symptomatic), 90 (early symptomatic), 105 (late symptomatic), and 120 (end stage) days of age. Error bars: ±S.E.M. A *t*-test was performed for direct comparison of the levels of NfH^{SMI34} in the two groups at 105 and 120 days, and a Mann-Whitney Test was performed for the other time points as the data was not normally distributed. Non-parametric analyses take the median value into account more than the mean value in the statistical analysis. Black lines depict the median values of plasma NfH^{SMI34} levels in each group. * $p < 0.05$.

mean±S.E.M of plasma NfH^{SMI34} levels were 17.8±8.8 ng/mL in SOD1+A mice compared with 46.2±13.1 ng/mL in SOD1 mice (Mann-Whitney test, p=0.035). As disease progressed, plasma NfH^{SMI34} levels continued to be lower in Arimoclomol-treated than in vehicle-treated SOD1 mice. Thus, the mean±S.E.M NfH^{SMI34} levels in SOD1+A mice compared with SOD1 mice were 66.3±23.7: 81.8±15.8 (SOD1+A: SOD1) ng/mL at 90 days; 124.8±18.8: 155.4±19.3 ng/mL at 105 days and 231.7±23.9: 328.4±40.3 ng/mL at 120 days. However, the reduction in NfH^{SMI34} level in symptomatic SOD1+A mice compared with SOD1 mice only reached significance at 120 days (90 days p=0.154, Mann-Whitney test; 105 days, p=0.264, *t*-test; 120 days, p=0.048, *t*-test; Fig. 3.9).

Similarly, plasma levels of NfH^{SMI35} were also lower in SOD1+A mice (pink) compared with vehicle-treated SOD1 mice (light green) at all stages of the disease (Fig. 3.10). In contrast to NfH^{SMI34} levels, the assay for variably-phosphorylated NfH did not detect any significant effects of arimoclomol at pre-symptomatic stages. However, levels of NfH^{SMI35} in SOD1+A mice at 65 days of age were more consistent between different animals and at a lower level than observed in SOD1 mice, where there was a greater variation in plasma NfH^{SMI35} levels. Thus, the mean±S.E.M levels of plasma NfH^{SMI35} in SOD1+A and SOD1 mice (SODA: SOD) were 35.1±10.3: 74.0±20.8 ng/mL at 65 days; 55.4±15.5: 68.8±14.8 ng/mL at 90 days; 77.0±10.1: 104.8±17.0 ng/mL at 105 days and 92.0±15.5: 161.0±21.5 ng/mL at 120 days (Mann-Whitney test, p-values: 0.391; 0.327; <0.001 and 0.009 at 65, 90, 105 and 120 days, respectively; Mann-Whitney test).

These results show that the disease modifying effects of Arimoclomol in SOD1^{G93A} mice are reflected in a reduction in plasma NfH levels compared to vehicle-treated SOD1 littermates. Furthermore, a comparison of the relative plasma levels of the two NfH phosphoforms, which is summarised in Table 3.2, revealed that NfH^{SMI34} levels were significantly lower in SOD1+A mice than vehicle-treated SOD1 mice at 65 days of age (Mann-Whitney test, p=0.015). Vehicle-treated SOD1 mice had smaller ranks for NfH^{SMI34} even at 65 days; the increase in NfH^{SMI34} levels started from 90 days, although it was not significant. In contrast, SOD1+A mice had a similar ranks for NfH^{SMI34} and NfH^{SMI35} at 90 days of age, and levels of NfH^{SMI34} levels became significant greater than NfH^{SMI35} at 105 days (p=0.04). Further reduction of NfH^{SMI35} in SOD1+A mice was also observed at end-stage (p<0.0001). Thus, the disease modifying effects of Arimoclomol in SOD1 mice were reflected in

Figure 3.10

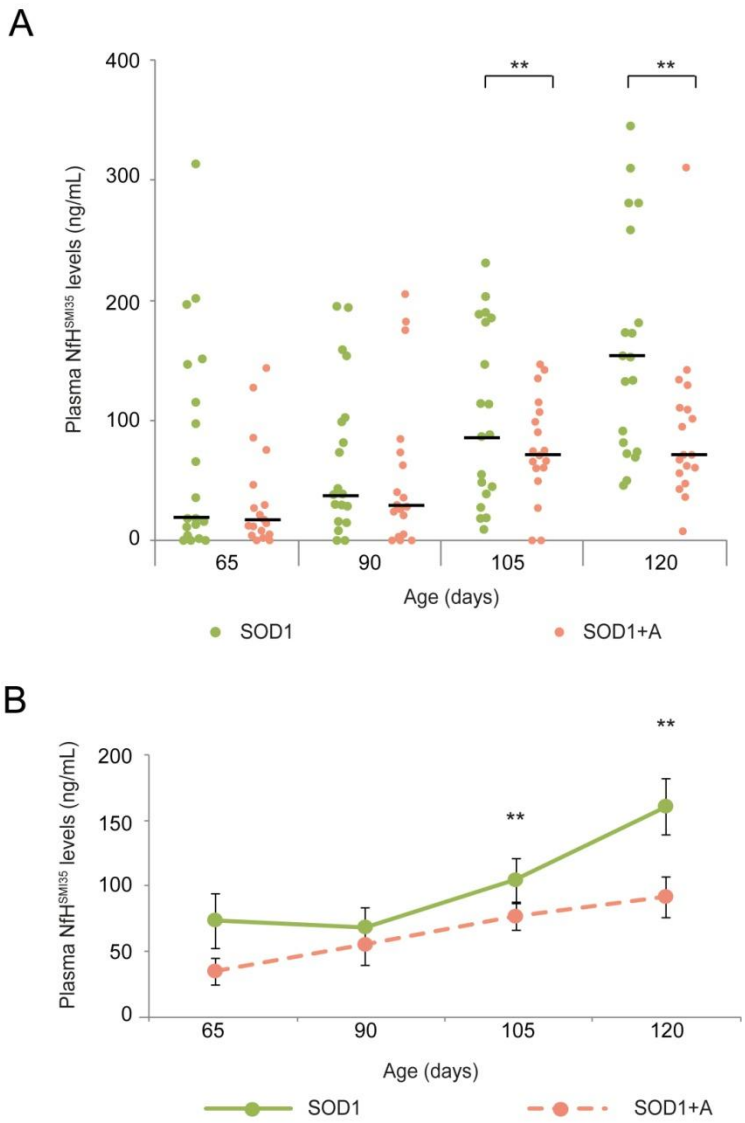

Figure 3.10. Longitudinal assessment of plasma NfH^{SMI35} levels in Arimoclomol-treated SOD1 mice. The graphs show the mean plasma level (ng/mL) of NfH^{SMI35} in (**A**) individual values and in (**B)** group mean values in vehicle-treated SOD1 mice (light green; n=19) and Arimoclomol-treated SOD1+A mice (pink; n=19), at 65 (pre-symptomatic), 90 (early symptomatic), 105 (late symptomatic), and 120 (end stage) days of age. Error bars: ±S.E.M. A *t*-test was performed for direct comparison of the levels of NfH^{SMI34} in the two groups at 105 and 120 days, and a Mann-Whitney Test was performed for the other time points as the data was not normally distributed. Non-parametric analyses take the median value into account more than the mean value in the statistical analysis. Black lines depict the median values of plasma NfH^{SMI35} levels in each group. ** $p < 0.01$.

Table 3.2. A summary of the statistical analysis (Mann-Whitney test) of the difference in the plasma levels of the two NfH phosphoforms in vehicle-treated SOD1 and Arimoclomol-treated SOD1+A mice at 65, 90, 105 and 120 days of age.

		SOD1 mice			SOD1+A mice		
Age (days)	NfH phosphoforms	Mean Rank	Sum of Ranks	p-Value	Mean Rank	Sum of Ranks	p-Value
65	SMI34	18.83	376.50	0.507	15.16	288.00	***0.015***
	SMI35	21.14	403.50		23.84	465.00	
90	SMI34	**21.08**	**421.50**	0.546	**19.66**	**373.50**	0.930
	SMI35	**18.87**	**358.50**		**19.34**	**367.50**	
105	SMI34	23.25	465.00	0.068	23.21	441.00	***0.040***
	SMI35	16.58	315.00		15.79	300.00	
120	SMI34	25.15	503.00	0.004	27.42	521.00	***<0.0001***
	SMI35	14.58	277.00		11.58	220.00	

lower levels of both NfH phosphoforms as well as a more even composition of plasma NfH phosphoforms than in vehicle-treated SOD1 mice.

3.3.4 Using plasma NfH levels as a biomarker in a novel preclinical trial in SOD1^{G93A} mice

The above results have shown that the beneficial effects of a known therapeutic agent are reflected in a reduction in plasma NfH levels in SOD1^{G93A} mice. In order to further test whether plasma NfH levels could be used as a good surrogate marker of treatment response in a clinical trial, I next examined plasma NfH levels as part of a novel preclinical study in SOD1^{G93A} mice.

In this study, blood samples were taken from SOD1^{G93A} mice in which the potential therapeutic effects of a new drug, Cogane, were under investigation. In this study the following experimental groups were examined:

i) Vehicle;
ii) Cogane alone;
iii) Congane in combination with Riluzole;
iv) Riluzole alone.

A Riluzole group was included in this study as most ALS patients are offered this option as the standard treatment for ALS. Treatment was initiated at 70 days of age, at symptom onset. NfH levels were examined at 105 and 120 days of age, when results presented in Fig. 3.9 and Fig 3.10 showed there were significant increases in plasma NfH phosphoforms in vehicle-treated SOD1^{G93A} mice. The effects of these treatments on disease progression in SOD1^{G93A} mice was determined at 120 days in treated and untreated mice by assessment of muscle force, motor unit and motor neuron survival. These physiological experiments were undertaken by Dr Bernadett Kalmar, a postdoc in our lab (Kalmar et al., 2012a). The results are summarised in Fig. 3.11, which shows that i) treatment with Cogane alone or in combination with Riluzole had beneficial effects and as shown in Fig. 3.11, there was a significant improvement in EDL muscle force and MU survival. In contrast, no improvement was observed in mice treated with Riluzole alone. However, as can be seen in Fig. 3.11C, treatment with Cogane and Riluzole, alone or in combination, resulted in an improvement in motor neuron survival compared to vehicle-treated SOD1^{G93A} mice.

Figure 3.11

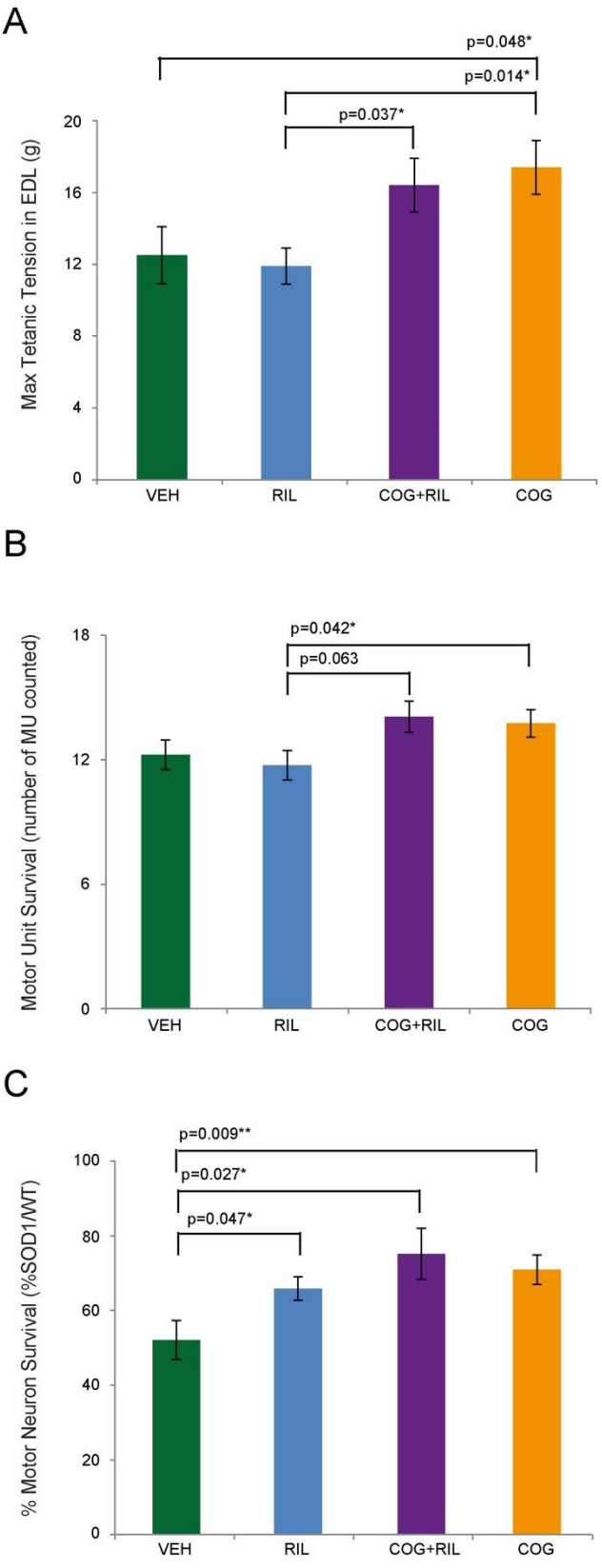
A
p=0.048*
p=0.014*
p=0.037*
Max Tetanic Tension in EDL (g)
20
16
12
8
4
0
VEH
RIL
COG+RIL
COG
B
p=0.042*
p=0.063
Motor Unit Survival (number of MU counted)
18
12
6
0
VEH
RIL
COG+RIL
COG
C
p=0.009**
p=0.027*
p=0.047*
% Motor Neuron Survival (%SOD1/WT)
100
80
60
40
20
0
VEH
RIL
COG+RIL
COG

Figure 3.11. Functional and morphological assessment of SOD1^{G93A} mice treated with Cogane and Riluzole from onset of disease (70 days of age). The bar chart summarises **(A)** maximum tetanic force of EDL muscle, **(B)** motor unit survival in EDL, and **(C)** motor neuron survival in SOD1^{G93A} mice treated with Cogane or Riluzole, alone or in combination. In mice treated with Cogane alone there was a significant improvement in EDL muscle force compared to vehicle- or Riluzole-treated mice. Riluzole treatment alone or in combination with Cogane had no effect on muscle force. (B) Treatment with Cogane alone or together with Riluzole increased motor unit survival compared to treatment with Riluzole alone. (C) Treatment with Cogane and Riluzole, alone or in combination, increased motor neuron survival compared to vehicle treatment. Error bars: ±S.E.M. Mann-Whitney U Test. *p<0.05. **p<0.01. **The experiments shown in this Figure were undertaken by Dr Bernadett Kalmar and data reproduced from Kalmar et al., 2012a.**

Interestingly, Cogane's superior beneficial effect on EDL muscle force and motor unit survival over Riluzole was not replicated in plasma NfH levels. As can be seen in Fig. 3.12, Cogane had no effect on plasma NfH^{SMI34} levels in $SOD1^{G93A}$ mice compared to vehicle, and although NfH^{SMI34} levels were reduced in mice treated with Cogane in combination with Riluzole, this reduction was not significant either at 105 days or 120 days. In contrast, mice treated with Riluzole alone had significantly lower plasma NfH^{SMI34} levels than either vehicle- or Cogane-treated mice at both 105 days and 120 days (Fig. 3.12A and Fig. 3.12 B). As for plasma NfH^{SMI35} levels, Cogane alone also had no effect compared to Vehicle. In contrast, in mice treated with Cogane in combination with Riluzole plasma NfH^{SMI35} was largely reduced than Cogane alone at 105 days of age (Fig. 3.12C). In mice treated with Riluzole alone, there was a small, but insignificant reduction in plasma NfH^{SMI35} levels at 105 days (Fig. 3.12C), but by 120 days this reduction in plasma NfH^{SMI35} was significantly lower than in Cogane-treated SOD1 mice (Fig. 3.12D).

3.3.5 Plasma NfH levels reflect disease progression in a slowly progressing mouse model of ALS

The results presented in this Chapter have shown that plasma NfH levels correlate with disease progression and can be used to monitor this functional parameter in preclinical trials which utilize the $SOD1^{G93A}$ mouse model of ALS. However, the $SOD1^{G93A}$ mouse model has a very aggressive, rapid disease. Therefore, in the next set of experiments, I examined whether plasma NfH levels also reflected disease progression in a more slowly progressing mouse model of ALS, the $SOD1^{G93Adl}$ mouse, in order to establish whether this approach was applicable to models other than that in which it was developed. The $SOD1^{G93Adl}$ mouse has a significantly slower disease course than the SOD^{G93A} model. The earliest phenotypic change detected in these mice is mild tremor, detected at 18 weeks of age, followed by deficits in grip strength at approximately 21 weeks (Acevedo-Arozena et al., 2011). Analysis of muscle force, motor unit and motor neuron survival revealed that deficits of these parameters were first detectable at 24 weeks of age and by 34 weeks these defects had worsened significantly. These physiological and morphological experiments were undertaken by Dr Bernadett Kalmar, a postdoc in our lab (Acevedo-Arozena et al., 2011). These findings are summarised in Fig. 3.13A-C.

In the same $SOD1^{G93Adl}$ mice used for analysis of disease progression, plasma NfH levels were determined between 15 and 38 weeks of age. The results are

Figure 3.12

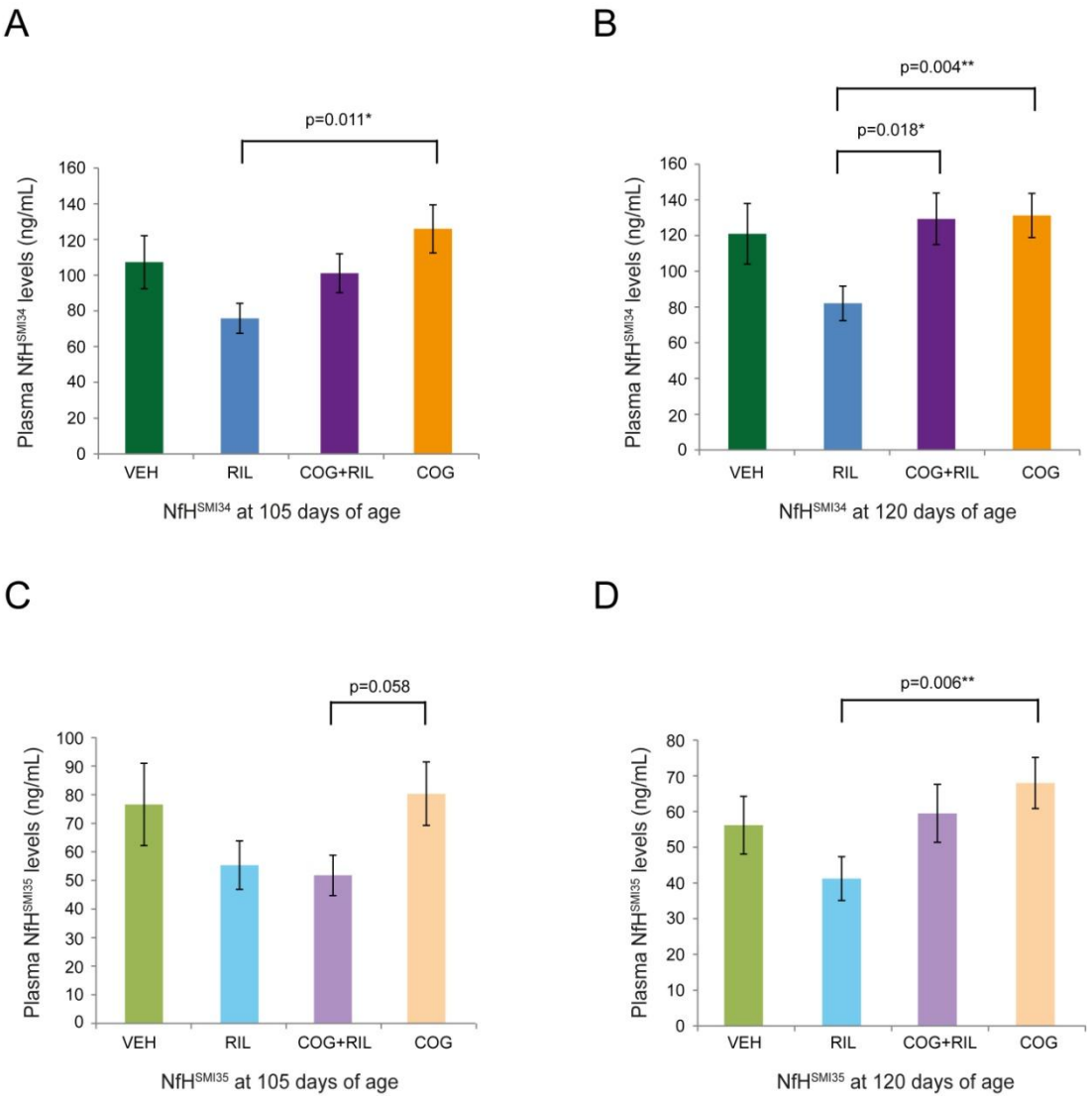
A
p=0.011*
Plasma NfH^SMI34 levels (ng/mL)
160
140
120
100
80
60
40
20
0
VEH
RIL
COG+RIL
COG
NfH^SMI34 at 105 days of age
B
p=0.004**
p=0.018*
Plasma NfH^SMI34 levels (ng/mL)
160
140
120
100
80
60
40
20
0
VEH
RIL
COG+RIL
COG
NfH^SMI34 at 120 days of age
C
p=0.058
Plasma NfH^SMI35 levels (ng/mL)
100
90
80
70
60
50
40
30
20
10
0
VEH
RIL
COG+RIL
COG
NfH^SMI35 at 105 days of age
D
p=0.006**
Plasma NfH^SMI35 levels (ng/mL)
80
70
60
50
40
30
20
10
0
VEH
RIL
COG+RIL
COG
NfH^SMI35 at 120 days of age

Figure 3.12. Summary of plasma NfH levels in SOD1^{G93A} mice treated with Cogane and Riluzole from onset of disease (70 days of age). The bar chart shows the mean plasma NfH^{SMI34} levels in **(A)** 105-day-old mice and **(B)** 120-day-old mice as well as plasma NfH^{SMI35} levels in mice at **(C)** 105 days and **(D)** 120 days of age. Figures **(A)** and **(B)** show that treatment of SOD1^{G93A} mice with Cogane has no effect on plasma NfH^{SMI34} levels compared to vehicle, and although NfH^{SMI34} levels are reduced in mice treated with Cogane in combination with Riluzole, this reduction is not significant either at 105 days or 120 days. Mice treated with Riluzole alone have significantly lower plasma NfH^{SMI34} levels than either vehicle- or Cogane-treated mice at both 105 days and 120 days. Figures **(C)** and **(D)** demonstrate that Cogane alone has no effect on NfH^{SMI35} levels at 105 and 120 days, although a significant reduction in levels is observed in the mice treated with Cogane in combination with Riluzole and Riluzole alone also decrease plasma NfH^{SMI35} levels at 105 days of age, which is not significant. However, by 120 days, Riluzole treatment results in a significant reduction in plasma NfH^{SMI35} levels compared to Cogane-treated mice. Error bars: ±S.E.M. Mann-Whitney U test. *$p<0.05$, **$p<0.01$.

Figure 3.13

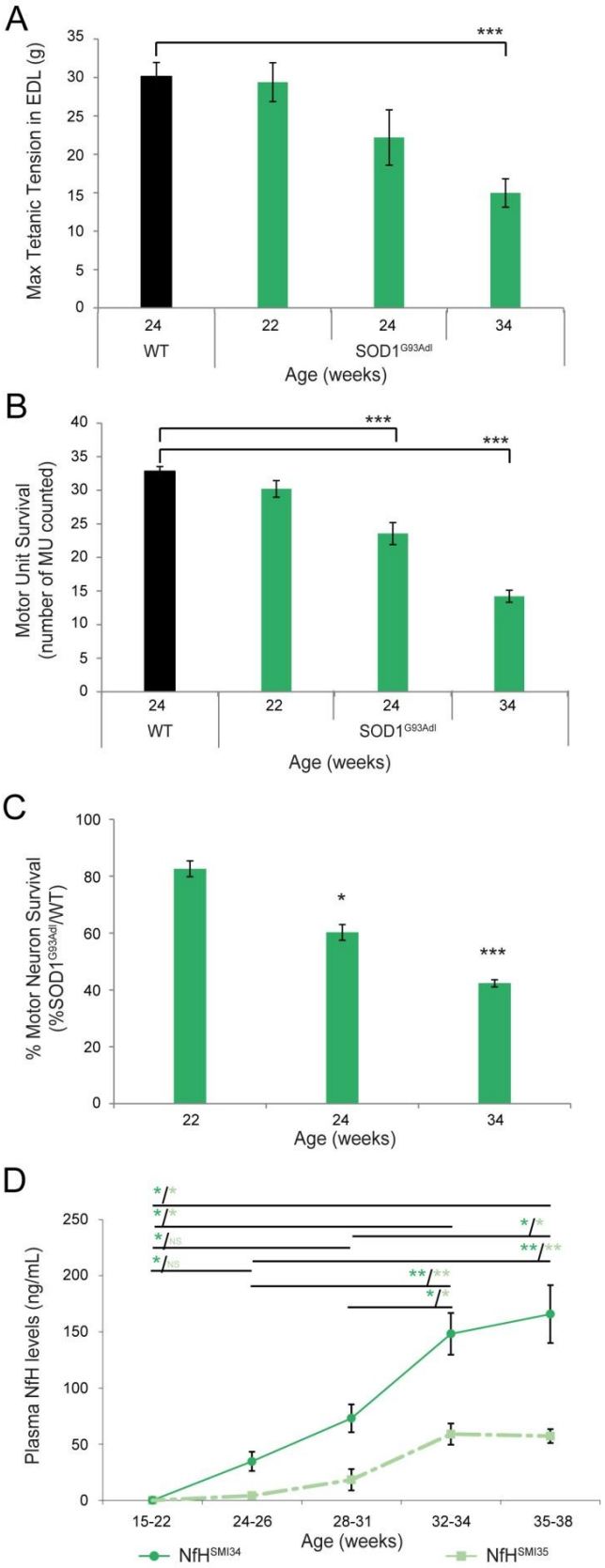
A
Max Tetanic Tension in EDL (g)
35
30
25
20
15
10
5
0
***
24
WT
22
24
34
SOD1G93Adl
Age (weeks)
B
Motor Unit Survival
(number of MU counted)
40
35
30
25
20
15
10
5
0
***
***
24
WT
22
24
34
SOD1G93Adl
Age (weeks)
C
% Motor Neuron Survival
(%SOD1G93Adl/WT)
100
80
60
40
20
0
*
***
22
24
34
Age (weeks)
D
Plasma NfH levels (ng/mL)
250
200
150
100
50
0
15-22
24-26
28-31
32-34
35-38
Age (weeks)
NfHSMI34
NfHSMI35

Figure 3.13. The decline in neuromuscular function and motor neuron survival and change in plasma NfH levels during disease progression in SOD1^{G93Adl} mouse model of ALS. The bar charts summarise data showing the decrease in **(A)** EDL tetanic force, **(B)** EDL motor unit survival, **(C)** Motor neuron survival at different stages of disease progression in SOD1^{G93Adel} mice (green bars) and their WT littermates (black bars). **(D)** Mean plasma NfH^{SMI34} (bright green solid line) and mean plasma NfH^{SMI35} (light green dashed line) levels in SOD1^{G93Adl} mice from 15-22 weeks of age onwards are shown. Plasma NfH became detectable from weeks 24-26, and increase largely during disease progression, particularly between weeks 28-31 and weeks 32-34, the late disease stage in this model. Error bars: ±S.E.M. *p<0.05, **p<0.01, ***p<0.001. **The experiments in (A), (B) and (C) were undertaken by Dr Bernadett Kalmar and data reproduced from Acevedo-Arozena et al., 2011.**

summarised in Fig 3.13D. It can be seen that plasma NfH levels, both NfH^{SMI34} and NfH^{SMI35} phosphoforms, were undetectable up to 22 weeks of age. By 24 weeks, however, plasma NfH levels began to increase and increased further as disease progressed, particularly between weeks 28-31 and 32-34, a late stage of disease in this model.

3.4 Discussion

In this Chapter I examined i) the potential of phosphorylated NfH as a biomarker of disease progression in $SOD1^{G93A}$ mice; ii) the ability of this method to detect the disease modifying effects of therapies under study in preclinical trials, and iii) the use of phosphorylated NfH levels to monitor disease progression in an alternative mouse model of ALS.

3.4.1 Plasma NfH levels are a biomarker of disease progression in the $SOD1^{G93A}$ mouse model of ALS and reflect the beneficial effects of a disease-modifying therapy

In this Chapter, plasma NfH levels were validated as a marker of late stage disease progression and treatment response in an animal model of ALS. Plasma is a readily available biological fluid that is easy to sample in longitudinal studies of progressive neurodegenerative disorders such as ALS. As shown in Fig. 3.1, the results show that plasma NfH levels increase significantly during disease progression, between 65-120 days, in the $SOD1^{G93A}$ mouse model of ALS (Friedman test: $p< 0.0001$). Moreover, this increase in plasma NfH in $SOD1^{G93A}$ mice correlates with the loss of muscle force, the decline in motor unit survival and most significantly, with the extent of motor neuron degeneration that occurs during later stages of disease. Furthermore, the results also show that plasma NfH levels are a sensitive readout of late stage disease severity that can reflect the effects of a disease modifying therapy. Thus, in $SOD1^{G93A}$ mice treated with Arimoclomol, I observed a significant delay in disease progression as previously reported (Kalmar et al., 2008; Kieran et al., 2004), as reflected in an improvement in muscle force, motor unit and motor neuron survival, and these improvements were linked to a reduction in plasma NfH levels compared with vehicle treated age-matched $SOD1^{G93A}$ littermates. Arimoclomol is currently in a Phase II/III clinical trial in ALS patients with *SOD1* mutations (Cudkowicz et al., 2008; Lanka et al., 2009; NCT00706147). The findings of this study therefore may represent an important step in the development of an easily accessible, comprehensive marker for disease progression in ALS that may have

utility in future clinical trials, particularly since patients are usually diagnosed and recruited into trials well after the onset of symptoms.

3.4.2 The use of NfHs as a biomarker of disease

Although previous reports have suggested that NfH levels may be a candidate biomarker for ALS and other progressive neurodegenerative diseases including AD and PD (Constantinescu et al., 2009; de Jong et al., 2007; van Eijk et al., 2010; Zetterberg et al., 2007), most of these studies have examined CSF as the target biological fluid. This approach necessitates the use of a relatively invasive procedure i.e. a lumbar puncture, which is not suitable for repeated sampling in longitudinal assessment of disease progression, particularly in individuals suffering from ALS, with significant physical and often respiratory impairment. Analysis of plasma NfH is the obvious solution to this problem, but this can be technically challenging due to the so-called NfH 'Hook Effect'. This technical hurdle is caused by the tendency of proteins such as neurofilaments to aggregate, resulting in the masking of its epitopes and consequently, lower and un-representative yields in commonly used ELISA techniques (Lu et al., 2011). The NfH 'Hook Effect' has to date, therefore prevented the reliable measurement of neurofilament levels in ALS and other diseases where NfH aggregate formation occurs by standard immunoassay. In this respect, the methodology developed in Chapter 2 and used in this Chapter to determine plasma NfH levels is unique, in so far it is the first method specifically devised to overcome the NfH 'Hook Effect' (Lu et al., 2011).

Although the anatomically defined blood-brain barrier (BBB) and the functionally defined blood-CSF barrier (BCB) limit CNS-to-blood transfer, molecules expressed in the CNS can still enter the blood under both normal and pathological conditions. It is therefore not surprising that neurofilaments leak into the circulation in both SOD1 mice and ALS patients. The method I have developed (Lu et al., 2011) and used in this study was capable of detecting both hyperphosphorylated (NfH^{SMI34}) and variably-phosphorylated (NfH^{SMI35}) forms of NfH in plasma of WT animals at all ages studied. Although the two forms of NfH were present in approximately equal amounts, the detection of hyperphosphorylated NfH in the plasma of healthy WT mice shows that the presence of hyperphosphorylated NfH in the peripheral blood is not in itself indicative of pathology. Moreover, since NfH have been detected in several pathological conditions (Perrot et al., 2008), their presence is not disease specific and one of the important conclusions from this Chapter is that plasma NfH

cannot therefore be used as a primary diagnostic biomarker for neurodegenerative conditions such as ALS. However, increased plasma NfH levels do not reflect the earlier stages of disease in SOD1^{G93A} mice, where NfH levels were similar in SOD1^{G93A} and WT mice. Nonetheless, a far larger variation in plasma NfH levels in SOD1^{G93A} mice than WT mice was observed, even prior to symptom onset (65 days). Plasma NfH levels increased significantly in SOD1 mice between 105 to 120 days of age (Fig. 3.1 and 3.2). Similarly in another SOD1^{G93Adl} mouse model, a significant increase of plasma NfH^{SMI34} and NfH^{SMI35} were found in parallel with the decline in muscle force, motor unit survival and motor neuron survival. However, I did not have enough data/mice to correlate these disease progression markers with NfH levels in SOD1^{G93Adel} mice, as tested in SOD1^{G93A} mice.

The sensitivity and reliability of the method used in the present study is highlighted by a comparison of our results with those of previous reports investigating plasma NfH as a potential biomarker of ALS. Thus, one study failed to detect any NfHs in plasma from WT mice and reported NfH levels in end-stage SOD1^{G93A} mice on average below 75 ng/mL (Boylan et al., 2009) and the other study only detected NfH in plasma of end-stage SOD1^{G93A} mice at very low levels (on average, 8 ng/mL) (Gnanapavan et al., 2012). In contrast, using the method employed in the present study, plasma NfH levels can be detected in WT mice at all ages studied, as well as in pre-symptomatic and end-stage SOD1^{G93A} mice, in which mean NfH levels rise to as high as 318.11 ng/mL (Lu et al., 2011).

In addition to examining changes in plasma NfH levels in SOD1^{G93A} mice, I also compared the relative levels of the two different NfH phosphoforms, NfH^{SMI35} and NfH^{SMI34}. The results show that at 65 days of age, in both WT and SOD1 mice, the plasma levels of NfH^{SMI35} and NfH^{SMI34} were similar to each other. However, by 90 days, a clear change in the relative levels of the two NfH phosphoforms was detected, with an increase in NfH^{SMI34} levels and a decline in NfH^{SMI35}. It is possible that this change in the relative levels of hyperphosphorylated NfH is a better indicator of pathology than simply the presence of this phosphoform per se. Thus, the results i) demonstrate the early involvement of NfH in pathology in SOD1^{G93A} mice, ii) reveal the true abundance of NfH in the plasma of these mice and iii) suggest that an increase in the ratio of hyperphosphorylated NfH: variably phosphorylated NfH is indicative of pathology, at least in the SOD1^{G93A} mouse model of ALS.

3.4.3 Plasma NfH levels correlate with functional and morphological read-outs of neuromuscular decline in SOD1^{G93A} mice

In order to examine whether the increase in plasma NfH reflected the decline in neuromuscular function that occurs during disease progression in SOD1^{G93A} mice, I performed a correlation analysis of plasma NfH levels with longitudinal and acute outcome measures. There was a strong-moderate inverse correlation between plasma NfH levels (both NfH^{SMI34} and NfH^{SMI35}) and grip strength in SOD1^{G93A} mice between 65-120 days of age (Fig. 3.4). Grip strength is a general functional test widely used to evaluate general motor function in mouse models (Crawley, 2008; Rogers et al., 1997; Rogers et al., 2001). However, grip strength is an overall measure of neuromuscular function that predominantly reflects the function of forelimb muscles, which are affected relatively late in disease progression in SOD1^{G93A} mice. I therefore also correlated NfH levels with acute, quantitative, reproducible *in vivo* physiological assessments of neuromuscular function in hindlimbs. A moderate-strong correlation in the decline in muscle force and increased plasma NfH (Fig. 3.5D) and a mild correlation between plasma NfH and EDL motor unit loss (Fig. 3.6C) in SOD1^{G93A} mice was observed. The mild correlation between NfH levels and motor unit survival is likely to be a reflection of the relatively late involvement of the EDL muscle in disease in SOD1 mice (Kalmar et al., 2008; Sharp et al., 2005). It is therefore possible that motor unit loss in other muscles such as TA, which is affected earlier and to a greater extent than EDL, may correlate better with NfH levels than EDL. However, it is technically more difficult to accurately estimate motor unit survival in large muscles such as TA, which has a large number of motor units. Instead, assessment of motor unit loss in any individual muscle may not be a good measure of overall disease progression, particularly in a disease such as ALS, where the site of disease onset and degeneration of different muscle groups varies.

Among the most direct measures of disease progression in ALS is the extent of motor neuron survival. It has been proposed that the loss of motor neurons in ALS patients is linear (Chio et al., 2009) and in the present study, morphological assessment of motor neuron survival at different ages confirms that motor neuron survival appears to decline linearly in SOD1^{G93A} mice. More importantly, we found a strong correlation between the extent of motor neuron degeneration and plasma NfH levels in SOD1^{G93A} mice (Fig. 3.7C). These results show that plasma NfH levels, at least detected by the method described in this study, can be used to reflect the

extent of motor neuron degeneration. Thus, longitudinal measurement of plasma NfH levels in SOD1^{G93A} mice reveals that plasma NfH levels increase as disease progresses, particularly in later stages between 105-120 days, the most critical period of disease progression in SOD1^{G93A} mice, and this increase in NfH levels correlate with the decline in neuromuscular function and death of motor neurons, the defining phenotypic characteristics of ALS.

However, it should be noted that, there is likely to be a significant delay between the time that the first physical manifestations of disease occur in ALS, such as muscle denervation (Fischer et al., 2004), and when these deficits result in functional, symptomatic deficits (such as reduced muscle force), and the eventual appearance of Nfs in the peripheral blood. Thus, when the timeline between muscle denervation, axonal degeneration, formation of NfH-containing aggregates, motor neuron degeneration and the eventual entry of NfH into peripheral blood is taken into account, it is not surprising that there is a discrepancy in the time between the detection of early physical manifestations of the disease (90 days) and the first significant elevation in plasma NfH levels (105 days). However, the invasive physiological and morphological approaches used to determine the extent of disease in SOD1^{G93A} mice in this study, although very sensitive, quantitative and accurate, are irreversible and not practical for longitudinal follow-up in mice. Moreover, these measures are, in the mice, not clinically relevant for humans as they may not reflect the state of disease in patients when they first present to their physician with symptoms. Therefore, the correlations we report between the increases in plasma NfH levels and the decline in neuromuscular function may provide a safe and easy measure for the evaluation of later disease progression in ALS.

3.4.4 Plasma NfH levels reflect the effects of disease-modifying therapies in SOD1^{G93A} mice

The results presented in this Chapter also show that plasma NfH levels reflect the disease modifying effects of Arimoclomol in SOD1^{G93A} mice. In confirmation of our previous findings (Kalmar et al., 2008; Kieran et al., 2004), we found that treatment with Arimoclomol significantly delays the decline in neuromuscular function and the degeneration of motor neurons in SOD1^{G93A} mice (Table 3.1). Furthermore, plasma NfH levels were in general lower in Arimoclomol-treated SOD1+A mice than vehicle-treated SOD1 littermates at all ages studied, but most significantly at later stages of

disease, from 105-120 days of age (Fig. 3.9 and Fig 3.10). Hence, at 65 days, a pre-symptomatic age, plasma levels of NfH^{SMI34} were significantly lower in Arimoclomol-treated SOD1+A mice compared to vehicle-treated SOD1 littermates, possibly due to the early beneficial effects of Arimoclomol in the periphery, at the neuromuscular junction (NMJ) (Kalmar et al., 2012b). Arimoclomol acts as a co-inducer of the heat shock response, so that it only acts in cells under conditions of cellular stress to augment the heat shock response (HSR) (Hargitai et al., 2003). Thus, although the neuroprotective effects of Arimoclomol in $SOD1^{G93A}$ mice only manifest later in the disease when motor neurons are under considerable stress (Kalmar et al., 2008; Kieran et al., 2004), a recent study shows that its beneficial effects in the periphery manifest earlier in the disease, prior to symptom onset (Kalmar et al., 2012b). It has now been established that the earliest physical manifestation of disease in $SOD1^{G93A}$ mice occurs at the NMJ, where significant muscle denervation occurs prior to any motor neuron death (Fischer et al., 2004; Kalmar et al., 2012b). The recent work in our lab has shown that this early denervation is accompanied by an increase in the HSR and correspondingly, in Arimoclomol-treated $SOD1^{G93A}$ mice, this stress response is augmented, resulting in a delay in muscle denervation (Kalmar et al., 2012b). Therefore, since the levels of NfH remain steady in WT mice throughout the study, the difference in plasma NfH levels observed in SOD1+A and SOD1 mice at 65 days of age is likely to be the result of Arimoclomol's early beneficial effects in the periphery and the maintenance of neuromuscular contacts.

As shown in Fig. 3.9 & 3.10 and Table 3.1, the significant improvement in muscle force, motor unit and motor neuron survival observed from 105 days of age in Arimoclomol-treated SOD1+A mice compared to their vehicle-treated SOD1 littermates is reflected in a decrease in plasma NfH levels. Although the significance of reduction of NfH^{SMI35} observed from 105 days was in line with the physiological improvement, the reduction of NfH^{SMI34} became significantly reduced only at 120 days of age. However, further analysis of the levels of the two NfH phosphoforms showed that the relative increase in the more pathological plasma NfH^{SMI34} compared with NfH^{SMI35} occurred later in Arimoclomol-treated SOD1+A mice than vehicle-treated SOD1 mice (Table 3.2). It is likely that the difference in the timing of the effects of Arimoclomol treatment on NfH^{SMI35} and NfH^{SMI34} levels may be related to their different levels of phosphorylation. Since the stability of NfH increases with the degree of phosphorylation (Petzold, 2005), it will take longer for proteases to cleave hyperphosphorylated NfH compared with variable-phosphorylated NfH.

Because neurofilament aggregates containing a large quantity of hyperphosphorylated NfH are a hallmark of disease in SOD1^{G93A} mice, it will take longer for hyperphosphorylated NfH levels to decrease following treatment with Arimoclomol compared with variable-phosphorylated NfH.

Furthermore, in this Chapter I also examined the utility of phosphorylated NfH measurements to detect the effects of therapeutic agents in a novel preclinical trial undertaken in the group. In this study, the efficacy of a new potential drug candidate called Cogane was examined. As part of this study, SOD1^{G93A} mice were also treated with Riluzole either alone or in combination with Cogane, as Riluzole is the standard treatment for ALS and in any human ALS clinical trial it is likely that patients will be receiving Riluzole. The effects these treatments in neuromuscular function and motor neuron survival were analysed. In addition, blood was collected from these mice at key time points in disease when data collection from vehicle-treated SOD1 mice had shown the most significant changes in phosphorylated NfH levels, i.e. at 105 and 120 days of age (Fig. 3.1 and Fig. 3.2). As can be seen in Fig. 3.12, distinct plasma NfH levels were observed in mice treated with Riluzole and Cogane, in which Riluzole is more effective in reducing plasma NfH levels than Cogane. Together with the findings in Kalmar et al., 2012a, it is therefore possible that Cogane primarily improves muscle function, whereas Riluzole appears to have neuroprotective effects. The changes in phosphorylated NfH may therefore reflect the different therapeutic mechanisms of Cogane and Riluzole in disease progression in SOD1^{G93A} mice.

Lastly, a large difference in NfH levels was observed in the vehicle-treated SOD1^{G93A} mice in the Arimoclomol trial (Fig. 3.1 & 3.2) and the Cogane trial (Fig. 3.13). As the goal in the Arimoclomol trial was to investigate the possibility of NfH as a disease biomarker in SOD1^{G93A} mice, male mice, which are usually only used for breeding in most of other studies, were used in order to obtain the maximal blood samples in serial blood samplings, while still complying with UK Home Office regulations. In contrast, female mice were chosen to investigate novel therapeutic effects on disease progression in SOD1^{G93A} mice, the main goal in the Cogane trial. As there is a gender difference in body mass, disease progression, survival days and response to Arimoclomol in SOD1^{G93A} mice (Kalmar et al., 2008), the difference in plasma NfH levels observed in these two trials in vehicle-treated SOD1^{G93A} mice is likely to be due to gender differences.

3.5 Conclusions

Taken together, the results presented in this Chapter show that the late stage decline in neuromuscular function and motor neuron survival in SOD1^{G93A} mice and SOD1^{G93Adl} mice is correlated with an increase in plasma NfH phosphoform levels. Furthermore, plasma NfH phosphoform levels reflect the improvement in disease phenotype induced by disease-modifying treatments such as Arimoclomol. Plasma NfH phosphoform levels may therefore be a useful marker to determine late stage disease progression in ALS and that may eventually be used as a sensitive outcome measure in clinical trials, particularly since ALS patients are likely to exhibit significant disease symptoms by the time of enrolment.

The accurate and sensitive assessment of plasma NfH phosphoform levels may therefore provide a quick and easy readout of disease progression in individual patient in future clinical trials. In addition, plasma NfH levels may also serve as a safety biomarker as rapid increases in plasma NfH phosphoform levels following administration of test drugs might indicate a detrimental treatment effect (Petzold et al., 2010b). The use of plasma NfH as an outcome measure may therefore help to improve the safety of clinical trials by speeding up the time taken to detect deleterious effects. Furthermore, reductions in the time taken to complete these studies will reduce the costs of Phase III trials, which account for 70% of costs of clinical drug development in ALS (Cudkowicz et al., 2010). Whether the findings presented in this Chapter in animal models of ALS can be translated to ALS patients will become clear through further longitudinal investigation on cohorts of ALS patients. This is the focus of the experiments next presented in Chapter 4. If the results observed in this study in animal models of ALS are translated into patient samples, accurately measured plasma NfH phosphoform levels may become a valuable biomarker of disease progression, especially in later stages, for the ALS community.

- Some of the results presented in this Chapter have been published:
  Ching-Hua Lu, Axel Petzold, Bernadett Kalmar, James Dick, Andrea Malaspina, Linda Greensmith. (2012). Plasma neurofilament heavy chain levels correlate to markers of late stage disease progression and treatment response in SOD1^{G93A} mice that model ALS. PLoS ONE, 7(7):e40998.

Chapter 4

Plasma neurofilaments as a biomarker of disease progression in ALS: Insights from a longitudinal study

4.1 Introduction

In Chapter 3, I examined whether plasma phosphorylated NfH levels may be used as a biomarker of disease progression in SOD1^{G93A} mice. My results showed that plasma NfH levels correlate well with functional and morphological read-outs of disease progression in this well-characterised mouse model of ALS, which exhibits a homogenous disease phenotype. Moreover, my results also showed that plasma NfH levels were sensitive enough to reflect the disease modifying effects of known and novel therapies in SOD1^{G93A} mice. In addition, analysis of plasma NfH levels in the more slowly progressing SOD1^{G93Adel} mouse model of ALS established that the correlation between disease progression and plasma NfH levels was not restricted to the aggressive, rapidly progressing ALS phenotype observed in SOD1^{G93A} mice. Taken together, these findings suggest that plasma NfH levels may be a biomarker of disease progression in human ALS. In this Chapter, I investigated the relevance of the findings outlined in Chapter 3 in ALS patients, by analysing the longitudinal pattern of plasma NfH levels in a heterogeneous group of ALS patients and examining its correlation with disease progression in these ALS patients.

4.1.1 Current limitations and merits in biomarkers of disease progression in ALS

Similar to other neurodegenerative disorders, it is generally accepted that the neurodegenerative processes driving ALS start long before the appearance of overt signs and symptoms of disease. In addition to this period of unrecognized pathology and of its detrimental effect to neuronal integrity, there is typically a 9-14 month delay between symptom onset and a final diagnosis of ALS (Cellura et al., 2012; Iwasaki et al., 2002). It is therefore reasonable to assume that this overall delay in the recognition of the disease may be a major obstacle to the development of treatments, whose efficacy largely depends on an early rescuing strategy for still healthy or partially functioning motor neurons (Ganesalingam and Bowser, 2010).

Indeed, the diagnostic latency remains to date one of the strongest predictors of a worse prognosis in ALS (Chio et al., 2009; Turner et al., 2010a). The significant

clinical heterogeneity in ALS, which encompasses different anatomical sites of disease initiation as well as different patterns of disease progression, and overall survivals ranging from 6 months to 10 years, adds an additional layer of complexity in any effort to identify biomarkers of disease progression and of treatment response in ALS (Kiernan et al., 2011).

The clinical diversity in the progression of ALS can be captured by clinimetrics such as the ALS Functional Rating Scale_Revised (ALSFRS_R) (Castrillo-Viguera et al., 2010; Cedarbaum et al., 1999; Kollewe et al., 2008), which recapitulates the main components of the neurological impairment in ALS and provides a measure of the level of involvement based on commonly recognized disease milestones, such as the need for gastrostomy and for non-invasive ventilation. The ALSFRS_R score and its ratio have a strong correlation with disease progression and survival (Kaufmann et al., 2005; Kollewe et al., 2008), and have been widely used as primary or secondary outcome measure of efficacy in ALS clinical trials (Beghi et al., 2011). The ALSFRS_R score and its ratio have also been used as a parameter of disease progression in several biomarker development studies (Boylan et al., 2013; Keil et al., 2012; Tortelli et al., 2012; Zhang et al., 2011b). However, the ALSFRS_R is far from perfect and still requires refinement, as some of its rating categories were recently found not to be sensitive enough, with a reduced sensitivity of the raw scores in changes occurring in very high and very low functional ALS patients (Franchignoni et al., 2013). Therefore, it is possible that the 'not-so-perfect' ALSFRS_R, a clinimetric mostly used to validate the relevance of a developing disease progression biomarker in ALS, might also contribute to the uncertainty of current biomarker development in ALS.

However, attempts to establish molecular indicators to predict or monitor the rate of disease progression in ALS have produced initial encouraging results, for example, evidence of a correlation between the numbers of regulatory T-lymphocytes (Tregs) & their FoxP3 protein expressions and disease progression rates in ALS (Beers et al., 2008; Henkel et al., 2013). With recent discoveries of new genetics and pathomechanisms in ALS as well as advances in technologies and platforms for biomarker development (discussed in Chapter 1 Section 5**)** it is still possible that novel biomarkers for disease progression in ALS may be identified in the near future.

4.1.2 Recent progress in developing neurofilaments as a biomarker of disease progression in ALS

Nfs have emerged as one of the most promising candidates amongst potential biomarkers of disease progression in extracellular fluid (ECF), in cerebrospinal fluid (CSF), and in blood extracted from patients with ALS (Ganesalingam et al., 2013). The reported direct pathological involvement of Nf phosphophorms in ALS and the fact that Nfs are the main by-product of axonal loss and motor neuron degeneration clearly identify Nfs as a suitable target for any investigation into disease biomarkers of neurodegeneration. The CSF is in a privileged position to be the main bio-repository for molecules synthetized or excreted during physiological or pathological events within the CNS. As a result, most of the biomarkers studies in neurodegenerative disorders, including the study of Nf, have been undertaken in CSF. In ALS, levels of Nfs in CSF have been found to be much higher than in other neurodegenerative disorders such as AD (Brettschneider et al., 2006c; Ganesalingam et al., 2011; Norgren et al., 2003; Rosengren et al., 1996; Tortelli et al., 2012) and to correlate inversely with disease duration (Zetterberg et al., 2007), inversely with diagnostic delay & ALSFRS_R score and positively with disease progression (Tortelli et al., 2012).

However, due to the invasive nature of spinal taps, serial CSF sampling, although not impossible, is certainly not practical for the purpose of monitoring disease progression, particularly in frail and advanced ALS patients. Studies to uncover the Nf plasma profile in ALS patients have been undertaken in small cohorts of patients and have shown a 2-fold increase of pNfH in ALS, although both patients and controls display very low detection levels (Boylan et al., 2009). Levels of pNfH in blood-based bio-fluids, serum and plasma, correlated well with CSF pNfH levels, although the correlation with ALSFRS_R slope was the best in CSF, followed by serum and then plasma, according to a recent study (Boylan et al., 2013). However, the major disadvantage with previous investigations into the bioavailability of NfH in peripheral blood is that they have been conducted in cohorts of rather small group size, which are unlikely to be representative of the heterogeneous ALS population (Chio et al., 2011a; Chio et al., 2011b).

Both CSF and current blood-based Nf studies extrapolate prognostic information based on a single time point sampling followed by short follow-up periods, tracking only a fraction of the disease course from the baseline sampling. Large scale of

longitudinal investigations defining Nf expression at multiple time points in association with the observed rate of neurological decline would be a better approach to test the relationship between the bioavailability of a protein and the natural development of the disease. This approach would also help the study design of clinical trials which plan to use plasma NfH as a biomarker of treatment response.

4.1.3 Hypotheses and Aims of this Chapter

In this Chapter, I examined the hypothesis that plasma NfH levels may be a marker of disease progression in ALS. To test this possibility, I examined NfH levels in plasma samples collected from 136 ALS patients and 104 controls with the following Aims:

i) To conduct a baseline cross-sectional examination of plasma NfH levels in ALS patients and controls;

ii) To establish the longitudinal pattern of plasma NfH levels in ALS patients;

iii) To examine whether the plasma NfH levels correlate with disease progression in ALS, using ALSFRS_R score;

iv) To establish whether plasma NfH levels have any prognostic value in ALS;

v) To explore a possible mechanism affecting NfH homeostasis in peripheral blood.

4.2 Method and Materials

4.2.1 Experimental participants

Ethical approval for the study was obtained from the East London and the City Research Ethics Committee 1 (09/H0703/27) and patients were recruited at different clinics within the University College London Partner-Motor Neuron Disease (UCLP-MND) Care Centres (St Bartholomew's Hospital, London; Royal London Hospital, London; Basildon Hospital, Essex; National Hospital for Neurology and Neurosurgery, London) and at the Musgrove Park Hospital, Somerset. All subjects provided written informed consent. All subjects were evaluated in MND clinics. The study design involved study visits and blood samplings every 3 months in the follow-up period, but time intervals varied between 2 and 4 months.

4.2.1.1 ALS patients

In this project, we recruited only clinically sporadic ALS patients, who had a diagnosis of definite, probable, laboratory supported probable or possible ALS according to the El Escorial Criteria (Table 4.1) (Brooks et al., 2000). Only patients able to consent and to attend the designated out-patient clinics were included in this study. 90% of ALS participants were consented in the study either at diagnosis or within 2-3 months from diagnosis. Exclusion criteria included neurological co-morbidity which are likely to affect Nf homeostasis including neurosurgical operations prior to enrolment, concomitant peripheral neuropathies (idiopathic, diabetes-induced or following chemotherapy) and recent history of significant neurotrauma (Petzold et al., 2010a; Petzold et al., 2006a; Petzold et al., 2006b; Petzold et al., 2008; Petzold et al., 2010b; Tisdall and Petzold, 2012). A total of 136 ALS patients were recruited into the study.

4.2.1.2 Control subjects

Control subjects included healthy individuals and patients with a variety of neurological conditions, seen in the Neuromuscular Clinics within UCLP; these subjects were divided into two groups:

i) Healthy controls (HC), mainly the unrelated spouse/partner of patients;
ii) Neurological disease controls (NC);

Group NC included 14 multiple sclerosis (MS) individuals with a diagnosis of relapsing remitting MS (n=5), secondary progressive MS (n=6) and primary progressive MS (n=3), 10 individuals with inflammatory demyelinating neuropathies including chronic inflammatory demyelinating polyneuropathy, paraproteinemia related and multifocal motor neuropathy, 15 individuals with a diagnosis of single-level or multi-level compressive cervical or lumbar radiculopathy, 10 cases of idiopathic or genetically determined neuropathy including Charcot-Marie-Tooth and 4 cases with benign fasciculations and cramp syndrome. It is important to investigate neurological disease controls as these NCs represent some ALS mimic conditions. A total of 104 control subjects were included into the study.

4.2.2 Characterisation of disease progression ALS

4.2.2.1 Change in function

Disease duration was calculated from the reported symptom onset onwards. Disease progression was evaluated using the ALS Functional Rating Scale

Table 4.1 Diagnostic guidelines for ALS (Brooks et al., 2000).

Diagnostic Criteria:	
(A) Presence	1. Evidence of LMN degeneration by clinical, electrophysiological or neuropathologic examination;
	2. Evidence of UMN degeneration by clinical examination;
	3. Progressive spread of symptoms or signs within a region or to other regions as determined by history or examination.
(B) Absence	1. Electrophysiological or pathological evidence of other disease processes that might explain the signs of LMN and/or UMN degeneration;
	2. Neuroimaging evidence of other disease processes that might explain the observed signs.
Diagnostic certainty categories:	
Definite ALS: Clinical evidence of UMN and LMN signs in three regions;	
Probable ALS: Clinical signs of UMN and LMN deterioration in at least two regions, with some UMN signs rostral to LMN signs;	
Probable Laboratory-Supported ALS: Clinical signs of UMN and LMN degeneration in one region, or UMN signs alone in one region and electromyographic LMN signs in at least two regions;	
Possible ALS: Clinical signs of UMN and LMN degeneration in only one region, or UMN signs alone in two or more regions, or LMN signs found rostral to UMN signs.	

(ALSFRS_R) and disease duration over a specific period. The details of the ALSFRS_R, a composite functional outcome measure used for clinical trials and biomarker studies in ALS (Castrillo-Viguera et al., 2010; Chio et al., 2009; Kollewe et al., 2008), are shown in Table 4.2. In this study, the sum of scores from Questions 1-12 of the ALSFRS_R is taken as the 'score' for that visit. The maximal score is 48, which represents no functional deficit, and is used as the pre-onset status. A number of parameters of disease progression derived from the ALSFRS_R score were used in this Chapter:

i) ***Progression rate***: the progression rate from onset to each evaluation is calculated as [48 - the ALSFRS_R score at an assessment/duration in month between the reported time of ALS onset and the evaluation].

ii) ***Overall progression rate***: the progression rate between the reported time of ALS onset and the last assessment in the study period, determined as [(48 - the last ALSFRS_R score)/ duration in month between reported time of onset and the last available assessment in our follow-up]. This parameter was used to characterize the speed of progression of the disease and to separate ALS individuals with a fast disease development (ALS-F) from ALS individuals displaying a slower rate of progression (ALS-S). In general, those patients with an overall-progression rate ≥1.0 were considered as ALS-F, whereas those with an overall-progression rate of ≤ 0.5 were considered ALS-S.

iii) ***ALSFRS_R slope***: the *change* in functional score between two consecutive visits determined as [△ALSFRS_R score/duration in months]; this value can be negative.

4.2.2.1 Disease duration to baseline

For the purpose of our cross-sectional and longitudinal analyses, the ALS cohort was divided into 4 sub-groups according to the disease duration to baseline: 1) <12 months; 2) between 12-24 months; 3) between 24-36 months and 4) >36 months.

4.2.3 Plasma collection

All participants were evaluated in the out-patient clinics and blood samples were taken and processed within 1 hour. The interval between each visit was usually 3 months, but could vary according to patients' clinical progression. Blood was collected, into EDTA-coated tubes and spun down at 20°C 3500 rpm for 10 minutes,

Table 4.2 ALS Functional Rating Scale _ Revised (ALSFRS_R).

0	Questionnaire collected:	1	From patient in clinic
		2	From patient by phone
		3	From carer by phone (patient response) Must be done by carer only when dysarthric patient cannot communicate by phone. Must be patient view.

1	Speech	4	Normal speech processes
		3	Detectable speech disturbance
		2	Intelligible with repeating
		1	Speech combined with nonvocal communication
		0	Loss of useful speech

2	Salivation	4	Normal
		3	Slight but definite excess of saliva in mouth; may have night-time drooling
		2	Moderately excessive saliva; may have minimal drooling
		1	Marked excess of saliva with some drooling
		0	Marked drooling; requires constant tissue or handkerchief

3	Swallowing	4	Normal eating habits
		3	Early eating problems – occasional choking
		2	Dietary consistency changes
		1	Needs supplemental tube feeding
		0	NPO (exclusively parenteral or enteral feeding)

4	Handwriting	4	Normal
		3	Slow or sloppy: all words are legible
		2	Not all words are legible
		1	Able to grip pen but unable to write
		0	Unable to grip pen

5a	Cutting food and handling utensils (patients without gastrostomy)	4	Normal
		3	Somewhat slow and clumsy, but no help needed
		2	Can cut most foods, although clumsy and slow; some help needed
		1	Food must be cut by someone, but can still feed slowly
		0	Need to be fed

or

5b	Cutting food and handling utensils (patients with gastrostomy)	4	Normal
		3	Clumsy but able to perform all manipulations independently
		2	Some help needed with closures and fasteners
		1	Provides minimal assistance to caregiver
		0	Unable to perform any aspect of task

6	Dressing and Hygiene	4	Normal function
		3	Independent and complete self-care with effort or decreased efficiency
		2	Intermittent assistance or substitute methods
		1	Needs attendant for self-care
		0	Total dependence

7	Turning in bed and adjusting bed clothes	4	Normal
		3	Somewhat slow and clumsy, but no help needed
		2	Can turn alone or adjust sheets, but with great difficulty
		1	Can initiate, but not turn or adjust sheets alone
		0	Helpless

8	Walking	4	Normal
		3	Early ambulation difficulties
		2	Walks with assistance
		1	Nonambulatory functional movement
		0	No purposeful leg movement

9	Climbing stairs	4	Normal
		3	Slow
		2	Mild unsteadiness or fatigue
		1	Needs assistance
		0	Cannot do

10	Dyspnea	4	None
		3	Occurs when walking
		2	Occurs with one or more of the following: eating, bathing, dressing (ADL)
		1	Occurs at rest, difficulty breathing when either sitting or lying
		0	Significant difficulty, considering using mechanical respiratory support

11	Orthopnea	4	None
		3	Some difficulty sleeping at night due to shortness of breath, does not routinely use more than two pillows
		2	Needs extra pillows in order to sleep (more than two)
		1	Can only sleep sitting up
		0	Unable to sleep

12	Respiratory insufficiency	4	None
		3	Intermittent use of BiPAP
		2	Continuous use of BiPAP during the night
		1	Continuous use of BiPAP during the night and day
		0	Invasive mechanical ventilation by intubation or tracheotomy

with acceleration and deceleration set at 5 and 4 respectively. Plasma was then aliquoted and stored at -80°C until assayed.

4.2.3.1 Cross-sectional study sampling

Baseline plasma samples collected from the 136 ALS and 104 control participants were used for a cross-sectional study of plasma NfH levels.

4.2.3.2 Longitudinal study sampling

For longitudinal analysis, serial blood samples for plasma analysis were obtained from 74 of the 136 patients with a mean±S.E.M. follow-up period of 12.2±1.0 months (Max: 39.0, Min 1.1, 25%: 4.1, 75%: 17.9 months). The longitudinal study design involved visits and blood sampling every 3 months in the follow-up period, although time intervals varied between 2-4 months.

4.2.4 NfH ELISA

4.2.2.1 Analytical procedure using ELISA method originally designed for CSF samples

For detail procedures, please refer to Chapter 2, section 2.2.5.

4.2.2.2 Analytical procedure using ELISA method designed for plasma samples (developed in Chapter 2)

For detail procedures, please refer to Table 2.3.

4.2.2.3 ELISA data analysis

Hyperphosphorylated NfH was detected with the SMI-34R capture antibody labelled as NfH^{SMI34} (averaged intra-assay coefficient of variation (CV): 3.11%, averaged inter-assay CV: 3.76% at 12.5 ng/mL, 1.94% at 50 ng/mL), while variably phosphorylated NfH was detected with the SMI-35R capture antibody, labelled as NfH^{SMI35} (averaged intra-assay CV: 2.97%, averaged inter-assay CV: 3.29% at 12.5 ng/mL, 3.65% at 50 ng/mL). The sensitivity (blank + 3SD) of the assay calculates to 0.74 ng/mL, with a detection limit of 1.56 ng/mL. Total NfH refers to the sum of NfH^{SMI34} and NfH^{SMI35}. Measurements with a CV higher than 10%, the intra-assay CV in the ELISA method original designed for measuring NfH in human CSF, were repeated to keep up with the standard in the original assay (Petzold et al., 2003). Quality control samples were used throughout the analyses and absorbance

readouts from different microtitre plates were adjusted to the quality control readout to allow comparison of results across different plates (Petzold et al., 2010c).

4.2.4 Western Blots

4.2.4.1 Sample preparation

Western blot (WB) analysis of NfH^{SMI34} was carried out using plasma from ALS patients and purified bovine NfH protein (USBiological; N2160-15B). Each set of samples contained plasma pooled from 3 patients. All sets of samples were filtered twice through the Amicon® Ultra Centrifugal filter (Millipore; UFC510024) to remove low molecular weight proteins in the plasma. Next, to check for presence of aggregates, concentrated plasma samples were divided into two groups: one with 1-hour urea incubation prior protein denaturation and the other without incubation. The urea pre-incubation group was processed with a 1:1 dilution factor, with 0.5 M urea-$Barb_2$EDTA buffer incubation for 1 hour (RT), while the non-urea group was kept at 4°C during that hour before diluting 1:1 with $Barb_2$EDTA buffer prior protein denaturation. Samples were then mixed with lithium dodecyl sulfate sample buffer and 0.5 M dithiothreitol before being denatured at 70ºC in a water bath for 10 minutes. Purified bovine NfH protein was incubated using the above conditions to have a final amount of 100 ng NfH in each denatured sample.

4.2.4.2 Blotting procedures

HiMark™ Pre-stained high molecular weight (MW) protein standard (ranged between 460-30 kDa; Invitrogen, LC5699), purified bNfH protein and plasma samples were loaded into 3-8% NuPAGE® Noves® Tris-Acetate gels (Invitrogen, EA0375BOX) and run at 150 V for 1 hours before transferred on a nitrocellulose membrane. The membrane was then blocked with $Barb_2$EDTA buffer containing 5% skimmed milk at room temperature for 1 hour. After washing (4 x 10 minutes), the membrane was incubated in $Barb_2$EDTA buffer containing 0.1% skimmed milk with SMI-34R (1:1000) at 4ºC overnight. The membrane was then washed (6 x 15 minutes), followed by 2-hour incubation with HRP-labelled rabbit anti-mouse IgG (Dako, P0260, 1:1000, RT) and washed (6 x 15 minutes). The membrane was then treated with the chemiluminescence substrate (SuperSignal West Pico, Thermo Scientific, #34078) for 5 minutes. The dried membrane was visualised on an AlphaEase SP CCD camera.

Then, the blots were stripped of the antibodies and re-probed with HRP conjugated-Anti-Human immunoglobulin G (IgG) (Dako, P0214, 1:1000, 4°C, overnight) following the manufacturer's instructions (Abcam®). The membrane was then treated with the chemiluminescence substrate (SuperSignal West Pico, Thermo Scientific, #34078) for 1 minute and then visualized. Pre-absorption of the primary antibodies abolished all the bands at high MW.

4.2.5 Statistical analysis

Numerical variables were summarized by the sample mean±S.E.M., median and interquartile range (IQR). A Mann-Whitney U test was performed for group comparison between ALS patients and controls. The correlations between plasma NfH levels and the monthly rate of change in ALSFRS_R score, diagnostic latency in months and overall progression rate as well as plasma NfH levels and age were carried with Spearman's rank correlation coefficient (rho). Fisher's exact test was used to examine the dominant group of patients with different patterns of longitudinal plasma NfH levels and ALSFRS_R score. A p value of less than 0.05 was considered as statistically significant. All analyses were performed using SPSS (V.20; IBM SPSS statistics, UK).

4.3 Results

In this Chapter, I examined whether the findings presented in Chapter 3, in which I showed that plasma NfH levels correlated with markers of disease progression in the $SOD1^{G93A}$ mouse model of ALS and increased towards end-stage disease, were reflected in plasma of ALS patients. I examined i) whether the NfH 'Hook effect' observed in $SOD1^{G93A}$ mouse model is present in human plasma, and ii) if so, can the ELISA method developed in Chapter 2 overcome this NfH 'Hook effect' in human plasma samples? Having established a suitable assay for the detection of NfH in human plasma, I next examined i) both the cross-sectional and the longitudinal pattern of plasma NfH in ALS patients, and ii) whether plasma NfH levels are of prognostic value in ALS. Finally, I investigated the possibility of that alternative mechanisms may affect plasma NfH homeostasis, aside from disease progression.

4.3.1 A NfH 'hook effect' is present in human plasma

In the first set of experiments, I examined whether the NfH 'Hook Effect' observed in the plasma of $SOD1^{G93A}$ mice is also present in human plasma. Samples selected

from a small number of healthy controls, and limb-onset ALS patients at an early stage (ALSFRS_R score ≥40) and a late stage (ALSFRS_R score ≤25) of disease were examined, using the method originally developed for human CSF samples which is described in Chapter 2 (Section 2.2.5).

A NfH 'Hook Effect' was observed from the serial dilution of plasma samples from early-ALS (eALS), late-ALS (lALS) as well as in healthy controls (HC) (Fig. 4.1A). The resulting lack of parallelism between human plasma samples and standards introduced an analytical error averaging up to 46.9, 101.5, and 22.5 times higher levels for a 1:16 dilution (4^{th}), when compared with 1:2 dilution (1^{st}) for HC, eLAS, and lALS, respectively (Fig. 4.1B). Taken together, plasma NfH^{SMI34} levels in human can be up to 32.3 times higher at the 4^{th} serial dilution than the 1^{st} one (Fig. 4.1C).

4.3.2 The NfH 'Hook Effect' in human plasma is overcome by urea

A number of different approaches were tested as described in Chapter 2 Section 3.2 to overcome the NfH 'Hook Effect' in human plasma. These tests showed that the same modification used for analysis of mouse plasma can overcome the NfH 'Hook Effect' in human plasma and subsequently improved parallelism (Fig. 4.2A-C). This involved **incubation of the plasma samples in 0.5 M urea-$Barb_2$EDTA buffer at a 1:8 dilution for 1 hour at RT before adding to the ELISA plate**. Hence, the protocol described in Table 2.3 Chapter 2 was used for further experiments on human plasma described in this Chapter.

4.3.3 Plasma levels of NfH in ALS patients and controls

The demographic and clinical characteristics of the 136 ALS patients and 104 Control subjects examined in the cross-sectional study are summarized in Table 4.3. The median (Interquartile range; IQR) of diagnostic latency in our ALS cohort was 11.99 (7.03, 20.98) months, in line with other large-scale population studies in ALS (Cellura et al., 2012; Iwasaki et al., 2002). We observed a strong negative correlation between the *Overall Progression Rate* in ALS patients and their diagnostic latency (Spearman's rho = -0.511, $p<0.0001$; Fig. 4.3). This confirms previous observations that short diagnostic latencies are generally associated with a worse prognosis in ALS (Chio et al., 2009; Turner et al., 2010a).

Figure 4.1

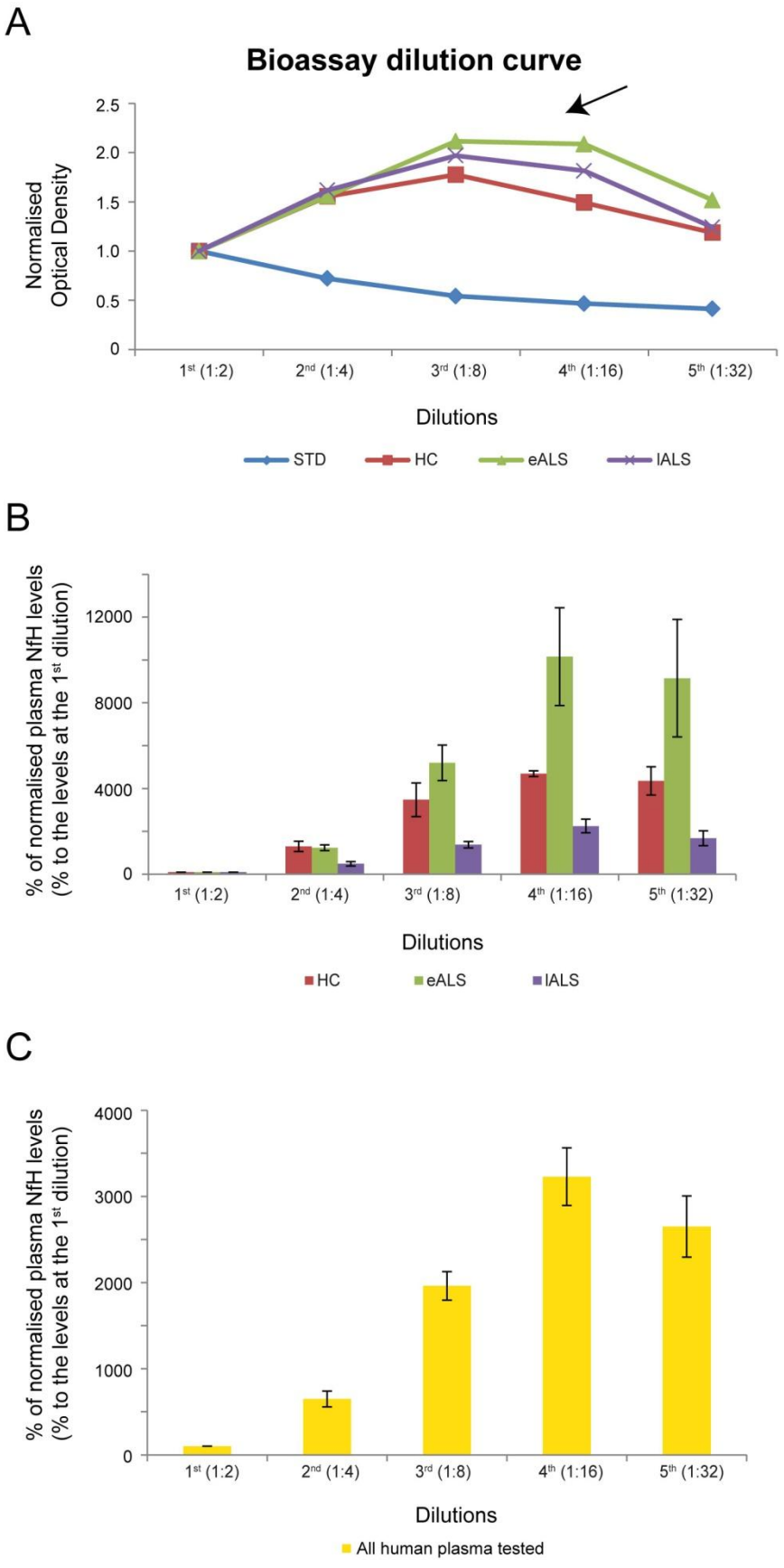
A
Bioassay dilution curve
Normalised Optical Density
2.5
2.0
1.5
1.0
0.5
0
1st (1:2)
2nd (1:4)
3rd (1:8)
4th (1:16)
5th (1:32)
Dilutions
STD
HC
eALS
IALS
B
% of normalised plasma NfH levels (% to the levels at the 1st dilution)
12000
8000
4000
0
1st (1:2)
2nd (1:4)
3rd (1:8)
4th (1:16)
5th (1:32)
Dilutions
HC
eALS
IALS
C
% of normalised plasma NfH levels (% to the levels at the 1st dilution)
4000
3000
2000
1000
0
1st (1:2)
2nd (1:4)
3rd (1:8)
4th (1:16)
5th (1:32)
Dilutions
All human plasma tested

Figure 4.1. The Hook effect and lack of parallelism for NfH in human plasma. **(A)** Normalised optical density (NOD) in serial dilution of plasma samples from healthy controls (HC; red), early stage ALS (eALS; green), and late stage ALS (lALS; purple) showed a 'Hook' (arrow) and a lack of parallelism with the standard curve (blue), i.e. increase in NOD, while the NOD of the standard attenuated. **(B)** shows the percentage change of NfH concentrations obtained during serial dilutions normalised to the concentration obtained from the first dilution in HC, eALS and lALS. NfH concentration obtained from more diluted samples had much higher levels than the concentration obtained from less diluted samples in all three sample groups, with the maximum effect observed at 1:16 dilution. Note the effect seemed to be more prominent in eALS samples than lALS. (C) shows averaged percentage change of NfH concentrations during serial dilutions normalised to the concentration obtained from the first dilution, containing the three groups shown in (B). Error bars: ±S.E.M.

Figure 4.2

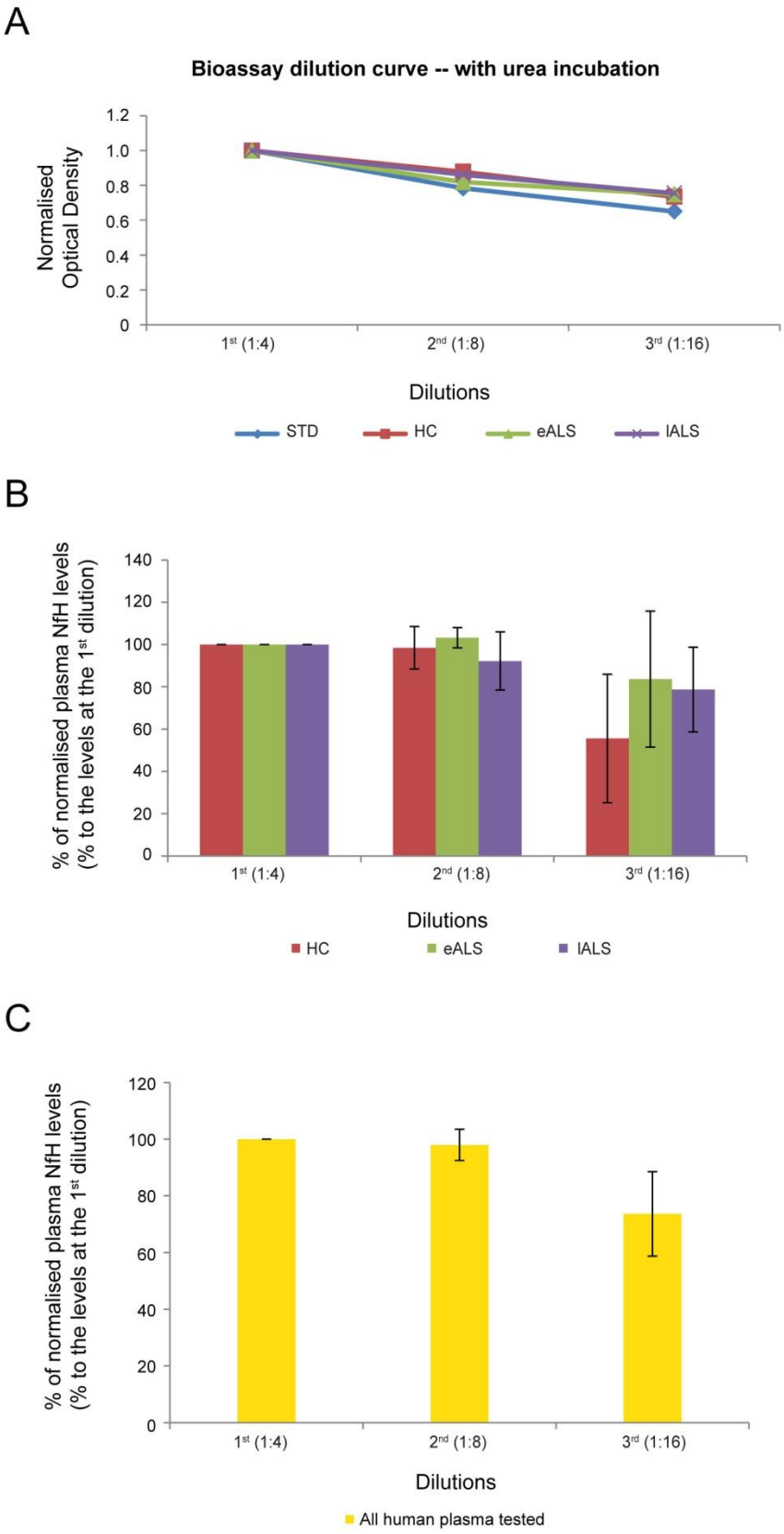
A
Bioassay dilution curve -- with urea incubation
Normalised Optical Density
1.2
1.0
0.8
0.6
0.4
0.2
0
1st (1:4)
2nd (1:8)
3rd (1:16)
Dilutions
STD
HC
eALS
lALS
B
% of normalised plasma NfH levels (% to the levels at the 1st dilution)
140
120
100
80
60
40
20
0
1st (1:4)
2nd (1:8)
3rd (1:16)
Dilutions
HC
eALS
lALS
C
% of normalised plasma NfH levels (% to the levels at the 1st dilution)
120
100
80
60
40
20
0
1st (1:4)
2nd (1:8)
3rd (1:16)
Dilutions
All human plasma tested

Figure 4.2. The effects of 1 hour incubation of 0.5 M Urea-Barb$_2$EDTA buffer at room temperature on plasma NfH levels in human plasma. (A) The 'hook effect' disappeared and parallelism was improved, using the urea-timed method (Incubation in 0.5 M Urea-Barb$_2$EDTA buffer at room temperature for 1 hour). **(B)** Using serial dilution of samples, more consistent NfH levels were detected at the 1:8 (16%) for both controls and ALS. However, plasma NfH levels degraded for controls and lALS at 1:16 dilution, respectively. **(C)** Urea pre-incubation delivered consistent levels for controls and ALS plasma (the three groups shown in B) up to 1:8 dilution, but not beyond. Error bar: ±SEM.

Table 4.3. Characteristics of ALS patients and controls in the cross-sectional study for plasma NfH levels.

Groups	**Patient No**	**Plasma NfH^{SMI34} levels (ng/mL)** Mean±SEM (1^{st} quartile, median, 3^{rd} quartile)	**Plasma NfH^{SMI35} levels (ng/mL)** Mean±SEM (1^{st} quartile, median, 3^{rd} quartile)	**Plasma pNfH levels (ng/mL)** Mean±SEM (1^{st} quartile, median, 3^{rd} quartile)	**Age at sampling (yrs)** Mean±SEM (1^{st} quartile, median, 3^{rd} quartile)	**Gender** F/M	**Ethnicity** % Non-Caucasian	**Age of onset (yrs)** Mean±SEM (1^{st} quartile, median, 3^{rd} quartile)	**Clinical onset sites** **B**ulbar/Limb/Both	**ALSFRS_R score at sampling** Mean±SEM (1^{st} quartile, median, 3^{rd} quartile)	**Progression rate at sampling** Mean±SEM (1^{st} quartile, median, 3^{rd} quartile)	**Riluzole treatment** % on treatment
ALS[§]	136 at Visit 1	17.4±1.4 (8.6, 15.1, 24.3)	14.5±1.6 (4.1, 10.8, 20.7)	32.0±2.5 (15.2, 29.0, 4.1)	63.7±1.0 (57.7, 65.1, 70.6)	48/88	6.62%	60.9±1.1 (53.9, 63.8, 68.2)	29/104/3	35.3±0.7 (29.0, 37.0,42.0)	0.68±0.06 (0.23, 0.51, 0.92)	75
All Controls *	104	16.7±1.4 (5.0, 14.0, 26.5)	11.1±1.0 (4.3, 9.1, 16.3)	27.8±2.1 (11.5, 24.9, 40.1)	57.4±1.2 (50.1, 59.1, 64.8)	60/44	1.92%					
HC	51	16.9±1.9 (6.1, 14.5, 27.4)	11.8±1.2 (6.5, 9.4, 15.0)	28.7±2.6 (14.2, 27.7, 40.1)	55.3±1.8 (45.5, 57.9, 62.7)	38/13	0%					
NC	53	16.4±2.2 (4.0, 13.7, 24.9)	10.5±1.5 (0.1, 7.7, 17.8)	26.9±3.3 (6.9, 23.8, 40.0)	59.4±1.7 (51.4, 60.3, 67.3)	22/31	3.77%					

[§]The ALS cohort includes 62 patients sampled only at baseline (visit 1) and 74 patients sampled longitudinally during disease progression (total 136 patients). *Controls include i) HC: Healthy controls, ii) NC: Neurological disease controls. The NC group includes 14 MS individuals with a diagnosis of relapsing remitting MS (n=5), secondary progressive MS (n=6) and primary progressive MS (n=3) and 10 individuals with inflammatory demyelinating neuropathies including chronic inflammatory demyelinating polyneuropathy, paraproteinemia related and multifocal motor neuropathy, 15 individuals with a diagnosis of single-level or multi-level compressive cervical or lumbar radiculopathy, 10 cases of idiopathic or genetically determined neuropathy including Charcot-Marie-Tooth and 4 cases with benign fasciculations and cramp syndrome.

Figure 4.3

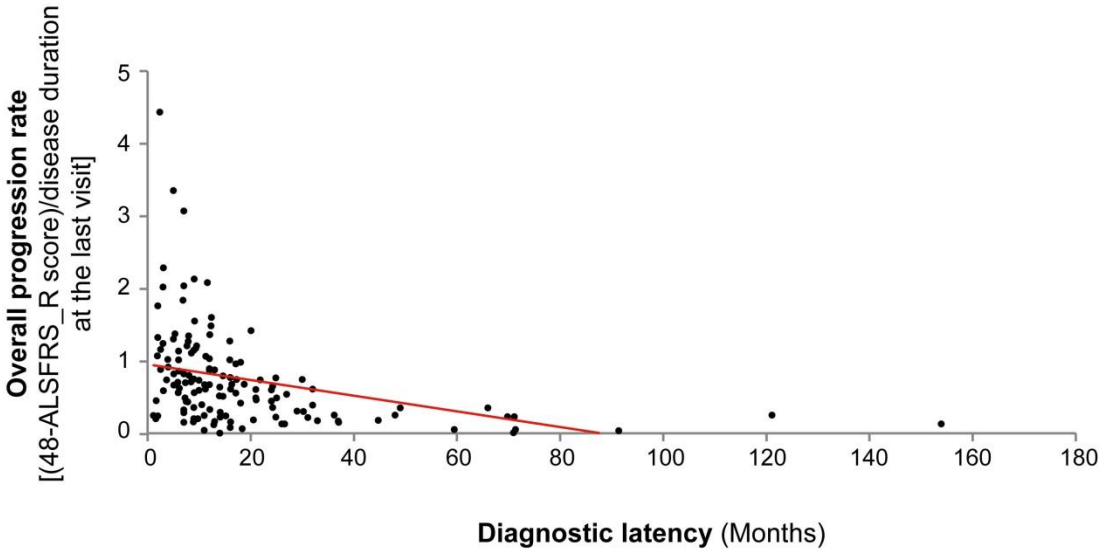

Figure 4.3 A shorter diagnostic latency is associated with a poorer prognosis in ALS. A strong negative correlation was observed between the overall progression rate in ALS patients and their diagnostic latency expressed in months (from the reported onset of symptoms). Spearman's rho= -0.511, p<0.0001. The best-fit trend-line is shown in red.

4.3.3.1 Changes in plasma NfH levels in ALS patients

Plasma NfH levels were determined in our cohort of ALS patients (n=136) and control subjects (n=104). The results were first analysed in a cross-sectional study in which plasma NfH levels in ALS patients and control subjects were compared. Next, a longitudinal study in a proportion of our ALS cohort (n=74) was undertaken, in which changes in total plasma NfH levels, as well as changes in the more pathological form of NfH, hyperphosphorylated NfH^{SMI34}, during disease progression were examined.

In the control subjects enrolled into this study, no significant difference in plasma NfH levels between Healthy controls (HC) and Neurological controls (NC) was observed (p=0.247, 0.507 and 0.195 for total NfH, NfH^{SMI34} and NfH^{SMI35}, respectively; Mann-Whitney U test; See Table 4.3).

4.3.3.1.1 Cross-sectional study of plasma NfH levels in ALS patients and control subjects

I first undertook a cross-sectional study of plasma NfH levels in ALS patients and control subjects, to establish whether plasma NfH levels are distinct between ALS patients and controls at the time of enrolment into the study, irrespective of any disease parameter (e.g. disease duration, progression rate etc.). I determined levels of total NfH, as well as levels of the two NfH phosphoforms, hyperphosphorylated NfH^{SMI34} and less pathological NfH^{SMI35}.

4.3.3.1.1.1 There is no significant difference in plasma NfH levels between ALS patients and control subjects at baseline sampling

The cross-sectional analysis comparing NfH plasma levels measured at baseline (1^{st} sampling) in the ALS cohort and control subjects (HC plus NC), showed that there was no significant difference between these groups (p=0.202, 0.524 and 0.288, for total NfH, NfH^{SMI34} and NfH^{SMI35}, respectively; Fig. 4.4A). This finding is in contrast to previous reports of NfH levels in smaller cohorts of ALS patients and controls (Boylan et al., 2009), possibly due to the high clinical heterogeneity of our large ALS patient cohort.

Figure 4.4

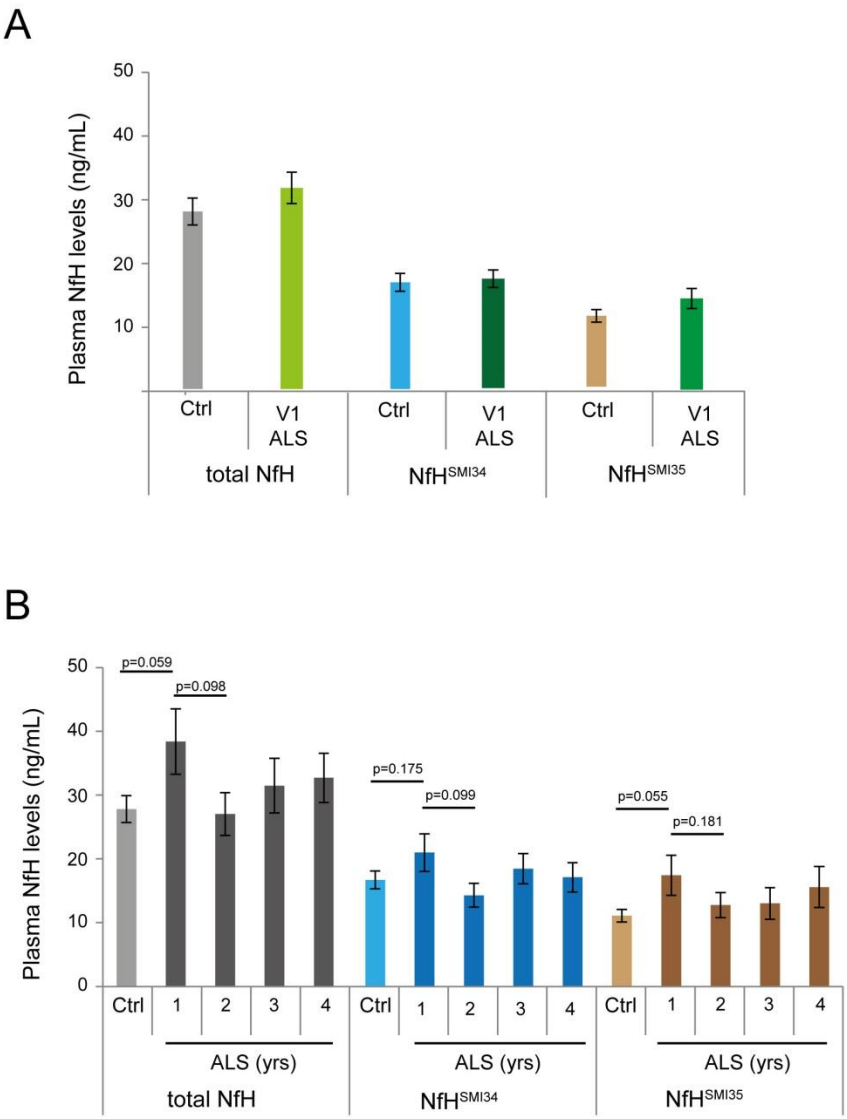

Figure 4.4 Cross-sectional analysis of plasma NfH levels in ALS patients and controls at baseline. (A) Analysis of NfH levels showed that there was no significant difference in total plasma NfH or its phosphoforms in ALS patients and controls (HC + NC). **(B)** When ALS patients were grouped according to time of disease duration to Visit 1, patients with the shortest disease duration (n=31) showed higher NfH levels compared to controls, and the difference in NfH^{SMI35} and total NfH was very close to statistical significance (p=0.055 and 0.059, respectively). Mann-Whitney U test. ALS duration: 1= <12 months; 2= <24m; 3= <36m; 4= >36m. Error bars: ±S.E.M.

4.3.3.1.1.2 Plasma NfH levels may change during disease progression

Since plasma NfH levels are likely to change throughout the course of disease progression, the time of plasma sampling with respect to the time of disease onset was considered to be a likely key determinant of NfH expression levels. Therefore, we undertook an additional cross-sectional analysis between the control subjects and sub-groups of ALS patients that were homogeneous with respect to disease duration, defined as the time interval between reported disease onset and baseline plasma sampling (Visit 1). In this analysis, the cohort of ALS patients was divided into four sub-groups according to the ***disease duration*** to Visit 1. Analysis of plasma NfH levels showed that only the sub-group with the shortest disease duration (less than 12 months) showed higher levels of plasma NfH levels compared to controls, with a trend towards statistical significance (p= 0.059, 0.175, 0.055, for total NfH, NfH^{SMI34} and NfH^{SMI35}, respectively; Fig. 4.4B). In contrast, ALS patients with longer disease durations (greater than 12 months), had comparable levels of plasma NfH to control subjects. Since disease duration in our cohort of ALS patients was very close to the diagnostic latency (in most patients baseline sampling occurred within 3 months of diagnosis), this data suggests that patients with a shorter diagnostic latency (and disease duration) were likely to progress faster and to have higher plasma NfH levels in samples taken during the early stages of the disease, as previously described by others (Boylan et al., 2013).

4.3.3.1.2 Longitudinal changes in plasma NfH levels in ALS patients

On the basis of these observations, I next undertook a longitudinal analysis of NfH expression in a subset of our clinically heterogeneous ALS cohort. I examined the overall pattern of change in plasma NfH levels during the progression of disease in a subset of our ALS cohort, followed longitudinally for up to 2 years from first sampling, and assessed whether the pattern of NfH changes was related to the rate of disease progression. Plasma samples were collected longitudinally during the follow-up of 74 ALS patients and the profile of *total* plasma NfH expression during the natural progression of the disease was first determined. Samples were collected at several time-points, ranging between 2 and 11 times, with the interval between visits ranging between 2 to 4 months.

4.3.3.1.2.1 Total plasma NfH levels in ALS patients are affected by the progression rate during disease

Patients were grouped according to their **overall progression rate** and defined as having either fast progressing disease (ALS-F) or slow progressing disease (ALS-S), as defined by the monthly decline in the ALSFRS_R score. The characteristics of these patients are summarized in Table 4.4. The results shown in Fig. 4.5 summarize the longitudinal pattern of plasma NfH levels from the baseline for 18 ALS-F (overall progression rate >1.0/month) and 35 ALS-S (overall progression rate <0.5/month) patients followed-up longitudinally for up to 15 months from the first sampling. Plasma NfH levels were higher in both ALS-F and ALS-S patients at baseline than controls. In ALS-F patients, there was a decline in NfH levels over time towards end-stage disease. In contrast, plasma NfH levels in ALS-S patients remained stable during the first 6 months after baseline sampling and subsequently began to slightly increase with disease progression, although they remained above control levels throughout the study period (Fig. 4.5).

4.3.3.1.3 Longitudinal changes in levels of hyperphosphorylated NfH in ALS patients: the change in expression from symptom onset

The results presented in Fig. 4.5 suggest that the overall pattern of plasma NfH levels is different in ALS patients with different rates of disease progression. I therefore sought to examine plasma NfH levels in ALS patients in more detail, by undertaking an analysis of the changes in levels of the more pathological NfH phosphoform, NfH^{SMI34}, in addition to taking into account both the time of disease duration as well as the rate of disease progression. Thus, I next examined the changes in expression of hyperphoshorylated NfH^{SMI34} in ALS patients during disease progression.

4.3.3.1.3.1 Hyperphosphorylated NfH^{SMI34} plasma levels in ALS patients and the effects of disease duration and progression rate

The characteristics of the ALS patients included in this analysis are summarized in Table 4.5, which also details the classification of the rate of disease progression in this analysis. The 74 ALS individuals followed up longitudinally were divided into 4 groups based on disease duration, defined as the time interval from the reported clinical onset of ALS symptoms to the first sampling of plasma.

Table 4.4. Patient characteristics of the ALS patients studied longitudinally and sub-grouped according to their overall progression rates. Serial plasma NfH levels for all ALS patients were recorded from the baseline visit.

Pattern 2: Overall progression rate* **	**Patient n.**	**Time points**	**Age of onset[N.S.]**	**Gender**	**Duration: onset to baseline sampling*** **	**Duration: onset to diagnosis** **	**Duration: onset to the last sampling*** **	**ALSFRS_R at baseline** **	**Ethnicity**	**Clinical onset**
(Mean±SEM)		range	(Mean±SEM)	F/M	(Months; Mean±SEM)	(Months; Mean±SEM)	(Months; Mean±SEM)	(Mean±SEM)	% non-Caucasian	Bulbar/Limb/Both
ALS-F (1.258±0.06)	18	2 to 8	65.9±1.1	7/10	12.2±1.6	7.9±1.0	20.8±1.6	34.9±1.7	none	5/12/1
ALS-S (0.253±0.02)	35	2 to 11	59.6±2.1	6/29	44.5±8.6	23.3±4.2	60.1±8.7	41.1±1.1	5.80%	8/26/1

ALS patients with overall progression rates of >1.0 and <0.5 were grouped as fast (ALS-F) and slow (ALS-S) progressors, respectively. There is a significant difference between the two groups of patients in the ALSFRS_R score at baseline, overall progression rate, duration to the baseline and the last sampling, as well as diagnostic latency. However, there is no difference between age of onset in these patients *p<0.05, **p<0.01, ***p<0.0001, N.S.: not significant.

Figure 4.5

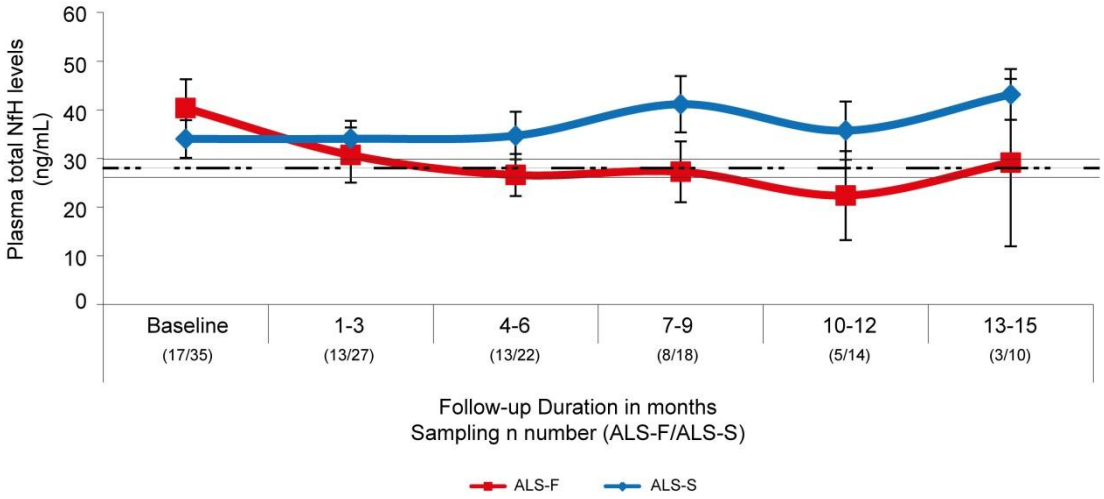

Figure 4.5. The profile of total plasma NfH levels in a 15-month follow-up from baseline in ALS patients with different rates of disease progression. Mean total plasma NfH levels are shown in red for patients with a faster progression rate (ALS-F) and in blue for patients with a slower progression rate (ALS-S). The dashed line represents the mean total plasma NfH level in control subjects. The two solid lines encasing the dashed lines represent the error bars for controls. Values in the parentheses are number of ALS-F and ALS-S patients at each time point (ALS-F/ALS-S). Error bars: ±S.E.M.

Table 4.5. Characteristics of ALS patients followed longitudinally: ALS patients are sub-grouped according to the time interval between ALS onset and their first study visit.

Patient Groups§: time from ALS onset to sampling (overall progression rate (Mean±SEM))	**Patients n.**	**Time points** range	**Age of onset** (Mean±SEM)	**Gender** F/M	**Duration: onset to baseline sampling** (Months; Mean±SEM)	**Duration: onset to diagnosis** (Months; Mean±SEM)	**Duration: onset to the last sampling** (Months; Mean±SEM)	**ALSFRS_R at baseline** (Mean±SEM)	**Ethnicity** % non-Caucasian	**Clinical onset** Bulbar/Limb/Both
< 1year ALS-Ft (1.29±0.08)	13	2 to 8	63.9±1.9	4/9	8.8±0.7	6.0±0.8	19.3±1.6	37.8±1.6	none	5/8/0
< 1year ALS-S (0.57±0.13)	5	2 to 7	61.4±3.4	1/4	9.1±1.2	5.9±1.1	17.0±3.3	44.4±1.8	none	0/5/0
1 to 2 years ALS-F (0.82±0.06)	15	2 to 7	65.0±2.3	8/7	17.6±0.9	12.6±1.3	26.5±1.7	35.3±1.4	none	3/12/0
1 to 2 years ALS-S (0.23±0.03)	11	2 to 11	58.8±4.1	2/9	17.2±1.2	9.7±1.7	34.5±4.4	44.3±0.6	9%	2/9/0
2 to 3 years ALS-F (0.73±0.06)	10	2 to 8	64.7±4.5	4/6	29.3±1.2	20.6±2.4	38.2±2.0	30.2±2.0	none	1/8/1
2 to 3 years ALS-S (0.34±0.04)	10	2 to 11	65.9±2.6	3/7	28.0±1.0	19.2±2.1	45.0±4.2	40.8±1.5	none	3/7/0
> 3 years ALS-S (0.31±0.05)	10	2 to 10	57.7±3.3	1/9	47.7±2.3	27.9±4.3	62.0±3.3	34.1±3.3	none	4/6/0

§ ALS patients were first sub-grouped according to the interval from symptom onset to their first sampling, and then further sub-divided according to their overall progression rate. For sub-groups in Year 2 and beyond, slow progressing ALS patients (ALS-S) had an overall progression rate < 0.5; the remaining patients were grouped as fast progressors (ALS-F). For ALS patients with a baseline sampling within 12 months of ALS onset, the majority was ALS-F and had a progression rate > 1.0, the remaining 5 patients were grouped as ALS-S.

As can be seen in Fig. 4.6, the profile of plasma NfH^{SMI34} expression in the follow-up period varied according to both disease duration (from symptom onset) and to overall progression rate. Patients with a fast progression rate (ALS-F) enrolled in the study within the first year from ALS onset (Fig. 4.6A; Year 1), had higher plasma NfH^{SMI34} levels than those with a slow progression rate (ALS-S), throughout the study period. Patients enrolled in the study more than 12 months after disease onset (Fig. 4.6B; Year 2), had similar levels of plasma NfH^{SMI34} in ALS-F and ALS-S disease, over the study period. However, for those ALS patients enrolled in the study more than 24 months after disease onset (Fig. 4.6C; Year 3), the longitudinal pattern of NfH expression of ALS-F and ALS-S appeared to diverge between 4-6 months from the levels detected at baseline, with the ALS-F group displaying a gradual decline in NfH^{SMI34} levels and the ALS-S group showing an increase followed by stabilization of NfH^{SMI34} levels, which typically remained above the mean NfH^{SMI34} level detected in the control group (Fig. 4.6C). All ALS patients in our cohort enrolled during the 4^{th} year after symptom onset were defined as ALS-S, and their mean plasma NfH^{SMI34} levels were consistently higher than control levels throughout the study (see Fig. 4.6D; Year 4).

Taken together, these results show that in this heterogeneous ALS patient cohort, plasma NfH levels are dependent on both disease duration (from time of symptom onset to sampling) as well as the rate of disease progression.

4.3.3.2 Do changes in plasma NfH levels have any prognostic value?

The conclusions drawn from the data above come from an overall, retrospective analysis of plasma NfH levels in ALS patients. In order to examine whether plasma NfH levels could be of any prognostic value in a prospective study, I next undertook a correlation analysis between plasma NfH levels and disease progression.

4.3.3.2.1 Plasma NfH levels correlate with progression of disease between visits

In order to establish whether the changes in plasma NfH levels in ALS patients were a good indicator of the rate of disease progression, I examined the correlation between disease progression, determined by the ALSFRS_R slope between two consecutive visits (average interval of 2-4 months between visits) and the plasma NfH levels at the later visit, in patients from whom plasma samples and clinical

Figure 4.6

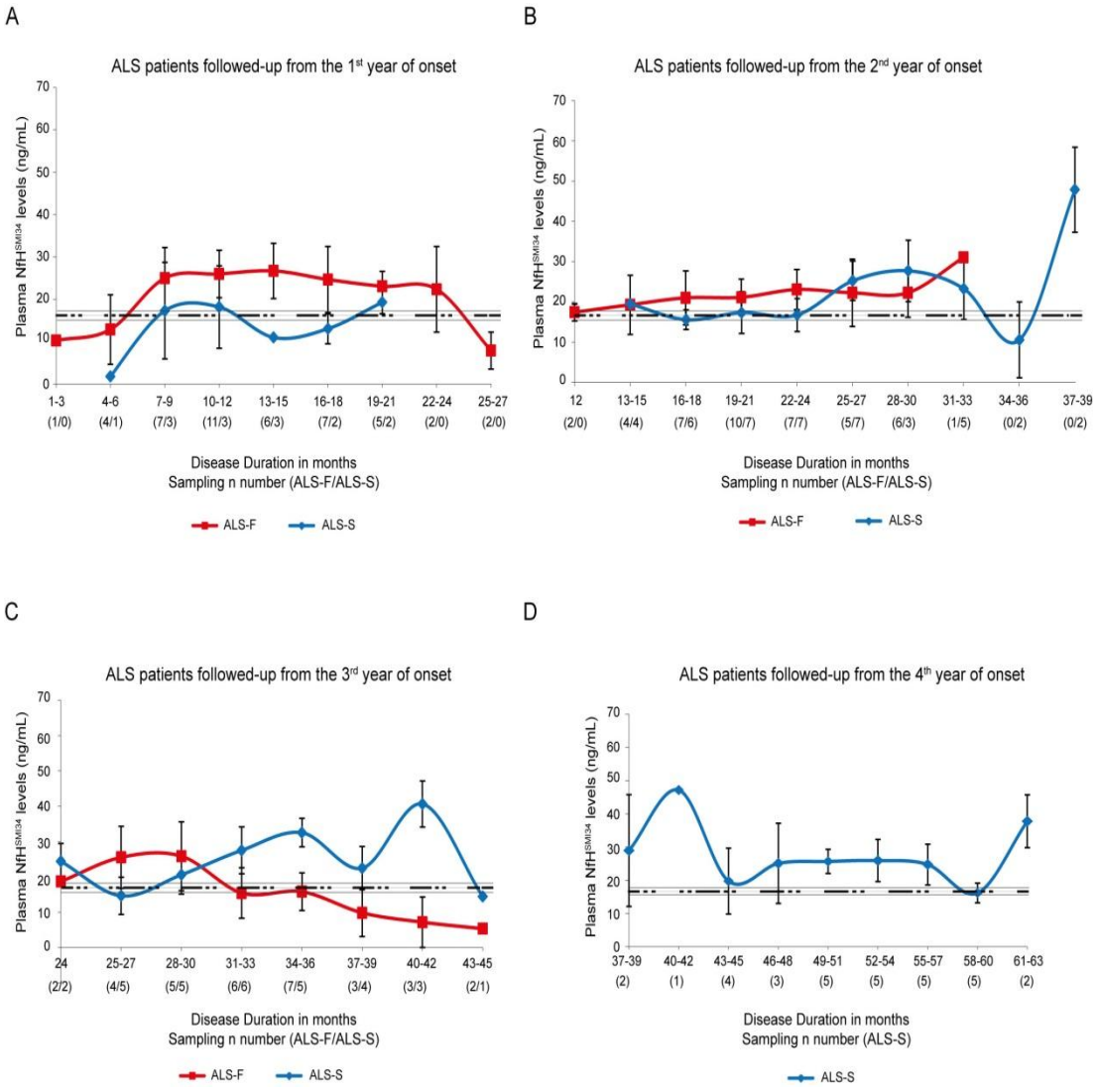
A
ALS patients followed-up from the 1st year of onset
Plasma NfH SMI34 levels (ng/mL)
0 10 20 30 40 50 60 70
1-3 (1/0)
4-6 (4/1)
7-9 (7/3)
10-12 (11/3)
13-15 (6/3)
16-18 (7/2)
19-21 (5/2)
22-24 (2/0)
25-27 (2/0)
Disease Duration in months
Sampling n number (ALS-F/ALS-S)
ALS-F
ALS-S
B
ALS patients followed-up from the 2nd year of onset
Plasma NfH SMI34 levels (ng/mL)
0 10 20 30 40 50 60 70
12 (2/0)
13-15 (4/4)
16-18 (7/6)
19-21 (10/7)
22-24 (7/7)
25-27 (5/7)
28-30 (6/3)
31-33 (1/5)
34-36 (0/2)
37-39 (0/2)
Disease Duration in months
Sampling n number (ALS-F/ALS-S)
ALS-F
ALS-S
C
ALS patients followed-up from the 3rd year of onset
Plasma NfH SMI34 levels (ng/mL)
0 10 20 30 40 50 60 70
24 (2/2)
25-27 (4/5)
28-30 (5/5)
31-33 (6/6)
34-36 (7/5)
37-39 (3/4)
40-42 (3/3)
43-45 (2/1)
Disease Duration in months
Sampling n number (ALS-F/ALS-S)
ALS-F
ALS-S
D
ALS patients followed-up from the 4th year of onset
Plasma NfH SMI34 levels (ng/mL)
0 10 20 30 40 50 60 70
37-39 (2)
40-42 (1)
43-45 (4)
46-48 (3)
49-51 (5)
52-54 (5)
55-57 (5)
58-60 (5)
61-63 (2)
Disease Duration in months
Sampling n number (ALS-S)
ALS-S

Figure 4.6. The longitudinal profile of plasma NfH^{SMI34} levels in a 2 year follow-up varies according to the rate of disease progression and duration. ALS patients were grouped according to the time of their first, baseline sampling of plasma relative to the time of symptom onset: **(A)** within the 1st, **(B)** 2nd, **(C)** 3rd and **(D)** 4th year from the reported onset of ALS. The graphs show the mean plasma NfH^{SMI34} levels in patients sampled at 3-month intervals, grouped according to their *Overall Progression Rate.* The results from patients with faster progression rates (ALS-F) are shown in red, and those with slower progression rates (ALS-S) are shown in blue. The dashed lines represent the mean plasma NfH^{SMI34} levels from Control subjects (HC plus NC); the two solid lines encasing the dashed line represent the variability of error bars in control samples. Error bars: ±S.E.M. Values in the parentheses are number of ALS-F and ALS-S patients at each time point (ALS-F/ALS-S). For patients recruited *within* the 1st year of symptom onset, patients classified as ALS-F have an overall-progression rate ≥1.0, and those patients classified as ALS-S have a progression rate of ≤1.0. For patients recruited *after* the 1st year of symptom onset, patients classified as ALS-S have an overall progression rate of ≤ 0.5, and those defined as ALS-F have a rate of ≥0.5.

information were collected longitudinally. In this analysis, data from 206 'pairs' of visits from 74 patients were examined. For each pair of visits (i.e. one visit and the next follow-up visit) the ALSFRS_R slope was determined and the level of plasma NfH at the follow-up visit was correlated with the ALSFRS_R slope for that period. The ALSFRS_R slope ranged between -9 and 3 per month [mean±S.E.M. = -0.866±1.34; median (IQR) = -0.5 (-1.33, 0)]. As can be seen in Fig. 4.7, there was a mild positive correlation between the ALSFRS_R slope and NfH^{SMI34} levels (Spearman's rho=0.186, p=0.009; Fig. 4.7A), but no correlation between the ALSFRS_R slope and NfH^{SMI35} levels (Spearman's rho=0.076, p=0.281; Fig. 4.7B), in 206 pairs of consecutive visits.

However, this correlation was strengthened for both NfH^{SMI34} (Spearman's rho=0.256, p=0.01) and NfH^{SMI35} (Spearman's rho=0.215, p=0.032), when only those patients with a relatively fast progression rate were included in the analysis, i.e. patients with a confirmed decrease in the ALSFRS_R score of >0.5 points per month. Lower plasma NfH levels correlate with a faster decline in the ALSFRS_R score, particularly in patients in whom a loss of >0.5 points in the ALSFRS_R score per month indicates a faster disease progression. This finding is similar to that observed in the longitudinal analysis of changes in plasma NfH levels during disease progression (Fig. 4.6) in which ALS-F patients had lower plasma NfH levels during the more advanced stages of disease, when the ALSFRS_R slopes between visits were more marked and mostly negative.

These results therefore indicate that there is a correlation between plasma NfH levels and the rate of disease progression in ALS patients, where surprisingly, low levels of plasma NfH correlate with a poor prognosis. These findings are in contrast with previous reports which show that high levels of plasma NfH correlate with a faster disease progression (Boylan et al., 2013).

4.3.3.2.2 Changes in plasma NfH levels do not predict patterns of disease progression

I next examined whether a specific pattern of disease progression was reflected in a change in plasma NfH levels. 74 ALS patients followed-up longitudinally were assessed to establish the overall pattern of disease progression as determined by the ALSFRS_R score and sub-grouped these patients according to the pattern of plasma NfH changes. The pattern of disease progression, as determined by the

Figure 4.7

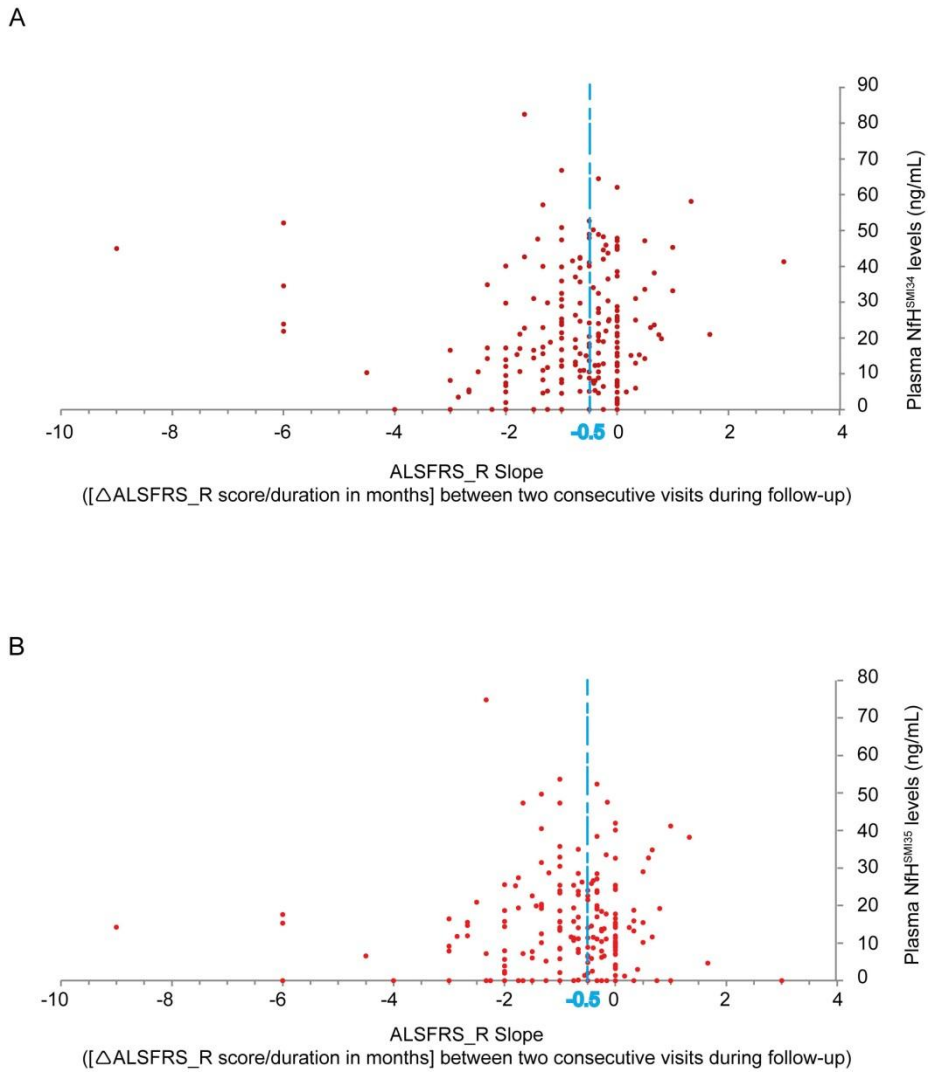

Figure 4.7. NfH plasma levels correlate with the decline in the monthly ALSFRS_R slope. The ALSFRS_R slope between two consecutive visits correlated with the change in plasma NfH^{SMI34} **(A)** and NfH^{SMI35} **(B)** levels in the total of 206 pairs of consecutive visits. A significant correlation was found between the ALSFRS_R slope and NfH^{SMI34} levels in the second visit of each sampling pair (Spearman's rho=0.186, p=0.009), but not between the ALSFRS_R slope and NfH^{SMI35} (Spearman's rho=0.076, p=0.281). For those pairs of consecutive visits in which the ALSFRS_R slope was less than -0.5 (patients who lost more than 0.5 points per month, as shown to the left side of the blue dashed lines; 100 sampling pairs), the correlation between the ALSFRS_R slopes and both NfH^{SMI34} (Spearman's rho=0.256, p=0.01) and NfH^{SMI35} (Spearman's rho=0.215, p=0.032) levels were strengthened.

ALSFRS_R score, showed that patients either progressed or stabilised during the follow-up period of this study. In each of these two groups of patients, we found that plasma NfH either increased in some patients or decreased/no change. Thus, as can be seen in Fig. 4.8, we identified 4 main patterns of combined behaviours of these two parameters: (A) deterioration of the ALSFRS_R score with increased NfH levels; (B) deterioration of the ALSFRS_R score with decreased/no change NfH levels; (C) stable ALSFRS_R score with decreased/no change NfH levels; and (D) stable ALSFRS_R score with increased NfH levels. The proportion of gender and onset site of patients in these four groups is also presented in Fig. 4.8, which shows that group (B) has the highest proportion of female and bulbar onset ALS patients. Statistical analysis of each group was undertaken to determine whether increased NfH levels could predict deterioration in function (as determined by a decrease in the ALSFRS_R score). As shown in Table 4.6, the results showed that there was a trend toward significance for plasma NfH^{SMI34} levels (Fisher Exact test p= 0.0704), but not for NfH^{SMI35} levels (Fisher Exact test p=0.1674).

Taken together, these results show that changes in plasma NfH levels do not appear to predict disease progression in a large, heterogeneous population of ALS patients. However, if the patient cohort under study is relatively small or homogenous, it is more likely that one pattern of disease will predominate. This may lead to a false positive correlation between plasma NfH levels and rate of disease progression that is not representative of the heterogeneous ALS population. Thus, our results suggest that cross-sectional biomarker studies consisting of small sample sizes may be subject to sampling bias, since they may consist of a relatively high number of one particular group of patients.

4.3.3.3 Sampling bias leads to misinterpretation of relevance of NfH levels in cross-sectional studies in ALS

In order to establish how significant the sampling bias may be in cross-sectional studies, we next divided our cohort of 74 ALS patients studied longitudinally into two groups: (a) those in which plasma NfH levels *increase* from baseline during the course of the disease (n=45), and (b) those in which NfH levels *decrease* from baseline during the course of the disease (n=48). In these patients we compared plasma NfH levels at baseline sampling at Visit 1 (V_1) to either the maximum level of plasma NfH (V_{Max}) determined in Group (a) patients, or the minimum level of plasma NfH (V_{Min}) determined in Group (b) patients.

Figure 4.8

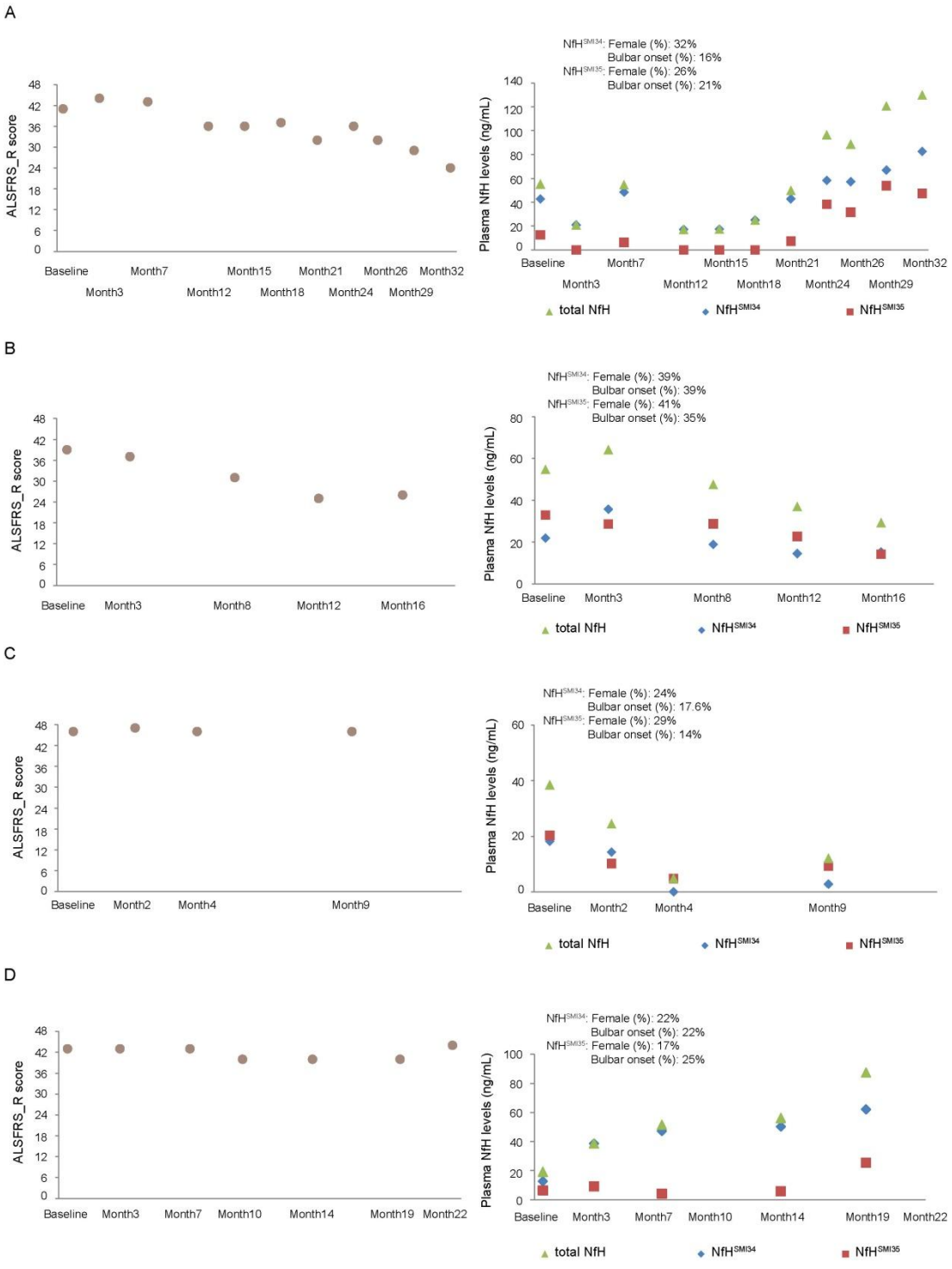
A
ALSFRS_R score
Baseline
Month3
Month7
Month12
Month15
Month18
Month21
Month24
Month26
Month29
Month32
NfH^SMI34: Female (%): 32%
Bulbar onset (%): 16%
NfH^SMI35: Female (%): 26%
Bulbar onset (%): 21%
Plasma NfH levels (ng/mL)
total NfH
NfH^SMI34
NfH^SMI35
B
NfH^SMI34: Female (%): 39%
Bulbar onset (%): 39%
NfH^SMI35: Female (%): 41%
Bulbar onset (%): 35%
Month8
Month16
C
NfH^SMI34: Female (%): 24%
Bulbar onset (%): 17.6%
NfH^SMI35: Female (%): 29%
Bulbar onset (%): 14%
Month2
Month4
Month9
D
NfH^SMI34: Female (%): 22%
Bulbar onset (%): 22%
NfH^SMI35: Female (%): 17%
Bulbar onset (%): 25%
Month10
Month14
Month19
Month22

Figure 4.8. Analysis of the change in plasma NfH levels and ALSFRS_R score during a follow-up period of up to 32 months identifies four main groups of ALS patients. The graphs show the four groups of ALS patients revealed by dividing the patients according to the pattern of change of plasma NfH levels and disease progression. The graphs on the left show the 4 main patterns of change in plasma NfH levels (Total plasma NfH=Triangles; NfH^{SMI34}=Diamonds; and NfH^{SMI35}=Squares); the graphs on the right show the corresponding pattern of change in the ALSFRS_R score. The 4 groups of patients represent Group **(A)**: Increased NfH levels with deterioration of ALSFRS_R; Group **(B)**: Decreased NfH levels with deteriorated ALSFRS_R; Group **(C)** Decreased NfH levels with a stable ALSFRS_R; and Group **(D)** Increased NfH levels with a stable ALSFRS_R.

Table 4.6. Change in plasma NfH levels and its prognostic value for disease progression: summary of the statistical analysis.

		ALSFRS_R score Decrease	**ALSFRS_R score Increase or stabilised**	**Fisher Exact Test (p value)**
Plasma NfH^{SMI34} levels	Increase	25	9	p=0.0704
	Decrease/no change	23	17	
Plasma NfH^{SMI35} levels	Increase	19	12	p=0.1674
	Decrease/no change	29	14	

The Table shows the number of ALS patients who fulfilled the criteria for sub-grouping according to the change in NfH^{SMI34} or NfH^{SMI35} levels together with the change in the ALSFRS_R score during the study period. The p value obtained from Fisher exact test is also presented. No significant correlation between the change of plasma NfH and the change of ALSFRS_R score was observed in this cohort of ALS patients.

The plasma V_1 and V_{Max} NfH levels for ALS patients in Group (a) in which plasma NfH levels increased during disease are shown in Fig. 4.9A, where they are compared to mean NfH levels for healthy controls (HC; n=51). It can be seen that NfH plasma levels at V_{Max} are significantly higher than NfH plasma levels at V_1 and in HCs. In ALS patients in Group (b), in which plasma NfH levels decreased during disease progression to $V_{Min,}$ NfH levels at baseline (V_1) are significantly higher than V_{Min} levels and from HC levels (Fig. 4.9B). Thus, for both groups of patients, determination of NfH levels at a specific point in disease progression in a snap-shot cross-sectional study would result in a completely different estimation of NfH levels from samples taken at a different stage of the disease. For example, if the total NfH levels determined at V_1 and V_{max} are compared, it can be seen that if the sample at V_1 was used in a cross-sectional study NfH levels would be taken as 25.3±2.7 ng/mL (mean±S.E.M.), which is not different from HCs, in contrast to NfH levels at V_{Max}, 49.6±3.6 ng/mL (mean±S.E.M.), which would be taken as significantly higher than HCs 28.7±2.6 ng/mL (mean±S.E.M.). These results therefore confirm that sampling bias can significantly affect the interpretation of cross-sectional studies of plasma NfH levels in ALS patients.

4.3.4 The immune response to neurofilaments; NfH fragments co-localise with anti-human IgG immunoglobulin

The results presented above show that plasma NfH levels do not always increase as disease progresses in ALS patients. This finding is in contrast to my previous findings in the $SOD1^{G93A}$ mouse model of ALS, which present a very homogenous pattern of disease progression and in which I observed a clear increase in plasma NfH levels during disease progression (Lu et al., 2012). I therefore next investigated a possible mechanism that may explain the contradictory patterns of plasma NfH levels in ALS patients during disease progression. It has been previously shown that auto-antibodies can be produced in response to the presence of neuron-specific proteins in peripheral blood (Couratier et al., 1998; Fialova et al., 2010). We thus undertook a preliminary study to examine whether auto-antibodies against NfHs and their proteolytic by-products could be detected in plasma of ALS patients, since these may affect the level of NfHs in plasma.

High molecular weight NfH aggregates were detected in the plasma of ALS patients, as can be seen in the immunoblot in Fig. 4.10A (green dashed arrow; bands

Figure 4.9

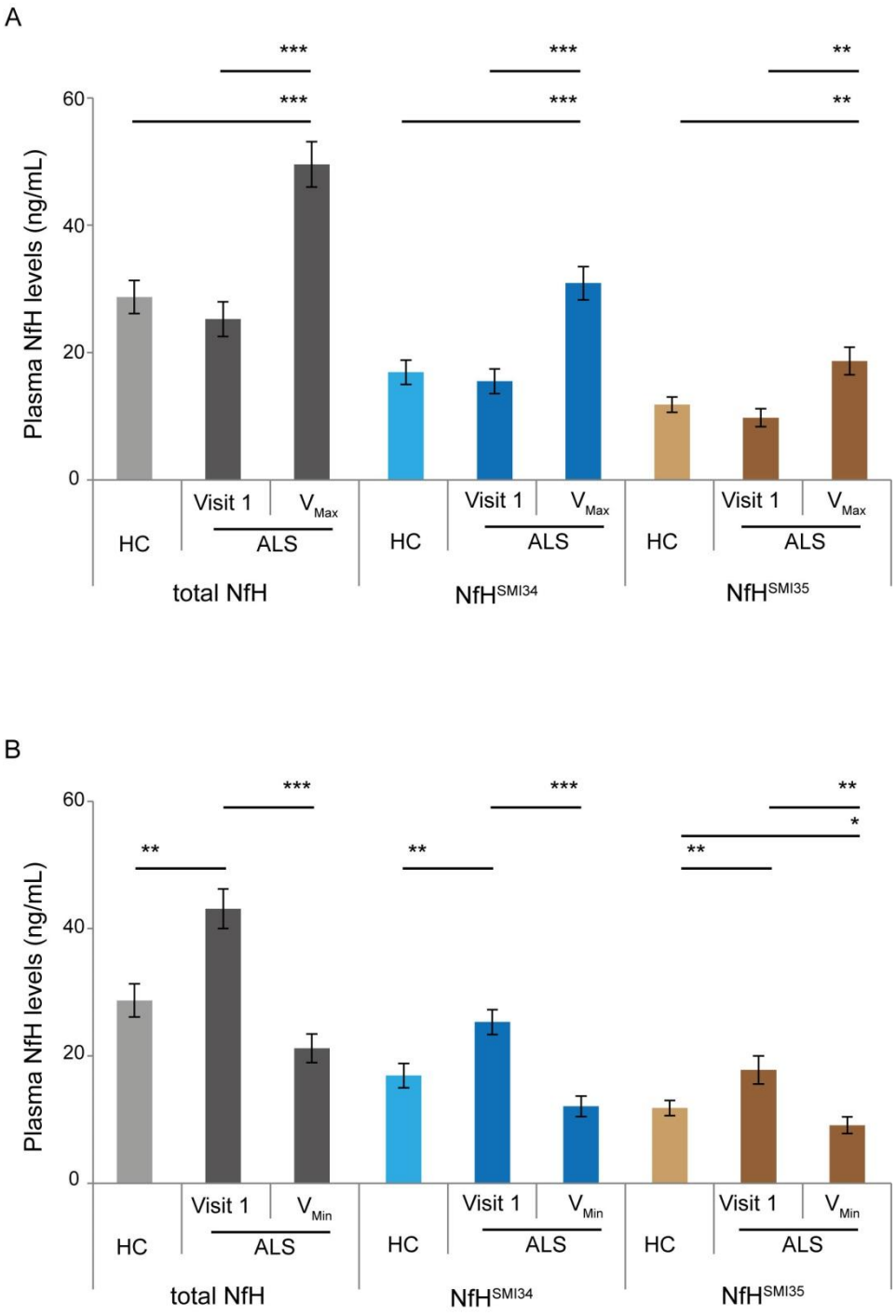
A
***
***
***
***
**
**
60
40
20
0
Plasma NfH levels (ng/mL)
Visit 1
V Max
HC
ALS
total NfH
NfHSMI34
NfHSMI35
B
***
***
**
**
**
**
*
60
40
20
0
Plasma NfH levels (ng/mL)
Visit 1
V Min
HC
ALS
total NfH
NfHSMI34
NfHSMI35

Figure 4.9. A comparative cross-sectional analysis of plasma NfH levels in ALS patients and healthy controls: NfH levels vary according to the chosen sampling time. (A) In 45 ALS patients, NfH levels were significantly higher than in healthy controls at Visit 1 and were also much higher in a later stage of the disease. (B) In 48 ALS patients, NfH levels were significantly higher than in healthy controls at Visit 1, but later decreased to a much lower level compared to both healthy controls and to NfH levels at Visit 1. Grey bars= Total NfH levels: light grey bars: Healthy Controls (HC), Dark Grey Bars: ALS patients from Visit 1, V_{Max} and V_{Min}. Blue bars= NfH^{SMI34} levels: Light Blue bars: Healthy Controls (HC), Dark Blue bars: ALS patients from Visit 1, V_{Max} and V_{Min}. Brown bars= NfH^{SMI35} levels: Light brown bars: Healthy Controls (HC), Dark brown bars: ALS patients from Visit 1, V_{Max} and V_{Min}. Error bars: ±S.E.M. **p<0.01, ***p<0.0001. Kruskal-Wallis Test.

Figure 4.10

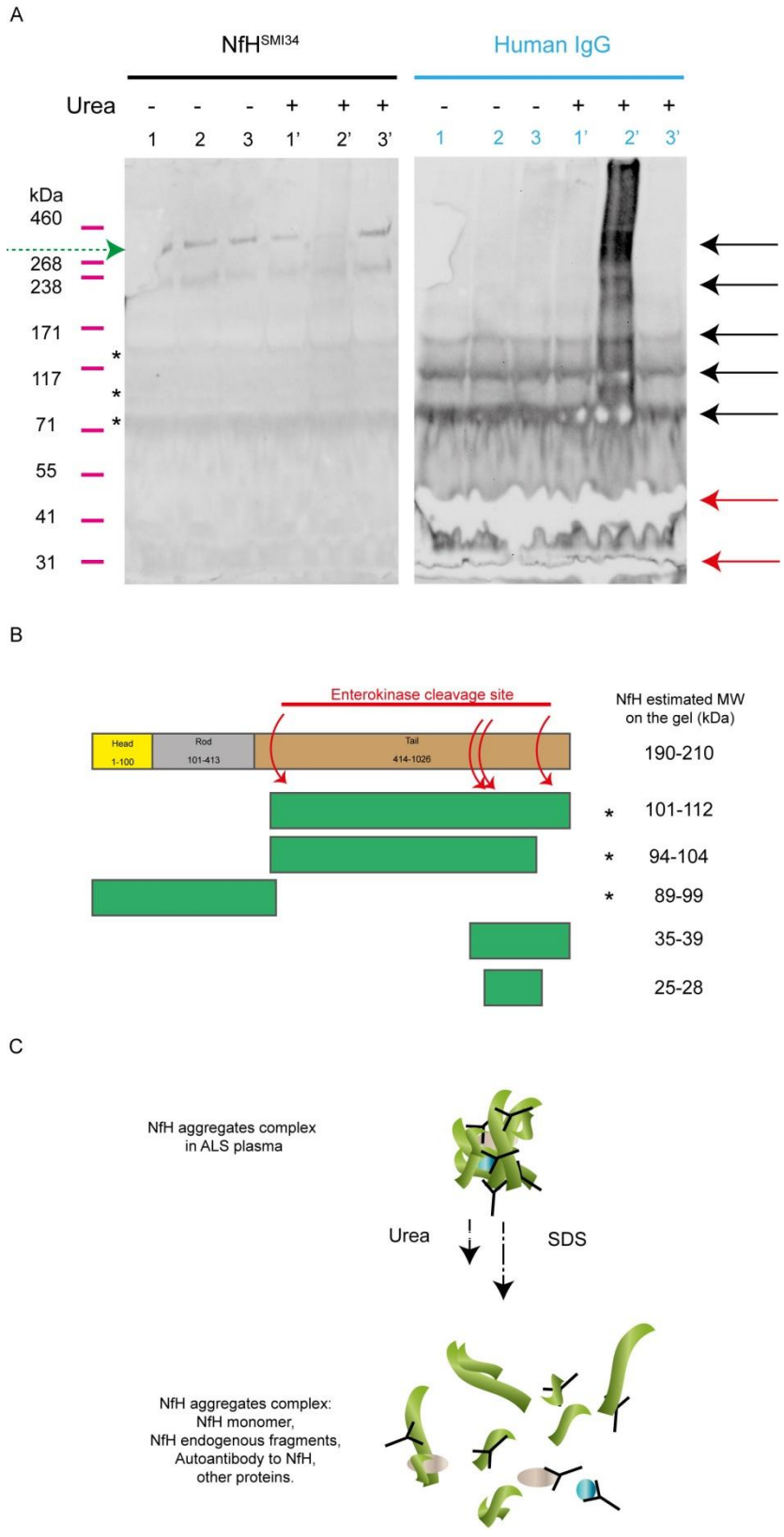
A
NfH SMI34
Human IgG
Urea
- - - + + +
1 2 3 1' 2' 3'
kDa
460
268
238
171
117
71
55
41
31
B
Enterokinase cleavage site
Head
1-100
Rod
101-413
Tail
414-1026
NfH estimated MW on the gel (kDa)
190-210
101-112
94-104
89-99
35-39
25-28
C
NfH aggregates complex in ALS plasma
Urea
SDS
NfH aggregates complex:
NfH monomer,
NfH endogenous fragments,
Autoantibody to NfH,
other proteins.

Figure 4.10. Immune response to NfH and NfH aggregates. (A) Immunoblots of plasma samples from ALS patients. Three sets of plasma samples, each containing plasma samples from 3 ALS patients were examined. Lane 1-3 and 1'-3': samples pre-treated without and with 0.5M urea incubation, respectively. The blot on the Left is probed with NfH^{SMI34}: bands at high molecular weight are present in ALS plasma (bands between 238-460 kDa; green dashed arrow) and endogenous binding of NfH cleavage products at lower MW areas (bands below ~205 kDa). Addition of 0.5 M urea partly dissolves the aggregates, particularly in lane 2'. On the right-side, the same blot re-probed with anti-Human IgG immunoglobulin is shown after stripping of the NfH antibody. Multiple bands showing intense staining for Human IgG were revealed; both the expected bands for the light chain (25kDa) and heavy chain (53 kDa) (red arrows) as well as bands at the MW of NfH endogenous fragments can be seen (black arrows). **(B)** The image shows the enterokinase cleavage sites for NfH (as described in Petzold et al., 2011a). **(C)** The diagram illustrates a hypothesis of NfH aggregates complex, which contain i) NfH high MW aggregates, a mixture of NfH monomer and NfH low MW fragments (endogenous cleavage products by Enterokinase), ii) human autoantibody to NfH, and iii) other proteins.

between 238-460 kD in lanes 1-3 of the NfH^{SMI34} blot). In addition, endogenous binding of NfH cleavage products were detected (see Fig. 4.10A: NfH^{SMI34} blot, bands below the expected ~205 kDa in lanes 1-3, marked by asterisks). This result is similar to our previous findings in plasma of $SOD1^{G93A}$ mice (Lu et al., 2011). The addition of 0.5 M Urea partly dissolves the aggregates after one hour (especially in lane 2' Fig. 4.10A, lanes 1'-3' in the NfH^{SMI34} blot). The NfH^{SMI34} blot shown in Fig. 4.10A was subsequently stripped of the NfH antibody and re-probed with HRP-conjugated anti-Human IgG immunoglobulin. This revealed multiple bands stained intensely for Human IgG, both for the expected bands for its light chain (25kDa) and heavy chain (53 kDa) (Fig. 4.10A, red arrows) as well as bands at the same MW of the NfH endogenous fragments (Fig. 4.10A, black arrows). These findings suggest firstly, that NfH aggregates are present in ALS plasma, and secondly, that both the high MW NfH aggregates and low MW fragments appear to co-localize with human IgG. Fig. 4.10B illustrates the enterokinase cleavage sites for NfHs (Petzold et al., 2011a)

The molecular weight of the NfH fragments produced following enterokinase cleavage (Fig. 4.10B, bands marked by asterisks), were of the same MW as the bands observed in the blot shown in Fig 4.10A (bands marked by asterisks) in the NfH^{SMI34} blot. These findings are similar to those reported in $SOD1^{G93A}$ mice (Lu et al., 2011). Taken together the results shown in Fig. 4.10 support the hypothesis that NfH aggregates may be present in the peripheral blood of ALS patients. Furthermore, as shown in Fig. 4.10C, these results also suggest that NfH aggregate complexes may contain: i) high MW NfH aggregates, a mixture of NfH monomers and low MW NfH fragments (endogenous cleavage products produced by enterokinases), ii) human auto-antibodies to NfHs, and iii) other possible proteins. The immune response to plasma NfHs and its proteolytic fragments may thus play a central role in the change in plasma NfH levels in ALS patients in different phases of the disease.

4.4 Discussion

In this Chapter I investigated whether plasma NfH levels may be used as a biomarker of disease progression in ALS. I have: i) validated whether the method developed in Chapter 2 is suitable for analysis of human plasma samples; ii) conducted a baseline cross-sectional comparison of plasma NfH levels between 104 control subjects and 136 ALS patients; iii) undertaken a longitudinal analysis of

serial samples from 74 ALS patients; iv) tested the prognostic value and functional correlation of plasma NfH levels in ALS patients; v) identified a potential sampling bias in ALS patients that may be a general practical challenge in biomarker studies of all neurodegenerative disorders that do not have a clear-cut disease onset; and vi) identified a possible additional mechanism that influences the plasma NfH levels in ALS patients.

4.4.1 Plasma NfH levels are related to disease duration and disease progression in ALS and may also be affected by the immune response: NfH is not a ready-to-use biomarker of disease progression for ALS

In this Chapter, I firstly confirmed the presence of the 'Hook Effect,' a technical obstacle caused by the form of NfH aggregates, which prevent accurate quantification of plasma NfH using ELISA methods. This hurdle was overcome by the use of a modified version of ELISA method for plasma NfH detection developed in Chapter 2. Next, using a large heterogeneous cohort of ALS patients, a cross-sectional analysis of plasma NfH levels showed that there was no significant difference in plasma NfH levels between ALS patients and control groups at baseline, the time of the first sampling. This finding is in contrast to previous reports of NfH levels (Boylan et al., 2009). However, since these previous studies involved smaller cohorts of ALS patients and controls than the present study, it is likely that our results more closely reflect the high clinical heterogeneity of large ALS patient cohorts.

Analysis of longitudinal changes in plasma NfH levels, showed that patients with a shorter diagnostic latency and disease duration, are not only more likely to progress faster, a finding that has been also described by others (Chio et al., 2009; Turner et al., 2010b), but to also have higher plasma NfH levels during the early stages of the disease (Fig. 4.6). Thus, in the ALS patient cohort examined in this Chapter, I found a correlation between plasma NfH levels and the rate of disease progression in ALS patients, where surprisingly, low levels of plasma NfH correlate with a poor prognosis. These findings also are in contrast to those reported by Boylan and colleagues, which suggested that high levels of plasma NfH correlate with a faster disease progression (Boylan et al., 2013), and may again be explained by the larger and more heterogeneous ALS population examined in the present study.

I also investigated whether a specific pattern of disease progression was reflected in a change in plasma NfH levels. Four main patterns of combined behaviors of these two parameters were identified, where patients either progressed or stabilised, accompanied by either an increase or decrease in NfH levels. These results show that changes in plasma NfH levels do not predict disease progression, in our large, heterogeneous population of ALS patients. It is possible, however, that in studies of small homogenous patient cohorts, one pattern of disease may predominate, resulting in an increased chance of detecting a false positive correlation between plasma NfH levels and rate of disease progression. Therefore, my results show that sampling bias may have a significant impact on the interpretation of cross-sectional biomarker studies, particularly those consisting of small sample sizes.

My results also clearly show that, contrary to expectations, plasma NfH levels do not always increase as disease progresses in ALS patients. Since previous studies have detected the presence of auto-antibodies to other neuron-specific proteins in peripheral blood (Couratier et al., 1998; Fialova et al., 2010), it is possible that the rise of auto-antibodies may influence the levels of NfH in plasma of ALS patients. I therefore examined whether auto-antibodies against NfHs and their proteolytic by-products could be detected in plasma of ALS patients. My results showed that NfH aggregate complexes in plasma of ALS patients may contain not only high MW NfH aggregates, a mixture of NfH monomers and low MW NfH fragments (endogenous cleavage products produced by enterokinases), but also human auto-antibodies to NfHs. The immune response to plasma NfHs and its proteolytic fragments may thus play a central role in the change in plasma NfH levels in ALS patients in different phases of the disease.

4.4.2 Plasma NfH levels do not always increase as disease progresses in ALS

The results presented in this Chapter have thus significantly increased our understanding of the relationship between disease progression in ALS, the bioavailability of NfH and the importance of the time of sampling in the disease course, which is key to the interpretation of case-control and cross-sectional studies. The large and heterogeneous cohort of ALS patients and controls subjects examined in this study is representative of the wider ALS population with regard to the delay from symptom onset to disease recognition, and the median (IQR) of diagnostic latency in our ALS patients is in line with other large population studies (Cellura et al., 2012; Iwasaki et al., 2002). For NfH detection, I have used an

efficient, sensitive and reproducible blood-based analysis, circumventing the need for invasive lumbar punctures. Using the immunoassay described in Chapter 2 for analysis of human plasma samples, I have significantly improved the sensitivity of NfH detection in plasma by overcoming the 'hook effect' created by NfH aggregates Fig 4.1 and Fig. 4.2).

The longitudinal analysis of a biomarker throughout disease progression provides an unquestionable methodological advantage over cross-sectional studies. In this Chapter, I have obtained information which cannot be easily extracted from single time point measurements.

In ALS, the invariably progressive nature of the condition may suggest a linear change in time of any biological signal that reflects the pathological process. This can be seen quite clearly in the SOD1 mouse model of ALS, where plasma NfH levels increase towards end-stage disease (Boylan et al., 2009; Lu et al., 2012). Furthermore, in this experimental model, we have been able to demonstrate a treatment effect of a known neuroprotective agent on plasma NfH levels (Lu et al., 2012). However, the situation in the human pathology, as the present study demonstrates, is completely different. The profile of plasma NfH, at least within the disease time frame studied, varies significantly and depends on both the speed of disease progression and the delay from reported disease onset to baseline and subsequent NfH measurements, which may result from different expression levels of NfH mRNA in the neurons, different rates in the breakdown of NfH, and the reaction to the autoantibodies against NfH (Fig. 4.5). The differences in NfH bioavailability in sub-groups of ALS patients is likely to reflect not only the clinical heterogeneity of the disease, but also other unknown factors such as the rate of motor neuron and axonal degeneration in different disease phenotypes, NfH catabolism in biological fluids and possibly, as suggested in this study, the immune response to NfHs.

4.4.3 Immune response against neuroglia-specific proteins in the peripheral blood

My results also suggest that the rise of antibodies against NfH may accelerate the clearance of NfH and interfere with the detection power of antibody-based assays. Our immunoblotting results suggest a co-localisation of NfH fragments and human IgG components, which is in keeping with an immune response to the changing levels of NfH in plasma (Fig. 4.10A). Although we have not established the role of

these auto-antibodies in determining plasma NfH levels, these findings suggest that these antibodies may be responsible for a faster NfH clearance and may also interfere with the actual sensitivity of our antibody-based assay.

The potential importance of auto-antibodies to NfHs in ALS has been discussed previously. Recent studies have re-addressed the findings of significant elevations in serum auto-antibodies against neuronal and glial specific-proteins such as tau, microtubule-associated protein-2, tubulin, myelin basic protein, glial fibrillary acid protein and Nfs in airline crews (Abou-Donia et al., 2013) and in serum/CSF against Nfs in early MS patients (Fialova et al., 2013). It is therefore possible that the humoral immune response to plasma NfHs may itself be the primary target of future exploratory studies into biomarkers of disease progression in ALS.

4.4.4 Possible explanations for the discrepancy in plasma NfH levels between animal models and men

The Results presented in Chapter 3 showed that plasma NfH increase as disease progresses in SOD1 mice. This finding is in contrast to the Results of this Chapter, which show that this is not the case in human ALS patients. There may be several reasons for this discrepancy between the mouse models of ALS. Firstly, in contrast to ALS patients, SOD1 mice exhibit a very well characterised, homogeneous pattern of disease, with minimal variation in disease onset, site of onset, duration and end-stage, especially in colonies which are well maintained, managed, and monitored for gene copy numbers, fluctuations in lifespan of male stud mice. This homogeneity is enhanced when mice of a single gender are examined as in Chapter 3, as gender is known to affect disease progression in the SOD1 mouse model (Kalmar et al., 2008). Furthermore, disease progression in this model is extremely aggressive and $SOD1^{G93A}$ mice in our colony die, on average, by Day 130, showing for a clear neuromuscular deficit around 100-110 days. This phenotype, of homogeneity and rapid disease progression, is very different from the disease phenotype observed in a large cohort of ALS patients, which are clearly characterised by a significant heterogeneity in all aspects of the disease. Furthermore, it is possible that the rapidity of the disease observed in SOD1 mice is such that an immune response to plasma NfH is not initiated, unlike in ALS patients, where the prolonged duration of disease makes this more likely.

4.4.5 The impact of this study for biomarker studies in ALS

In addition, whilst the transgenic animal model of the ALS provides the opportunity to study the very early stages of the disease process when the animal is largely asymptomatic, investigations in humans capture only the later stages of disease. Ultimately, the use of NfHs or other proteins as prognostic biomarkers for ALS will be best served by study designs that allow a preliminary longitudinal evaluation of their expression. The use of a biomarker as an outcome measure in clinical trials implies a projected change of the area under the curve of the longitudinal measurement reflecting a treatment response. This, as findings described in this Chapter shown, can only be achieved with prior knowledge of the expression profile of the biomarker in the natural course of the disease and of the specific expression profile that each phenotypic variant of the disease may entail.

The data presented in this Chapter also suggest that the asymptomatic phase of ALS and the delay to diagnosis or plasma sampling have a significant effect on NfH measurements performed in the symptomatic phase. ALS patients in the study were sub-grouped according to the delay from ALS onset to baseline sampling. This time interval reflects the diagnostic delay, as baseline sampling in most of patients occurred either at diagnosis or up to 3 months later. Plasma NfH levels in ALS-F patients were higher during earlier stages of disease and reduce as the disease progresses, possibly as a consequence of the depletion of the motor neuron population. In contrast, ALS-S patients tend to have relatively low levels of NfHs during earlier stages of disease, which increase in the later stage of the disease. It is possible that plasma NfH levels may reflect neuropathological changes driven by a disease that proceeds at different speeds in different patients. The higher NfH levels detected in ALS-S patients may indicate the development of a level of neurodestruction that occurs earlier in ALS-F patients. Whether ALS-S subjects would exhibit, at later disease stages, a decrease of NfH levels as observed in end-stage ALS-F cannot be determined from our study. However, it is clear that the results of the longitudinal study presented here show that the level of information that cross-sectional studies can provide is severely limited, as the results are subject to significant sampling bias and are critically dependent on the chosen sampling time in the study population. Thus, cross-sectional studies alone cannot provide a comprehensive representation of the bioavailability of markers such as NfHs, whose expression changes throughout the disease course.

4.5 Conclusions

Taken together, the results presented in this Chapter show that plasma NfH levels in ALS patients differ from the pattern observed in SOD1 mouse models of ALS (presented in Chapter 3). In the animal models, the materials used for investigation are homogenous and are also neatly time-controlled. However, in neurodegenerative disorders so heterogeneous as ALS, the pre-diagnosis variation between patients are still huge, even though researchers can achieve a short diagnosis-to-sampling/study delay. Cross-sectional studies with strict enrolment criteria can certainly reduce the heterogeneity in the study cohorts, although this approach simultaneously raises the concern of low representative such patient cohorts are. This is a dilemma commonly faced in ALS biomarker studies and clinical trials.

My findings from the longitudinal analysis of plasma NfH levels in a large heterogeneous ALS cohort reveal several limitations that are not revealed in studies of small homogenous ALS cohorts. Although plasma NfH is correlated with disease progression in ALS, as shown in this Chapter, NfH levels are not only determined by the progression and disease course of ALS itself, but might also be affected by the immune response in individual patients. This is a very important finding in blood-based biomarker research, as several studies have now shown that auto-antibodies against neuroglia-specific proteins are produced in the blood (Abou-Donia et al., 2013; Fialova et al., 2013). Hence, for any blood-based neurochemical biomarker study, it is not possible to draw any positive or negative conclusions from small homogenous patient cohorts, particularly in studies involving proteins that are directly related to the pathology of ALS. Moreover, the findings of this study also highlight the role that the immune system may play in ALS biomarker studies.

From this study I conclude that there are several ways by which blood-based biomarker studies for ALS could be improved:

i) Studies should be undertaken longitudinally and in a large comprehensive cohort of ALS patients to gain an overview of the target biomarker as a function of disease progression. From such a study, patients sub-groups can be subsequently identified and analysed;

ii) The probability of an immune response to the target biomarker must be considered and investigated, as auto-antibodies may have a significant effect on the levels of the target molecules.

- The Results presented in this Chapter was submitted to *Neurology,* under Review.

  Ching-Hua Lu, Axel Petzold, Jo Topping, Kezia Allen, Jan Clarke, Jens Kuhle, Gavin Giovannoni, Pietro Fratta, Katie Sidle, Mark Fish, Richard Orrell, Robin Howard, Linda Greensmith, and Andrea Malaspina. Plasma NfH levels and group-based trajectories of disease progression in ALS: Insights from a longitudinal study.

Chapter 5

Discussion

The experiments described in this Thesis have examined whether plasma NfH levels may be a biomarker of disease progression in SOD1 mouse models of ALS and in ALS patients.

5.1 The development of a sensitive, reliable immunoassay for the quantification of NfH in plasma of SOD1 mice and ALS patients.

In the experiments described in Chapter 2, I first evaluated the suitability of methods that have been previously used for measuring NfH in the CSF (Petzold et al., 2003) to be employed for the detection of plasma NfH in $SOD1^{G93A}$ mice. As can be seen in Table 2.2, the assayed values for serial sample dilutions of SOD1 plasma increased as the dilution factor increased, while NfH in the WT animals remained undetectable. A similar phenomenon was observed using plasma samples from ALS patients. The identification of the 'Hook Effect' and the presence of high MW NfH aggregates in the plasma of SOD1 mice and ALS patients, phenomena thought to be due to endogenous binding of protein fragments, were overcome by pre-incubation of plasma samples with 0.5 M urea. This enables the accurate and consistent detection of NfH not only in plasma from diseased animals and from ALS patients, but also in plasma from healthy individuals. The sensitivity and reliability of the method developed in this study is clear if our results are compared with those of previous reports investigating plasma NfH as a potential biomarker of ALS. These studies have shown low or late detection of plasma NfH in SOD1 mice and undetectable plasma NfH in WT mice (Boylan et al., 2009; Gnanapavan et al., 2012). In addition, the detection in our study of hyperphosphorylated NfH in plasma from healthy WT mice and from healthy controls shows that the presence of hyperphosphorylated NfH in the peripheral blood is not in itself indicative of pathology.

5.2 Plasma NfH levels in clinically homogeneous SOD1 mouse models of ALS

As a proof of principle, serial experiments examining plasma NfH levels in different mouse models of ALS were undertaken and correlated with readouts of disease

progression and the therapeutic effects of various known and potential therapeutic agents.

5.2.1 Plasma NfH levels increase during disease progression is detected in both rapidly-progressing SOD1^{G93A} and slowly-progressing SOD1^{G93Adl} mouse models of ALS

SOD1^{G93A} mice have a homogeneous, aggressive, rapidly progressing disease phenotype in which neurofilament pathology is a disease hallmark. The Results presented in Chapter 3 show that plasma NfH levels increase significantly in SOD1^{G93A} mice between 105 to 120 days of age. Increased plasma NfH levels do not reflect the earlier stages of disease in SOD1^{G93A} mice, where NfH levels were similar in SOD1^{G93A} and WT mice. Nonetheless, even prior to symptom onset, there was a larger variation in plasma NfH levels in SOD1^{G93A} mice than WT mice, suggesting the beginning of the release of NfH into the peripheral blood. Similarly, but not identically, in the slow-progressed SOD1^{G93Adel} mice, plasma NfH levels increased in parallel with disease progression, although there was a limitation of small numbers of samples analysed in this set of experiments. These findings suggest that plasma NfH levels increase during disease progression not only in rapidly-progressing SOD1^{G93A} mice, but also in the more slowly-progressing SOD1^{G93Adl} model which may be more relevant to the pattern of disease progression in ALS patients.

5.2.2 Plasma NfH levels correlate with readouts of disease progression in SOD1^{G93A} mice

In SOD1^{G93A} mice, plasma NfH levels correlate well with functional and morphological readouts of disease progression. There is a good correlation between plasma NfH levels and the decline in grip strength in SOD1^{G93A} mice in the longitudinal assessment presented in Chapter 3. Moreover, the increase in NfH levels parallels the loss of muscle force and motor unit survival in the acute, cross-sectional physiological assessment of disease phenotype. Amongst the most important readouts, there is a good correlation between plasma NfH levels and the motor neuron death in the spinal cord of SOD1^{G93A} mice in the morphological assessment.

5.2.3 Plasma NfH levels reflect the therapeutic effects of established and new agents in SOD1^{G93A} mice

In SOD1^{G93A} mice, plasma NfH levels were found to reflect the therapeutic effect of several test drugs. The first drug tested in this Thesis was Arimoclomol, a co-inducer of the heat shock response, which has previously been shown to have beneficial effects in SOD1^{G93A} mice, improving neuromuscular function and prolonging lifespan (Kalmar et al., 2008; Kieran et al., 2004). The Results presented in Chapter 3 show that lower plasma NfH^{SMI34} levels are observed during the pre-symptomatic stages in Arimoclomol-treated SOD1 mice, suggesting a beneficial effect of Arimoclomol which is reflected in the reduction in NfH^{SMI34} levels in the blood. In the later disease stages, Arimoclomol-treated SOD1 mice tend to have lower levels of plasma NfH, although the difference in treated and untreated mice only reach significance at end-stage.

Interestingly, in the preclinical study of Cogane and Riluzole, mice treated with the two drugs have very different morphological and physiological profiles as well as plasma NfH levels. For example, in Riluzole-treated SOD1 mice, although their muscle strength and motor unit survival were not different from Vehicle-treated mice, these mice presented with an improved motor neuron survival and a reduction of plasma NfH levels. In contrast, in Cogane-treated SOD1 mice, there is an improvement in muscle strength, motor unit survival and motor neuron survival, compared to untreated mice, and these mice also present with significantly higher plasma NfH levels than those treated with Riluzole. These results suggest it is likely that Riluzole and Cogane target two very distinct mechanisms so that their neuromuscular profiles and plasma NfH levels are therefore different. These findings also imply that plasma NfH levels may be a potential candidate to be used as an outcome measure in clinical trials of new agents.

5.3 Plasma NfH levels in a cohort of clinically heterogeneous ALS patients

The Results presented in Chapter 3 from homogenous SOD1 mouse models of ALS suggest that plasma NfH levels a promising biomarker of disease progression in ALS, at least in these mouse models. In Chapter 4, I next examined the possibility that plasma NfH may also be a biomarker in a large, heterogeneous cohort of ALS patients.

5.3.1 Plasma NfH levels are influenced by disease duration, rate of disease progression, composition of study cohorts, and likely auto-antibody to NfH as well

The pattern of plasma NfH levels in ALS patients were not as straightforward as those detected in SOD1 mice as a function of disease progression. The Results presented in Chapter 4 show that there is no significant difference in plasma NfH levels between ALS (n=136) and control subjects (n=104) in a cross-sectional study at baseline sampling. However, if ALS patients are further sub-grouped according to the disease duration from the reported onset of symptom to their baseline sampling, patients sampled within the first year of disease onset tend to have higher plasma NfH levels than the controls and those sampled in the second year. These results suggest that disease duration may play a role in determination of plasma NfH levels.

The analysis of the longitudinal pattern of plasma NfH from baseline sampling amongst our 74 patients who had serial samplings showed that fast-progressing ALS patients (ALS-F) had plasma NfH levels that declined during disease progression while the levels in slowly-progressing ALS patients (ALS-S) remained steady, then increased later during the follow-up. These results suggest that plasma NfH levels are dependent on the rate of disease progression. Furthermore, the analysis of the longitudinal pattern of plasma NfH from the onset of symptoms, with further sub-grouping according to the overall disease progression rate, revealed distinct patterns between ALS-F and ALS-S patients at different disease durations. These results suggest that plasma NfH levels are influenced not only by the rate of disease progression but also by the disease course.

A correlation between plasma NfH levels and the disease progression rate, determined by the ALSFRS_R, is more likely to be observed over short periods, i.e. between visits in the study rather than overall, from onset to baseline sampling or to the last available visit. However, this correlation is dependent on the composition of the patient cohort in the study as patients with different disease progression rates and disease durations at the time of sampling will affect the pattern of plasma NfH and hence its correlation with disease progression.

Since plasma NfH levels do not always increase during disease progression in a large cohort of ALS patients, unlike in $SOD1^{G93A}$ mice, I examined the possibility that other factors/mechanisms may be influencing plasma NfH levels. Previous studies

have shown that an immune response to neuroglial specific proteins can be detected in the peripheral blood (Abou-Donia et al., 2013; Couratier et al., 1998; Fialova et al., 2010). I therefore examined whether there was any evidence of an immune response to the presence of NfH in plasma ALS patients. In the preliminary study, western blot, bands stained for anti-human IgG strikingly co-localised with bands stained for NfH, at high MW aggregates, monomers and proteolytic fragments, suggesting a possible role played by auto-antibodies against NfH in the peripheral blood in the determination of plasma NfH levels.

5.3.2 Sampling bias is likely in small homogeneous cross-sectional studies of ALS patients: The need to re-think the use of baseline sampling

The Results presented in Chapter 4 have shown that plasma NfH levels in ALS are influenced by the progression of ALS itself. Hence for neurochemical markers that are pathologically relevant to ALS, it is likely that small homogeneous cross-sectional studies at baseline, particularly in studies targeting patients with an aggressive phenotype which enables them to be diagnosed as definite ALS with a short diagnostic interval, are un-representative of the clinical heterogeneity of ALS. Results from such studies may cause sampling bias, which can lead to a false conclusion about this marker. Moreover, the value of the data obtained at baseline should also be re-examined, as the baseline is an arbitrary time-point and could reflect very different stages of disease for different patients with different disease course. Only by increasing the number and the heterogeneity of patients in the cohort is it possible to further sub-classify patients in order to examine ALS as a whole disease, rather just a limited disease phenotype as currently undertaken in most of cross-sectional studies of ALS biomarkers.

5.4 Conclusion

In this Thesis, I have presented the results of experiments which resulted in the development of an improved immunoassay for the sensitive and reliable detection of NfH levels in plasma of mice and humans. In SOD1 mouse models of ALS, plasma NfH levels correlate well with disease progression and were a good outcome measure of the therapeutic effects of test drugs. In spite of the technical improvements and the promising results from SOD1 mice, the findings in a large heterogeneous ALS patient cohort are in contrast to the findings in the animal models. Figure 5.1 summarises the timeline of key clinical events and the use of

Figure 5.1

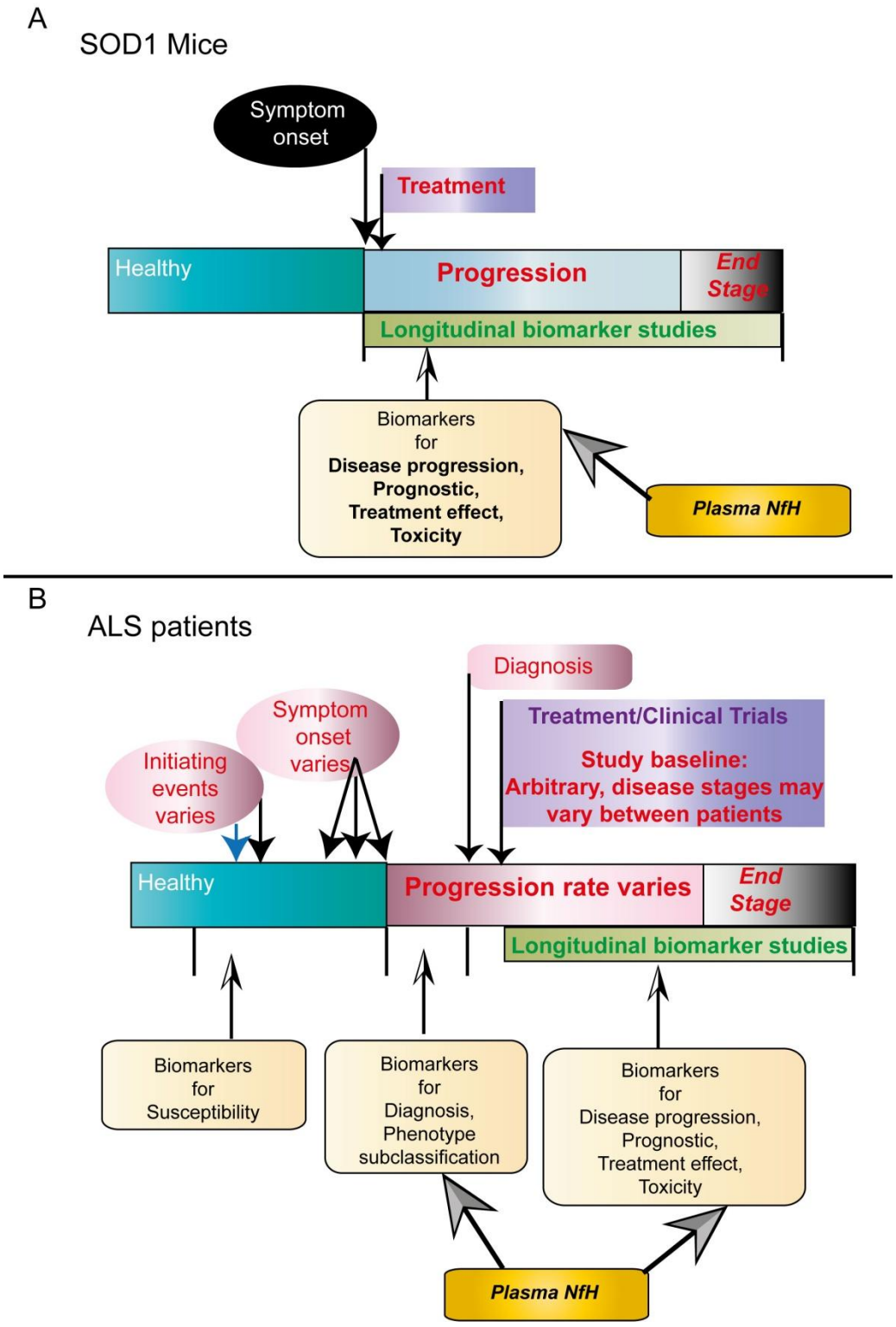
A
SOD1 Mice
Symptom onset
Treatment
Healthy
Progression
End Stage
Longitudinal biomarker studies
Biomarkers for Disease progression, Prognostic, Treatment effect, Toxicity
Plasma NfH
B
ALS patients
Diagnosis
Symptom onset varies
Initiating events varies
Treatment/Clinical Trials
Study baseline: Arbitrary, disease stages may vary between patients
Healthy
Progression rate varies
End Stage
Longitudinal biomarker studies
Biomarkers for Susceptibility
Biomarkers for Diagnosis, Phenotype subclassification
Biomarkers for Disease progression, Prognostic, Treatment effect, Toxicity
Plasma NfH

Figure 5.1. Timeline of key clinical events and the use of biomarkers in SOD1 mice and in ALS patients. Schematic illustrations show the timeline of key events and the potential use of biomarkers in clinically homogeneous SOD1 mice **(A)** and in clinically heterogeneous ALS patients **(B)**. SOD1 mice have well-characterised disease phenotypes, age of onset, rates of disease progression and duration of survival. In longitudinal biomarker studies in mice, it is possible to develop biomarkers for disease progression, prognosis, treatment effect and toxicity due to their disease homogeneity, as observed with plasma NfH levels in the experiments presented in this Thesis (Chapter 3). In contrast, ALS patients are highly heterogeneous with regard to initiating events, age of onset, disease phenotypes, rates of disease progression and disease duration. Therefore, the baseline in clinical trials and cross-sectional biomarker studies is arbitrary and may represent different disease stages amongst individual patients. Nonetheless, it is still possible to develop biomarkers of disease progression when patients are sub-classified according to disease phenotype in large comprehensive longitudinal biomarker studies, as observed in the study presented in Chapter 4, for plasma NfH levels in ALS patients.

biomarkers in SOD1 mice and in ALS patients, according to the results obtained from this Thesis. These results provide new insights into biomarker studies in ALS.

Several important lessons have been learned from the experiments presented in this Thesis, including:

i) Blood-based biomarker studies in ALS should be undertaken longitudinally and in a large comprehensive cohort of ALS patients in order to gain an overview of the target biomarker as a function of disease progression. From such a study, patient sub-groups can be subsequently identified and then analysed;

ii) The possibility of an immune response to the target biomarker should be considered and investigated, as auto-antibodies may have a significant effect on the levels of the target molecules;

iii) Despite the promising results observed in SOD1 mice and the correlation with disease progression in ALS patients shown both in Chapter 4 and in previous studies (Boylan et al., 2009; Boylan et al., 2013), plasma NfH levels are not a simple marker of disease progression in ALS patients. However, with the insights obtained from this Thesis, it is possible that the correlation between plasma NfH and disease progression may be revealed in further studies.

List of References

Abou-Donia, M.B., Abou-Donia, M.M., Elmasry, E.M., Monro, J.A., and Mulder, M.F. (2013). Autoantibodies to nervous system-specific proteins are elevated in sera of flight crew members: biomarkers for nervous system injury. Journal of toxicology and environmental health Part A *76*, 363-380.

Abrahams, S., Goldstein, L.H., Suckling, J., Ng, V., Simmons, A., Chitnis, X., Atkins, L., Williams, S.C., and Leigh, P.N. (2005). Frontotemporal white matter changes in amyotrophic lateral sclerosis. J Neurol *252*, 321-331.

Acevedo-Arozena, A., Kalmar, B., Essa, S., Ricketts, T., Joyce, P., Kent, R., Rowe, C., Parker, A., Gray, A., Hafezparast, M.*, et al.* (2011). A comprehensive assessment of the SOD1G93A low-copy transgenic mouse, which models human amyotrophic lateral sclerosis. Disease models & mechanisms *4*, 686-700.

Achi, E.Y., and Rudnicki, S.A. (2012). ALS and Frontotemporal Dysfunction: A Review. Neurol Res Int *2012*, 806306.

Aggarwal, A., and Nicholson, G. (2001). Normal complement of motor units in asymptomatic familial (SOD1 mutation) amyotrophic lateral sclerosis carriers. J Neurol Neurosurg Psychiatry *71*, 478-481.

Aggarwal, A., and Nicholson, G. (2002). Detection of preclinical motor neurone loss in SOD1 mutation carriers using motor unit number estimation. J Neurol Neurosurg Psychiatry *73*, 199-201.

Aggarwal, S.P., Zinman, L., Simpson, E., McKinley, J., Jackson, K.E., Pinto, H., Kaufman, P., Conwit, R.A., Schoenfeld, D., Shefner, J.*, et al.* (2010). Safety and efficacy of lithium in combination with riluzole for treatment of amyotrophic lateral sclerosis: a randomised, double-blind, placebo-controlled trial. Lancet neurology *9*, 481-488.

Al-Chalabi, A., Andersen, P.M., Nilsson, P., Chioza, B., Andersson, J.L., Russ, C., Shaw, C.E., Powell, J.F., and Leigh, P.N. (1999). Deletions of the heavy neurofilament subunit tail in amyotrophic lateral sclerosis. Hum Mol Genet *8*, 157-164.

Al-Chalabi, A., Jones, A., Troakes, C., King, A., Al-Sarraj, S., and van den Berg, L.H. (2012). The genetics and neuropathology of amyotrophic lateral sclerosis. Acta Neuropathol *124*, 339-352.

Al-Saif, A., Al-Mohanna, F., and Bohlega, S. (2011). A mutation in sigma-1 receptor causes juvenile amyotrophic lateral sclerosis. Ann Neurol *70*, 913-919.

ALSTDI. TRO19622 (Olesoxime). Access Date: 16/04/2013 http://www.als.net/ALS-Research/Olesoxime/ALS-Topics/

Anand, A., Gupta, P.K., Sharma, N.K., and Prabhakar, S. (2012). Soluble VEGFR1 (sVEGFR1) as a novel marker of amyotrophic lateral sclerosis (ALS) in the North Indian ALS patients. Eur J Neurol *19*, 788-792.

Andersen, P.M., and Al-Chalabi, A. (2011). Clinical genetics of amyotrophic lateral sclerosis: what do we really know? Nature reviews Neurology *7*, 603-615.

Andres, P.L., Hedlund, W., Finison, L., Conlon, T., Felmus, M., and Munsat, T.L. (1986). Quantitative motor assessment in amyotrophic lateral sclerosis. Neurology *36*, 937-941.

Appel, S.H., Beers, D.R., and Henkel, J.S. (2010). T cell-microglial dialogue in Parkinson's disease and amyotrophic lateral sclerosis: are we listening? Trends in immunology *31*, 7-17.

Appel, S.H., Zhao, W., Beers, D.R., and Henkel, J.S. (2011). The microglial-motoneuron dialogue in ALS. Acta myologica : myopathies and cardiomyopathies : official journal of the Mediterranean Society of Myology / edited by the Gaetano Conte Academy for the study of striated muscle diseases *30*, 4-8.

Appel, V., Stewart, S.S., Smith, G., and Appel, S.H. (1987). A rating scale for amyotrophic lateral sclerosis: description and preliminary experience. Ann Neurol *22*, 328-333.

Archibald, D., Ingersoll, E., Mather, J., Schoenfeld, D., Kerr, D., Wang, Y.-C., Dong, Y., and Bozik, M. (2011). Statistical modeling to illustrate the contribution of and effects of differential mortality and functional change on joint rank test outcomes in ALS. Amyotrophic Lateral Sclerosis *12 (S1)*, 107.

Armon, C., and Brandstater, M.E. (1999). Motor unit number estimate-based rates of progression of ALS predict patient survival. Muscle Nerve *22*, 1571-1575.

Arts, I.M., Overeem, S., Pillen, S., Kleine, B.U., Boekestein, W.A., Zwarts, M.J., and Jurgen Schelhaas, H. (2012). Muscle ultrasonography: a diagnostic tool for amyotrophic lateral sclerosis. Clin Neurophysiol *123*, 1662-1667.

Arts, I.M., Overeem, S., Pillen, S., Schelhaas, H.J., and Zwarts, M.J. (2011a). Muscle changes in amyotrophic lateral sclerosis: a longitudinal ultrasonography study. Clin Neurophysiol *122*, 623-628.

Arts, I.M., Overeem, S., Pillen, S., Schelhaas, H.J., and Zwarts, M.J. (2011b). Muscle ultrasonography to predict survival in amyotrophic lateral sclerosis. J Neurol Neurosurg Psychiatry *82*, 552-554.

Arts, I.M., Pillen, S., Schelhaas, H.J., Overeem, S., and Zwarts, M.J. (2010). Normal values for quantitative muscle ultrasonography in adults. Muscle Nerve *41*, 32-41.

Ayala, Y.M., Zago, P., D'Ambrogio, A., Xu, Y.F., Petrucelli, L., Buratti, E., and Baralle, F.E. (2008). Structural determinants of the cellular localization and shuttling of TDP-43. J Cell Sci *121*, 3778-3785.

Bak, T.H., and Hodges, J.R. (2001). Motor neurone disease, dementia and aphasia: coincidence, co-occurrence or continuum? J Neurol *248*, 260-270.

Bak, T.H., and Hodges, J.R. (2004). The effects of motor neurone disease on language: further evidence. Brain Lang *89*, 354-361.

Baron, P., Bussini, S., Cardin, V., Corbo, M., Conti, G., Galimberti, D., Scarpini, E., Bresolin, N., Wharton, S.B., Shaw, P.J.*, et al.* (2005). Production of monocyte chemoattractant protein-1 in amyotrophic lateral sclerosis. Muscle Nerve *32*, 541-544.

Batulan, Z., Shinder, G.A., Minotti, S., He, B.P., Doroudchi, M.M., Nalbantoglu, J., Strong, M.J., and Durham, H.D. (2003). High threshold for induction of the stress response in motor neurons is associated with failure to activate HSF1. J Neurosci *23*, 5789-5798.

Beck, M., Giess, R., Wurffel, W., Magnus, T., Ochs, G., and Toyka, K.V. (1999). Comparison of maximal voluntary isometric contraction and Drachman's hand-held dynamometry in evaluating patients with amyotrophic lateral sclerosis. Muscle Nerve *22*, 1265-1270.

Beers, D.R., Henkel, J.S., Zhao, W., Wang, J., and Appel, S.H. (2008). CD4+ T cells support glial neuroprotection, slow disease progression, and modify glial morphology in an animal model of inherited ALS. Proc Natl Acad Sci U S A *105*, 15558-15563.

Beers, D.R., Henkel, J.S., Zhao, W., Wang, J., Huang, A., Wen, S., Liao, B., and Appel, S.H. (2011). Endogenous regulatory T lymphocytes ameliorate amyotrophic lateral sclerosis in mice and correlate with disease progression in patients with amyotrophic lateral sclerosis. Brain *134*, 1293-1314.

Beghi, E., Chio, A., Couratier, P., Esteban, J., Hardiman, O., Logroscino, G., Millul, A., Mitchell, D., Preux, P.M., Pupillo, E.*, et al.* (2011). The epidemiology and treatment of ALS: focus on the heterogeneity of the disease and critical appraisal of therapeutic trials. Amyotroph Lateral Scler *12*, 1-10.

Beghi, E., Logroscino, G., Chio, A., Hardiman, O., Mitchell, D., Swingler, R., and Traynor, B.J. (2006). The epidemiology of ALS and the role of population-based registries. Biochim Biophys Acta *1762*, 1150-1157.

Beleza-Meireles, A., and Al-Chalabi, A. (2009). Genetic studies of amyotrophic lateral sclerosis: controversies and perspectives. Amyotroph Lateral Scler *10*, 1-14.

Bento-Abreu, A., Van Damme, P., Van Den Bosch, L., and Robberecht, W. (2010). The neurobiology of amyotrophic lateral sclerosis. Eur J Neurosci *31*, 2247-2265.

Berry, J.D., Miller, R., Moore, D.H., Cudkowicz, M.E., Van Den Berg, L.H., Kerr, D.A., Dong, Y., Ingersoll, E.W., and Archibald, D. (2013). The Combined Assessment of Function and Survival (CAFS): A new endpoint for ALS clinical trials. Amyotroph Lateral Scler Frontotemporal Degener *14*, 162-168.

Beuche, W., Yushchenko, M., Mader, M., Maliszewska, M., Felgenhauer, K., and Weber, F. (2000). Matrix metalloproteinase-9 is elevated in serum of patients with amyotrophic lateral sclerosis. Neuroreport *11*, 3419-3422.

Bevan, J.S., Burke, C.W., Esiri, M.M., and Adams, C.B. (1987). Misinterpretation of prolactin levels leading to management errors in patients with sellar enlargement. Am J Med *82*, 29-32.

Black, L.F., and Hyatt, R.E. (1969). Maximal respiratory pressures: normal values and relationship to age and sex. Am Rev Respir Dis *99*, 696-702.

Blasco, H., Corcia, P., Moreau, C., Veau, S., Fournier, C., Vourc'h, P., Emond, P., Gordon, P., Pradat, P.F., Praline, J.*, et al.* (2010). 1H-NMR-based metabolomic profiling of CSF in early amyotrophic lateral sclerosis. PLoS ONE *5*, e13223.

Borchelt, D.R., Wong, P.C., Becher M.W., Pardo, C.A., Lee, M.K., Xu, Z.S., Thinakaran, G., Jenkins, N.A. Copeland, N.G., Sisodia, S.S., *et al*. (1998). Axonal transport of mutant superoxide dismutase 1 and focal axonal abnormalities in the proximal axons of transgenic mice. Neurobiol Dis *5*, 27-35.

Bosco, D.A., Lemay, N., Ko, H.K., Zhou, H., Burke, C., Kwiatkowski, T.J., Jr., Sapp, P., McKenna-Yasek, D., Brown, R.H., Jr., and Hayward, L.J. (2010a). Mutant FUS proteins that cause amyotrophic lateral sclerosis incorporate into stress granules. Hum Mol Genet *19*, 4160-4175.

Bosco, D.A., Morfini, G., Karabacak, N.M., Song, Y., Gros-Louis, F., Pasinelli, P., Goolsby, H., Fontaine, B.A., Lemay, N., McKenna-Yasek, D.*, et al.* (2010b). Wild-type and mutant SOD1 share an aberrant conformation and a common pathogenic pathway in ALS. Nat Neurosci *13*, 1396-1403.

Bose, J.K., Wang, I.F., Hung, L., Tarn, W.Y., and Shen, C.K. (2008). TDP-43 overexpression enhances exon 7 inclusion during the survival of motor neuron pre-mRNA splicing. J Biol Chem *283*, 28852-28859.

Bowser, R., Turner, M.R., and Shefner, J. (2011). Biomarkers in amyotrophic lateral sclerosis: opportunities and limitations. Nature reviews Neurology *7*, 631-638.

Boylan, K., Yang, C., Crook, J., Overstreet, K., Heckman, M., Wang, Y., Borchelt, D., and Shaw, G. (2009). Immunoreactivity of the phosphorylated axonal neurofilament H subunit (pNF-H) in blood of ALS model rodents and ALS patients: evaluation of blood pNF-H as a potential ALS biomarker. J Neurochem *111*, 1182-1191.

Boylan, K.B., Glass, J.D., Crook, J.E., Yang, C., Thomas, C.S., Desaro, P., Johnston, A., Overstreet, K., Kelly, C., Polak, M.*, et al.* (2013). Phosphorylated

neurofilament heavy subunit (pNF-H) in peripheral blood and CSF as a potential prognostic biomarker in amyotrophic lateral sclerosis. J Neurol Neurosurg Psychiatry *84*, 467-472.

Bozik, M., Ingersoll, E., Volles, L., Mather, J., Amburgey, C., Moritz, J., Archibald, D., Sullivan, M., Gribkoff, V., Miller, R.*, et al.* (2009). KNS-760704-CL201, Part 1: A 12-week phase 2 study of the safety, tolerability, and clinical effects of KNS-760704 in ALS subjects. Amyotroph Lateral Scler *10 (S1)*, 28-29.

Brettschneider, J., Lehmensiek, V., Mogel, H., Pfeifle, M., Dorst, J., Hendrich, C., Ludolph, A.C., and Tumani, H. (2010). Proteome analysis reveals candidate markers of disease progression in amyotrophic lateral sclerosis (ALS). Neurosci Lett *468*, 23-27.

Brettschneider, J., Mogel, H., Lehmensiek, V., Ahlert, T., Sussmuth, S., Ludolph, A.C., and Tumani, H. (2008). Proteome analysis of cerebrospinal fluid in amyotrophic lateral sclerosis (ALS). Neurochem Res *33*, 2358-2363.

Brettschneider, J., Petzold, A., Schottle, D., Claus, A., Riepe, M., and Tumani, H. (2006a). The neurofilament heavy chain (NfH) in the cerebrospinal fluid diagnosis of Alzheimer's disease. Dement Geriatr Cogn Disord *21*, 291-295.

Brettschneider, J., Petzold, A., Sussmuth, S.D., Landwehrmeyer, G.B., Ludolph, A.C., Kassubek, J., and Tumani, H. (2006b). Neurofilament heavy-chain NfH(SMI35) in cerebrospinal fluid supports the differential diagnosis of Parkinsonian syndromes. Mov Disord *21*, 2224-2227.

Brettschneider, J., Petzold, A., Sussmuth, S.D., Ludolph, A.C., and Tumani, H. (2006c). Axonal damage markers in cerebrospinal fluid are increased in ALS. Neurology *66*, 852-856.

Bromberg, M.B. (2004). Motor unit number estimation: new techniques and new uses. In Advances in Clinical Neurophysiology, M. Hallett, L.H. Phillips, H.D.L. Schomer, and J.M. Ma, eds. (Elsevier, B.V.), pp. 120-136.

Bromberg, M.B., Forshew, D.A., Nau, K.L., Bromberg, J., Simmons, Z., and Fries, T.J. (1993). Motor unit number estimation, isometric strength, and electromyographic measures in amyotrophic lateral sclerosis. Muscle Nerve *16*, 1213-1219.

Brooks, B.R. (1997). Guidelines for Administration and Scoring. In Handbook of Neurological Rating Scales, R.M. Herndon, ed. (New York: Demos Vermande), pp. 31-79.

Brooks, B.R. (2002). Functional scales: summary. Amyotroph Lateral Scler Other Motor Neuron Disord *3(S1)*, S13-18.

Brooks, B.R., Miller, R.G., Swash, M., and Munsat, T.L. (2000). El Escorial revisited: revised criteria for the diagnosis of amyotrophic lateral sclerosis. Amyotroph Lateral Scler Other Motor Neuron Disord *1*, 293-299.

Burrell, J.R., Kiernan, M.C., Vucic, S., and Hodges, J.R. (2011). Motor neuron dysfunction in frontotemporal dementia. Brain *134*, 2582-2594.

Byrne, S., Elamin, M., Bede, P., Shatunov, A., Walsh, C., Corr, B., Heverin, M., Jordan, N., Kenna, K., Lynch, C.*, et al.* (2012). Cognitive and clinical characteristics of patients with amyotrophic lateral sclerosis carrying a C9orf72 repeat expansion: a population-based cohort study. Lancet Neurol *11*, 232-240.

Campos-Melo, D., Droppelmann, C.A., He, Z., Volkening, K., and Strong, M.J. (2013). Altered microRNA expression profile in amyotrophic lateral sclerosis: a role in the regulation of NFL mRNA levels. Mol Brain *6*, 26.

Carden, M.J., Trojanowski, J.Q., Schlaepfer, W.W., and Lee, V.M. (1987). Two-stage expression of neurofilament polypeptides during rat neurogenesis with early establishment of adult phosphorylation patterns. J Neurosci *7*, 3489-3504.

Carpenter, S. (1968). Proximal axonal enlargement in motor neuron disease. Neurology *18,* 941-851.

Carvalho, M.D., and Swash, M. (2009). Awaji diagnostic algorithm increases sensitivity of El Escorial criteria for ALS diagnosis. Amyotroph Lateral Scler *10*, 53-57.

Castrillo-Viguera, C., Grasso, D.L., Simpson, E., Shefner, J., and Cudkowicz, M.E. (2010). Clinical significance in the change of decline in ALSFRS-R. Amyotroph Lateral Scler *11*, 178-180.

Cedarbaum, J.M., Stambler, N., Malta, E., Fuller, C., Hilt, D., Thurmond, B., and Nakanishi, A. (1999). The ALSFRS-R: a revised ALS functional rating scale that incorporates assessments of respiratory function. BDNF ALS Study Group (Phase III). J Neurol Sci *169*, 13-21.

Cellura, E., Spataro, R., Taiello, A.C., and La Bella, V. (2012). Factors affecting the diagnostic delay in amyotrophic lateral sclerosis. Clin Neurol Neurosurg *114*, 550-554.

Chang, J.L., Lomen-Hoerth, C., Murphy, J., Henry, R.G., Kramer, J.H., Miller, B.L., and Gorno-Tempini, M.L. (2005). A voxel-based morphometry study of patterns of brain atrophy in ALS and ALS/FTLD. Neurology *65*, 75-80.

Charrie, A., Charriere, G., and Guerrier, A. (1995). Hook effect in immunometric assays for prostate-specific antigen. Clin Chem *41*, 480-481.

Cheah, B.C., Vucic, S., Krishnan, A.V., Boland, R.A., and Kiernan, M.C. (2011). Neurophysiological index as a biomarker for ALS progression: validity of mixed effects models. Amyotroph Lateral Scler *12*, 33-38.

Chen, H.J., Anagnostou, G., Chai, A., Withers, J., Morris, A., Adhikaree, J., Pennetta, G., and de Belleroche, J.S. (2010). Characterization of the properties of a novel mutation in VAPB in familial amyotrophic lateral sclerosis. J Biol Chem *285*, 40266-40281.

Chen, Y., Zeng, Y., Huang, R., Yang, Y., Chen, K., Song, W., Zhao, B., Li, J., Yuan, L., and Shang, H.F. (2012). No association of five candidate genetic variants with amyotrophic lateral sclerosis in a Chinese population. Neurobiol Aging *33*, 2721 e2723-2725.

Chen, Y.Z., Bennett, C.L., Huynh, H.M., Blair, I.P., Puls, I., Irobi, J., Dierick, I., Abel, A., Kennerson, M.L., Rabin, B.A*., et al.* (2004). DNA/RNA helicase gene mutations in a form of juvenile amyotrophic lateral sclerosis (ALS4). Am J Hum Genet *74*, 1128-1135.

Chen, Z., and Ma, L. (2010). Grey matter volume changes over the whole brain in amyotrophic lateral sclerosis: A voxel-wise meta-analysis of voxel based morphometry studies. Amyotroph Lateral Scler *11*, 549-554.

Chin, T.K., Eagles, P.A., and Maggs, A. (1983). The proteolytic digestion of ox neurofilaments with trypsin and alpha-chumotrypsin. Biochem J *215*, 239-252.

Chio, A., Calvo, A., Moglia, C., Mazzini, L., and Mora, G. (2011a). Phenotypic heterogeneity of amyotrophic lateral sclerosis: a population based study. J Neurol Neurosurg Psychiatry *82*, 740-746.

Chio, A., Canosa, A., Gallo, S., Cammarosano, S., Moglia, C., Fuda, G., Calvo, A., and Mora, G. (2011b). ALS clinical trials: do enrolled patients accurately represent the ALS population? Neurology *77*, 1432-1437.

Chio, A., Logroscino, G., Hardiman, O., Swingler, R., Mitchell, D., Beghi, E., and Traynor, B.G. (2009). Prognostic factors in ALS: A critical review. Amyotroph Lateral Scler *10*, 310-323.

Chiu, I.M., Chen, A., Zheng, Y., Kosaras, B., Tsiftsoglou, S.A., Vartanian, T.K., Brown, R.H., Jr., and Carroll, M.C. (2008). T lymphocytes potentiate endogenous neuroprotective inflammation in a mouse model of ALS. Proc Natl Acad Sci U S A *105*, 17913-17918.

Choi, K., Ni, L., and Jonakait, G.M. (2011). Fas ligation and tumor necrosis factor alpha activation of murine astrocytes promote heat shock factor-1 activation and heat shock protein expression leading to chemokine induction and cell survival. J Neurochem *116*, 438-448.

Chow, C.Y., Landers, J.E., Bergren, S.K., Sapp, P.C., Grant, A.E., Jones, J.M., Everett, L., Lenk, G.M., McKenna-Yasek, D.M., Weisman, L.S.*, et al.* (2009). Deleterious variants of FIG4, a phosphoinositide phosphatase, in patients with ALS. Am J Hum Genet *84*, 85-88.

Ciccarelli, O., Catani, M., Johansen-Berg, H., Clark, C., and Thompson, A. (2008). Diffusion-based tractography in neurological disorders: concepts, applications, and future developments. Lancet Neurol *7*, 715-727.

Clement, A.M., Nguyen, M.D., Roberts, E.A., Garcia, M.L., Boillee, S., Rule, M., McMahon, A.P., Doucette, W., Siwek, D., Ferrante, R.J.*, et al.* (2003). Wild-type nonneuronal cells extend survival of SOD1 mutant motor neurons in ALS mice. Science *302*, 113-117.

Cohlberg, J.A., Hajarian, H., Tran, T., Alipourjeddi, P., and Noveen, A. (1995). Neurofilament protein heterotetramers as assembly intermediates. J Biol Chem *270*, 9334-9339.

Constantinescu, R., Zetterberg, H., Holmberg, B., and Rosengren, L. (2009). Levels of brain related proteins in cerebrospinal fluid: an aid in the differential diagnosis of parkinsonian disorders. Parkinsonism & related disorders *15*, 205-212.

Cooper-Knock, J., Hewitt, C., Highley, J.R., Brockington, A., Milano, A., Man, S., Martindale, J., Hartley, J., Walsh, T., Gelsthorpe, C.*, et al.* (2012a). Clinico-pathological features in amyotrophic lateral sclerosis with expansions in C9ORF72. Brain *135*, 751-764.

Cooper-Knock, J., Kirby, J., Ferraiuolo, L., Heath, P.R., Rattray, M., and Shaw, P.J. (2012b). Gene expression profiling in human neurodegenerative disease. Nat Rev Neurol *8*, 518-530.

Corcia, P., Mayeux-Portas, V., Khoris, J., de Toffol, B., Autret, A., Muh, J.P., Camu, W., and Andres, C. (2002). Abnormal SMN1 gene copy number is a susceptibility factor for amyotrophic lateral sclerosis. Ann Neurol *51*, 243-246.

Corrado, L., Carlomagno, Y., Falasco, L., Mellone, S., Godi, M., Cova, E., Cereda, C., Testa, L., Mazzini, L., and D'Alfonso, S. (2011). A novel peripherin gene (PRPH) mutation identified in one sporadic amyotrophic lateral sclerosis patient. Neurobiol Aging *32*, 552 e551-556.

Cote, F., Collard, J.F., and Julien, J.P. (1993). Progressive neuronopathy in transgenic mice expressing the human neurofilament heavy gene: a mouse model of amyotrophic lateral sclerosis. Cell *73*, 35-46.

Couillard-Despres, S., Zhu, Q., Wong, P.C., Price, D.L., Cleveland, D.W., and Julien J.P. (1998). Protective effect of nuerofilament heavy gene overexpression in motor neuron disease induced by mutant superoxide dismutase. Proc Natl Acad Sci U S A 95, 9626-9630.

Couratier, P., Yi, F.H., Preud'homme, J.L., Clavelou, P., White, A., Sindou, P., Vallat, J.M., and Jauberteau, M.O. (1998). Serum autoantibodies to neurofilament proteins in sporadic amyotrophic lateral sclerosis. J Neurol Sci *154*, 137-145.

Crawley, J.N. (2008). Behavioral phenotyping strategies for mutant mice. Neuron *57*, 809-818.

Crul, T., Toth, N., Piotto, S., Literati-Nagy, P., Tory, K., Haldimann, P., Kalmar, B., Greensmith, L., Torok, Z., Balogh, G.*, et al.* (2013). Hydroximic acid derivatives: pleiotropic hsp co-inducers restoring homeostasis and robustness. Curr Pharm Des *19*, 309-346.

Cudkowicz, M., Bozik, M.E., Ingersoll, E.W., Miller, R., Mitsumoto, H., Shefner, J., Moore, D.H., Schoenfeld, D., Mather, J.L., Archibald, D.*, et al.* (2011). The effects of dexpramipexole (KNS-760704) in individuals with amyotrophic lateral sclerosis. Nat Med *17*, 1652-1656.

Cudkowicz, M., Qureshi, M., and Shefner, J. (2004). Measures and markers in amyotrophic lateral sclerosis. NeuroRx *1*, 273-283.

Cudkowicz, M.E., Katz, J., Moore, D.H., O'Neill, G., Glass, J.D., Mitsumoto, H., Appel, S., Ravina, B., Kieburtz, K., Shoulson, I.*, et al.* (2010). Toward more efficient clinical trials for amyotrophic lateral sclerosis. Amyotroph Lateral Scler *11*, 259-265.

Cudkowicz, M.E., Shefner, J.M., Schoenfeld, D.A., Brown, R.H., Jr., Johnson, H., Qureshi, M., Jacobs, M., Rothstein, J.D., Appel, S.H., Pascuzzi, R.M.*, et al.* (2003). A randomized, placebo-controlled trial of topiramate in amyotrophic lateral sclerosis. Neurology *61*, 456-464.

Cudkowicz, M.E., Shefner, J.M., Simpson, E., Grasso, D., Yu, H., Zhang, H., Shui, A., Schoenfeld, D., Brown, R.H., Wieland, S.*, et al.* (2008). Arimoclomol at dosages up to 300 mg/day is well tolerated and safe in amyotrophic lateral sclerosis. Muscle Nerve *38*, 837-844.

Dangond, F., Hwang, D., Camelo, S., Pasinelli, P., Frosch, M.P., Stephanopoulos, G., Brown, R.H., Jr., and Gullans, S.R. (2004). Molecular signature of late-stage human ALS revealed by expression profiling of postmortem spinal cord gray matter. Physiol Genomics *16*, 229-239.

Daoud, H., Valdmanis, P.N., Dion, P.A., and Rouleau, G.A. (2010). Analysis of DPP6 and FGGY as candidate genes for amyotrophic lateral sclerosis. Amyotroph Lateral Scler *11*, 389-391.

de Carvalho, M., Evangelista, T., and Sales-Luis, M.L. (2002). The corticomotor threshold is not dependent on disease duration in amyotrophic lateral sclerosis (ALS). Amyotroph Lateral Scler *3*, 39-42.

de Carvalho, M., Scotto, M., Lopes, A., and Swash, M. (2003a). Clinical and neurophysiological evaluation of progression in amyotrophic lateral sclerosis. Muscle Nerve *28*, 630-633.

de Carvalho, M., Scotto, M., Lopes, A., and Swash, M. (2005). Quantitating progression in ALS. Neurology *64*, 1783-1785.

de Carvalho, M., and Swash, M. (2000). Nerve conduction studies in amyotrophic lateral sclerosis. Muscle Nerve *23*, 344-352.

de Carvalho, M., Turkman, A., and Swash, M. (2003b). Motor responses evoked by transcranial magnetic stimulation and peripheral nerve stimulation in the ulnar innervation in amyotrophic lateral sclerosis: the effect of upper and lower motor neuron lesion. J Neurol Sci *210*, 83-90.

de Jong, D., Jansen, R.W., Pijnenburg, Y.A., van Geel, W.J., Borm, G.F., Kremer, H.P., and Verbeek, M.M. (2007). CSF neurofilament proteins in the differential diagnosis of dementia. J Neurol Neurosurg Psychiatry *78*, 936-938.

DeJesus-Hernandez, M., Mackenzie, I.R., Boeve, B.F., Boxer, A.L., Baker, M., Rutherford, N.J., Nicholson, A.M., Finch, N.A., Flynn, H., Adamson, J.*, et al.* (2011). Expanded GGGGCC hexanucleotide repeat in noncoding region of C9ORF72 causes chromosome 9p-linked FTD and ALS. Neuron *72*, 245-256.

Delisle, M.B. and Carpenter, S. (1984). Neurofibrillary axonal swellings and smyotrophic lateral sclerosis. J Neurol Sci *63,* 241-250.

Deng, H.X., Chen, W., Hong, S.T., Boycott, K.M., Gorrie, G.H., Siddique, N., Yang, Y., Fecto, F., Shi, Y., Zhai, H.*, et al.* (2011). Mutations in UBQLN2 cause dominant X-linked juvenile and adult-onset ALS and ALS/dementia. Nature *477*, 211-215.

Devos, D., Moreau, C., Lassalle, P., Perez, T., De Seze, J., Brunaud-Danel, V., Destee, A., Tonnel, A.B., and Just, N. (2004). Low levels of the vascular endothelial growth factor in CSF from early ALS patients. Neurology *62*, 2127-2129.

Dewey, C.M., Cenik, B., Sephton, C.F., Johnson, B.A., Herz, J., and Yu, G. (2012). TDP-43 aggregation in neurodegeneration: are stress granules the key? Brain Res *1462*, 16-25.

Dormann, D., Rodde, R., Edbauer, D., Bentmann, E., Fischer, I., Hruscha, A., Than, M.E., Mackenzie, I.R., Capell, A., Schmid, B.*, et al.* (2010). ALS-associated fused in sarcoma (FUS) mutations disrupt Transportin-mediated nuclear import. EMBO J *29*, 2841-2857.

Dunckley, T., Huentelman, M.J., Craig, D.W., Pearson, J.V., Szelinger, S., Joshipura, K., Halperin, R.F., Stamper, C., Jensen, K.R., Letizia, D.*, et al.* (2007). Whole-genome analysis of sporadic amyotrophic lateral sclerosis. N Engl J Med *357*, 775-788.

Dupre, N., and Valdmanis, P. (2009). Genome-wide association studies in amyotrophic lateral sclerosis. Eur J Hum Genet *17*, 137-138.

Dupuis, L., Gonzalez de Aguilar, J.L., di Scala, F., Rene, F., de Tapia, M., Pradat, P.F., Lacomblez, L., Seihlan, D., Prinjha, R., Walsh, F.S.*, et al.* (2002). Nogo provides a molecular marker for diagnosis of amyotrophic lateral sclerosis. Neurobiol Dis *10*, 358-365.

Dupuis, L., Pradat, P.F., Ludolph, A.C., and Loeffler, J.P. (2011). Energy metabolism in amyotrophic lateral sclerosis. Lancet Neurol *10*, 75-82.

Ehlers, M.D., Fung, E.T., O'Brien, R.J., and Huganir, R.L. (1998). Splice variant-specific interaction of the NMSA receptro subunit NR1 with neuronal intermediate filaments. J Neurosci *18*, 720-730.

Eisen, A., and Swash, M. (2001). Clinical neurophysiology of ALS. Clin Neurophysiol *112*, 2190-2201.

Eisen, A., and Weber, M. (2000). Neurophysiological evaluation of cortical function in the early diagnosis of ALS. Amyotroph Lateral Scler *1(S1)*, S47-51.

Elamin, M., Phukan, J., Bede, P., Jordan, N., Byrne, S., Pender, N., and Hardiman, O. (2011). Executive dysfunction is a negative prognostic indicator in patients with ALS without dementia. Neurology *76*, 1263-1269.

Ellis, C.M., Simmons, A., Jones, D.K., Bland, J., Dawson, J.M., Horsfield, M.A., Williams, S.C., and Leigh, P.N. (1999). Diffusion tensor MRI assesses corticospinal tract damage in ALS. Neurology *53*, 1051-1058.

Eyer, J. Cleveland, D.W., Wong, P.C., and Peterson, A.C. (1998). Pathogenesis of two axonopathies does not require axonal neurofilments. Nature *391*, 584-587.

Ezzi, S.A., Urushitani, M., and Julien, J.P. (2007). Wild-type superoxide dismutase acquires binding and toxic properties of ALS-linked mutant forms through oxidation. J Neurochem *102*, 170-178.

Farina, C., Aloisi, F., and Meinl, E. (2007). Astrocytes are active players in cerebral innate immunity. Trends Immunol *28*, 138-145.

Feinstein, A.R. (1987). Clinimetric perspectives. J Chronic Dis *40*, 635-640.

Felice, K.J. (1997). A longitudinal study comparing thenar motor unit number estimates to other quantitative tests in patients with amyotrophic lateral sclerosis. Muscle Nerve *20*, 179-185.

Fernandez-Santiago, R., Sharma, M., Berg, D., Illig, T., Anneser, J., Meyer, T., Ludolph, A., and Gasser, T. (2011). No evidence of association of FLJ10986 and ITPR2 with ALS in a large German cohort. Neurobiol Aging *32*, 551.e1-4.

Ferraiuolo, L., Kirby, J., Grierson, A.J., Sendtner, M., and Shaw, P.J. (2011). Molecular pathways of motor neuron injury in amyotrophic lateral sclerosis. Nat Rev Neurol *7*, 616-630.

Ferreira-Gonzalez, I., Permanyer-Miralda, G., Busse, J.W., Bryant, D.M., Montori, V.M., Alonso-Coello, P., Walter, S.D., and Guyatt, G.H. (2007). Methodologic discussions for using and interpreting composite endpoints are limited, but still identify major concerns. J Clin Epidemiol *60*, 651-657; discussion 658-662.

Fialova, L., Bartos, A., Svarcova, J., Zimova, D., and Kotoucova, J. (2013). Serum and cerebrospinal fluid heavy neurofilaments and antibodies against them in early multiple sclerosis. J Neuroimmunol *259*, 81-87.

Fialova, L., Svarcova, J., Bartos, A., Ridzon, P., Malbohan, I., Keller, O., and Rusina, R. (2010). Cerebrospinal fluid and serum antibodies against neurofilaments in patients with amyotrophic lateral sclerosis. Eur J Neurol *17*, 562-566.

Figlewicz, D.A., Krizus, A., Martinoli, M.G., Meininger, V., Dib, M., Rouleau, G.A., and Julien, J.P. (1994). Variants of the heavy neurofilament subunit are associated with the development of amyotrophic lateral sclerosis. Hum Mol Genet *3*, 1757-1761.

Filippini, N., Douaud, G., Mackay, C.E., Knight, S., Talbot, K., and Turner, M.R. (2010). Corpus callosum involvement is a consistent feature of amyotrophic lateral sclerosis. Neurology *75*, 1645-1652.

Fischer, L.R., Culver, D.G., Tennant, P., Davis, A.A., Wang, M., Castellano-Sanchez, A., Khan, J., Polak, M.A., and Glass, J.D. (2004). Amyotrophic lateral sclerosis is a distal axonopathy: evidence in mice and man. Exp Neurol *185*, 232-240.

Fogh, I., D'Alfonso, S., Gellera, C., Ratti, A., Cereda, C., Penco, S., Corrado, L., Soraru, G., Castellotti, B., Tiloca, C.*, et al.* (2011). No association of DPP6 with amyotrophic lateral sclerosis in an Italian population. Neurobiol Aging *32*, 966-967.

Franchignoni, F., Mora, G., Giordano, A., Volanti, P., and Chio, A. (2013). Evidence of multidimensionality in the ALSFRS-R Scale: a critical appraisal on its measurement properties using Rasch analysis. J Neurol Neurosurg Psychiatry. Epub ahead of print. PMID: 23516308.

Frey, D., Schneider, C., Xu, L., Borg, J., Spooren, W., and Caroni, P. (2000). Early and selective loss of neuromuscular synapse subtypes with low sprouting competence in motoneuron diseases. J Neurosci *20*, 2534-2542.

Frieze, T.W., Mong, D.P., and Koops, M.K. (2002). "Hook effect" in prolactinomas: case report and review of literature. Endocr Pract *8*, 296-303.

Furuya, Y., Cho, S., Ohta, S., Sato, N., Kotake, T., and Masai, M. (2001). High dose hook effect in serum total and free prostate specific antigen in a patient with metastatic prostate cancer. J Urol *166*, 213.

Gal, J., Zhang, J., Kwinter, D.M., Zhai, J., Jia, H., Jia, J., and Zhu, H. (2011). Nuclear localization sequence of FUS and induction of stress granules by ALS mutants. Neurobiol Aging *32*, 2323 e2327-2340.

Ganesalingam, J., An, J., Bowser, R., Andersen, P.M., and Shaw, C.E. (2013). pNfH is a promising biomarker for ALS. Amyotroph Lateral Scler Frontotemporal Degener *14*, 146-149.

Ganesalingam, J., An, J., Shaw, C.E., Shaw, G., Lacomis, D., and Bowser, R. (2011). Combination of neurofilament heavy chain and complement C3 as CSF biomarkers for ALS. J Neurochem *117*, 528-537.

Ganesalingam, J., and Bowser, R. (2010). The application of biomarkers in clinical trials for motor neuron disease. Biomark Med *4*, 281-297.

Giess, R., Beck, M., Goetz, R., Nitsch, R.M., Toyka, K.V., and Sendtner, M. (2000). Potential role of LIF as a modifier gene in the pathogenesis of amyotrophic lateral sclerosis. Neurology *54*, 1003-1005.

Giess, R., Holtmann, B., Braga, M., Grimm, T., Muller-Myhsok, B., Toyka, K.V., and Sendtner, M. (2002). Early onset of severe familial amyotrophic lateral sclerosis with a SOD-1 mutation: potential impact of CNTF as a candidate modifier gene. Am J Hum Genet *70*, 1277-1286.

Gifondorwa, D.J., Jimenz-Moreno, R., Hayes, C.D., Rouhani, H., Robinson, M.B., Strupe, J.L., Caress, J., and Milligan, C. (2012). Administration of Recombinant Heat Shock Protein 70 Delays Peripheral Muscle Denervation in the SOD1(G93A) Mouse Model of Amyotrophic Lateral Sclerosis. Neurol Res Int *2012*, 170426.

Glass, J.D., Boulis, N.M., Johe, K., Rutkove, S.B., Federici, T., Polak, M., Kelly, C., and Feldman, E.L. (2012). Lumbar intraspinal injection of neural stem cells in patients with amyotrophic lateral sclerosis: results of a phase I trial in 12 patients. Stem Cells *30*, 1144-1151.

Gnanapavan, S., Grant, D., Pryce, G., Jackson, S., Baker, D., and Giovannoni, G. (2012). Neurofilament a biomarker of neurodegeneration in autoimmune encephalomyelitis. Autoimmunity *45*, 298-303.

Goldknopf, I.L., Sheta, E.A., Bryson, J., Folsom, B., Wilson, C., Duty, J., Yen, A.A., and Appel, S.H. (2006). Complement C3c and related protein biomarkers in amyotrophic lateral sclerosis and Parkinson's disease. Biochem Biophys Res Commun *342*, 1034-1039.

Goldstein, M.E., Sternberger, N.H., and Sternberger, L.A. (1987). Phosphorylation protects neurofilaments against proteolysis. J Neuroimmunol *14*, 149-160.

Gordon, T., Tyreman, N., Li, S., Putman, C.T., and Hegedus, J. (2010). Functional over-load saves motor units in the SOD1-G93A transgenic mouse model of amyotrophic lateral sclerosis. Neurobiol Dis *37*, 412-422.

Greenway, M.J., Andersen, P.M., Russ, C., Ennis, S., Cashman, S., Donaghy, C., Patterson, V., Swingler, R., Kieran, D., Prehn, J.*, et al.* (2006). ANG mutations segregate with familial and 'sporadic' amyotrophic lateral sclerosis. Nat Genet *38*, 411-413.

Griffin, J.W. and Watson, D.F. (1988). Axonal transport in neurological disease. Ann Neurol *23*, 3–13.

Groeneveld, G.J., Veldink, J.H., van der Tweel, I., Kalmijn, S., Beijer, C., de Visser, M., Wokke, J.H., Franssen, H., and van den Berg, L.H. (2003). A randomized sequential trial of creatine in amyotrophic lateral sclerosis. Ann Neurol *53*, 437-445.

Gros-Louis, F., Lariviere, R., Gowing, G., Laurent, S., Camu, W., Bouchard, J.P., Meininger, V., Rouleau, G.A., and Julien, J.P. (2004). A frameshift deletion in peripherin gene associated with amyotrophic lateral sclerosis. J Biol Chem *279*, 45951-45956.

Gros-Louis, F., Soucy, G., Lariviere, R., and Julien, J.P. (2010). Intracerebroventricular infusion of monoclonal antibody or its derived Fab fragment against misfolded forms of SOD1 mutant delays mortality in a mouse model of ALS. J Neurochem *113*, 1188-1199.

Guiloff, R.J. (2002). Functional scales in ALS: cons. Amyotroph Lateral Scler *3 (S1)*, S11-12.

Gurney, M.E., Pu, H., Chiu, A.Y., Dal Canto, M.C., Polchow, C.Y., Alexander, D.D., Caliendo, J., Hentati, A., Kwon, Y.W., Deng, H.X.*, et al.* (1994). Motor neuron degeneration in mice that express a human Cu,Zn superoxide dismutase mutation. Science *264*, 1772-1775.

Hadano, S., Hand, C.K., Osuga, H., Yanagisawa, Y., Otomo, A., Devon, R.S., Miyamoto, N., Showguchi-Miyata, J., Okada, Y., Singaraja, R.*, et al.* (2001). A gene encoding a putative GTPase regulator is mutated in familial amyotrophic lateral sclerosis 2. Nat Genet *29*, 166-173.

Hand, C.K., Khoris, J., Salachas, F., Gros-Louis, F., Lopes, A.A., Mayeux-Portas, V., Brewer, C.G., Brown, R.H., Jr., Meininger, V., Camu, W.*, et al.* (2002). A novel locus for familial amyotrophic lateral sclerosis, on chromosome 18q. Am J Hum Genet *70*, 251-256.

Hanisch, U.K., and Kettenmann, H. (2007). Microglia: active sensor and versatile effector cells in the normal and pathologic brain. Nat Neurosci *10*, 1387-1394.

Hardiman, O., van den Berg, L.H., and Kiernan, M.C. (2011). Clinical diagnosis and management of amyotrophic lateral sclerosis. Nat Rev Neurol *7*, 639-649.

Hargitai, J., Lewis, H., Boros, I., Racz, T., Fiser, A., Kurucz, I., Benjamin, I., Vigh, L., Penzes, Z., Csermely, P.*, et al.* (2003). Bimoclomol, a heat shock protein co-inducer,

acts by the prolonged activation of heat shock factor-1. Biochem Biophys Res Commun *307*, 689-695.

Haverkamp, L.J., Appel, V., and Appel, S.H. (1995). Natural history of amyotrophic lateral sclerosis in a database population. Validation of a scoring system and a model for survival prediction. Brain *118*, 707-719.

Hegedus, J., Putman, C.T., and Gordon, T. (2007). Time course of preferential motor unit loss in the SOD1 G93A mouse model of amyotrophic lateral sclerosis. Neurobiol Dis *28*, 154-164.

Henkel, J.S., Beers, D.R., Wen, S., Rivera, A.L., Toennis, K.M., Appel, J.E., Zhao, W., Moore, D.H., Powell, S.Z., and Appel, S.H. (2013). Regulatory T-lymphocytes mediate amyotrophic lateral sclerosis progression and survival. EMBO Mol Med *5*, 64-79.

Henkel, J.S., Beers, D.R., Zhao, W., and Appel, S.H. (2009). Microglia in ALS: the good, the bad, and the resting. J Neuroimmune Pharmacol *4*, 389-398.

Herrmann, D.N. and Griffin, J.W. (2002). Intermediate filaments. A common thread in neuromuscular disorders. Neurology 58, 1141-1143.

Hirano, A., Donnenfeld, H. Sasaki, S., and Nakano, I. (1984). Fine structural observations of neurofilamentous changes in amyotrophic lateral sclerosis patients. J Neuropathol Exp Neurol *43*, 461-470.

Hisanaga, S., and Hirokawa, N. (1990). Molecular architecture of the neurofilament. II. Reassembly process of neurofilament L protein in vitro. J Mol Biol *211*, 871-882.

Hoagland, R.J., Mendoza, M., Armon, C., Barohn, R.J., Bryan, W.W., Goodpasture, J.C., Miller, R.G., Parry, G.J., Petajan, J.H., and Ross, M.A. (1997). Reliability of maximal voluntary isometric contraction testing in a multicenter study of patients with amyotrophic lateral sclerosis. Syntex/Synergen Neuroscience Joint Venture rhCNTF ALS Study Group. Muscle Nerve *20*, 691-695.

Hodges, J.R., Davies, R., Xuereb, J., Kril, J., and Halliday, G. (2003). Survival in frontotemporal dementia. Neurology *61*, 349-354.

Hoffman, P.N., and Lasek, R.J. (1975). The slow component of axonal transport. Identification of major structural polypeptides of the axon and their generality among mammalian neurons. J Cell Biol *66*, 351-366.

Hu, W.T., Seelaar, H., Josephs, K.A., Knopman, D.S., Boeve, B.F., Sorenson, E.J., McCluskey, L., Elman, L., Schelhaas, H.J., Parisi, J.E.*, et al.* (2009). Survival profiles of patients with frontotemporal dementia and motor neuron disease. Arch Neurol *66*, 1359-1364.

Hutton, M., Lendon, C.L., Rizzu, P., Baker, M., Froelich, S., Houlden, H., Pickering-Brown, S., Chakraverty, S., Isaacs, A., Grover, A.*, et al.* (1998). Association of missense and 5'-splice-site mutations in tau with the inherited dementia FTDP-17. Nature *393*, 702-705.

Ilzecka, J. (2004). Cerebrospinal fluid vascular endothelial growth factor in patients with amyotrophic lateral sclerosis. Clin Neurol Neurosurg *106*, 289-293.

Imuta, N., Ogawa, S., Maeda, Y., Kuwabara, K., Hori, O., Ueda, H., Yanagihara, T., and Tohyama, M. (1998). Induction of 72-kDa inducible heat shock protein (HSP72) in cultured rat astrocytes after energy depletion. J Neurochem *70*, 550-557.

Iwasaki, Y., Ikeda, K., Ichikawa, Y., Igarashi, O., and Kinoshita, M. (2002). The diagnostic interval in amyotrophic lateral sclerosis. Clin Neurol Neurosurg *104*, 87-89.

Iwata, N.K., Kwan, J.Y., Danielian, L.E., Butman, J.A., Tovar-Moll, F., Bayat, E., and Floeter, M.K. (2011). White matter alterations differ in primary lateral sclerosis and amyotrophic lateral sclerosis. Brain *134*, 2642-2655.

Jain, S., and Roy, P. (2013). The discovery and analysis of P bodies. In Ten years of progress in GW/P body research, E.K.L. Chan, and M.J. Fritzler, eds. (New York: Springer New York), pp. 23-43

Jassam, N., Jones, C.M., Briscoe, T., and Horner, J.H. (2006). The hook effect: a need for constant vigilance. Ann Clin Biochem *43*, 314-317.

Jelsone-Swain, L.M., Fling, B.W., Seidler, R.D., Hovatter, R., Gruis, K., and Welsh, R.C. (2010). Reduced interhemispheric functional connectivity in the motor cortex during rest in limb-onset amyotrophic lateral sclerosis. Front Syst Neurosci *4*, 158.

Jillapalli, D., and Shefner, J.M. (2004). Single motor unit variability with threshold stimulation in patients with amyotrophic lateral sclerosis and normal subjects. Muscle Nerve *30*, 578-584.

Johnson, B.S., Snead, D., Lee, J.J., McCaffery, J.M., Shorter, J., and Gitler, A.D. (2009). TDP-43 is intrinsically aggregation-prone, and amyotrophic lateral sclerosis-linked mutations accelerate aggregation and increase toxicity. J Biol Chem *284*, 20329-20339.

Johnson, J.O., Mandrioli, J., Benatar, M., Abramzon, Y., Van Deerlin, V.M., Trojanowski, J.Q., Gibbs, J.R., Brunetti, M., Gronka, S., Wuu, J.*, et al.* (2010). Exome sequencing reveals VCP mutations as a cause of familial ALS. Neuron *68*, 857-864.

Johnston, C.A., Stanton, B.R., Turner, M.R., Gray, R., Blunt, A.H., Butt, D., Ampong, M.A., Shaw, C.E., Leigh, P.N., and Al-Chalabi, A. (2006). Amyotrophic lateral sclerosis in an urban setting: a population based study of inner city London. J Neurol *253*, 1642-1643.

Jokic, N., Gonzalez de Aguilar, J.L., Dimou, L., Lin, S., Fergani, A., Ruegg, M.A., Schwab, M.E., Dupuis, L., and Loeffler, J.P. (2006). The neurite outgrowth inhibitor Nogo-A promotes denervation in an amyotrophic lateral sclerosis model. EMBO Rep *7*, 1162-1167.

Julien, J.P. (1999). Neurofilament functions in health and disease. Curr Opin Neurobiol *9*:554–560.

Julien, J.P. and Mushynski, W.E. (1982). Multiple phosphorylation sites in mammaliam neurofilament polypeptides. J. Biol Chem *257*, 10467-10470.

Julien, J.P. and Myshynski, W.E. (1983). The distribution of phosphorylation sites among identified proteolytic fragments of mammaliam neurofilaments. J Biol Chem 258, 4019-4025.

Kabashi, E., Valdmanis, P.N., Dion, P., Spiegelman, D., McConkey, B.J., Vande Velde, C., Bouchard, J.P., Lacomblez, L., Pochigaeva, K., Salachas, F.*, et al.* (2008). TARDBP mutations in individuals with sporadic and familial amyotrophic lateral sclerosis. Nat Genet *40*, 572-574.

Kalmar, B., Burnstock, G., Vrbova, G., Urbanics, R., Csermely, P., and Greensmith, L. (2002). Upregulation of heat shock proteins rescues motoneurones from axotomy-induced cell death in neonatal rats. Exp Neurol *176*, 87-97.

Kalmar, B., Dick, J., and Greensmith, L. (2012a). Treatment with PYM50028 improves neuromuscular function in a mouse model of ALS. Amyotroph Lateral Scler *13*, 64.

Kalmar, B., Edet-Amana, E., and Greensmith, L. (2012b). Treatment with a coinducer of the heat shock response delays muscle denervation in the SOD1-G93A mouse model of amyotrophic lateral sclerosis. Amyotroph Lateral Scler *13*, 378-392.

Kalmar, B., and Greensmith, L. (2008). Heat shock proteins as therapeutic targets in amyotrophic lateral sclerosis. In Heat shock proteins and the brain: Implications for neurodegenerative diseases and neuroprotection, A.A.A Asea, and I.R. Brown, eds. (Springer), pp. 69-107.

Kalmar, B., and Greensmith, L. (2009). Activation of the heat shock response in a primary cellular model of motoneuron neurodegeneration-evidence for neuroprotective and neurotoxic effects. Cell Mol Biol Lett *14*, 319-335.

Kalmar, B., Lu, C.H., and Greensmith, L. (2013). The role of heat shock proteins in Amyotrophic Lateral Sclerosis: The therapeutic potential of Arimoclomol. Pharmacol Ther, doi: 10.1016/j.pharmthera.2013.08.003. [Epub ahead of print]

Kalmar, B., Novoselov, S., Gray, A., Cheetham, M.E., Margulis, B., and Greensmith, L. (2008). Late stage treatment with arimoclomol delays disease progression and prevents protein aggregation in the SOD1 mouse model of ALS. J Neurochem *107*, 339-350.

Kasai, T., Tokuda, T., Ishigami, N., Sasayama, H., Foulds, P., Mitchell, D.J., Mann, D.M., Allsop, D., and Nakagawa, M. (2009). Increased TDP-43 protein in cerebrospinal fluid of patients with amyotrophic lateral sclerosis. Acta Neuropathol *117*, 55-62.

Kaufmann, P., Levy, G., Montes, J., Buchsbaum, R., Barsdorf, A.I., Battista, V., Arbing, R., Gordon, P.H., Mitsumoto, H., Levin, B.*, et al.* (2007). Excellent inter-rater, intra-rater, and telephone-administered reliability of the ALSFRS-R in a multicenter clinical trial. Amyotroph Lateral Scler *8*, 42-46.

Kaufmann, P., Levy, G., Thompson, J.L., Delbene, M.L., Battista, V., Gordon, P.H., Rowland, L.P., Levin, B., and Mitsumoto, H. (2005). The ALSFRSr predicts survival time in an ALS clinic population. Neurology *64*, 38-43.

Keil, C., Prell, T., Peschel, T., Hartung, V., Dengler, R., and Grosskreutz, J. (2012). Longitudinal diffusion tensor imaging in amyotrophic lateral sclerosis. BMC neuroscience *13*, 141.

Kertesz, A., McMonagle, P., Blair, M., Davidson, W., and Munoz, D.G. (2005). The evolution and pathology of frontotemporal dementia. Brain *128*, 1996-2005.

Kieran, D., Kalmar, B., Dick, J.R., Riddoch-Contreras, J., Burnstock, G., and Greensmith, L. (2004). Treatment with arimoclomol, a coinducer of heat shock proteins, delays disease progression in ALS mice. Nat Med *10*, 402-405.

Kieran, D., Sebastia, J., Greenway, M.J., King, M.A., Connaughton, D., Concannon, C.G., Fenner, B., Hardiman, O., and Prehn, J.H. (2008). Control of motoneuron survival by angiogenin. J Neurosci *28*, 14056-14061.

Kiernan, M.C., Vucic, S., Cheah, B.C., Turner, M.R., Eisen, A., Hardiman, O., Burrell, J.R., and Zoing, M.C. (2011). Amyotrophic lateral sclerosis. Lancet *377*, 942-955.

Kim, H.J., Kim, N.C., Wang, Y.D., Scarborough, E.A., Moore, J., Diaz, Z., Maclea, K.S., Freibaum, B., Li, S., Molliex, A.*, et al.* (2013). Mutations in prion-like domains in hnRNPA2B1 and hnRNPA1 cause multisystem proteinopathy and ALS. Nature *495*, 467-473.

Kim, S., Chang, R., Teunissen, C., Gebremichael, Y., and Petzold, A. (2011). Neurofilament stoichiometry simulations during neurodegeneration suggest a remarkable self-sufficient and stable in vivo protein structure. J Neurol Sci *307*, 132-138.

Kimura, F., Fujimura, C., Ishida, S., Nakajima, H., Furutama, D., Uehara, H., Shinoda, K., Sugino, M., and Hanafusa, T. (2006). Progression rate of ALSFRS-R at time of diagnosis predicts survival time in ALS. Neurology *66*, 265-267.

King, O.D., Gitler, A.D., and Shorter, J. (2012). The tip of the iceberg: RNA-binding proteins with prion-like domains in neurodegenerative disease. Brain Res *1462*, 61-80.

Kollewe, K., Mauss, U., Krampfl, K., Petri, S., Dengler, R., and Mohammadi, B. (2008). ALSFRS-R score and its ratio: a useful predictor for ALS-progression. J Neurol Sci *275*, 69-73.

Kong, J. and Xu, Z. (2000). Overexpression of neurofilament subunit NF-L and NF-H extends survival of a mouse model for amyotrophic lateral sclerosis. Neurosci Lett *281*, 72-74.

Kudo, L.C., Parfenova, L., Vi, N., Lau, K., Pomakian, J., Valdmanis, P., Rouleau, G.A., Vinters, H.V., Wiedau-Pazos, M., and Karsten, S.L. (2010). Integrative gene-tissue microarray-based approach for identification of human disease biomarkers: application to amyotrophic lateral sclerosis. Hum Mol Genet *19*, 3233-3253.

Kuhle, J., Lindberg, R.L., Regeniter, A., Mehling, M., Steck, A.J., Kappos, L., and Czaplinski, A. (2009). Increased levels of inflammatory chemokines in amyotrophic lateral sclerosis. Eur J Neurol *16*, 771-774.

Kushkuley, J., Chan, W.K., Lee, S., Eyer, J., Leterrier, J.F., Letournel, F., and Shea, T.B. (2009). Neurofilament cross-bridging competes with kinesin-dependent association of neurofilaments with microtubules. J Cell Sci *122*, 3579-3586.

Kushkuley, J., Metkar, S., Chan, W.K., Lee, S., and Shea, T.B. (2010). Aluminum induces neurofilament aggregation by stabilizing cross-bridging of phosphorylated c-terminal sidearms. Brain Res *1322*, 118-123.

Kwiatkowski, T.J., Jr., Bosco, D.A., Leclerc, A.L., Tamrazian, E., Vanderburg, C.R., Russ, C., Davis, A., Gilchrist, J., Kasarskis, E.J., Munsat, T.*, et al.* (2009). Mutations in the FUS/TLS gene on chromosome 16 cause familial amyotrophic lateral sclerosis. Science *323*, 1205-1208.

Lagier-Tourenne, C., Polymenidou, M., and Cleveland, D.W. (2010). TDP-43 and FUS/TLS: emerging roles in RNA processing and neurodegeneration. Hum Mol Genet *19*, R46-64.

Lagier-Tourenne, C., Polymenidou, M., Hutt, K.R., Vu, A.Q., Baughn, M., Huelga, S.C., Clutario, K.M., Ling, S.C., Liang, T.Y., Mazur, C.*, et al.* (2012). Divergent roles of ALS-linked proteins FUS/TLS and TDP-43 intersect in processing long pre-mRNAs. Nat Neurosci *15*, 1488-1497.

Lakes, G., and Group, A.S. (2003). A comparison of muscle strength testing techniques in amyotrophic lateral sclerosis. Neurology *61*, 1503-1507.

Lambrechts, D., Storkebaum, E., Morimoto, M., Del-Favero, J., Desmet, F., Marklund, S.L., Wyns, S., Thijs, V., Andersson, J., van Marion, I.*, et al.* (2003). VEGF is a modifier of amyotrophic lateral sclerosis in mice and humans and protects motoneurons against ischemic death. Nat Genet *34*, 383-394.

Landers, J.E., Melki, J., Meininger, V., Glass, J.D., van den Berg, L.H., van Es, M.A., Sapp, P.C., van Vught, P.W., McKenna-Yasek, D.M., Blauw, H.M.*, et al.* (2009).

Reduced expression of the Kinesin-Associated Protein 3 (KIFAP3) gene increases survival in sporadic amyotrophic lateral sclerosis. Proc Natl Acad Sci U S A *106*, 9004-9009.

Lange, D.J., Andersen, P.M., Remanan, R., Marklund, S., and Benjamin, D. (2013). Pyrimethamine decreases levels of SOD1 in leukocytes and cerebrospinal fluid of ALS patients: A phase I pilot study. Amyotroph Lateral Scler Frontotemporal Degener *14*, 199-204.

Lanka, V., Wieland, S., Barber, J., and Cudkowicz, M. (2009). Arimoclomol: a potential therapy under development for ALS. Expert Opin Investig Drugs *18*, 1907-1918.

Law, W.J., Cann, K.L., and Hicks, G.G. (2006). TLS, EWS and TAF15: a model for transcriptional integration of gene expression. Brief Funct Genomic Proteomic *5*, 8-14.

Leboeuf, R., Langlois, M.F., Martin, M., Ahnadi, C.E., and Fink, G.D. (2006). "Hook effect" in calcitonin immunoradiometric assay in patients with metastatic medullary thyroid carcinoma: case report and review of the literature. J Clin Endocrinol Metab *91*, 361-364.

Lee, C.D., Song, Y., Peltier, A.C., Jarquin-Valdivia, A.A., and Donofrio, P.D. (2010). Muscle ultrasound quantifies the rate of reduction of muscle thickness in amyotrophic lateral sclerosis. Muscle Nerve *42*, 814-819.

Lee, M.K., Marszalek, J.R., and Cleveland, D.W. (1994). A mutant neurofilament subunit causes massive, selective motor neuron death: implications for the pathogenesis of human motor neuron disease. Neuron *13*, 975-988.

Lee, Y., Morrison, B.M., Li, Y., Lengacher, S., Farah, M.H., Hoffman, P.N., Liu, Y., Tsingalia, A., Jin, L., Zhang, P.W.*, et al.* (2012). Oligodendroglia metabolically support axons and contribute to neurodegeneration. Nature *487*, 443-448.

Leigh, P.N., Swash, M., Iwasaki, Y., Ludolph, A., Meininger, V., Miller, R.G., Mitsumoto, H., Shaw, P., Tashiro, K., and Van Den Berg, L. (2004). Amyotrophic lateral sclerosis: a consensus viewpoint on designing and implementing a clinical trial. Amyotroph Lateral Scler *5*, 84-98.

Lepore, A.C., Rauck, B., Dejea, C., Pardo, A.C., Rao, M.S., Rothstein, J.D., and Maragakis, N.J. (2008). Focal transplantation-based astrocyte replacement is neuroprotective in a model of motor neuron disease. Nat Neurosci *11*, 1294-1301.

Leung, C.L., He, C.Z., Kaufmann, P., Chin, S.S., Naini, A., Liem, R.K., Mitsumoto, H., and Hays, A.P. (2004). A pathogenic peripherin gene mutation in a patient with amyotrophic lateral sclerosis. Brain Pathol *14*, 290-296.

Li, Y.J., Pericak-Vance, M.A., Haines, J.L., Siddique, N., McKenna-Yasek, D., Hung, W.Y., Sapp, P., Allen, C.I., Chen, W., Hosler, B.*, et al.* (2004). Apolipoprotein E is

associated with age at onset of amyotrophic lateral sclerosis. Neurogenetics *5*, 209-213.

Li, Y.R., King, O.D., Shorter, J., and Gitler, A.D. (2013). Stress granules as crucibles of ALS pathogenesis. J Cell Biol *201*, 361-372.

Lillo, P., Garcin, B., Hornberger, M., Bak, T.H., and Hodges, J.R. (2010). Neurobehavioral features in frontotemporal dementia with amyotrophic lateral sclerosis. Arch Neurol *67*, 826-830.

Lindquist, S. (1986). The heat-shock response. Annu Rev Biochem *55*, 1151-1191.

Linseman, D.A., and Loucks, F.A. (2008). Diverse roles of Rho family GTPases in neuronal development, survival, and death. Front Biosci *13*, 657-676.

Liu-Yesucevitz, L., Bilgutay, A., Zhang, Y.J., Vanderweyde, T., Citro, A., Mehta, T., Zaarur, N., McKee, A., Bowser, R., Sherman, M.*, et al.* (2010). Tar DNA binding protein-43 (TDP-43) associates with stress granules: analysis of cultured cells and pathological brain tissue. PLoS ONE *5*, e13250.

Liu, A.Y., Mathur, R., Mei, N., Langhammer, C.G., Babiarz, B., and Firestein, B.L. (2011). Neuroprotective drug riluzole amplifies the heat shock factor 1 (HSF1)- and glutamate transporter 1 (GLT1)-dependent cytoprotective mechanisms for neuronal survival. J Biol Chem *286*, 2785-2794.

Logroscino, G., Traynor, B.J., Hardiman, O., Chio, A., Mitchell, D., Swingler, R.J., Millul, A., Benn, E., and Beghi, E. (2010). Incidence of amyotrophic lateral sclerosis in Europe. J Neurol Neurosurg Psychiatry *81*, 385-390.

Lomen-Hoerth, C., Anderson, T., and Miller, B. (2002). The overlap of amyotrophic lateral sclerosis and frontotemporal dementia. Neurology *59*, 1077-1079.

Lomen-Hoerth, C., Murphy, J., Langmore, S., Kramer, J.H., Olney, R.K., and Miller, B. (2003). Are amyotrophic lateral sclerosis patients cognitively normal? Neurology *60*, 1094-1097.

Lorenzl, S., Albers, D.S., LeWitt, P.A., Chirichigno, J.W., Hilgenberg, S.L., Cudkowicz, M.E., and Beal, M.F. (2003). Tissue inhibitors of matrix metalloproteinases are elevated in cerebrospinal fluid of neurodegenerative diseases. J Neurol Sci *207*, 71-76.

Lu, C.H., Kalmar, B., Malaspina, A., Greensmith, L., and Petzold, A. (2011). A method to solubilise protein aggregates for immunoassay quantification which overcomes the neurofilament "hook" effect. J Neurosci Methods *195*, 143-150.

Lu, C.H., Petzold, A., Kalmar, B., Dick, J., Malaspina, A., and Greensmith, L. (2012). Plasma neurofilament heavy chain levels correlate to markers of late stage disease

progression and treatment response in SOD1^{G93A} mice that model ALS. PLoS ONE *7*.

Lule, D., Ludolph, A.C., and Kassubek, J. (2009). MRI-based functional neuroimaging in ALS: an update. Amyotroph Lateral Scler *10*, 258-268.

Luty, A.A., Kwok, J.B., Dobson-Stone, C., Loy, C.T., Coupland, K.G., Karlstrom, H., Sobow, T., Tchorzewska, J., Maruszak, A., Barcikowska, M.*, et al.* (2010). Sigma nonopioid intracellular receptor 1 mutations cause frontotemporal lobar degeneration-motor neuron disease. Ann Neurol *68*, 639-649.

Mackenzie, I.R., Bigio, E.H., Ince, P.G., Geser, F., Neumann, M., Cairns, N.J., Kwong, L.K., Forman, M.S., Ravits, J., Stewart, H.*, et al.* (2007). Pathological TDP-43 distinguishes sporadic amyotrophic lateral sclerosis from amyotrophic lateral sclerosis with SOD1 mutations. Ann Neurol *61*, 427-434.

Magnus, T., Beck, M., Giess, R., Puls, I., Naumann, M., and Toyka, K.V. (2002). Disease progression in amyotrophic lateral sclerosis: predictors of survival. Muscle Nerve *25*, 709-714.

Majounie, E., Renton, A.E., Mok, K., Dopper, E.G., Waite, A., Rollinson, S., Chio, A., Restagno, G., Nicolaou, N., Simon-Sanchez, J.*, et al.* (2012). Frequency of the C9orf72 hexanucleotide repeat expansion in patients with amyotrophic lateral sclerosis and frontotemporal dementia: a cross-sectional study. Lancet Neurol *11*, 323-330.

Malaspina, A., and de Belleroche, J. (2004). Spinal cord molecular profiling provides a better understanding of amyotrophic lateral sclerosis pathogenesis. Brain Res Brain Res Rev *45*, 213-229.

Malaspina, A., Kaushik, N., and de Belleroche, J. (2001). Differential expression of 14 genes in amyotrophic lateral sclerosis spinal cord detected using gridded cDNA arrays. J Neurochem *77*, 132-145.

Malik, M.N., Fenko, M.D., Iqbal, K., and Wisniewski, H.M. (1983). Purification and characterization of two forms of Ca^{2+}-activated neutral protease from calf brain. J Biol Chem 258, 8955-8962.

Manetto, V., Sternberger, N.H., Perry, G., Sternberger, L.A., and Gambetti, P. (1988). Phosphorylation of neurofilaments is altered in amyotrophic lateral sclerosis. J Neuropathol Exp Neurol *47*, 642-653.

Maruyama, H., Morino, H., Ito, H., Izumi, Y., Kato, H., Watanabe, Y., Kinoshita, Y., Kamada, M., Nodera, H., Suzuki, H.*, et al.* (2010). Mutations of optineurin in amyotrophic lateral sclerosis. Nature *465*, 223-226.

McComas, A.J. (1995). Motor unit estimation: anxieties and achievements. Muscle Nerve *18*, 369-379.

McDonald, K.K., Aulas, A., Destroismaisons, L., Pickles, S., Beleac, E., Camu, W., Rouleau, G.A., and Vande Velde, C. (2011). TAR DNA-binding protein 43 (TDP-43) regulates stress granule dynamics via differential regulation of G3BP and TIA-1. Hum Mol Genet *20*, 1400-1410.

McHanwell, S., and Biscoe, T.J. (1981). The localization of motoneurons supplying the hindlimb muscles of the mouse. Philos Trans R Soc Lond B Biol Sci *293*, 477-508.

Meier, J., Couillard-Despres, S., Jacomy, H., Gravel, C., and Julien, J.P. (1999). Extra neurofilament NF-L subunits rescue motor neuron dsiease cuased by overexpression ot the human NF-H gene in mice. J Neuropathol Exp Neurol *58*, 1099-1110.

Miles, L.E., Lipschitz, D.A., Bieber, C.P., and Cook, J.D. (1974). Measurement of serum ferritin by a 2-site immunoradiometric assay. Anal Biochem *61*, 209-224.

Miller, R.G., Mitchell, J.D., Lyon, M., and Moore, D.H. (2007). Riluzole for amyotrophic lateral sclerosis (ALS)/motor neuron disease (MND). Cochrane Database Syst Rev, CD001447.

Miller, R.G., Moore, D.H., 2nd, Gelinas, D.F., Dronsky, V., Mendoza, M., Barohn, R.J., Bryan, W., Ravits, J., Yuen, E., Neville, H.*, et al.* (2001). Phase III randomized trial of gabapentin in patients with amyotrophic lateral sclerosis. Neurology *56*, 843-848.

Miller, T.M., Pestronk, A., David, W., Rothstein, J., Simpson, E., Appel, S.H., Andres, P.L., Mahoney, K., Allred, P., Alexander, K.*, et al.* (2013). An antisense oligonucleotide against SOD1 delivered intrathecally for patients with SOD1 familial amyotrophic lateral sclerosis: a phase 1, randomised, first-in-man study. Lancet Neurol *12*, 435-442.

Misawa, S., Noto, Y., Shibuya, K., Isose, S., Sekiguchi, Y., Nasu, S., and Kuwabara, S. (2011). Ultrasonographic detection of fasciculations markedly increases diagnostic sensitivity of ALS. Neurology *77*, 1532-1537.

Mitchell, J., Paul, P., Chen, H.J., Morris, A., Payling, M., Falchi, M., Habgood, J., Panoutsou, S., Winkler, S., Tisato, V.*, et al.* (2010). Familial amyotrophic lateral sclerosis is associated with a mutation in D-amino acid oxidase. Proc Natl Acad Sci U S A *107*, 7556-7561.

Mitchell, R.M., Freeman, W.M., Randazzo, W.T., Stephens, H.E., Beard, J.L., Simmons, Z., and Connor, J.R. (2009). A CSF biomarker panel for identification of patients with amyotrophic lateral sclerosis. Neurology *72*, 14-19.

Mohammadi, B., Kollewe, K., Samii, A., Krampfl, K., Dengler, R., and Munte, T.F. (2009). Changes of resting state brain networks in amyotrophic lateral sclerosis. Exp Neurol *217*, 147-153.

Mora, G. (2002). Functional scales: pro. Amyotroph Lateral Scler *3(S1)*, S9-10.

Moreau, C., Devos, D., Brunaud-Danel, V., Defebvre, L., Perez, T., Destee, A., Tonnel, A.B., Lassalle, P., and Just, N. (2005). Elevated IL-6 and TNF-alpha levels in patients with ALS: inflammation or hypoxia? Neurology *65*, 1958-1960.

Moreau, C., Devos, D., Brunaud-Danel, V., Defebvre, L., Perez, T., Destee, A., Tonnel, A.B., Lassalle, P., and Just, N. (2006). Paradoxical response of VEGF expression to hypoxia in CSF of patients with ALS. J Neurol Neurosurg Psychiatry *77*, 255-257.

Morita, M., Al-Chalabi, A., Andersen, P.M., Hosler, B., Sapp, P., Englund, E., Mitchell, J.E., Habgood, J.J., de Belleroche, J., Xi, J.*, et al.* (2006). A locus on chromosome 9p confers susceptibility to ALS and frontotemporal dementia. Neurology *66*, 839-844.

Mougeot, J.L., Li, Z., Price, A.E., Wright, F.A., and Brooks, B.R. (2011). Microarray analysis of peripheral blood lymphocytes from ALS patients and the SAFE detection of the KEGG ALS pathway. BMC Med Genomics *4*, 74.

Muller, H.P., Unrath, A., Huppertz, H.J., Ludolph, A.C., and Kassubek, J. (2012). Neuroanatomical patterns of cerebral white matter involvement in different motor neuron diseases as studied by diffusion tensor imaging analysis. Amyotroph Lateral Scler *13*, 254-264.

Munch, C., Sedlmeier, R., Meyer, T., Homberg, V., Sperfeld, A.D., Kurt, A., Prudlo, J., Peraus, G., Hanemann, C.O., Stumm, G.*, et al.* (2004). Point mutations of the p150 subunit of dynactin (DCTN1) gene in ALS. Neurology *63*, 724-726.

Munoz, D.G., Greene, C., Perl, D.P., Selkoe, D.J. (1988). Accumulation of phosphorylated neurofilaments in anterior horn motoneurons of amyotrophic lateral slcerosis patients. J. Neuropathol Exp Neruol *47*, 9-18.

MuscularDystrophyCampaign. Clinical trial of ACE-031 for Duchenne suspended. Access date: 17/04/2013 http://www.muscular-ystrophy.org/research/news/3862_clinical_trial_of_ace-031_for_duchenne_suspended

NCT00349622. Clinical Trial Ceftriaxone in Subjects With Amyotrophic Lateral Sclerosis (ALS). Access date: 16/04/2013 http://www.clinicaltrials.gov/ct2/show/NCT00349622

NCT00420719. Multi-Center Pivotal Study of Motor-Point Stimulation for Conditioning the Diaphragm of Patients With Amyotrophic Lateral Sclerosis (ALS). Access date: 16/04/2013 http://clinicaltrials.gov/ct2/show/NCT00420719?term=NCT00420719&rank=1

NCT00647296. A 2-Part, Randomized, Double-Blind, Safety and Tolerability Study Evaluating KNS-760704 in Patients With Amyotrophic Lateral Sclerosis (ALS). Access date: 16/04/2013 http://www.clinicaltrials.gov/ct2/show/NCT00647296?term=dexpramipexole+%28KNS-760704%29&rank=2

NCT00706147. Phase II/III Randomized, Placebo-controlled Trial of Arimoclomol in SOD1 Positive Familial Amyotrophic Lateral Sclerosis. Access date: 16/04/2013 http://clinicaltrials.gov/show/NCT00706147

NCT00748501. A Phase 2 Repeat-Dosing Clinical Trial of SB-509 in Subjects With Amyotrophic Lateral Sclerosis. Access date: 16/04/2013 http://www.clinicaltrials.gov/ct2/show/NCT00748501?term=SB-509&rank=1

NCT00800501. A Double-blind, Randomised, Parallel Group Safety and Tolerability Study of Intracerebroventricular Administration of sNN0029 to Patients With Amyotrophic Lateral Sclerosis, Using an Implanted Catheter and SynchroMed® II Pump. Access date" 16/04/2013 http://www.clinicaltrials.gov/ct2/show/NCT00800501?term=sNN0029&rank=2

NCT00801333. Derivation of Induced Pluripotent Stem Cells From an Existing Collection of Human Somatic Cells. Access date: 16/04/2013 http://clinicaltrials.gov/ct2/show/NCT00801333?term=iPS+cells+in+ALS&rank=1

NCT00868166. Phase II/III, Multicenter, Randomized, Parallel Group, Double-blind, Placebo Controlled Study to Assess Safety and Efficacy of TRO19622 in Amyotrophic Lateral Sclerosis (ALS) Patients Treated With Riluzole. Access date: 16/04/2013 http://www.clinicaltrials.gov/ct2/show/NCT00868166?term=NCT00868166&rank=1

NCT00931944. An Open-Label, Safety and Tolerability, Study Evaluating KNS-760704 in Patients With Amyotrophic Lateral Sclerosis. Access date: 16/04/2013 http://www.clinicaltrials.gov/ct2/show/NCT00931944?term=dexpramipexole+%28KNS-760704%29&rank=5

NCT00952887. A Randomized, Double-Blind, Placebo-Controlled, Multiple-Dose, Dose-Escalation Study to Evaluate the Safety, Tolerability, Pharmacokinetic and Pharmacodynamic Effects of ACE-031 (ActRIIB-IgG1) in Healthy Postmenopausal Women. Access date: 17/04/2013 http://clinicaltrials.gov/ct2/show/NCT00952887?term=ACE-031&rank=1

NCT01041222. A Phase 1, Double-Blind, Placebo-Controlled, Dose-Escalation Study of the Safety, Tolerability, and Pharmacokinetics of ISIS 333611 Administered Intrathecally to Patients With Familial Amyotrophic Lateral Sclerosis Due to Superoxide Dismutase 1 Gene Mutations. Access date: 16/04/2013 http://www.clinicaltrials.gov/ct2/show/NCT01041222?term=SOD1Rx&rank=1

NCT01083667. Phase I/II Study of SOD1 Inhibition by Pyrimethamine in Familial ALS. Access date: 17/04/2013 http://clinicaltrials.gov/show/NCT01083667

NCT01091142. Single-Ascending-Dose Safety and Tolerability Study of NP001 in Subjects With Amyotrophic Lateral Sclerosis. Access date: 16/04/2013 http://www.clinicaltrials.gov/ct2/show/NCT01091142?term=NP001&rank=1

NCT01099761. A Randomized, Double-Blind, Placebo-Controlled, Multiple Ascending-Dose Study to Evaluate the Safety, Tolerability, Pharmacokinetics, and Pharmacodynamics of ACE-031 (ActRIIB-IgG1) in Subjects With Duchenne Muscular Dystrophy. Access date: 17/04/2013 http://clinicaltrials.gov/ct2/show/NCT01099761?term=ACE-031&rank=2

NCT01281189. A Randomized, Double-Blind, Placebo-Controlled, Multi-Center Study of the Safety and Efficacy of Dexpramipexole in Subjects With Amyotrophic Lateral Sclerosis. Access date: 16/04/2013 http://www.clinicaltrials.gov/ct2/show/NCT01281189?term=NCT01281189&rank=1

NCT01281631. A Phase 2 Randomized, Double-Blind, Placebo-Controlled, Multicenter Study of NP001 in Subjects With Amyotrophic Lateral Sclerosis. Access date: 16/04/2013 http://www.clinicaltrials.gov/ct2/show/NCT01281631?term=NP001&rank=2

NCT01348451. A Phase I, Open-label, First in Human, Feasibility and Safety Study of Human Spinal Cord Derived Neural Stem Cell Transplantation for the Treatment of Amyotrophic Lateral Sclerosis. Access date: 16/04/2013 http://clinicaltrials.gov/ct2/show/NCT01348451?term=Neuralstem&rank=4

NCT01384162. An Open Label, Safety and Tolerability Continuation Study of Intracerebroventricular Administration of sNN0029 to Patients With Amyotrophic Lateral Sclerosis, Using an Implanted Catheter and SynchroMed® II Pump. Access date: 16/04/2013 http://www.clinicaltrials.gov/ct2/show/NCT01384162?term=sNN0029&rank=1

NCT01605006. Humanitarian Device Exemption Post-Approval Study of NeuRx Diaphragm Pacing System for Amyotrophic Lateral Sclerosis. Access date: 16/04/2013 http://clinicaltrials.gov/ct2/show/NCT01605006?term=NeuRX+DPS&rank=1

NCT01639391. Creation of a Bank of Fibroblast From Patients With Amyotrophic Lateral Sclerosis: Pilot Study. Access date: 16/04/2013 http://clinicaltrials.gov/ct2/show/NCT01639391?term=iPS+cells+in+ALS&rank=2

NCT01709149. A Phase IIb, Multi-National, Double-Blind, Randomized, Placebo-Controlled Study to Evaluate the Safety, Tolerability and Efficacy of CK-2017357 in Patients With Amyotrophic Lateral Sclerosis (ALS) (BENEFIT-ALS). Access date:

17/04/2013 http://clinicaltrials.gov/ct2/show/NCT01709149?term=CK-2017357&rank=6

NCT01753076. Study NOG112264, a Phase II Study of Ozanezumab (GSK1223249) Versus Placebo in the Treatment of Amyotrophic Lateral Sclerosis. Access date: 17/04/2013 http://clinicaltrials.gov/ct2/show/NCT01753076?term=GSK-1223249&rank=4

Neary, D., Snowden, J.S., Gustafson, L., Passant, U., Stuss, D., Black, S., Freedman, M., Kertesz, A., Robert, P.H., Albert, M.*, et al.* (1998). Frontotemporal lobar degeneration: a consensus on clinical diagnostic criteria. Neurology *51*, 1546-1554.

Neary, D., Snowden, J.S., and Mann, D.M. (2000). Cognitive change in motor neurone disease/amyotrophic lateral sclerosis (MND/ALS). J Neurol Sci *180*, 15-20.

Neumann, M., Rademakers, R., Roeber, S., Baker, M., Kretzschmar, H.A., and Mackenzie, I.R. (2009). A new subtype of frontotemporal lobar degeneration with FUS pathology. Brain *132*, 2922-2931.

Neumann, M., Sampathu, D.M., Kwong, L.K., Truax, A.C., Micsenyi, M.C., Chou, T.T., Bruce, J., Schuck, T., Grossman, M., Clark, C.M.*, et al.* (2006). Ubiquitinated TDP-43 in frontotemporal lobar degeneration and amyotrophic lateral sclerosis. Science *314*, 130-133.

Nguyen, M.D., Lariviere, R.C., and Julien, J.P. (2001). Deregulation of Cdk5 in a mouse model of ALS: toxicity alleviated by perikaryal neurofilament inclusions. Neuron *30*, 135-147.

Niebroj-Dobosz, I., Janik, P., Sokolowska, B., and Kwiecinski, H. (2010). Matrix metalloproteinases and their tissue inhibitors in serum and cerebrospinal fluid of patients with amyotrophic lateral sclerosis. Eur J Neurol *17*, 226-231.

Nirmalananthan, N., and Greensmith, L. (2005). Amyotrophic lateral sclerosis: recent advances and future therapies. Curr Opin Neurol *18*, 712-719.

Nishimura, A.L., Mitne-Neto, M., Silva, H.C., Richieri-Costa, A., Middleton, S., Cascio, D., Kok, F., Oliveira, J.R., Gillingwater, T., Webb, J.*, et al.* (2004). A mutation in the vesicle-trafficking protein VAPB causes late-onset spinal muscular atrophy and amyotrophic lateral sclerosis. Am J Hum Genet *75*, 822-831.

Nixon, R.A. (1993). The regulation of neurofilament protein dynamics by phosphorylation—clues to neurofibrillary pathoiology. Brian Pathol *3*, 29-38.

Norgren, N., Rosengren, L., and Stigbrand, T. (2003). Elevated neurofilament levels in neurological diseases. Brain Res *987*, 25-31.

Noto, Y., Shibuya, K., Sato, Y., Kanai, K., Misawa, S., Sawai, S., Mori, M., Uchiyama, T., Isose, S., Nasu, S.*, et al.* (2011). Elevated CSF TDP-43 levels in amyotrophic lateral sclerosis: specificity, sensitivity, and a possible prognostic value. Amyotroph Lateral Scler *12*, 140-143.

Nygren, I., Larsson, A., Johansson, A., and Askmark, H. (2002). VEGF is increased in serum but not in spinal cord from patients with amyotrophic lateral sclerosis. Neuroreport *13*, 2199-2201.

Okamoto, K., Hirai, S., Amari, M., Watanabe, M., and Sakurai, A. (1993). Bunina bodies in amyotrophic lateral sclerosis immunostained with rabbit anti-cystatin C serum. Neurosci Lett *162*, 125-128.

Okamoto, K., Mizuno, Y., and Fujita, Y. (2008). Bunina bodies in amyotrophic lateral sclerosis. Neuropathology *28*, 109-115.

Onders, R., Katirji, B., So, Y., Katz, J., Miller, R., Newman, D., Simpson, E., Appel, S., Boylan, K., Maragakis, N.*, et al.* (2010). Positive clinical results of diaphragm pacing in ALS/MND with chronic hypoventilation and upper motor neuron respiratory deficits with intact lower motor neuron phrenic motor function. Amyotroph Lateral Scler *11*, 137.

Ono, S., Hu, J., Shimizu, N., Imai, T., and Nakagawa, H. (2001). Increased interleukin-6 of skin and serum in amyotrophic lateral sclerosis. J Neurol Sci *187*, 27-34.

Orlacchio, A., Babalini, C., Borreca, A., Patrono, C., Massa, R., Basaran, S., Munhoz, R.P., Rogaeva, E.A., St George-Hyslop, P.H., Bernardi, G.*, et al.* (2010). SPATACSIN mutations cause autosomal recessive juvenile amyotrophic lateral sclerosis. Brain *133*, 591-598.

Orsetti, V., Pegoraro, E., Cima, V., D'Ascenzo, C., Palmieri, A., Querin, G., Volpe, M., Ermani, M., Angelini, C., and Soraru, G. (2011). Genetic variation in KIFAP3 is associated with an upper motor neuron-predominant phenotype in amyotrophic lateral sclerosis. Neurodegener Dis *8*, 491-495.

Otto, M., Bowser, R., Turner, M., Berry, J., Brettschneider, J., Connor, J., Costa, J., Cudkowicz, M., Glass, J., Jahn, O.*, et al.* (2012). Roadmap and standard operating procedures for biobanking and discovery of neurochemical markers in ALS. Amyotroph Lateral Scler *13*, 1-10.

Pant, H.C. (1988). Dephosphorylation of neurofilament proteins enhances their susceptibility to degradation by calpain. Biochem J *256*, 608-665.

Parker, R., and Sheth, U. (2007). P bodies and the control of mRNA translation and degradation. Mol Cell *25*, 635-646.

Parkinson, N., Ince, P.G., Smith, M.O., Highley, R., Skibinski, G., Andersen, P.M., Morrison, K.E., Pall, H.S., Hardiman, O., Collinge, J.*, et al.* (2006). ALS phenotypes

with mutations in CHMP2B (charged multivesicular body protein 2B). Neurology *67*, 1074-1077.

Pasinetti, G.M., Ungar, L.H., Lange, D.J., Yemul, S., Deng, H., Yuan, X., Brown, R.H., Cudkowicz, M.E., Newhall, K., Peskind, E.*, et al.* (2006). Identification of potential CSF biomarkers in ALS. Neurology *66*, 1218-1222.

Perrot, R., Berges, R., Bocquet, A., and Eyer, J. (2008). Review of the multiple aspects of neurofilament functions, and their possible contribution to neurodegeneration. Mol Neurobiol *38*, 27-65.

Petakov, M.S., Damjanovic, S.S., Nikolic-Durovic, M.M., Dragojlovic, Z.L., Obradovic, S., Gligorovic, M.S., Simic, M.Z., and Popovic, V.P. (1998). Pituitary adenomas secreting large amounts of prolactin may give false low values in immunoradiometric assays. The hook effect. J Endocrinol Invest *21*, 184-188.

Petzold, A. (2005). Neurofilament phosphoforms: surrogate markers for axonal injury, degeneration and loss. J Neurol Sci *233*, 183-198.

Petzold, A., Groves, M., Leis, A.A., Scaravilli, F., and Stokic, D.S. (2010a). Neuronal and glial cerebrospinal fluid protein biomarkers are elevated after West Nile virus infection. Muscle Nerve *41*, 42-49.

Petzold, A., Hinds, N., Murray, N.M., Hirsch, N.P., Grant, D., Keir, G., Thompson, E.J., and Reilly, M.M. (2006a). CSF neurofilament levels: a potential prognostic marker in Guillain-Barre syndrome. Neurology *67*, 1071-1073.

Petzold, A., Keir, G., Green, A.J., Giovannoni, G., and Thompson, E.J. (2003). A specific ELISA for measuring neurofilament heavy chain phosphoforms. J Immunol Methods *278*, 179-190.

Petzold, A., Keir, G., Kay, A., Kerr, M., and Thompson, E.J. (2006b). Axonal damage and outcome in subarachnoid haemorrhage. J Neurol Neurosurg Psychiatry *77*, 753-759.

Petzold, A., Michel, P., Stock, M., and Schluep, M. (2008). Glial and axonal body fluid biomarkers are related to infarct volume, severity, and outcome. J Stroke Cerebrovasc Dis *17*, 196-203.

Petzold, A., Mondria, T., Kuhle, J., Rocca, M.A., Cornelissen, J., te Boekhorst, P., Lowenberg, B., Giovannoni, G., Filippi, M., Kappos, L.*, et al.* (2010b). Evidence for acute neurotoxicity after chemotherapy. Ann Neurol *68*, 806-815.

Petzold, A., Tisdall, M.M., Girbes, A.R., Martinian, L., Thom, M., Kitchen, N., and Smith, M. (2011a). In vivo monitoring of neuronal loss in traumatic brain injury: a microdialysis study. Brain *134*, 464-483.

Petzold, A., Tozer, D.J., and Schmierer, K. (2011b). Axonal damage in the making: neurofilament phosphorylation, proton mobility and magnetisation transfer in multiple sclerosis normal appearing white matter. Exp Neurol *232*, 234-239.

Petzold, A., Verwey, N.A., van Uffelen, K., Blankenstein, M.A., and Teunissen, C. (2010c). Batch prepared protein standards for cerebrospinal fluid (CSF) biomarkers for neurodegeneration. J Neurosci Methods *193*, 296-299.

Pflumm, M. (2012). Meeting Report: ALS/MND 2012: Trials & Tribulations. Access date: 16/04/2013 http://blogs.als.net/post/ALSMND-2012-Clinical-Trials-Tribulations.aspx

Phatnani, H.P., Guarnieri, P., Friedman, B.A., Carrasco, M.A., Muratet, M., O'Keeffe, S., Nwakeze, C., Pauli-Behn, F., Newberry, K.M., Meadows, S.K.*, et al.* (2013). Intricate interplay between astrocytes and motor neurons in ALS. Proc Natl Acad Sci U S A *110*, E756-765.

Philips, T., and Robberecht, W. (2011). Neuroinflammation in amyotrophic lateral sclerosis: role of glial activation in motor neuron disease. Lancet Neurol *10*, 253-263.

Piepers, S., Veldink, J.H., de Jong, S.W., van der Tweel, I., van der Pol, W.L., Uijtendaal, E.V., Schelhaas, H.J., Scheffer, H., de Visser, M., de Jong, J.M.*, et al.* (2009). Randomized sequential trial of valproic acid in amyotrophic lateral sclerosis. Ann Neurol *66*, 227-234.

Pillen, S., Arts, I.M., and Zwarts, M.J. (2008). Muscle ultrasound in neuromuscular disorders. Muscle Nerve *37*, 679-693.

Plikaytis, B.D., Holder, P.F., Pais, L.B., Maslanka, S.E., Gheesling, L.L., and Carlone, G.M. (1994). Determination of parallelism and nonparallelism in bioassay dilution curves. J Clin Microbiol *32*, 2441-2447.

Pohl, C., Block, W., Karitzky, J., Traber, F., Schmidt, S., Grothe, C., Lamerichs, R., Schild, H., and Klockgether, T. (2001). Proton magnetic resonance spectroscopy of the motor cortex in 70 patients with amyotrophic lateral sclerosis. Arch Neurol *58*, 729-735.

Poloni, M., Facchetti, D., Mai, R., Micheli, A., Agnoletti, L., Francolini, G., Mora, G., Camana, C., Mazzini, L., and Bachetti, T. (2000). Circulating levels of tumour necrosis factor-alpha and its soluble receptors are increased in the blood of patients with amyotrophic lateral sclerosis. Neurosci Lett *287*, 211-214.

Polymenidou, M., Lagier-Tourenne, C., Hutt, K.R., Huelga, S.C., Moran, J., Liang, T.Y., Ling, S.C., Sun, E., Wancewicz, E., Mazur, C.*, et al.* (2011). Long pre-mRNA depletion and RNA missplicing contribute to neuronal vulnerability from loss of TDP-43. Nat Neurosci *14*, 459-468.

Pradat, P.F., Dubourg, O., de Tapia, M., di Scala, F., Dupuis, L., Lenglet, T., Bruneteau, G., Salachas, F., Lacomblez, L., Corvol, J.C.*, et al.* (2012). Muscle gene

expression is a marker of amyotrophic lateral sclerosis severity. Neurodegener Dis *9*, 38-52.

Quigley, H., Colloby, S.J., and O'Brien, J.T. (2011). PET imaging of brain amyloid in dementia: a review. Int J Geriatr Psychiatry *26*, 991-999.

Quinones, M.P., and Kaddurah-Daouk, R. (2009). Metabolomics tools for identifying biomarkers for neuropsychiatric diseases. Neurobiol Dis *35*, 165-176.

Ranganathan, S., Williams, E., Ganchev, P., Gopalakrishnan, V., Lacomis, D., Urbinelli, L., Newhall, K., Cudkowicz, M.E., Brown, R.H., Jr., and Bowser, R. (2005). Proteomic profiling of cerebrospinal fluid identifies biomarkers for amyotrophic lateral sclerosis. J Neurochem *95*, 1461-1471.

Ravits, J.M., and La Spada, A.R. (2009). ALS motor phenotype heterogeneity, focality, and spread: deconstructing motor neuron degeneration. Neurology *73*, 805-811.

Renton, A.E., Majounie, E., Waite, A., Simon-Sanchez, J., Rollinson, S., Gibbs, J.R., Schymick, J.C., Laaksovirta, H., van Swieten, J.C., Myllykangas, L.*, et al.* (2011). A hexanucleotide repeat expansion in C9ORF72 is the cause of chromosome 9p21-linked ALS-FTD. Neuron *72*, 257-268.

Ringholz, G.M., Appel, S.H., Bradshaw, M., Cooke, N.A., Mosnik, D.M., and Schulz, P.E. (2005). Prevalence and patterns of cognitive impairment in sporadic ALS. Neurology *65*, 586-590.

Rogers, D.C., Fisher, E.M., Brown, S.D., Peters, J., Hunter, A.J., and Martin, J.E. (1997). Behavioral and functional analysis of mouse phenotype: SHIRPA, a proposed protocol for comprehensive phenotype assessment. Mamm Genome *8*, 711-713.

Rogers, D.C., Peters, J., Martin, J.E., Ball, S., Nicholson, S.J., Witherden, A.S., Hafezparast, M., Latcham, J., Robinson, T.L., Quilter, C.A.*, et al.* (2001). SHIRPA, a protocol for behavioral assessment: validation for longitudinal study of neurological dysfunction in mice. Neurosci Lett *306*, 89-92.

Roots, B.I. (1983). Neurofilament accumulation induced in synapses by leupeptin. Science 221, 971-972.

Rosen, D.R., Siddique, T., Patterson, D., Figlewicz, D.A., Sapp, P., Hentati, A., Donaldson, D., Goto, J., O'Regan, J.P., Deng, H.X.*, et al.* (1993). Mutations in Cu/Zn superoxide dismutase gene are associated with familial amyotrophic lateral sclerosis. Nature *362*, 59-62.

Rosengren, L.E., Karlsson, J.E., Karlsson, J.O., Persson, L.I., and Wikkelso, C. (1996). Patients with amyotrophic lateral sclerosis and other neurodegenerative diseases have increased levels of neurofilament protein in CSF. J Neurochem *67*, 2013-2018.

Roy, J., Minotti, S., Dong, L., Figlewicz D.A., and Durham, H.D. (1998). Glutamtae potentiates the toxicity of mutant Cu/Zn-superoxide dismutase in motor neurons by postsynaptic calcium-dependent mechanisms. J. Neurosci *18*, 9673-9684.

Roy, S., Coffee, P., Smith, G., Liem, R.K., Brady, S.T. and Black, M.M. (2000). Neurofilaments are transported rapidly but intermittently in axons: implications for slow axonal transport. J Neurosci *20*, 6849-6861.

Rozen, S., Cudkowicz, M.E., Bogdanov, M., Matson, W.R., Kristal, B.S., Beecher, C., Harrison, S., Vouros, P., Flarakos, J., Vigneau-Callahan, K.*, et al.* (2005). Metabolomic analysis and signatures in motor neuron disease. Metabolomics *1*, 101-108.

Rudnicki, S.A., Berry, J.D., Ingersoll, E., Archibald, D., Cudkowicz, M.E., Kerr, D.A., and Dong, Y. (2013). Dexpramipexole effects on functional decline and survival in subjects with amyotrophic lateral sclerosis in a Phase II study: Subgroup analysis of demographic and clinical characteristics. Amyotroph Lateral Scler Frontotemporal Degener *14*, 44-51.

Russell, A.J., Hartman, J.J., Hinken, A.C., Muci, A.R., Kawas, R., Driscoll, L., Godinez, G., Lee, K.H., Marquez, D., Browne, W.F.t.*, et al.* (2012). Activation of fast skeletal muscle troponin as a potential therapeutic approach for treating neuromuscular diseases. Nat Med *18*, 452-455.

Rutkove, S.B., Aaron, R., and Shiffman, C.A. (2002). Localized bioimpedance analysis in the evaluation of neuromuscular disease. Muscle Nerve *25*, 390-397.

Rutkove, S.B., Caress, J.B., Cartwright, M.S., Burns, T.M., Warder, J., David, W.S., Goyal, N., Maragakis, N.J., Clawson, L., Benatar, M.*, et al.* (2012). Electrical impedance myography as a biomarker to assess ALS progression. Amyotroph Lateral Scler *13*, 439-445.

Ryberg, H., An, J., Darko, S., Lustgarten, J.L., Jaffa, M., Gopalakrishnan, V., Lacomis, D., Cudkowicz, M., and Bowser, R. (2010). Discovery and verification of amyotrophic lateral sclerosis biomarkers by proteomics. Muscle Nerve *42*, 104-111.

Ryberg, H., Askmark, H., and Persson, L.I. (2003). A double-blind randomized clinical trial in amyotrophic lateral sclerosis using lamotrigine: effects on CSF glutamate, aspartate, branched-chain amino acid levels and clinical parameters. Acta Neurol Scand *108*, 1-8.

Ryberg, H., and Bowser, R. (2008). Protein biomarkers for amyotrophic lateral sclerosis. Expert Rev Proteomics *5*, 249-262.

Saha, S., and Das, K.P. (2007). Unfolding and refolding of bovine alpha-crystallin in urea and its chaperone activity. Protein J *26*, 315-326.

Salzer, J., Svenningsson, A., and Sundstrom, P. (2010). Neurofilament light as a prognostic marker in multiple sclerosis. Mult Scler *16*, 287-292.

Sangamo BioSciences press release. SB-509. Access Date: 16/04/2013 http://investor.sangamo.com/releasedetail.cfm?ReleaseID=531441 http://investor.sangamo.com/releasedetail.cfm?ReleaseID=610157

Sapp, P.C., Hosler, B.A., McKenna-Yasek, D., Chin, W., Gann, A., Genise, H., Gorenstein, J., Huang, M., Sailer, W., Scheffler, M.*, et al.* (2003). Identification of two novel loci for dominantly inherited familial amyotrophic lateral sclerosis. Am J Hum Genet *73*, 397-403.

Saris, C.G., Horvath, S., van Vught, P.W., van Es, M.A., Blauw, H.M., Fuller, T.F., Langfelder, P., DeYoung, J., Wokke, J.H., Veldink, J.H.*, et al.* (2009). Weighted gene co-expression network analysis of the peripheral blood from Amyotrophic Lateral Sclerosis patients. BMC Genomics *10*, 405.

Saxena, S., Cabuy, E., and Caroni, P. (2009). A role for motoneuron subtype-selective ER stress in disease manifestations of FALS mice. Nat Neurosci *12*, 627-636.

Schrohl, A.S., Wurtz, S., Kohn, E., Banks, R.E., Nielsen, H.J., Sweep, F.C., and Brunner, N. (2008). Banking of biological fluids for studies of disease-associated protein biomarkers. Mol Cellular Proteomics *7*, 2061-2066.

Sekizawa, T., Openshaw, H., Ohbo, K., Sugamura, K., Itoyama, Y., and Niland, J.C. (1998). Cerebrospinal fluid interleukin 6 in amyotrophic lateral sclerosis: immunological parameter and comparison with inflammatory and non-inflammatory central nervous system diseases. J Neurol Sci *154*, 194-199.

Sharp, P.S., Dick, J.R., and Greensmith, L. (2005). The effect of peripheral nerve injury on disease progression in the SOD1(G93A) mouse model of amyotrophic lateral sclerosis. Neuroscience *130*, 897-910.

Shea, T.B. (1994). Triton-soluble phosphovariants of the high molecular weight neurofilament subunit from NB2a/d1 cells are assembly-competent. Implications for normal and abnormal neurofilament assembly. FEBS Lett *343*, 131-136.

Shefner, J., Meininger, V., and Group, T.T.A.S. (2010). Results of a clinical trial of talampanel in patients with ALS. Amyotroph Lateral Scler *11*, 44-45.

Shefner, J.M., Cudkowicz, M.E., Zhang, H., Schoenfeld, D., and Jillapalli, D. (2004). The use of statistical MUNE in a multicenter clinical trial. Muscle Nerve *30*, 463-469.

Shefner, J.M., Cudkowicz, M.E., Zhang, H., Schoenfeld, D., and Jillapalli, D. (2007). Revised statistical motor unit number estimation in the Celecoxib/ALS trial. Muscle Nerve *35*, 228-234.

Shorter, J. (2011). The mammalian disaggregase machinery: Hsp110 synergizes with Hsp70 and Hsp40 to catalyze protein disaggregation and reactivation in a cell-free system. PLoS ONE *6*, e26319.

Shtilbans, A., Choi, S.G., Fowkes, M.E., Khitrov, G., Shahbazi, M., Ting, J., Zhang, W., Sun, Y., Sealfon, S.C., and Lange, D.J. (2011). Differential gene expression in patients with amyotrophic lateral sclerosis. Amyotroph Lateral Scler *12*, 250-256.

Siciliano, G., Manca, M.L., Sagliocco, L., Pastorini, E., Pellegrinetti, A., Sartucci, F., Sabatini, A., and Murri, L. (1999). Cortical silent period in patients with amyotrophic lateral sclerosis. J Neurol Sci *169*, 93-97.

Simpson, C.L., Lemmens, R., Miskiewicz, K., Broom, W.J., Hansen, V.K., van Vught, P.W., Landers, J.E., Sapp, P., Van Den Bosch, L., Knight, J.*, et al.* (2009). Variants of the elongator protein 3 (ELP3) gene are associated with motor neuron degeneration. Hum Mol Genet *18*, 472-481.

Slowik, A., Tomik, B., Wolkow, P.P., Partyka, D., Turaj, W., Malecki, M.T., Pera, J., Dziedzic, T., Szczudlik, A., and Figlewicz, D.A. (2006). Paraoxonase gene polymorphisms and sporadic ALS. Neurology *67*, 766-770.

Sofroniew, M.V., and Vinters, H.V. (2010). Astrocytes: biology and pathology. Acta Neuropathol *119*, 7-35.

Sreedharan, J., Blair, I.P., Tripathi, V.B., Hu, X., Vance, C., Rogelj, B., Ackerley, S., Durnall, J.C., Williams, K.L., Buratti, E.*, et al.* (2008). TDP-43 mutations in familial and sporadic amyotrophic lateral sclerosis. Science *319*, 1668-1672.

Sreedharan, J., and Shaw, C.E. (2009). The genetics of amyotrophic lateral sclerosis. Adv Clin Neurosci & Rehabil *9*, 10-15.

St-Jean, E., Blain, F., and Comtois, R. (1996). High prolactin levels may be missed by immunoradiometric assay in patients with macroprolactinomas. Clin Endocrinol (Oxf) *44*, 305-309.

Stagg, C.J., Knight, S., Talbot, K., Jenkinson, M., Maudsley, A.A., and Turner, M.R. (2013). Whole-brain magnetic resonance spectroscopic imaging measures are related to disability in ALS. Neurology *80*, 610-615.

Sternberger, L.A. and Sternberger, N.H. (1983). Monoclonal antibodies distinguish phosphoryalted and non-phosphorylated forms of neurofilaments in situe. Proc Natl Acad Sci U S A *82*, 6126-6130.

Storkebaum, E., Lambrechts, D., Dewerchin, M., Moreno-Murciano, M.P., Appelmans, S., Oh, H., Van Damme, P., Rutten, B., Man, W.Y., De Mol, M.*, et al.* (2005). Treatment of motoneuron degeneration by intracerebroventricular delivery of VEGF in a rat model of ALS. Nat Neurosci *8*, 85-92.

Strong, M.J., Kesavapany, S., and Pant, H.C. (2005). The pathobiology of amyotrophic lateral sclerosis: a proteinopathy? J Neuropathol Exp Neurol *64*, 649-664.

Sunyach, C., Michaud, M., Arnoux, T., Bernard-Marissal, N., Aebischer, J., Latyszenok, V., Gouarne, C., Raoul, C., Pruss, R.M., Bordet, T.*, et al.* (2012). Olesoxime delays muscle denervation, astrogliosis, microglial activation and motoneuron death in an ALS mouse model. Neuropharmacology *62*, 2346-2352.

Sussmuth, S.D., Brettschneider, J., Ludolph, A.C., and Tumani, H. (2008). Biochemical markers in CSF of ALS patients. Curr Med Chem *15*, 1788-1801.

Sussmuth, S.D., Sperfeld, A.D., Hinz, A., Brettschneider, J., Endruhn, S., Ludolph, A.C., and Tumani, H. (2010). CSF glial markers correlate with survival in amyotrophic lateral sclerosis. Neurology *74*, 982-987.

Swarup, V., Phaneuf, D., Bareil, C., Robertson, J., Rouleau, G.A., Kriz, J., and Julien, J.P. (2011). Pathological hallmarks of amyotrophic lateral sclerosis/frontotemporal lobar degeneration in transgenic mice produced with TDP-43 genomic fragments. Brain *134*, 2610-2626.

Takeuchi, S., Fujiwara, N., Ido, A., Oono, M., Takeuchi, Y., Tateno, M., Suzuki, K., Takahashi, R., Tooyama, I., Taniguchi, N.*, et al.* (2010). Induction of protective immunity by vaccination with wild-type apo superoxide dismutase 1 in mutant SOD1 transgenic mice. J Neuropathol Exp Neurol *69*, 1044-1056.

Tanaka, M., Kikuchi, H., Ishizu, T., Minohara, M., Osoegawa, M., Motomura, K., Tateishi, T., Ohyagi, Y., and Kira, J. (2006). Intrathecal upregulation of granulocyte colony stimulating factor and its neuroprotective actions on motor neurons in amyotrophic lateral sclerosis. J Neuropathol Exp Neurol *65*, 816-825.

Tarasiuk, J., Kulakowska, A., Drozdowski, W., Kornhuber, J., and Lewczuk, P. (2012). CSF markers in amyotrophic lateral sclerosis. J Neural Transm *119*, 747-757.

Tarulli, A.W., Garmirian, L.P., Fogerson, P.M., and Rutkove, S.B. (2009). Localized muscle impedance abnormalities in amyotrophic lateral sclerosis. J Clin Neuromuscul Dis *10*, 90-96.

Ticozzi, N., Tiloca, C., Morelli, C., Colombrita, C., Poletti, B., Doretti, A., Maderna, L., Messina, S., Ratti, A., and Silani, V. (2011). Genetics of familial Amyotrophic lateral sclerosis. Arch Ital Biol *149*, 65-82.

Tisdall, M., and Petzold, A. (2012). Comment on "chronic traumatic encephalopathy in blast-exposed military veterans and a blast neurotrauma mouse model". Science translational medicine *4*, 157le158; author reply 157lr155.

Todd, S., Whitehead, A., Stallard, N., and Whitehead, J. (2001). Interim analyses and sequential designs in phase III studies. Br J Clin Pharmacol *51*, 394-399.

Tokutake, S. (1990). On the assembly mechanism of neurofilaments. Int J Biochem *22*, 1-6.

Tomkins, J. Usher, P., Slade, J.Y., Ince, P.G., Curtis, A., Bushby, K., and Shaw, P.J. (1998). Novel insertion in the KSP region of the neurofilament heavy gene in amyotrophic lateral sclerosis (ALS). Neuroreport *9*, 3967-3970.

Tortelli, R., Ruggieri, M., Cortese, R., D'Errico, E., Capozzo, R., Leo, A., Mastrapasqua, M., Zoccolella, S., Leante, R., Livrea, P.*, et al.* (2012). Elevated cerebrospinal fluid neurofilament light levels in patients with amyotrophic lateral sclerosis: a possible marker of disease severity and progression. Eur J Neurol *19*, 1561-1567.

Tsuda, H., Han, S.M., Yang, Y., Tong, C., Lin, Y.Q., Mohan, K., Haueter, C., Zoghbi, A., Harati, Y., Kwan, J.*, et al.* (2008). The amyotrophic lateral sclerosis 8 protein VAPB is cleaved, secreted, and acts as a ligand for Eph receptors. Cell *133*, 963-977.

Tu, P.H., Raju, P., Robinson, K.A., Gurney, M.E., Trojanowski, J.Q., and Lee, V.M. (1996). Transgenic mice carrying a human mutant superoxide dismutase transgene develop neuronal cytoskeletal pathology resembling human amyotrophic lateral sclerosis lesions. Proc Natl Acad Sci U S A *93*, 3155-3160.

Turner, M.R., Brockington, A., Scaber, J., Hollinger, H., Marsden, R., Shaw, P.J., and Talbot, K. (2010a). Pattern of spread and prognosis in lower limb-onset ALS. Amyotroph Lateral Scler *11*, 369-373.

Turner, M.R., Cagnin, A., Turkheimer, F.E., Miller, C.C., Shaw, C.E., Brooks, D.J., Leigh, P.N., and Banati, R.B. (2004). Evidence of widespread cerebral microglial activation in amyotrophic lateral sclerosis: an [11C](R)-PK11195 positron emission tomography study. Neurobiol Dis *15*, 601-609.

Turner, M.R., Kiernan, M.C., Leigh, P.N., and Talbot, K. (2009). Biomarkers in amyotrophic lateral sclerosis. Lancet Neurol *8*, 94-109.

Turner, M.R., and Modo, M. (2010). Advances in the application of MRI to amyotrophic lateral sclerosis. Expert Opin Med Diagn *4*, 483-496.

Turner, M.R., Scaber, J., Goodfellow, J.A., Lord, M.E., Marsden, R., and Talbot, K. (2010b). The diagnostic pathway and prognosis in bulbar-onset amyotrophic lateral sclerosis. J Neurol Sci *294*, 81-85.

Urban, P.P., Vogt, T., and Hopf, H.C. (1998). Corticobulbar tract involvement in amyotrophic lateral sclerosis. A transcranial magnetic stimulation study. Brain *121*, 1099-1108.

Urushitani, M., Ezzi, S.A., and Julien, J.P. (2007). Therapeutic effects of immunization with mutant superoxide dismutase in mice models of amyotrophic lateral sclerosis. Proc Natl Acad Sci U S A *104*, 2495-2500.

Valdmanis, P.N., and Rouleau, G.A. (2008). Genetics of familial amyotrophic lateral sclerosis. Neurology *70*, 144-152.

van Blitterswijk, M., DeJesus-Hernandez, M., and Rademakers, R. (2012). How do C9ORF72 repeat expansions cause amyotrophic lateral sclerosis and frontotemporal dementia: can we learn from other noncoding repeat expansion disorders? Curr Opin Neurol. 2012 Dec;25(6):689-700.

van der Graaff, M.M., Sage, C.A., Caan, M.W., Akkerman, E.M., Lavini, C., Majoie, C.B., Nederveen, A.J., Zwinderman, A.H., Vos, F., Brugman, F.*, et al.* (2011). Upper and extra-motoneuron involvement in early motoneuron disease: a diffusion tensor imaging study. Brain *134*, 1211-1228.

van Eijk, J.J., van Everbroeck, B., Abdo, W.F., Kremer, B.P., and Verbeek, M.M. (2010). CSF neurofilament proteins levels are elevated in sporadic Creutzfeldt-Jakob disease. J Alzheimers Dis *21*, 569-576.

van Es, M.A., Diekstra, F.P., Veldink, J.H., Baas, F., Bourque, P.R., Schelhaas, H.J., Strengman, E., Hennekam, E.A., Lindhout, D., Ophoff, R.A.*, et al.* (2009). A case of ALS-FTD in a large FALS pedigree with a K17I ANG mutation. Neurology *72*, 287-288.

van Es, M.A., Van Vught, P.W., Blauw, H.M., Franke, L., Saris, C.G., Andersen, P.M., Van Den Bosch, L., de Jong, S.W., van 't Slot, R., Birve, A.*, et al.* (2007). ITPR2 as a susceptibility gene in sporadic amyotrophic lateral sclerosis: a genome-wide association study. Lancet Neurol *6*, 869-877.

van Es, M.A., van Vught, P.W., Blauw, H.M., Franke, L., Saris, C.G., Van den Bosch, L., de Jong, S.W., de Jong, V., Baas, F., van't Slot, R.*, et al.* (2008). Genetic variation in DPP6 is associated with susceptibility to amyotrophic lateral sclerosis. Nat Genet *40*, 29-31.

Van Langenhove, T., van der Zee, J., and Van Broeckhoven, C. (2012). The molecular basis of the frontotemporal lobar degeneration-amyotrophic lateral sclerosis spectrum. Ann Med *44*, 817-828.

Vance, C., Al-Chalabi, A., Ruddy, D., Smith, B.N., Hu, X., Sreedharan, J., Siddique, T., Schelhaas, H.J., Kusters, B., Troost, D.*, et al.* (2006). Familial amyotrophic lateral sclerosis with frontotemporal dementia is linked to a locus on chromosome 9p13.2-21.3. Brain *129*, 868-876.

Vance, C., Rogelj, B., Hortobagyi, T., De Vos, K.J., Nishimura, A.L., Sreedharan, J., Hu, X., Smith, B., Ruddy, D., Wright, P.*, et al.* (2009). Mutations in FUS, an RNA processing protein, cause familial amyotrophic lateral sclerosis type 6. Science *323*, 1208-1211.

Varrato, J., Siderowf, A., Damiano, P., Gregory, S., Feinberg, D., and McCluskey, L. (2001). Postural change of forced vital capacity predicts some respiratory symptoms in ALS. Neurology *57*, 357-359.

Verstraete, E., Kuiperij, H.B., van Blitterswijk, M.M., Veldink, J.H., Schelhaas, H.J., van den Berg, L.H., and Verbeek, M.M. (2012a). TDP-43 plasma levels are higher in amyotrophic lateral sclerosis. Amyotroph Lateral Scler *13*, 446-451.

Verstraete, E., Veldink, J.H., Huisman, M.H., Draak, T., Uijtendaal, E.V., van der Kooi, A.J., Schelhaas, H.J., de Visser, M., van der Tweel, I., and van den Berg, L.H. (2012b). Lithium lacks effect on survival in amyotrophic lateral sclerosis: a phase IIb randomised sequential trial. J Neurol Neurosurg Psychiatry *83*, 557-564.

Visanji, N.P., Orsi, A., Johnston, T.H., Howson, P.A., Dixon, K., Callizot, N., Brotchie, J.M., and Rees, D.D. (2008). PYM50028, a novel, orally active, nonpeptide neurotrophic factor inducer, prevents and reverses neuronal damage induced by MPP+ in mesencephalic neurons and by MPTP in a mouse model of Parkinson's disease. FASEB J *22*, 2488-2497.

Volkening, K., Leystra-Lantz, C., Yang, W., Jaffee, H., and Strong, M.J. (2009). Tar DNA binding protein of 43 kDa (TDP-43), 14-3-3 proteins and copper/zinc superoxide dismutase (SOD1) interact to modulate NFL mRNA stability. Implications for altered RNA processing in amyotrophic lateral sclerosis (ALS). Brain Res *1305*, 168-182.

Vucic, S., Burke, D., and Kiernan, M.C. (2007). Diagnosis of motor neuron disease. In The motor neuron disease handbook, M.C. Kiernan, ed. (Sydney: Australasian Medical Publishing Company Limited), pp. 89-115.

Vucic, S., Nicholson, G.A., and Kiernan, M.C. (2008). Cortical hyperexcitability may precede the onset of familial amyotrophic lateral sclerosis. Brain *131*, 1540-1550.

Wang, X.S., Lee, S., Simmons, Z., Boyer, P., Scott, K., Liu, W., and Connor, J. (2004). Increased incidence of the Hfe mutation in amyotrophic lateral sclerosis and related cellular consequences. J Neurol Sci *227*, 27-33.

Whitehead, J. (1999). A unified theory for sequential clinical trials. Stat Med *18*, 2271-2286.

Willard, M., and Simon, C. (1983). Modulations of neurofilament axonal transport during the developemnt of rabbit retinal ganglion cells. Cell *35*, 551-559.

Williams, K.L., Fifita, J.A., Vucic, S., Durnall, J.C., Kiernan, M.C., Blair, I.P., and Nicholson, G.A. (2013). Pathophysiological insights into ALS with C9ORF72 expansions. J Neurol Neurosurg Psychiatry *84*, 931-935.

Williamson, T.L., Bruijn, L.I., Zhu, Q., Anderson, K.L, Anderson, S.D., Julien, J.P., and Cleveland, D.W. (1998). Absence of neurofilaments reduces the selective vulnerability of motor neurons and slows disease caused by a familial amyotrophic lateral sclerosis-linked superoxide dismutase 1 mutant. Proc Natl Acad Sci USA *95*, 9631-9636.

Wilms, H., Sievers, J., Dengler, R., Bufler, J., Deuschl, G., and Lucius, R. (2003). Intrathecal synthesis of monocyte chemoattractant protein-1 (MCP-1) in amyotrophic lateral sclerosis: further evidence for microglial activation in neurodegeneration. J Neuroimmunol *144*, 139-142.

Wilson, M.E., Boumaza, I., Lacomis, D., and Bowser, R. (2010). Cystatin C: a candidate biomarker for amyotrophic lateral sclerosis. PLoS ONE *5*, e15133.

Winhammar, J.M., Rowe, D.B., Henderson, R.D., and Kiernan, M.C. (2005). Assessment of disease progression in motor neuron disease. Lancet Neurol *4*, 229-238.

Wittkop, L., Smith, C., Fox, Z., Sabin, C., Richert, L., Aboulker, J.P., Phillips, A., Chene, G., Babiker, A., and Thiebaut, R. (2010). Methodological issues in the use of composite endpoints in clinical trials: examples from the HIV field. Clin Trials *7*, 19-35.

Wolf, C., and Quinn, P.J. (2008). Lipidomics: practical aspects and applications. Prog Lipid Res *47*, 15-36.

Wolfensohn, S. and Lloyd, M. (eds) (2007) Conduct of Minor Procedures. In Handbook of Laboratory Animal Management and Welfare. Third Edition. (Blackwell Publishing Ltd, Oxford, UK). pp 150-181.

Wong, N.K., He, B.P., and Strong, M.J. (2000). Characterization of neuronal intermediate filament protein expression in cervical spinal motor neurons in sporadic amyotrophic lateral sclerosis (ALS). J Neuropathol Exp Neurol *59*, 972-982.

Wong, P.C., Marszalek, J. Crawford, T.O. Xu, Z., Hsieh, S.T., Griffin, J.W. and Cleveland, D.W. (1995). Increasing neurofilament subunit NF-M expression reduces axonal NF-H, inhibits radial nrowth, and results in neurofilamentous accumulation in motro neurons. J Cell Biol *130*, 1413-1422.

Wu, C.H., Fallini, C., Ticozzi, N., Keagle, P.J., Sapp, P.C., Piotrowska, K., Lowe, P., Koppers, M., McKenna-Yasek, D., Baron, D.M.*, et al.* (2012). Mutations in the profilin 1 gene cause familial amyotrophic lateral sclerosis. Nature *488*, 499-503.

Wuolikainen, A., Andersen, P.M., Moritz, T., Marklund, S.L., and Antti, H. (2012). ALS patients with mutations in the SOD1 gene have an unique metabolomic profile in the cerebrospinal fluid compared with ALS patients without mutations. Mol Genet Metab *105*, 472-478.

Wuolikainen, A., Hedenstrom, M., Moritz, T., Marklund, S.L., Antti, H., and Andersen, P.M. (2009). Optimization of procedures for collecting and storing of CSF for studying the metabolome in ALS. Amyotroph Lateral Scler *10*, 229-236.

Xu, Z., Cork, L.C., Griffin, J.W., and Cleveland, D.W. (1993). Increased expression of neurofilament subunit NF-L produces morphological alterations that resemble the pathology of human motor neuron disease. Cell *73*, 23-33.

Yabe, J.T., Chylinski, T., Wang, F.S., Pimenta, A., Kattar, S.D., Linsley, M.D., Chan, W.K., and Shea, T.B. (2001a). Neurofilaments consist of distinct populations that can be distinguished by C-terminal phosphorylation, bundling, and axonal transport rate in growing axonal neurites. J Neurosci *21*, 2195-2205.

Yabe, J.T., Wang, F.S., Chylinski, T., Katchmar, T., and Shea, T.B. (2001b). Selective accumulation of the high molecular weight neurofilament subunit within the distal region of growing axonal neurites. Cell Motil Cytoskeleton *50*, 1-12.

Yamanaka, K., Chun, S.J., Boillee, S., Fujimori-Tonou, N., Yamashita, H., Gutmann, D.H., Takahashi, R., Misawa, H., and Cleveland, D.W. (2008). Astrocytes as determinants of disease progression in inherited amyotrophic lateral sclerosis. Nat Neurosci *11*, 251-253.

Yang, J., Bridges, K., Chen, K.Y., and Liu, A.Y. (2008). Riluzole increases the amount of latent HSF1 for an amplified heat shock response and cytoprotection. PLoS ONE *3*, e2864.

Yang, Y., Hentati, A., Deng, H.X., Dabbagh, O., Sasaki, T., Hirano, M., Hung, W.Y., Ouahchi, K., Yan, J., Azim, A.C*., et al.* (2001). The gene encoding alsin, a protein with three guanine-nucleotide exchange factor domains, is mutated in a form of recessive amyotrophic lateral sclerosis. Nat Genet *29*, 160-165.

Yuan, A, Rao, M.V., Sasaki, T., Chen, Y., Kimar, A., Veeranna, Liem, R.K., Eyer, J., Peterson, A.C., Julien, J.P., *et al.* (2006). Alpha-internexin is structurally and functionally associated with the neurofilament triplet proteins in the mature CNS. J Neurosci *26*, 10006-10019.

Zangi, R., Zhou, R., and Berne, B.J. (2009). Urea's action on hydrophobic interactions. J Am Chem Soc *131*, 1535-1541.

Zetterberg, H., Jacobsson, J., Rosengren, L., Blennow, K., and Andersen, P.M. (2007). Cerebrospinal fluid neurofilament light levels in amyotrophic lateral sclerosis: impact of SOD1 genotype. Eur J Neurol *14*, 1329-1333.

Zetterberg, H., Jacobsson, J., Rosengren, L., Blennow, K., and Andersen, P.M. (2008). Association of APOE with age at onset of sporadic amyotrophic lateral sclerosis. J Neurol Sci *273*, 67-69.

Zhang, R., Hadlock, K.G., Do, H., Yu, S., Honrada, R., Champion, S., Forshew, D., Madison, C., Katz, J., Miller, R.G*., et al.* (2011a). Gene expression profiling in peripheral blood mononuclear cells from patients with sporadic amyotrophic lateral sclerosis (sALS). J Neuroimmunol *230*, 114-123.

Zhang, Y., Schuff, N., Woolley, S.C., Chiang, G.C., Boreta, L., Laxamana, J., Katz, J.S., and Weiner, M.W. (2011b). Progression of white matter degeneration in amyotrophic lateral sclerosis: A diffusion tensor imaging study. Amyotroph Lateral Scler *12*, 421-429.

Zinman, L., and Cudkowicz, M. (2011). Emerging targets and treatments in amyotrophic lateral sclerosis. Lancet Neurol *10*, 481-490.

Zoing, M.C., Burke, D., Pamphlett, R., and Kiernan, M.C. (2006). Riluzole therapy for motor neurone disease: an early Australian experience (1996-2002). J Clin Neurosci *13*, 78-83.